

1990

EROSION AND ELECTRODE ENERGY DISTRIBUTION IN SWITCHES WITH SILVER-CADMIUM-OXIDE CONTACTS

NOURI, HASSAN

<http://hdl.handle.net/10026.1/2391>

<http://dx.doi.org/10.24382/4445>

University of Plymouth

All content in PEARL is protected by copyright law. Author manuscripts are made available in accordance with publisher policies. Please cite only the published version using the details provided on the item record or document. In the absence of an open licence (e.g. Creative Commons), permissions for further reuse of content should be sought from the publisher or author.

EROSION AND ELECTRODE ENERGY DISTRIBUTION IN
SWITCHES WITH SILVER-CADMIUM-OXIDE CONTACTS

by

HASSAN NOURI, BSc, MSc

A Thesis submitted to the Council for National Academic Awards in Partial
Fulfilment for the Degree of Doctor of Philosophy

Sponsoring Establishment: Plymouth Polytechnic South West

Department of Electrical, Electronics and Communication Engineering

Collaborating Establishment: Ranco Control Ltd., Plymouth, Devon

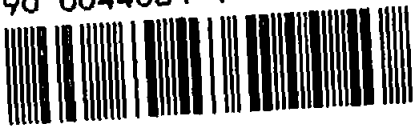
September 1990

POLYTECHNIC SOUTH WEST LIBRARY SERVICES	
Item No.	900044034-9
Class No.	T-621.381537
Contl No.	X 702351236

Now

90 0044034 9

TELEPEN



REFERENCE ONLY

I dedicate this work to my dear late

father in gratitude for his support and

encouragement throughout my education.

COPYRIGHT

"This copy of the thesis has been supplied on condition that anyone who consults it is understood to recognise that its copyright rests with its author and that no quotation from the thesis and no information derived from it may be published without the author's prior written consent".

CONTENTS

Acknowledgement

List of symbols and abbreviations

Declaration

Abstract 2

Chapter One Introduction 4

References - Chapter one 8

Chapter Two Electrical contact theory

2.1 Introduction 11

2.2 Theory of electric arc 11

2.2.1 The arc at break 12

2.2.2 The arc at make 18

2.2.3 The short arc 20

2.2.4 The long arc 23

2.2.5 The discharge transient 24

2.3 Theories of cathode emission 25

2.3.1 Thermionic emission 27

2.3.2 Field emission 29

2.4 The arc characteristics 31

2.5 The development of electrodes fall 34

2.5.1 The theory of electrodes fall 37

2.5.1.1 The cathode fall 39

2.5.1.2 The anode fall 43

2.6 Erosion 44

2.6.1 Erosion due to break arc 47

2.6.2 Erosion due to make arc 49

2.7	Power balance at the electrodes	53
2.7.1	Power balance at the cathode	55
2.7.1.1	Supplied power at the cathode	55
2.7.1.2	Used power by the cathode	56
2.7.2	Power balance at the anode	56
2.7.2.1	Supplied power at the anode	56
2.7.2.2	Used power by the anode	56
References – Chapter Two		57

Chapter Three The design and construction of experimental apparatus

3.1	Introduction	78
3.2	The equipment	78
3.3	Design of test rig	80
3.4	Design of constant current source in conjunction with timer	81
3.5	Techniques in thermocouple probe construction	83
3.5.1	Sensor construction	87
3.5.2	Sensor mounting	89
3.6	Thermocouple probe calibration system	97
3.7	Computer control ^{led} work station	100
References – Chapter Three		106

Chapter Four Experimental investigations

4.1	Introduction	107
4.2	Speed measurement	107
4.2.1	Opening speed	109
4.2.2	Closing speed	111
4.3	Electrode ^{voltage} fall measurement	111
4.3.1	Experimental details	112

4.3.2	Results, observations and discussion	117
4.4	Arcing at contacts of snap-action switches on closure; voltage step phenomena	136
4.4.1	The experiment	149
4.4.1.1	Dependence of steps on supply voltage and current	149
4.4.1.2	Dependence of steps on speed	155
4.4.1.3	Dependence of steps on surface condition	157
4.4.1.4	Dependence of steps on change of polarity	161
4.4.2	Development and formation of spikes	162
4.4.3	Theory of the arc at closure	164
4.4.4	Results and Discussion	166
4.5	Temperature-time curves of the electrodes	172
4.5.1	Procedure in testing	172
4.5.2	Calibration of the sensor	175
4.5.3	Results and Discussion	182
4.6	Power balance at the electrodes	188
4.6.1	Electrical model	188
4.6.1.1	Power balance at cathode	188
4.6.1.2	Power balance at anode	191
4.6.2	Thermal model	191
4.6.3	Results and Discussion	200
References – Chapter Four		221

Chapter Five Discussion Future Work And Conclusions

5.1	Discussion	225
5.2	Future work	233
5.3	Conclusions	234

Appendix I	:	Programme listing of the data collection software	A1
Appendix II	:	Data analysing programme listing	A9
Appendix III	:	Sample of temperature - time curves	A13
Appendix IV	:	Modelling heat transfer in the contact body using Finite Elements	A19

ACKNOWLEDGEMENT

I would like to thank my supervisors, Professor D.J. Mapps and Dr P.J. White, for their expert supervision and guidance throughout this work.

I am also grateful to Mr R. Purssel of Ranco Control Ltd. of Plymouth for his co-operation during this work.

Thanks are also due to all the technical staff who helped me in any way. In particular Dr R. Randell.

The author also wishes to thank Polytechnic South West (Plymouth) for providing financial support during his research assistantship in the Department of Electrical and Electronic Engineering.

Finally, I would like to express my deepest gratitude to my dear wife, Fiona, for her invaluable understanding and support during this research.

LIST OF SYMBOLS AND ABBREVIATIONS

J_a	Anode spot current density
V_a	Anode fall voltage
φ_a	Work function of the anode material
V_c	Cathode fall voltage
φ_c	Work function of the cathode material
a_a	Anode spot radius
a_c	Cathode spot radius
φ_{al}	Condensation heat of the electrons
$\varphi\beta$	Average evaporation energy of electrons
$\beta I\varphi$	Total power the cathode loses owing to the electron emission ($b = 1/3$)
V_e	Thermal energy of electron
J_p	Positive ion current density of cathode
J_e	Cathode spot current density
J_+	Density of the current carried by positive ions
V_i	Ionisation potential of the atoms of the cathode material
$V_i I_+$	Excitation energy
I	Total current
V_{arc}	Arc voltage
V_t	A part of thermal energy from column is carried by electrons
T_a	Anode surface temperature
T_c	Cathode surface temperature
t_c	Liquid temperature
T_1	Ambient temperature
T	Actual temperature in the spot

S	Specific heat capacity	
$V_c I_+$	Energy given off by positive ions to the cathode (K.E.)	
$V_a I$	Energy given off by electron to the anode	
Δ	Fraction of total power transferred to the cathode	
$(1-\Delta)$	Fraction of total power transferred to the anode	
C_l	Specific heat of liquid	
ρ_l	Density of liquid	
P_v	Power dissipated by vaporisation	
P_e	Power dissipated by the cooling effect of electron emission	
P_r	Power dissipated by radiation	
P_c	Power dissipated by thermalconduction into the cathode	
P_n	The power delivered to the anode spot by conversion of the K.E. of neutral atoms.	
P_r	Radiation energy from the column	
C_p	Power conducted from the hot gas to the electrodes	
Iwr	Power spent on evaporation (r for silver = 2.6×10^{10} J/M ³)	$\left\{ \begin{array}{l} w: \text{The rate of evaporation } M^3/\text{coul} \\ r: \text{Heat for } M^3 \text{ for both melting and evaporating } J/M^3 \end{array} \right.$
v^*	Excited atom energy	
f	Fraction of current I at the cathode carried by electrons	
F^*	Light flux to the cathode in quanta/sec (photon flux)	
e	Electron charge	
ξ	Yield of electron/excited atom	
R	Energy lost by radiation from region 2 to 3	
ϵ	Mean energy electrons carried the current from region 2 to 3	
C	$= a_c^2 \rho_l c_l t_c v$	
v	Random velocity of hot spot	
V_p	Plasma voltage (V)	
γ	Ratio of positive ion current to electron current	
ρ	Positive ion current	

I	Total current
α	Time constant of thermal system
θ_o	Thermocouple output temperature
Q_i	Input heat flow (watts)
V	Total voltage across the circuit
R_{th}	Thermal resistance of the system
h	Thermal heat transfer coefficient
T	Duration of the arc
V_{AE}	Total voltage drop across anode fall region
V_{CE}	Total voltage drop across cathode fall region

DECLARATION

I hereby declare that this thesis and its work of investigation has been completed by me and it has not been presented in any previous application for a higher degree.

H. NOURI

EROSION AND ELECTRODE ENERGY DISTRIBUTION IN SWITCHES WITH Ag Cd-O CONTACT

by

HASSAN NOURI

ABSTRACT

The cathode and the anode fall of the DC arcs are measured by fast oscilloscope for Ag-CdO contacts over a range of gap-lengths from 0.05 mm to 1 mm, and currents of 4-10 Amps at atmospheric pressure, with a known electrode closing speed, using the Moving Electrode Method.

It was observed that the anode fall can occur in a few places within the arc voltage waveform, and is dependent of the electrodes' surface condition. Both cathode and anode falls increase with gap-length and decrease with current.

It was found that when arc length is shorter than electrode separation, discontinuity within the arc voltage waveform during closure is caused, in many cases, by vapourisation of the first point of contact or by a high electric field set up between the two electrodes. These discontinuities are named as Voltage Step Phenomena. These voltage steps are related to the cathode and anode fall voltages, and their regular occurrences are a function of surface roughness.

The fluctuations in the arc voltage waveform are thought to originate mainly from the cathode.

A technique has been developed to measure the temperature of the electrodes accurately by using a T-type thermocouple, 0.075 mm diameter, in conjunction with a DC amplifier with a gain of 247.

The thermocouple is placed as close as possible under the electrode surface (200 μ m). This enables the temperature of the contact to be measured, after breaking contact, for an arc-duration even as short as 1ms.

The time-constant of the probe (contact containing the thermocouple) is measured to be approximately 18ms. With this technique the temperature of the electrodes are measured for currents and gap-lengths ranging 4-10 Amps and 0.05-1 mm respectively.

The effect of contacts being new and change of polarity have been investigated. From these results it is concluded that the co-existence of layers of foreign material on one, or both, surfaces causes the temperature of the electrodes to be high for the first 50-100 operations, before reaching to steady-state conditions. Change of polarity suggests that the moving electrode, either anode or cathode, due to the effect of air movement over its surface, is cooled relative to when fixed.

The power transfer to the electrodes is calculated for various currents and gap-length using thermal analogue formulae derived from the transient response of an RC circuit to a d.c. pulse.

The results show that below 0.2 mm the sum of the anode and cathode power is approximately equal to the arc power, and hence losses are negligible. At around 0.125 mm, for currents of about 6A and 12A, they both receive an equal amount of power from the arc. This has been related to the thermal energy of the electrons being negligible, at such separation, at the anode end of the plasma column.

The power balance equations are solved to calculate the positive ion current to the cathode, and the thermal energy of the electrons in the plasma column, under various test conditions.

In the investigation of erosion, the S.E.M. studies show that most of the power dissipated on the surface of the electrodes is used in melting and evaporation. The x-ray analysis shows that the melted metal is composed mostly of Silver.

To operate the test rig and collect the generated data automatically, a computerised test system, with a mini data acquisition system, has been designed and constructed here.

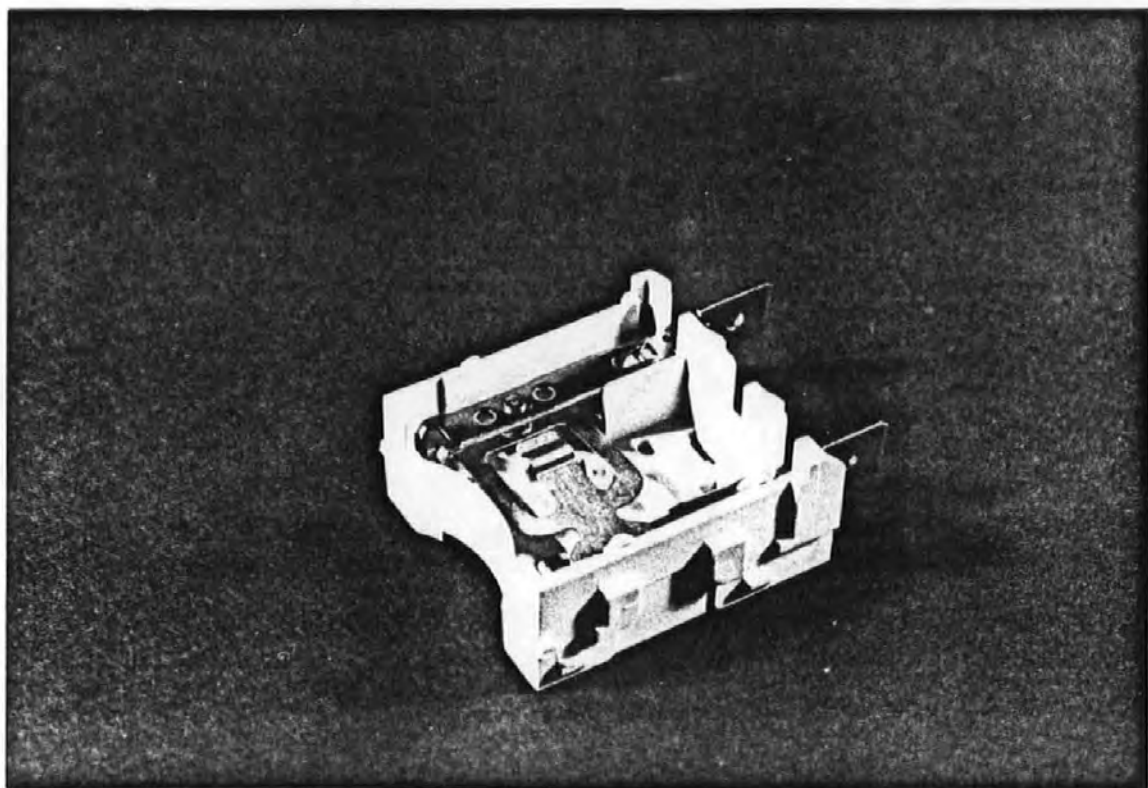


Figure 1.1: Photograph of Typical Snap-Action Switch

Electrical contacts have been known since the beginning of the 18th century and have been used extensively for a wide range of applications. In 1803 Petroff (1) and then in 1812 Sir Humphrey Davy (2) were probably the first who successfully observed an arc between carbon electrodes, and in the beginning of the nineteenth century Mrs H. Ayrton (3) was possibly the first to establish a relationship between the arc characteristics. The purpose of all electrical contacts is to perform the three operations of breaking the circuit, making the circuit and maintaining the circuit. These operations may take place at intervals of milliseconds in some cases and in others as long as years. The electrical contacts can be classified in the three main groups, depending upon the magnitude of the voltage and current at which they operate. These groups are:

- (1) High Power Contacts
- (2) Medium Power Contacts.
- (3) Low Power Contacts.

The fundamental process of the arc behaviour and the physical phenomena which occur in electrical contacts are described in standard literature(4-10).

The research described in this dissertation belongs to the third group above.

The electrical contact under investigation is a typical snap-action switch used in temperature controlled equipment and is shown in figure (1.1). These switches can be thought of as a topological variation of an electric contact which have found some specialised application in everyday life in domestic and commercial equipment. Since these switches must function reliably over a long period of time, especially for equipment which is designed to operate consistently, it is essential to increase their durability and reliability. For this reason, manufacturers are keen to optimise the performance of these switches for their own reputation through the consumers satisfaction. The unsuccessful operation of nearly all types of switches may be due to mechanical wear, chemical corrosion or electrical erosion. Of these, electrical

erosion is probably the most predominant factor, which is due to the amount of power being dissipated on each electrode during arcing (make or break).

The repeated operations of the switches results in metal being transferred from one electrode to the other. This produces a pip and crater on the electrodes. The disfigurement of the electrode surface may cause a switch to operate defectively and this may distort a waveform or eventually even fail to conduct a current. This is a common problem in telecommunication devices. The pip may also lock into the crater and prevent the switch to break.

In order to produce durable switches, a thorough understanding of the mechanisms underlining contact arcing is necessary.

There has already been substantial research in this area. For example, M. Sato (11) has investigated the welding of electric contacts for various metal and alloys. He concluded that the characteristics of the contact arcing mostly depend upon the softening temperature, melting temperature, specific heat, minimum voltage and the current necessary for a stationary arc to exist. Germer (12) has calculated the amount of heat dissipation at the electrodes on closure from a temperature difference measured by thermocouples. He deduced a relationship between contact erosion and heat dissipation. H.W. Turner (13) et al suggested ways of reducing the temperature rise in the contactor. The factors examined included not only the temperature rise due to carrying a steady current, but also the effect of arcing due to frequent switching of the contactor. Recently, with the development of powerful computers, a number of theoretical investigations into the effect of arcing on electrodes have been published (14,15). In the last decade, due to rapid technological progress, some of the electromechanical switches which have been employed in specialised equipment have been replaced by solid-state switches. A recent report by ^{the}Electronic Engineer Journal (16) states that over 50% of the switch market has been taken over by solid-state switches. The report by the Electrical Research Association suggests that in spite of the strong demand for solid-state switches, cost and flexibility considerations dictate that electromechanical switches will share the market for the

foreseeable future.

The switch model used for this research was especially built in the laboratory, and it has been described in section (3.3). It is similar to snap action switches in all functional aspects. The contacts were provided by RANCO Controls Ltd. of Plymouth, Devon. RANCO produces these switches at a rate of 200,000 per month for use in equipment requiring temperature control. These switches operate at 240 volts, at a current of up to 16A, for an average life time of 15 years, assuming a nominal usage of about 10,000 operations per year. This is typical of a very large proportion of switches.

Initial impetus for the present project arises from continuing and successful industry, SERC and local Education Authority-funded research, which started in 1974 with the collaboration of RANCO. The research has concentrated on the special properties of electric arcs which occur when switch contacts separate rapidly in snap-action switches controlling the temperature inside domestic refrigerators.

Here the need is for a means of providing a condition under which the operating characteristics can be adjusted so that the net contact erosion can be significantly reduced, hence leading to a major advance in switch technology which may be important not only for refrigerator switches, but also to the main research field of electrical interruption. Therefore, the project seeks to investigate the relationship between contact erosion and the energy dissipation due to arcing at the contacts. This arcing leads to the development of cathode and anode fall regions (Voltage drop) where power is developed to locally boil the contact material. Material transfer then occurs as a function of the polarity of the contacts and the energy dissipated at each contact surface, which in turn depends on the arc length and the current.

Research to date (18) has shown that the direction of material transfer can be reversed depending on the arc length, current and contact geometry. Recently published arc length/voltage/current data (19) suggests that the critical contact separation for equal contact power dissipation could be less than 0.2mm.

The initial approach to this investigation was to measure the anode and cathode

fall voltages for various currents and gap-lengths, using the method of Dickson and Von Engle⁽²⁰⁾, by drawing an arc and closing the contacts. Then to develop a technique to accurately measure the anode and cathode temperature rise during arcing, by placing a thermocouple of negligible thermal mass as close as possible under the electrode surface, before appreciable heat diffusion takes place. Because the duration of the arc is in the order of only 2 - 10 ms, the contact body does not reach a steady temperature.

Next, from the above measured data, to devise a power balance relation between electrical and thermal power. The degree of the difference in the correlation between them indicates the erosion rate, which may enable one to optimise the performance of these switches, as used in domestic appliances.

References - Chapter One

1. Petroff, W.
Rep. Acad. Chirurg. Med. Petersburg, 1803.
2. Davy, H.
"Elements of Chemical Philosophy",
French Translation 1813, pp 187-189.
3. Ayrton, H.
"The Electric Arc",
Electrician, London, 1902.
4. Windred, G.
"Electrical Contacts",
Macmillan & Co. Ltd., London, 1940.
5. Llewellyn Jones, F.
"Fundamental Processes of Electrical Contact Phenomena",
Her Majesty's Stationery Office, London, 1953.
6. Llewellyn Jones, F.
"Electrical Discharge",
The Physical Society, vol. XVI, 1953.
7. Llewellyn Jones, F.
"The Physics of Electrical Contacts",
The Clarendon Press, 1957.

8. Somerville, J.M.
"The Electric Arc",
Butler and Tanner Ltd., 1959.
9. Holm, R.
"Electric Contacts Theory of Application",
Fourth Edition, Springer-Verlag, Berlin, 1967,
10. Shmelcher, T.
"Low-voltage Switchgear",
Springer-Verlag, Berlin, 1983.
11. Sato, M.
"Studies on the silver base electrical contact materials",
Transactions of National Research Institute for Materials, vol. 18,
no. 2, 1976, pp 65-83.
12. Germer, L.H.
"Heat dissipation at the electrodes of a short electric arc",
The Bell System Technical Journals, Oct. 1951, pp 933-944.
13. Turner, H.W. et al
"Factors Reducing Temperature Rise in Contactors",
The Electrical Research Association, August 1967.
14. Robertson, S.R.
"A finite element analysis of the thermal behaviour of contact",
Proc. of the Holme Conference 1981, pp 115-123.

15. Nakagawa, Y and Yoshioka, Y.
"Theoretical calculation of the process of contact arc erosion
using a one-dimensional contact model",
Proc. of the 8th Int. Conf. on Electrical Contact Phenomena, Tokyo, Japan,
1976, pp 99-102.
16. Electronics Engineer
"Relays, Switches and Keyboards", August 1985, pp 48-60.
17. Electrical Research Association
"Future for Switching Components",
Leatherhead, Surrey, 1976.
18. Mapps, D.J. and White, P.J.
"Arc energy and erosion studies of snap-action switches",
Proc. of the Holme Conference, Chicago 1977, pp 85-91.
19. White, P.J.
"Investigation of parameters affecting the operating characteristics
of toggle-switches with Ag-cdo".
PhD Thesis, 1979.
20. Dickson, D.J. and Von Engel, A.
"Resolving of the electrode fall spaces of the electric arc",
Proc. of the Royal Society, A, vol. 300, 1966, pp 316-325.
21. Capp, B.J.
"The power balance in electrode-dominated arcs",
J. Physics., D. Appl. Physics, vol. 5, 1972, pp 2170-2178.

CHAPTER TWO

2.1 INTRODUCTION

There are some general properties of arc discharge phenomena which are applicable to snap-action switches. A detailed survey of these phenomena which are relevant to the present investigation is described in this chapter.

2.2 THEORY OF ELECTRIC ARC

An arc is defined as a discharge of electricity between two charged electrodes in a gas which is often called a space charge phenomenon. The term arc is only applied to a stable or quasi-stable discharge, and it has been regarded as the ultimate form of discharge (Dark discharge to glow discharge) and it is characterised as a continuous discharge phenomenon.

The process is derived from non-self sustaining discharge which relies for its maintenance upon external effects such as thermionic or non-thermionic emission to self-sustaining discharge in which the key mechanism for discharge formation is the magnitude of current through the gas, typically few tens of μA . This is beyond the saturation value.

The process involved in development of arc discharge has been discussed in several books⁽¹⁻³⁾ and by several workers^(4,5). A feature of the arc discharge which is of importance in electrical contacts is that it is not self-starting and must be initiated by separation of the contacts when carrying current or by approaching two charged electrodes. Each of these mechanisms will be discussed in sections 2.2.1 and 2.2.2.

It is well known that the occurrence of the arc depends on various factors such as contact resistance, pressure, speed, contact metal, contact geometry, ambient gas, voltage, current and circuit components.

The laws governing the circuit components are Ohm's Law (electrical resistance), Lenz' Law (electromagnetic inductance) and, finally, capacitance. A detailed study on the effect of each of these circuit components has been discussed fully by G. Windred⁽⁵⁾.

Since the occurrence of the arc to a large extent depends on voltage and current, F. Llewellyn-Jones⁽¹⁾ suggests that in high power contacts there is always a sufficient voltage across the gap to cause ionisation and this is especially true in the D.C. case as opposed to A.C. where the arc may be broken at the instant when the current is zero. This is because the residual ionisation tends to disappear at the moment of zero crossing. However, at high current, the current density exceeds the minimum required for arc maintenance.

The essential requirements for the arc maintenance are as follows:

- (i) Sufficient electron emission from the cathode
- (ii) Sufficient gas ionisation.

An arc may be regarded as a special form of discharge. It occurs in various types and has been classified as Short, Long and Transient Arcs. These are discussed in sections 2.2.3 - 2.2.5.

2.2.1 THE ARC AT BREAK

When the two electrodes with voltage and current which are greater than the minimum voltage (V_m) and minimum current (I_m) are pulled apart with decreasing load the contact area diminishes and contact resistance increases. Consequently, an arc occurs in the gap. The arc extinguishes as the current descends past the minimum current.

The minimum current is defined as the maximum current for a given voltage for which arc does not take place. The minimum voltage is defined as the voltage below which a current of any magnitude can be interrupted without arcing.

Minimum voltage and current are both functions of cathode materials and V_m in

general lies between 10-15 volts for most materials. The minimum arcing current is also found to be dependent on the shape of the contacts.

The values of I_m and V_m in normal atmosphere found by various observers (when electrode diameter \gg diameter of cathode spot, which is the seat of electron emission) is given by Holm⁽⁶⁾. In order to understand the processes of the arcing it is important to have knowledge about the formation and rupture of a Molten Metal Bridge.

MOLTEN METAL BRIDGE:

In general when two electrodes are at rest mechanically, the area of contact is very much smaller than the cross section of the electrodes⁽⁶⁾, and as a result of the flow of current from one electrode to the other is constrained through the microscopic contact area. F. Llewellyn Jones⁽⁷⁾ and Greenwood⁽⁸⁾ give a detailed calculation of constriction resistance for various shapes and for a random distribution of the microscopic contact spots.

As the electrodes are opened with decreasing load, there is an elastic and plastic relaxation of the area of the contact. Thus there is no immediate jump from the contact resistance to infinite resistance. The voltage across the contacts increases during this period until it reaches a value >1 volt when the current is forced to flow through one very small area where the current density is so high that melting of contact material occurs. This molten metal between the two electrodes is called the Molten Metal Bridge.

However, further decrease in contact load will not interrupt the current flow due to the Molten Metal Bridge, but continuous separation of the electrodes will draw out and lengthen the Bridge and so increases its resistance. Here, if the current is constant, the voltage across the bridge rises causing the temperature of the bridge (melting temperature) to reach the boiling temperature of the metal, when consequently the bridge breaks (ruptures) and sets up ^{an} induced e.m.f. across the gap. As soon as this induced e.m.f. reaches the minimum arcing voltage a sufficient gas

ionisation will take place and thus an arc discharge will take place in the metal vapour.

The spectroscopic studies by Thomas⁽⁹⁾ of the arc with Pd contacts have shown that the characteristics of the arc produced in the atmospheric air are not appreciably different from those of the arc in a vacuum. This result supports the view that the arc is initiated and maintained in metal vapour.

However, if the pressure of the metal vapour is not too high the discharge mechanism is known as Short arc, and as the gap between the electrodes increases the situation exhibits a Long arc. Both Short and Long arcs are discussed in sections 2.2.3 and 2.2.4.

The initiation and development of arc after rupture of the bridge has been studied by several workers (9,10) by means of simultaneous oscillographic recording of the variations of contact voltage and of current. Llewellyn Jones and Cowburn (12) and Thomas⁽⁹⁾ have also studied bridge rupture by means of time resolved spectroscopic measurements of the radiation emitted by the arc.

In the study of molten metal bridges, Llewellyn Jones (7) has calculated the maximum temperature of the bridge at rupture using ~~the~~ ψ, θ theorem. However, other researchers⁽¹³⁻¹⁵⁾ suggest that if the electrodes are opened more rapidly, the ψ, θ relationship will no longer be valid.

Koren et al⁽¹⁶⁾ have introduced the life of bridging into three periods, which are Melting period, Stable period and, finally, Unstable period, where eventually the bridge ruptures. They suggest that during the Unstable period the voltage can rise as high as the arc voltage, at which time a short duration arc is formed and can drop to a value as low as the melting voltage where the bridge reforms.

The occurrence of rebridging was first suggested by Jones⁽¹⁷⁾ and confirmed by Slade⁽¹⁸⁾ in oscillographic studies. This phenomenon was also studied by Thomas⁽¹⁹⁾ by means of high speed photography in which he suggested that each new bridge is formed from a droplet of molten metal from the previous bridge which is on the surface of the electrodes.

Jenkins⁽²⁰⁾ has suggested that the number of rebridgings and their life times is dependent on the circuit parameters.

The evidence linking boiling of bridge material with rupture was studied by Jones⁽¹⁷⁾, Thomas⁽¹⁹⁾ and Cowburn⁽²¹⁾.

Price and Llewellyn Jones⁽²³⁾, Thomas⁽²²⁾ and Cowburn⁽²¹⁾, by high speed photographic studies, showed that a bridge breaks explosively and, as a result, the metal vapour and droplets of molten metal are present between the electrodes after the rupture of a bridge.

Boddy and Utsumi⁽²⁴⁾ have related the cause of fluctuation of the arc voltage with metal vapour present after the rupture of a molten metal bridge.

Holm⁽⁶⁾ has introduced the concept of Short and Long bridge. A bridge is called Long when its length and its diameter are equal and their rupture can be caused by boiling in the hottest section, but probably more mechanically ^(i.e. due to surface tension in bridge) \wedge . A bridge is called Short when rupture occurs at a length small compared with its diameter. The rupture of such a bridge is not always accompanied by boiling or an arc⁽²⁵⁾. Nowadays it is customary to use some knowledge of the arc properties in the design of switches. The arc properties are defined as V-I characteristics and are outlined in the following:

V-I CHARACTERISTICS:

These are curves in which the voltage of the arc is plotted against the current with the arc length as a parameter. V-I characteristics have been published by several workers^(26,27). Holm⁽⁶⁾ produced a set of constant arc length curves at different voltages and currents, using silver electrodes in air. The observations refer to arcs shorter than 2mm and measurements were taken from an Ohmic circuit in which the arc was drawn at a rate slow enough to represent stationary conditions. At any point in time the velocity of the contact was 200mm/sec which has been suggested by Fink et al⁽²⁹⁾ as having a negligible effect on the arc characteristic.

Aida⁽³⁰⁾ using Holm's arc voltage-current characteristics presented a general

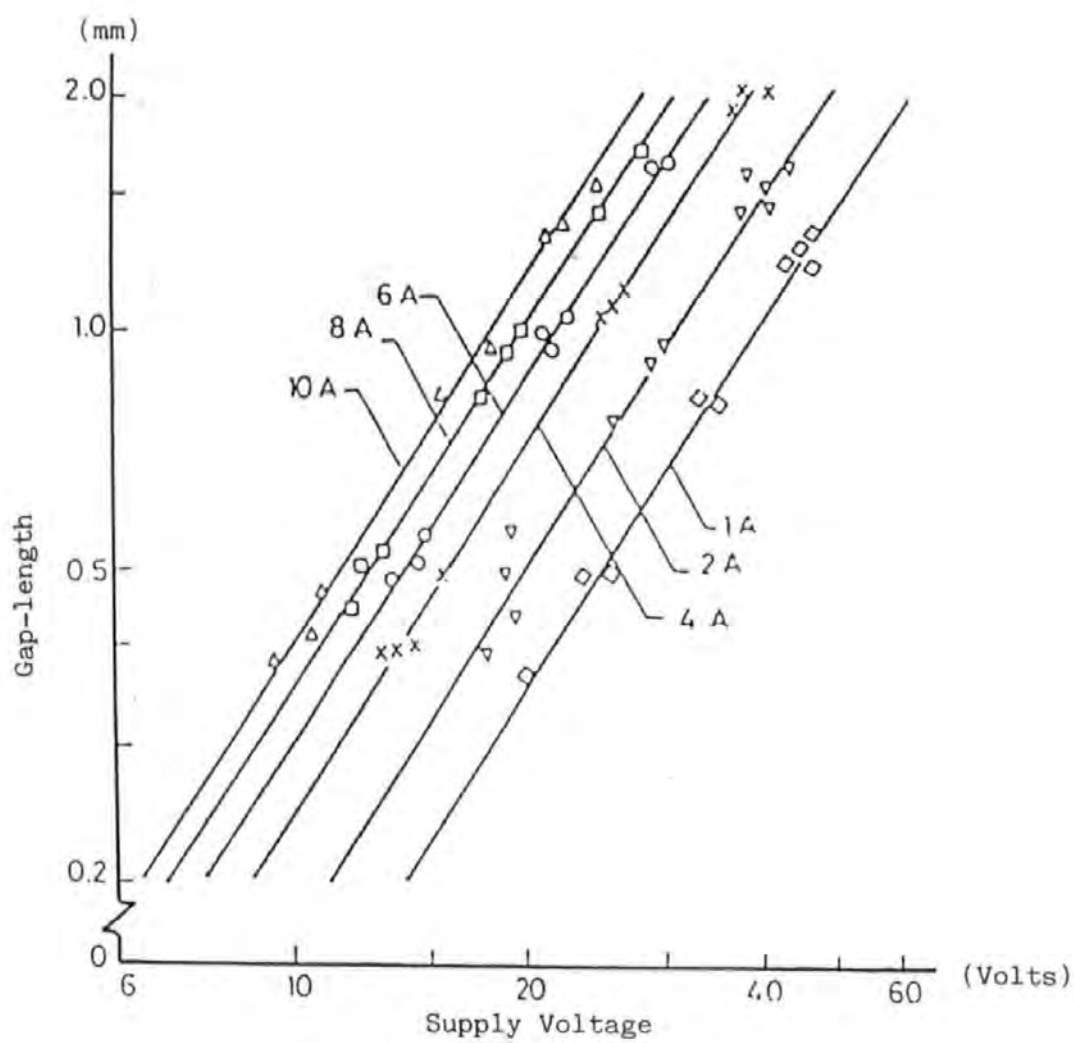


Figure 2.1: White's V-I Chart of Typical Snap-Action Switch for a current of 1-10 A.

formula for the arc duration at breaking operation of the contacts (gold, silver, copper, carbon and tungsten) as a function of arc voltage, current and breaking speed.

Sato et al^(31,32) have produced some equations defining the arc voltage and current in terms of circuit parameters at a constant opening velocity. By varying the values of the supply voltage and current, they produced different arc durations and obtained corresponding arc length by assuming a constant velocity characteristic.

In the study of snap-action switches where the opening characteristics are non linear⁽³³⁾. The chart of V-I characteristics has been produced by White⁽³³⁾ in which he adopted Holm's and Sato's methods. This is shown in figure 2.1. The data was obtained using high-speed camera and transient recorder. The film from a high-speed camera allows the arc length at any given time to be known and a transient recorder stores the simultaneous arc voltage and current. Since durability of switches up to a large extent depends on the duration of the arc between the electrodes, the factors affecting the life of the arc have been studied by several workers (34-37).

2.2.2 THE ARC AT MAKE

Since electrons are always present between two electrodes' gap or at the cathode surface due to a cosmic radiation or light, an initial avalanche of electrons can take place by introducing a voltage across the gap which eventually results in a transition from glow discharge to an arc.

The electric breakdown is known to be governed by Paschen's law which is a function of the electrode gap and gas pressure. In Paschen's law the minimum voltage required for $d > 10^{-2}$ cm and $pd = 7 \times 10^{-4}$ (atm x cm) at room temperature is 330 volts. This is known as break down or sparking potential (V_s). However, Germer and Haworth⁽³⁸⁾, in an experiment with the gap, reduced to 10^{-5} cm, discovered that at atmospheric pressure arc ignition occurs with V_s smaller than 330 volts, even down to 50 volts.

Several theories have been put forward for the initiation of arcs at make. Holm⁽⁶⁾ assumed that the arc at closure is initiated with preceding contact of asperity peak. The peak metal immediately evaporates by high current whereby the arc ignites in the heated and ionised vapour. He also observed a transition voltage drop to zero which indicates the contact make with the peak and the high current flows between two asperities in contact before vapourisation. However, Germer^(38,39) observed ignition without any transition voltage drop to zero (or was performed without preceding contact). They suggest that this is due to an enhanced field in which arc is initiated by field emission and its current density is higher than regular arc.

They also noticed that arc ignition appeared more readily at low voltages if the contacts were activated.

This high field emission has been confirmed by Llewellyn Jones⁽⁴⁰⁾, who stated that a layer of thin tarnish increases electron emission by a power of ten. Such a film also shortens the time lag of arc ignition.

Kisliuk⁽⁴¹⁾ considered a phenomenon called I-effect as an explanation to Germer

et al's(38,39) experiment in which ignition occurs without preceding contact.

Later, the concept of Whiskers was proposed by Holm⁽⁶⁾ as an explanation of Germer's experiment and it has been described as follows:

At high field the surface asperities form into a peak which is hair-like. At this situation as the contacts approach and the Whiskers come into contact, it is immediately heated to explosion with ignition of an arc in the vapour.

Contact at Whisker has a much smaller cross section compared with contact asperities and hence higher resistance and the transient current which flows before vapourisation is less than that which flows between two asperities in contact and consequently can not transiently lower the contact voltage to zero.

The concept of Whiskers has also been studied by other workers^(42,43). For example, Lawson⁽⁴²⁾ working with A.C. switches at 15 ampere and 120 volts describes the process of the arc as follows:

An initially drawn arc produces metal vapour in which Whiskers form in a fraction of a second, seemingly arranged along the field lines. The Whiskers short-circuit the gap, causing explosive breakdown and ignition of a new arc.

The arc ignition at closure before contact may be followed by a phenomenon which is named Floating⁽⁶⁾. Here electrodes are held separated by the high vapour pressure produced by an arc in spite of mechanical load. Floating may also occur when contacts are made and at rest, because the contact area is not able to increase to accommodate the inrush current.

Hueber in a series of papers^(44,45) has studied the initiation of Floating and its characteristics in different atmospheres.

Arcs at contact may also occur at rebound, since contact usually comes to a complete rest position after several make and breaks. In the study of ^{the} arc at closure, Phoney⁽⁴⁶⁾ with the aid of a fast storage oscilloscope has distinguished three types of closure phenomena.

- (i) Arc discharge with ^{out} preceding contact due to field emission.
- (ii) Arc discharge with preceding contact, either Whisker or

asperity, followed by vapourisation to an arc.

(iii) Closure with no arcing.

Germer⁽⁴⁷⁾ classified two types of arc discharge at closure, namely anodic arc and cathodic arc. These will be discussed in the next section.

2.2.3 THE SHORT ARC

The rate of ionisation for the occurrence of an arc is dependent on the contact gap. The minimum length required for considerable ionisation to take place is of the order of a few electron mean free path lengths.

In general it has been agreed that the short arc is initiated at a separation value less than the mean free path of an electron (or alternately where the mean free path of electrons exceeds the arc-length).

Since at separation of $\approx 10^{-4}$ cm the probability of ionisation of most atoms at energies near the ionisation potential is low $\approx 7-10\%$ ⁽⁴⁰⁾, a large number of electrons (about 90%) do not ionise and gain energy from the electric field travelling with high speed (105 cm/sec) towards the anode where they dissipate their energy as heat. This energy quickly raises the temperature of the contact to boiling point, creating a dense vapour at the surface to supply the arc with ions. The first molecule to leave the anode must be evaporated by the heating due to field emission electrons.

Prutton⁽⁵⁰⁾, in the study of surface properties, has explained fully the behaviour of the surface due to heating.

In general the short arc is characterised by its constant arc voltage, which is of the order of the ionising potential of the contact material⁽⁵¹⁾ and also, as has been suggested by Kisliuk⁽⁴⁸⁾, is a little greater than the sum of the ionisation potential of the metal vapour and the work function of the cathode surface. The current densities in such an arc are extremely high⁽⁴⁹⁾, at least 3×10^7 A/cm², and field emission possibly enhanced by the effect of the fields of individual ions approaching the cathode⁽⁵²⁾ is probably capable of supplying the cathode electron current⁽⁴⁸⁾.

Germer and Boyle in a series of papers^(53,54) suggest that the essential requirement for the maintenance of the arc is the metallic vapour which has been produced as the result of electron/ion bombardment on the electrodes. The same authors have also shown that two types of short arcs may exist which they named anode and cathode arcs. The defined anode arcs as being where ions are supplied chiefly by metal vapourised from the anode as a result of electron bombardment. However, in the cathode arc, metallic vapour is evaporated from the cathode, apparently by the blowing up of small points on the cathode by joule heating. Their classification of the short arc is based on their observations in which in a single anode arc a pit is seen on the anode and a roughened area on the cathode. However, in the single cathode arc, a widely dispersed array of individual pits appeared on the cathode and in many cases no mark was found on the anode. They have also reported on the experiment with different metals that the arc voltage of the cathode arc is higher than the anode, and they suggested that factors determining the types of arc are the potential between the electrodes and the nature of the cathode surface, but not the size of arc current. Short arcs initiated by voltages between the electrodes ≈ 50 volts are predominantly of the anode type, whilst those initiated by a voltage ≈ 400 volts are almost entirely of the cathode type.

In the cathode arc, transfer of metal is from the cathode to the anode only. In an anode arc, the metal is transferred in both directions, but the net transfer is from anode to cathode.

Smith and Boyle⁽⁵⁵⁾, in an experiment on a pair of gold electrodes at make with operating conditions of 200 volts, 2 ampere and an arc duration of $1\mu s$, suggested that if sufficient energy was applied to the anode arc the electrodes would be welded. Recently Fujiwara and Yamaguchi⁽⁵⁶⁾, in an investigation of short arc on closure, suggested that the weld can occur on some materials and this is independent of the contact force. They also reported that on some materials, such as Ag-60 Pd, the weld will never occur as the velocity of closing varied from 1mm/sec to 200mm/sec. Instead, adhesion takes place at the anode arc. However, this does not appear to

occur at the cathode arc in air because of surface oxidation. The phenomenon of adhesion has been explained thoroughly by Holm⁽⁶⁾.

In studies of arcing on opening contact, Hopkins and Jones⁽⁵⁷⁾ suggested that the short arc occurs after the explosion of the molten metal bridge provided the contact voltage can rise quickly to the ionisation potential of the atoms of the vapour. The pressure of the vapour in such an arc is shown by Slade⁽⁵⁸⁾ to be typically 6-8 atmospheres. The separation of the electrode surface at this stage may be comparable with the electron mean free path in the metal vapour. The electron crossing the gap will make few ionising collisions. The contact current will be carried mainly by electrons which will dissipate their energy in the form of heat at the anode.

Slade⁽⁵⁸⁾ in his test has suggested that the duration of the short arc is the product of local inductance and the current at bridge rupture.

Allen⁽⁵⁹⁾ has suggested that the conditions typical of a long arc may also be obtained immediately after rupture of the bridge due to vapour being produced at high pressure (typically 40 atmospheres) by the rupture of the bridge. An arc of this kind is known as a reverse short arc. This high pressure vapour initially may give a reverse short arc and then may diffuse into the surrounding atmosphere, quickly producing a condition for a short arc.

Holm⁽⁶⁾ has introduced the concept of anodic and cathodic dominated arcs in opening contacts, and remarks that since the anode spot increases with the gap, the transition from anode to cathode dominated arcs appears when the gap-length surpasses a critical value.

It seems from the review of the above literature that the short arc at Make is commonly called the Very Short or Extremely Short arc, and at Break is called the Micro arc. Since the short arc has been classified into two groups, at Make, being called the Anode arc or ^{the} Cathode arc, and at Break, the Anode and Cathode Dominated arc.

2.2.4 THE LONG ARC

When separating two touching electrodes between which a current is flowing, the final points of contact between the electrodes become very hot and may melt forming a liquid bridge between the electrodes. The nature of the bridge has been described in section 2.2.1. As the electrodes are drawn apart the bridge finally ruptures explosively, either by boiling at the hottest part or because of the failure of surface tension to maintain a stable liquid bridge. After rupture an arc discharge takes place between the electrodes. The first arc will usually be a short arc, like that described in section 2.2.3 which strikes when the distance between the electrode is $\approx 10^{-4}$ cm.

As separation between the two electrodes increases, if a sustained arc is to be formed, the short arc must change into a long arc in which the arc lengthens and electrons crossing the gap make more ionising and elastic collision with the gas atom which creates the ions. These positive ions under ^{the} influence of ^{the} electric field drift across the gap and produce the cathode fall and the column. This is the most characteristic feature of the long arc. In general, the long arc is defined where the arc length is greater than mean free path.

The cathode is only required to replace the lost electrons during ionisation. Those electrons which do not ionise an atom will continue their journey through a potential drop towards the anode in which they have lost most of their energies. The arrival of these low energy electrons at the anode is much less severe since their maximum energies lies within less than ^{mean} ^{of the} free path ^{of the} electrons and so the sudden evaporation is much less. On the other hand, the high field of the cathode fall results in the acceleration of some positive ions and consequently the cathode suffers a severe bombardment by massive positive ions which is likely to do greater damage.

It seems when breaking two electrodes, both electrodes lose matter by evaporation, first the anode and then the cathode, but in general it has been agreed

that the net transfer is from the cathode to the anode.

Holm⁽⁶⁾ classified the arc with duration of $\geq 3\mu s$ as Long arc and an arc with duration of $> 1ms$ as Normal arc. He also reported that the anode gain decreases with the arc duration and current. However, the material transfer is still from the cathode to the anode. Unless a sufficient anode fall is developed which is otherwise, this is as a result of the thin shape of the anode in which the anode spot is poorly cooled and little heat conduction takes place.

Llewellyn Jones ⁽⁷⁾ in a long arc discharge erosion suggests that for a low rate of erosion the electrodes should have metal with a high boiling point, high density and a high thermal conductivity.

2.2.5 DISCHARGE TRANSIENT

The arc will ignite and sustain provided the supply voltage is greater than the ionisation potential and the steady current is large enough.

However, in 1940 at Bell Laboratory, Curtis⁽⁶⁰⁾, in the study of telephone switching circuits where the steady circuit current was about 0.1 ampere, observed the phenomenon and named it Discharge Transient. His explanation is as follows:

The lead which constitutes a capacitance, inductance and a resistor will set up a mechanism in which the current flow from the inductance is used to charge the capacitance of the lead, causing the voltage of the separating contact to increase to 300 volts. This is enough to ignite a glow in the gap. The transition from glow to arc takes place as soon as the current is strong enough for the maintenance of an arc. The duration of the arc depends on the discharge capacitance time. This process is repeated several times until the gap becomes too large for break-down and consequently the remaining capacitive and inductive energy is dissipated in damped low frequency oscillations around the circuit.

Transient discharge similar to Curtis has also been observed by Martin and Stauss⁽⁶¹⁾ and Mill⁽⁶²⁾.

Germer⁽⁶³⁾ has discussed fully the influence of the lead capacity on the transient arc and also recently Sawa et al⁽⁶⁴⁾ studied the effect of atmospheric pressure on this kind of discharge.

The discharge transient has also been called the Transient Showering Arc or just Showering Arc.

2.3 THEORIES OF CATHODE EMISSION

A solid metal consists of atoms. The atoms may be pictured as arranged in regular order in the crystalline structure forming the metal. There are 10^{23} atoms per cm^3 of a metal, each atom consisting of a nucleus surround by its system of electrons, inner and outer, which, with the nuclei, form the ions, that is an atom minus one of its electrons.

The outermost (valence) electrons which are placed in orbits remote from the nucleus are bound to the atoms loosely and can move about freely at random and at high speed. They frequently change places. The atoms are also in motion, but their movement is so slow that they are practically stationary compared with the free electrons. The free electrons move through the electric field of the ion-lattice, but on average the resultant force on an electron is zero as it moves within the body of the metal. So, to the outer world, the metal presents an appearance of electrical neutrality.

When a voltage is applied to the ends of the metal conductor, there is a migration of electrons towards the point of highest positive potential. This constitutes the electric current in the conductor. Now consider the conditions in the space between two metal conductors, namely the anode and the cathode.

Since the electrons are in random motion inside the metal conductor, when they reach the surface and get ready to take off into space they come across a problem in which those that fly out beyond the surface will be returning back, as the result of leaving the atom positively charged, which creates electrostatic forces. To escape

Non Thermionic	Thermionic
Generally operate at temperature less than 3000°K	Generally operate at temperature greater than 3500 °K
Relatively high current density in range of 10^{-6} to 10^{-7} A/cm ²	Relatively low current density in range of 10^{-3} to 10^{-4} A/cm ²
Pressure on cathode spot in excess of ambient, as evidence by depression of liquid metal	No evidence of excess pressure on cathode spot

Table (2.1) : Characteristics of non thermionic and thermionic arc cathode given by Guile (83)

from the metal (Fermi levels) an electron must, therefore, have a kinetic energy at least equal to the work which it must do against this retarding (inward) force. This work is known as the Work Function, and must come from the cathode, which is consequently cooled. The work function is characteristic of a given material, and is generally quoted in electron volts or volts.

The process whereby the electrons leave an electrode is called Electron Emission. There are a number of mechanisms which can produce electron emission from metallic surfaces and these are as follows:

- (i) Thermionic emission
- (ii) Field or cold emission
- (iii) Field-Assisted thermionic emission, known as Schottky or T-F emission
- (iv) Photo-electric emission
- (v) Emission by positive ion and excited atom impact

The emission of electrons as a result of positive ions or photons impinging on the cathode is unlikely to play a significant roll in arcs, because the yield of electrons per positive ion or photon is much too small. In an arc, more efficient methods of production are essential in order to achieve the necessary transfer of current. These efficient methods are Thermionic and Field emission which will be discussed in the following sections. Here a comparison characteristic of Thermionic and Non Thermionic arc cathode is shown in table (2.1).

2.3.1 THERMIONIC EMISSION

This emission occurs when a sufficiently hot cathode is at a temperature below the boiling point of the cathode material. This is possible when the cathode is a member of the refractory (high boiling-point) materials.

Under this condition the conduction electrons are in constant motion inside the

cathode metal and have individual speed and hence energies. Their speed is from the violent thermal lattice vibration in the solid. A proportion of the electrons with enough energy could overcome the natural potential barrier which is known as the work function and then boils off the surface material uniformly. If there is a suitable electric field in the space they are swept away, otherwise they return to the cathode and an equilibrium is set up between those emerging and those returning. At room temperature the numbers involved are small, but if they ionise the gas in their path this may lead to other processes to enhance the emission.

The metal temperatures required for thermionic emission may be in the range of 1500–2500^o K. The maximum current of electrons which could pass through a given surface at a given temperature is given by the Richardson-Dushman equation which is based upon consideration of the concentrations of electrons inside and outside the cathode surface.

$$\underline{J_e = AT^2 e^{-b/T}}$$

A = Constant, has a value of about 60 A cm⁻² K² for most materials

b = $\varphi_0 e/K$

φ_0 = Thermionic work function of the cathode surface

e = Electron charge

K = Boltzman's constant

T = Temperature of the electrode metal

The above relations show that the current density is a function of φ_0 and T. It increases with decreasing work function and increasing temperature.

The energy required to maintain the cathode surface at a sufficiently high temperature may be supplied by the impinging positive ions which have been accelerated in the cathode fall, or it could be supplied from an external source. However, these days, inspite knowing the work function and boiling temperature of

some materials, thermionic emission which should occur has not been observed⁽²⁾. Waymouth⁽⁶⁵⁾ in his paper has described methods of measuring thermionic emission.

2.3.2 FIELD EMISSION

When non-refractory materials (low boiling-points) are used as a cathode, thermionic emission will not occur, because their boiling points are below the temperature at which appreciable thermionic emission would be expected. These materials are called Cold-Cathode materials or Non-Thermionic. Electrons may be drawn out of the surface of such materials by very high electric field in a range of 10^6 – 10^8 volts/cm⁽²⁾.

Froom⁽⁶⁷⁻⁷¹⁾ has shown that the cathode current density on mercury, sodium copper and liquid sodium - potassium alloy are of the order of 10^6 A/cm².

Cobine et al⁽⁷²⁾ have found values of 10^5 – 10^6 A/cm² on various metallic cathodes. Secker and George⁽⁷³⁾ used ^{the} scanning electron microscope to estimate the sum area of emission site and hence the current density.

Itoyama⁽⁷⁴⁾, using high speed camera techniques, has concluded that the current density of the cathode spot varies inversely with time at the initial stage of arcing and also that electrons are only emitted from a few sites in the cathode spot, whereas the positive ions enter the cathode spot uniformly. This confirms the early investigation of Somerville⁽²⁾ on copper (2582 °C boiling) and mercury (375 °C) in which he suggests that the cathode behaviour of such arcs is characterised by an extremely high cathode current density 10^6 A/cm² and by irregular movement of the cathode termination over the cathode surface, which often occurs by the simultaneous or successive existence of several cathode spots which increase in number with the increase of the current. This may be due because electrons from the cathode electrode can only escape from side where work function is locally reduced as temperature increases.

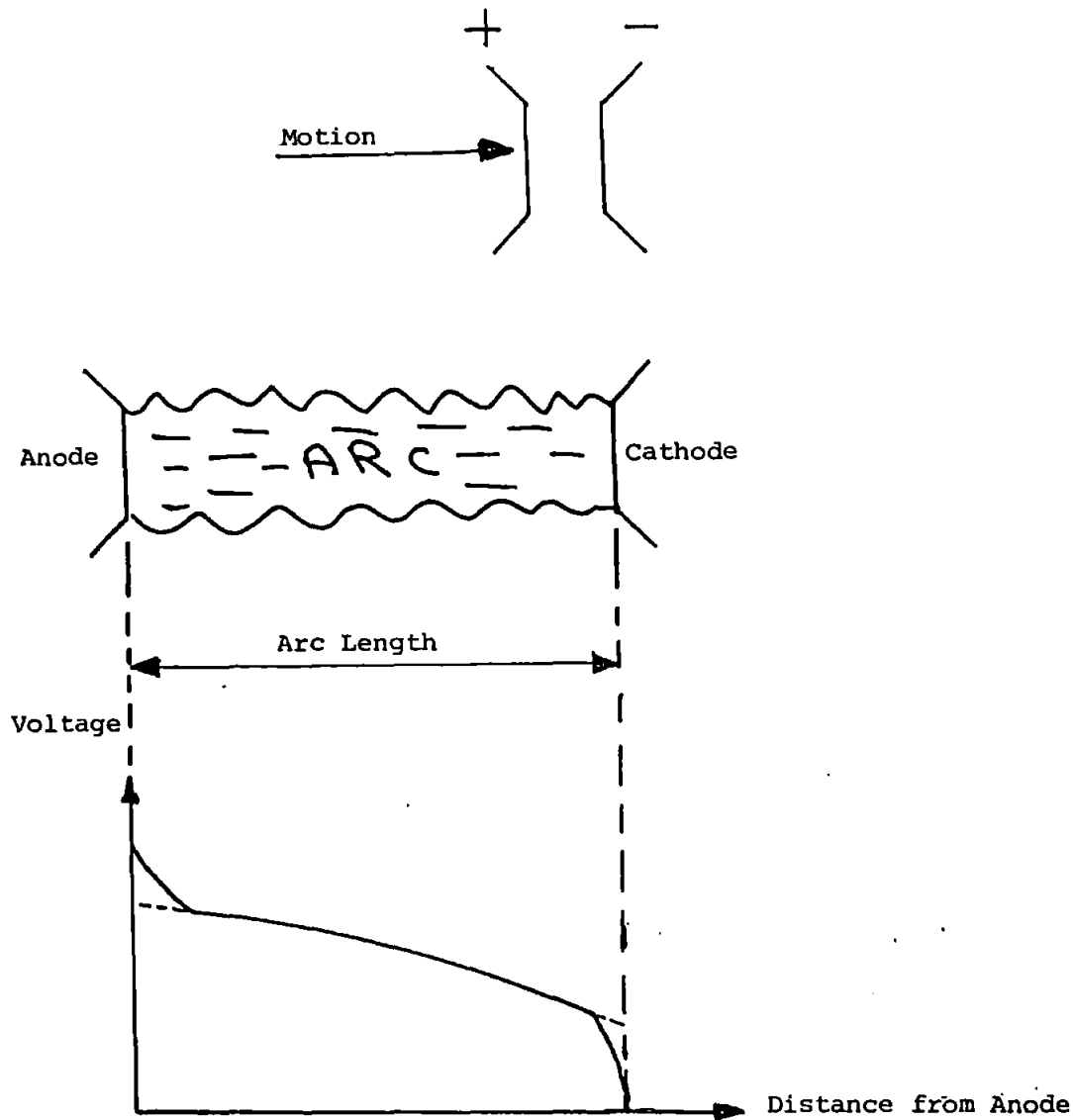


Figure 2.2: Non-Uniform Potential Distribution Along the Arc

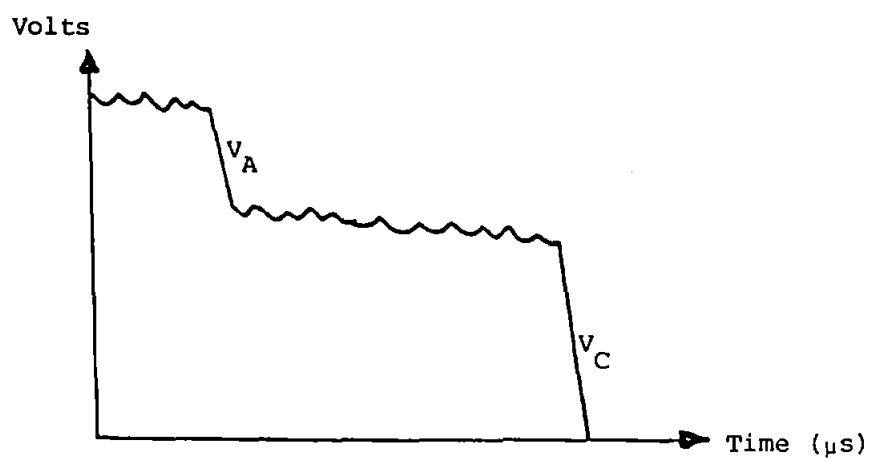


Figure 2.3: Component Parts of Voltage Drop Through the Arc

Djakov and Holmes⁽⁷⁵⁾ studied the cathode spot division in vacuum arcs with solid metal cathodes of Zinc, Copper, Aluminium, Lead and Bismuth for discharge current of 5-150 A. They concluded that above a certain current the number of spots increases linearly with current, except for Bismuth.

Various theories and explanations have been put forward for the mechanism of electron emission in cold cathode arcs as the result of strong field^(76,77).

Langmuir⁽⁷⁰⁾ has suggested that the strong field is produced by the space charge of the positive ions in the cathode fall space, and the major parts of cathode current are carried by electrons. Strong field may also occur when the metal is covered by a thin insulating layer (Oxide film) on which positive ions collected near or on the film^(79,80).

Meyer et al⁽⁸¹⁾ have shown that lack of Oxide and some destruction of the cathode surface leads to extinguishing of the arc.

Robson and Von Engel⁽⁸²⁾ suggest that electrons may be drawn out of the cathode of cold-cathode arc by the action of excited metal vapour atoms which diffuse back to the cathode in which their energy being used to extract electrons from the cathode surface. These electrons have sufficient energy to excite and ionise atoms and hence produce positive ions. The metal vapour atoms are produced by the impact of positive ions which gain sufficient energy in the cathode fall region.

2.4 THE ARC CHARACTERISTICS

If a current of more than a few micro-amperes flows through a self-sustained discharge, a nonuniform potential gradient between the electrodes will occur as is shown in figure (2.2).

This nonuniform characteristic is defined into three separate regions, namely electrodes fall (cathode, anode) and column. The former is the region of sharp-transition and discontinuity, electrically and thermally, between metallic and gaseous conductor. The condition in this region is less understood compared to the

arc column which is a region of gaseous conductor and is sandwiched between the electrodes region.

However, in the electrodes region, electrically a transition must take place in which the current is carried solely by electrons to a gaseous conductor where both electrons and ions are involved. Also there is a sharp drop in potential as shown in figure (2.3) and is known as the cathode and anode falls, where the former is larger than the latter, which may sometimes be absent altogether.

The characteristics of these drops are more dependent on the electrode materials and current than the ambient gas and the type of emission at the cathode. The actual drop is proportional to the arc length.

In the electrodes region, the anode presents less problems because electrons may enter the electrode freely from the gas, but in general ions do not enter the gas from the metal.

The other transition which must take place in the electrodes region is thermal transition, and it is gas pressure dependent. For example, at high gas pressure the transition is from relatively cool electrodes to a very hot plasma, and at lower gas pressure the situation is reversed.

The column (or as it is sometimes called, positive column of the arc) is the region of gaseous conduction and it is the most visible and longest part of the arc. Since the current flowing through it has to make the transition from gas to metal at both electrodes, such a channel must be electrically quasi-neutral, having approximately equal densities of positive and negative charge, where a net space charge is zero in a gas or $n_i = n_e = n$. Such a quasi-neutral is known as a Plasma. In such a Plasma the current density is of the order of $10-100 \text{ A/mm}^2$ and since it is composed of molecules, ions and electrons, in thermal equilibrium, it exhibits the Maxwellian energy distribution⁽⁶⁾. Since electrons have a faster rate of mobility than the ions, the current in the column is carried substantially by the electrons, the ions essentially serving to neutralise their space charge. However, if positive charge be absent in almost exactly equal density, a force of thousands of tons weight will be

acting on the electron in each cm^3 (2).

The arc column has also a potential gradient along its length which is a function of gas property in which the arc occurs, and its magnitude is typically 1-2 volts/mm in air and it is current dependent. The length and its cross section is arc dependent. For example, in the short arc where the electrodes are close together, the arc column is unable to develop to full cross-section and by reservation it can be said that short arc can exist without column.

The temperature of arc column can reach $5,000^\circ\text{K} - 50,000^\circ\text{K}$. It is dependent on gas pressure⁽⁸³⁾ and usually it has a certain minimum temperature to maintain, Saha's thermal ionisation, which is a consequence of the Maxwellian's distribution of energy.

The most characteristic feature of an arc is the low value of cathode fall, which generally lies between 8-20 volts, which is of the order of the excitation potential of the electrode vapour and in which the current flowing at atmosphere pressure is typically 30mA. At currents below this a glow discharge may occur with a voltage drop of about 300 volts. The glow and arc discharge are not completely separate phenomena as have been explained by^(84,85). Finally, there is a voltage drop at an arc anode which for metals generally lies between 1-12 volts, but it can be higher for some arcs with pure Carbon electrodes.

Since there are several discharges which are more or less alike, but lacking a common physical mechanism, it has been agreed that the arc be defined in terms of current and voltage drop only. The voltage drop of electrodes will be discussed in the next sections.

2.5 THE ELECTRODES FALL

After the discovery of the arc in 1803 by Petroff⁽⁸⁶⁾, attention was focussed on the nature of the charge carriers and on how the current passes from the anode through the intervening gas into the cathode. To explain this, in 1903 Mitkewicz⁽⁸⁷⁾ showed that the current is carried mainly by electrons moving towards the anode. This suggestion was confirmed a year later by Stark⁽⁸⁸⁾. They both suggested that these electrons originated from the hot spot on the cathode surface. The emission of electrons from the cathode has been described in section 2.3.

As previously discussed in section 2.4, there are in general three regions in the arc. However, research into the understanding of each region has led to the discovery of voltages drop within the electrode region ^(89,26). Since then there have been many attempts to measure the fall voltages. The principle methods used have been the Probe method and the Moving Electrodes Method.

The Probe method has been used in a few different ways. Some researchers have used the method to measure the potential difference between a wire probe and an electrode in order to determine the anode and cathode fall by linear extrapolation of the observed probe potential⁽⁹⁰⁻⁹⁴⁾, and others by measuring the potential difference which exists along the entire length of the arc and the potential being found by extrapolation⁽⁹⁵⁻⁹⁷⁾.

The above approach was tedious and discrepancies were observed among the results of different workers. These were largely due to the disturbance of the arc column by inserting a probe resulting in an increase of the arc voltage or due to cooling of the gas, and also to charge neutralisation at the probe surface and its holder. Other disturbances may be due to movement or melting of the probe. So, this method has, therefore, met with only limited success.

In the Moving Electrode Method, the magnitude of the last sudden voltage change which occurs when the electrodes are brought together, is measured. This idea was taken from observations by Gunthershulze⁽⁹⁸⁾ on a glow discharge in

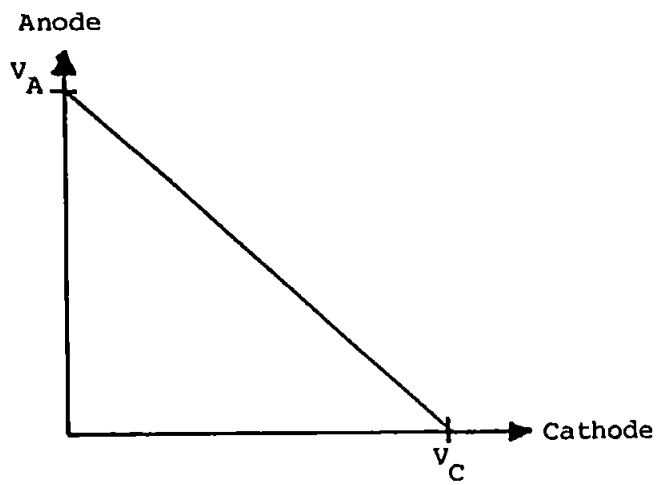
hydrogen at low pressure and currents of 1 mA in which the discharge voltage varies with lengths, and as the discharge length is reduced below a certain value the voltage (V) across the glow discharge drops suddenly by about 10–20 volts. Since this drop is small compared with cathode fall, which is in the order of 300 volts, this voltage is considered to be the anode fall, because its value is in the order of the ionisation potential in the glow discharge.

Since the arc discharge retains certain features of a glow discharge from which it can originate, Von Engel⁽⁹⁹⁾, by using Blondel–Buddel moving coil oscillograph (mirror–oscillograms), observed the existence of a minimum arc voltage as the length of the arc is reduced. The arc voltage decreases continuously by reaching a minimum value (V_m) just before the electrodes touch and the voltage becomes zero. V_m was taken to be equal to the sum of the anode and cathode falls. He suggested that it is possible to separate these falls in a single experiment by the use of two different electrode materials.

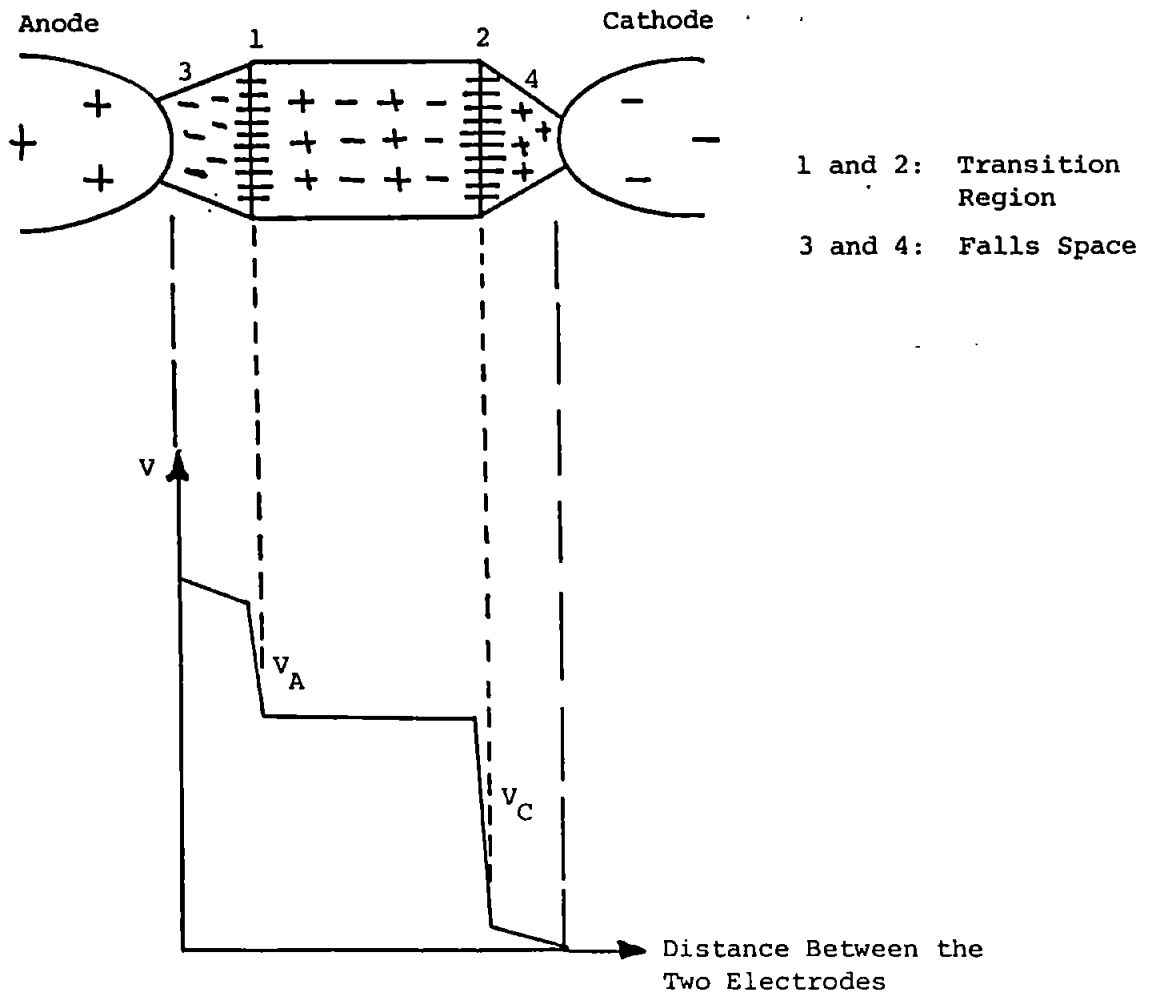
The value of V_m which is equal to the sum of anode and cathode fall in case of when electrodes are moved close together have been confirmed by Bauer et al⁽¹⁰⁰⁾. These authors also devised a method for the separation of V_a and V_c by observing the difference between the electrode temperatures for D.C. and A.C. arcs, the electrodes having a fixed polarity in the first case and acting alternatively as cathode and anode in the second. Their method was only applicable to enclosed arcs in various gases at variable pressures.

More attempts have been made to measure these fall voltage individually^(101,102), but the values obtained were low.

The early method of Von Engel using the mirror (Blondel) oscillograph may have been too slow to record the fall steps of short duration, but in 1967 Dickson and Von Engel⁽¹⁰³⁾ succeeded in a single experiment using a high speed cathode ray oscilloscope to separate the falls. The arc first being established, its anode is driven towards the stationary cathode. They suggested that the first discontinuity in arc voltage corresponds to the anode and the second as cathode fall where the arc length



a: Standard Field Theory (without arc)



b: Standard Field Theory (with arc)

Figure 2.4: Standard Field Theory Shows the Potential Gradient between Two Electrodes Without/With Arc.

is reduced to zero.

However, more recently Boddy and Utsumi⁽²⁴⁾ and Gray⁽¹⁰⁴⁾ have also found a similar discontinuity in the arc voltage when the closed electrodes are separated. They attributed this to a transition from the vapour arc to an arc with gaseous ions.

The theory of anode and cathode fall is discussed in the following section.

2.5.1 THEORY OF FALL VOLTAGES

If one considers the electrodes (anode and cathode) are separated by a distance d , then according to well known standard field theory, the potential gradient is as shown in figure (2.4a).

Since the arc introduces charges in between the electrodes, the redistribution of these charges along the arc length results in discontinuities in the potential as shown in figure (2.4b).

Many explanations have been put forward for these discontinuities (83,108-111), each of which deals with test conditions. Here these discontinuities are defined as follows:

The stream of electrons from the cathode are accelerated in the axial direction along the potential gradient. However, electron/atom collision reduce this axial velocity component and increase the transverse random component velocity distribution which results in accumulation of charges. The domination of positive ions⁽¹⁰⁹⁾ in the transition leads to a sharp drop in potential in cathode fall region. This is because the balance between positive ions and negative space charge requires copious emission of electrons from the cathode and also requires the width of this region to be equal to the column region and not small⁽²⁾.

In the plasma of the arc column, the electron and positive ion densities are equal, resulting in a uniform potential gradient. As the electrons leave the column end of the anode, they gain a randomised velocity component and electrons dominate over ions⁽¹⁰⁹⁾, though not as much as ions dominated in the first region. This

Cathode	Cathode Fall V_c (volts)	Method of Measurement	Author Reference
Hg	10	probe	95
Hg	9-11.3	probe	96
Hg	10	probe	97
Hg	8.1	Moving electrode	99
Cu	11.3	Moving electrode	99
Hg	7.8-8	Moving electrode	101
Cu	11-13	Probe	105
Cu	20.5	Probe	106
Cu	10.5-14.5	Probe	107
Mercury	7.5-8.5	Moving electrode	108
Mercury	8.6	Moving electrode	110

Table (2.2) : Catalogue of cathode fall voltage for various workers and various methods.

results in a smaller space charge field throughout the anode fall region.

It has been observed that the anode and cathode fall occur within a few microseconds of each other⁽¹⁰³⁾ and over a very short distance between the electrode surfaces, in which the electric field in these regions is extremely high⁽⁸³⁾. Somerville⁽²⁾ has suggested that the existence of electrode falls is due to space charge accumulation associated with the conditions required for the passage of a current across the junction between a metallic and a gaseous conduction, or it is a consequence of the passage of current across boundaries of conducting media.

A catalogue of measurements is shown in table (2.2).

2.5.1.1 THE CATHODE FALL

In general at the cathode of an arc there must exist a cathode fall of potential in order for the mechanisms responsible for regenerating the charged particles to be maintained, otherwise the discharge will extinguish.

The value of this fall which is thought to be of the order of the excitation potential of the electrode vapour (typically 8–20 volts) has been considered to be the most characteristic feature of the arc discharge. It is clear that the cathode has a more critical role in effecting the behaviour of the arc than the anode.

The nature of electron emission was found⁽⁸³⁾ to have a slight effect on the cathode fall values. For example, for thermionic mode V_c is higher than for the non thermionic mode. Also, there is always a high temperature gradient across the fall regions.

These days, due to the availability of fast storage oscilloscopes or similar equipment, most of the cathode fall measurements are based on the method of Von Engel and Dickson⁽¹⁰³⁾, 'The Moving Electrode Method'.

Dickson and Von Engel⁽¹⁰³⁾, using Tin cathode (flat shape, fixed) and Carbon anode (hemispherical shape, moveable), both of diameter 1 cm with the two electrodes 4 mm apart in Argon gas at 1 atm pressure and with the current range of 10–60 A, concluded that V_c is constant for currents up to about 30 A, but rising

Cathode	Anode	Gas	Pressure (mm Hg)	Current (A)	V _c (v)	V _a (v)
Sn	C	Ar	1-760	10-30	11	4
Sn	Sn	Ar	760	10	11	2
Sn	W	Ar	760	10	11	3
Sn	Cu	Ar	760	10	11	4
Cu	Cu	Ar	760	10	12	5
Cu	Cu	Ar	760	10	12	3
W	W	Air	760	10	15	3
C	C	Ar	760	10	*	*
C	C	Air	760	10	4	11
Sn	Cu	N ₂	769	10	11	3
Sn	Cu	N ₂	10-80	10	10	10
Cu	Cu	N ₂	60-150	10	16	10

* V_a+V_c = 22 volts

Table (2.3) : Measured values of cathode and anode fall voltages by Dickson and Von Engel⁽¹⁰³⁾ as function of Current, Gas, Pressure and Material.

Metal	Experimental values V_c (volts)	Theoretical values V_c (volts)
Cs	6.2	6.34
K	6.7-7.4	7.21
Sr	8.4-9.2	9.59
Bi	8.4-8.7	14.91
Cd	8.6-10.2	13.91
Na	8.7-9.0	8.65
Pd	8.8-10.2	13.27
In	9.5-11.9	12.02
Zn	9.8-11.1	14.67
Tl	10.5-11.5	11.64
Sn	10.6-13.0	14.42
Ca	10.8-11.4	10.30
Li	11.1-11.7	9.83
Te	11-12.4	15.31
Mg	11.6-13.0	12.48
Ag	12.1-13.6	14.44
Au	13.1-14.8	17.17
Cu	14.7-15.4	15.52
C	15.2-18.9	22.85
W	16.2-22.6	20.65
Al	17.2-18.6	13.05
Be	18.6-19.2	17.39
Nb	19.9-21.6	18.62

Table (2.4) : Vijh's⁽¹¹³⁾ experimental and theoretical fall
voltages values for various metals.

slowly as the current is increased. They also have carried out the fall measurements on various electrode materials with different currents, ranging from 10–30 A, with different gases at pressures between 10–750 mm Hg. The results shown in table (2.3) demonstrate that V_c is independent of the anode material.

Boylett and Maclean⁽¹⁰⁸⁾ on the oscillogram study with liquid Mercury cathode and Brass anode, at constant current of 10 A, observed a cathode fall of 7.5–8.5 volts, which is in good agreement with the Von Engel and Robson⁽¹¹⁰⁾ calculation of the cathode fall.

Capp⁽¹¹²⁾ in his work on the power balance in electrodes, on the basis of numerical work, has concluded that the cathode fall is constant as the gap-length is increased.

The cathode fall has also been calculated, based on electrochemical theory⁽¹¹³⁾ in which the comparison between experimental and theoretical values for various metals is shown in table (2.4).

More recently, Zhu and Von Engel⁽¹⁰⁹⁾ have confirmed the use of fast oscilloscope for separation of falls. They concluded that the cathode fall for Copper electrodes is the same in Argon as in Air. This suggests that Copper vapour is the dominant medium in the fall region.

The separation of falls using Graphite electrodes does occur when the cathode tip is uniformly covered with a thin layer of Copper powder. They also suggested that when a fast moving anode is mechanically reflected from the cathode, the arc which forms from a broken liquid bridge will generally exhibit two steps in the voltage trace. This is in agreement with the observation of Utsumi and Boddy⁽²⁴⁾. However, they ascribe these discontinuities to the absence of asperities in the arc.

2.5.1.2 THE ANODE FALL

In general, the existence of the anode fall is due to accumulation of negative space charge near the anode. Since the vital role of the anode is to preserve the current continuity by receiving an electron flow, it has less influence on the maintenance of the arc compared to the cathode.

The magnitude of anode fall depends on the number of positive ions present near the anode and, in fact, the actual value is determined by the energy requirement for their production. However, the energy required for the production of electrons and ions at the anode is much smaller at the anode than at the cathode.

The detailed theoretical investigation leading to the recognition that the function of the anode fall is the production of positive ions has been published in a series of papers⁽¹¹⁴⁻¹¹⁸⁾ by Bez and Hocker.

The measurement techniques of the anode fall are similar to the cathode, and the results vary widely from observer to observer, but mostly depend on arc parameter and conditions. The variation is as little as 1-2 volts at very high currents and up to 12 volts for low currents.

In the arc with pure Carbon anode at low current the fall of 35 volts occurring in two steps has been observed⁽²⁾, in which the larger value of 20 volts is very close to the anode, and 15 volts between this and column.

Finkelburg⁽¹¹⁹⁾, in a series of experiments, has concluded that if the anode is not pure Carbon, but has a core containing metallic Salts, the anode fall is much lower at low current, being of the order of 10-15 volts, and decreasing if the anode is made of Cadmium Oxide or Fluoride; the anode fall rises sharply with increasing current. But, when the anode is purely metallic, the anode fall is usually less than 12 volts at low current and may fall to only 1 or 2 volts at high currents.

The anode fall has also been estimated from subtracting the total arc voltage from the sum of the cathode fall and column voltage, using probes method, and has also been deduced from the power dissipated at the anode measured by water cooling. The values given are in the range of 5-10 volts ^(120,121).

Sugawara⁽¹²²⁾ determined the anode fall in Argon gas at atmospheric pressure by measuring the length of copper wire anode melted. The estimated value was 4.2 volts at 10 A arc. Dickson and Von Engel⁽¹⁰³⁾ observed that the anode fall has a constant value up to a current of 60 A, which is in good agreement with the Denney⁽¹²³⁾ suggestion that the anode fall voltage does not vary with the arc current up to a critical value. However, if the current is above this value, vaporisation may occur. This has been confirmed earlier by Cobine and Burger⁽¹²⁴⁾. They also suggested that any increase in the current tends to decrease the anode fall voltage.

Capp⁽¹¹²⁾ has numerically deduced the dependence of the anode fall with gap and hence arc voltage. He shows that the anode fall increases as the gap increases.

2.6 EROSION

Erosion due to the arc discharge occurs at break and make when the two charged electrodes are separated or brought together, in which case the arc energy is dissipated instantaneously in the form of heat on the contacts' surface. However, if the rate of generation of energy on the contact surface exceeds the rate of dissipation, then some energy will be used for evaporation of the contact material from the hot spot. The evaporated metal is displaced in the direction of the field.

In general, whichever way the contact material is liberated, the transfer of material from one contact to another is called erosion.

In D.C. operation the transfer material creates a pip on the anode and a crater on the cathode and it has been agreed that in general the transfer is from cathode to anode. But, in A.C. operation it is a function of polarity.

(Solid)					
Name	Thermal capacity J/Kg/k	Thermal conductivity W/m/K	Melting point °K	Boiling point °K	Density (ρ) Kg/m ³
Al	903	238	933	2720	2700
Bi	122	8.5	544	1810	9750
Cd	232	92	594	1037	8650
Fe	449	82	1808	3160	7870
Ag	236	418	1234	2466	10500
W	133	170	3653	5800	19300
Cu	385	400	1356	2855	8960
C	509	1.56	3820	5100	3000
Au	129	311	1336	3090	19320
(Fluid)					
Air	1010	0.026W/m	-	-	—
Ar	520	0.016	84	87.29	1.784
Hg	140	10.3	234.29	629.87	13540
N ₂	1040	0.027	63.30	77.36	1.250
O ₂	920	0.027	54.8	90.180	1.429

Table (2.5a) : Thermal properties of solid element and fluid

Element	Ionisation ev	Work ev
Aluminium (Al)	6.0	4.20
Argon (Ar)	15.8	-
Bismuth (Bi)	7.3	4.25
Cadmium (Cd)	9.0	4.11
Carbon (C)	11.3	-
Copper (Cu)	7.7	4.84
Gold (Au)	9.2	4.83
Iron (Fe)	7.9	4.63
Mercury (Hg)	10.4	4.53
Nitrogen (N ₂)	14.5	-
Oxygen (O ₂)	13.6	-
Silver (Ag)	7.6	4.54
Tin (Sn)	7.3	4.31
Tungsten (W)	8.0	4.57
Zinc (Zn)	9.4	4.34

Table (2.5b) Electrical properties of the elements.

Table (2.5) : Table of thermal and electrical properties of the elements extracted from physics handbook by C. Nordling and J. Osterman.

2.6.1 EROSION DUE TO BREAK ARC

The erosion which occurs when the contacts break is due to the following:

(i) Erosion due to molten metal bridge.

The bridge transfer usually takes place when current flow is about to be interrupted by separating two electrodes at the last point of contact, where the current density is extremely high. This results in local melting of the point at which the molten metal is formed, where some of the metal is displaced from its original position, and when the maximum temperature of the molten bridge reaches the boiling point of the metal then the bridge bursts.

Table (2.5) shows the melting and boiling temperature of various materials. The bridge transfer has also been named as the fine transfer (6) because the amount of material displaced per operation is small. This does not mean that their effect can be ignored in devices such as relay switches in which a large number of operations take place per day, and, in fact, this is thought to be one of many factors determining contact performance.

The direction of material transfer is debateable since the bridge bursting can occur near one of the contacts or at the centre of the bridge (1).

However, the significant effects of bridge transfer on low inductive circuit and current are studied by several workers^(19,21,25,57). The nature of the bridge formation and its transfer has been discussed by Lander (13).

(ii) Arc Transfer.

Arc transfer is the result of the bombardment of ions and electrons at the contact surface in which the unionised material is removed and lands on one of the electrodes in the direction of the field.

Turner et al⁽¹²⁵⁾ in the study of arc erosion have suggested that the main factors influencing arc erosion are current and arcing time. The contact erosion at

break occurs in succession from the bridge transfer to arc transfer. They also defined a region in their erosion plot as a discontinuous region in which for pure copper there is a sharp jump in erosion rate compared to more a gradual one of Ag-Cd O. They ascribed this to either melting of Silver in the surface resulting in a higher percentage of Oxide which retards further melting, or the movement of the arc around the Oxide spots restricting local heating but consuming Oxide. This suggestion has been modified later⁽¹²⁶⁾ by stating that the discontinuous erosion is as a result of transition from mainly evaporated loss to droplet loss. Their later suggestion comes from the concept which they introduced as Structural erosion. This was defined by a disintegration of the structure of the compound along weak boundaries, where particles of contact material detach themselves from the surface.

More recently, the same authors⁽¹²⁷⁾ have distinguished two types of material transfer in the study of high and low current erosion. They suggested that at low current pip and crater formation is the result of bridge transfer. Arc duration plays a less significant role in erosion, whereas at high current the bridge formation serves only to provide a means of arc initiation and the transfer is mainly arc transfer.

Kim and Peter⁽¹²⁸⁾ have studied the influence of Cd O on the rate of erosion from investigations into the microstructure of Ag-Cd O from a metallurgical point of view. They suggest that for a high energy arc, a high concentration of Cd O or a larger particle size is more favourable for low erosion. However, in the case of low energy application this suggestion is reversed.

El Koshairy et al⁽¹²⁹⁾, on the study of arc erosion by varying current and arc length, suggest that the rate of erosion is dependent on the contact gap. As they reduced the separation they observed reduction in losses particularly from the cathode. They related this to the fact that as the gap decreases, more metal vapour condenses back onto the contact surface.

Sato⁽³²⁾ has related the direction of material transfer in the A.C. condition to the peak current value. In the D.C. condition (40 volts, 1-50 A) he defined a transition region in current, in which the direction of material transfer is reversed.

His statement is derived from observation of Silver Cadmium Oxide contacts with an opening velocity of 63 mm/sec. The transition occurs at a current 6.5 A. For currents below this, material transfer was measured from cathode to anode, and for values above this anode to cathode. However, in the transition region no net directional transfer of metal occurred.

The transition region in arc transfer has also been observed by Slade and Holmes⁽¹³⁰⁾, but with different operating conditions and opening velocity (slow, 0.4mm/sec.). These workers state that for the current in the range of 5–12 A the transfer is mainly from cathode to anode, which results in formation of pip on the anode and crater on the cathode.

In the study of erosion in snap-action switches where the opening velocity is non-linear, White ⁽³³⁾ with operating conditions of 40 volts d.c., current range of 4,12 and 8 A, has shown that at 4 A net material transfer is from cathode to anode, at 12 A net material transfer is from anode to cathode, but at 8A he observed no movement of material transfer. This region is called the transition region which is in good agreement with Sato's⁽³²⁾ experiment. However, the opening velocity of Sato's experiment is 63 mm/sec., and gives an arc duration of 15 ms, which is seven times the arc duration in toggle switches. This suggests that more energy is dissipated in the arc in Sato's case.

White⁽³³⁾ also suggested that there is 40% reduction in energy dissipated in the arc when the contact gap is reduced from 2 mm to 0.2 mm. His test condition was 240 volts, 10 A peak, resistive load.

2.6.2 EROSION DUE TO MAKE ARC

The erosion at make can be categorised as follows:

- (i) Erosion due to bounce or 'bounce erosion'.

Bounce occurs when the kinetic energy of the moving contact is not

absorbed by the fixed contact as energy. In such a case the contact will go through the complete switching processes, but with different characteristics of break and make operation.

Since bounce involves drawing a molten metal bridge with consequent rupture and arcing, the contacts come to rest onto the molten material. However, if the rate of heat dissipation exceeds the rate of heat generation the contacts weld together. This is one of the main problems in telephone switching devices.

The number of bounces also depends on the strength of the weld after the first bounce. The weld strength has been the subject of studies by several workers^(131,132). These studies suggest that the weld is dependent on the contact material, arc voltage during bounce and size of contact.

In the study of contact material, the same authors (131, 132) found that Ag Cd O (85/12%) has the lowest energy dissipation, due to its low arc voltage during bounce – typically 10–12 volts.

Koepek and George⁽¹³³⁾ have observed that the Oxygen has a great influence on decreasing the weld strength on silver contact. They showed that when silver is in the molten state it absorbs Oxygen, which leads to the creation of an Oxide layer on the surface. This suggestion has been confirmed by Hewett⁽¹³⁴⁾.

(ii) Erosion due to breakdown voltage.

This is due to arc before the contact takes place. The arc is thought to be initiated by field emission of electrons from the cathode^(47,135).

Germer and Haworth⁽⁴⁹⁾ have related the arc erosion at make to inactive and active surfaces. They found that for inactive surface at 50 volts, an arc does not occur if the inductance is greater than 3 μ H. However, if the potential circuit is more than 50 volts, more than one arc discharge may take place. In general, transfer is to negative electrodes which is in good agreement with the suggestion made by Holm⁽⁶⁾. For an active surface in which foreign substances are present, the arc can occur in every closure, even when the inductance is very high.

They report that as the substance of the active surface may disappear due to arcing, this reduces the consistency of arcing during every closure after use. This leads to the suggestion that when there is no arc there is no erosion, but the energy of local capacity of the gap will be dissipated in the resistance of the circuit. The energy dissipated on the contacts surface is measured with the aid of a thermocouple⁽¹³⁶⁾, which is related to erosion.

In general, from the above literature review on erosion at break and make, one can conclude that the erosion is influenced by parameters such as circuit parameters (supply voltage, current, resistance and reactance), arc parameters (arc voltage, current, duration and length), and, finally, switch parameters (contact gap, velocity, shape, size and material).

Other parameters which are important are the thermal and electrical conductivities of the metal. Silver has a better thermal and electrical conductivity compared to Copper. Both have a low boiling point which means that evaporation can be excessive under arc.

It has been shown that Ag has less tendency to melt than copper but is also more expensive. Both metals may be combined by using a composite material with silver on a heavy Copper body as electrode. To assess the rate of erosion it is now customary to use the following techniques:

- (i) C.R.O. : V, I measurement.
- (ii) S.E.M. : surface examination.
- (iii) Weighing : material transfer evaluation.
- (iv) Talysurf : height and width of the pit and crater measurement.

The erosion of the contacts has also been studied from the analysis of the emission spectrum and measurement of arc duration⁽¹³⁷⁾.

Since the development of erosion is a result of arcing, numerous studies have been made to find a correlation between the arc energy and contact erosion⁽¹³⁸⁻¹⁴¹⁾.

Author Reference	Supplied Power	Used Power
6	$2V_c I + \Delta(VI - 2V_c I - V_a I)$	$\beta \varphi_c I + 4a_c \lambda (T - T_1) + I \omega r$
110	V_c	$\varphi_c + C + E + R + \epsilon$
	$(1-\eta)e^{**} V F + (1-f) I (V_c + V_l - \varphi_c)$	$I (C + E)$
112	$\rho (V_c + V_l) + C_p$	$I (\varphi_c + V_{ch})$
124	$J_p V_c$	$J_e \varphi_c + P_v$
146	$J_+ (V_l + V_c - \varphi_c)$	$P_v + P_c + P_r + P_e$

Table (2.6a) : Power balance equations at the cathode

Author Reference	Supplied power	Used power
6	$V_a I + (1-\Delta) (VI - 2V_c I - V_a I) + \varphi_a I$	$4a_a \lambda (T_a - T_1) + I \omega_a r$
112	$I (V_a + \varphi_a + V_e) + C_p$	$V_{ah} I$
124	$J_a (V_a + \varphi_a V_T) + P_n + P_r$	-

Table (2.6b) : Power balance equations at the anode

Table (2.6) : Power balance equations at the electrodes
given by various workers

A true correlation has not yet been revealed by workers. This may be due to the fact that some of the arc energy is used somewhere else within the arc region, especially in the column (which is the longest region of the arc) in the form of radiation and convection to the surrounding. This may suggest that only that part of arc energy generated very close to the electrodes can have profound influence on erosion, and it leads to the investigation of power balance at the electrodes to which the next section is devoted.

2.7 POWER BALANCE AT THE ELECTRODES

Disfigurement of an electrode's surface is a result of energy supplied close to its surface. This suggests that a balance must exist between supplied and used energies.

Since the duty of each electrode is different, their supplied and used energies are different. These will be discussed in the next sections.

The power balance at the electrodes also gives a picture of arc distribution within the gap, since some of this energy is used in elastic (thermal) and inelastic (exciting) collisions with the gas atoms in the gap. Some is used by thermal conduction through the metal, and, finally, some is used in evaporation of the metal from the surface.

Numerous studies have been made to correlate the energy supplied with that used, but it seems the results vary widely from worker to worker. A catalogue of these studies is tabulated and shown in table (2.6).

Experimentally, the amount of energy supplied to the electrodes is measured from surface temperature. For example, Somerville et al⁽¹⁴²⁾ and Blevin⁽¹⁴³⁾ have calculated the average surface temperature from the depth of melting into the electrodes, resulting from arcing of known duration. In their experiments the electrodes are made from metal foils with varying thickness.

Bolanowski⁽¹⁴⁴⁾ has studied the power given to the contact by arcing at break

from the contact surface temperature measurement. He derived an empirical relation between power received by the contact and arc power in terms of arc duration and arc current. This is shown in the following

$$P_K \approx P_{arc} \left[K - \frac{1}{1.5 t_{arc}^{(1.5)}} + 0.6 \frac{I_{arc}}{10^{-3}} \right]$$

$$K = 1 - 0.38 t_{arc} \dots\dots\dots \text{for } t_{arc} < 1\text{ms}$$

$$K = 6 \pm 0.62 t_{arc} \dots\dots\dots \text{for } t_{arc} > 1\text{ms}$$

- t_{arc} = arc time in ms
- I_{arc} = arc current in Amperes
- P_{arc} = arc Power
- P_K = Power absorbed by contact

The power of the arc was measured from oscilloscope readings. The empirical formula allows the calculation of the input power to the contact with accuracy of $\pm 20\%$. He also showed that the arc power is inversely proportional to the breaking speed. The speed of opening was in the range 250–700 mm/sec and arc current in the range 20–300 A.

Capp⁽¹¹²⁾ has also calculated the power absorbed by the electrodes due to arcing at break from contact surface temperature measurement. The electrodes were 8 mm in diameter and made of Cadmium or Zinc for cathode, and Tungsten for anode. They were mounted in a chamber containing Nitrogen at atmospheric pressure.

The ^{D.C} operating conditons were (0–80 volts, 0–5 A) and the arc was drawn up to a length of 2 mm, for a duration of 20 seconds. He found that as the gap increases, the power conducted into the anode increases at a greater rate than the corresponding rate into the cathode. He ascribed this to the fact that the anode fall voltage increases with gap and with arc voltage, as the cathode fall remains constant. He related the slow rate of increase in cathode power to an increase in

the thermal heat conducted to the cathode from the column.

He also suggested that the levelling off of this increase at the larger separation (about 8 mm) is the result of heat loss from the plasma column not going to the electrode and, instead, being lost to the surroundings. His arc model is used to explain the influence of energy transfer in flammable atmosphere such as underground mines.

More recently, the relation between contact surface temperature and power dissipated on the contact has been studied by Kubono⁽¹⁴⁵⁾. He showed that the cathode spot temperature and radius are dependent on cathode fall voltage and arc current. He also calculated the cathode loss from a relation between contact surface temperature and evaporation rate.

Since arc durations in snap-action switches are typically in the region of 2-3 ms and within this period the bulk of the cathode or anode materials do not reach steady state temperature, this implies that the transient condition exists for power balance investigations.

2.7.1 POWER BALANCE AT THE CATHODE

2.7.1.1 SUPPLIED POWER

- (i) Thermal energy (P.E.) of positive ions
- (ii) Kinetic energy of ions which they gain in
passing the electric field of the cathode fall
region ($I_p V_c$)
- (iii) Part of total neutralisation energy of ions
 $[e(V_p \phi)]$
- (iv) Heat conduction and radiation from the column
- (v) Joule heating of the cathode material

2.7.1.2 USED POWER

- (i) Energy for electron emission $e\phi$ /electron
- (ii) Energy for vaporisation of cathode material
- (iii) Radiation from hot spot on the cathode
- (iv) Heat conduction to the cathode

2.7.2 POWER BALANCE AT THE ANODE

2.7.2.1 POWER SUPPLIED

- (i) Potential energy of electron in which each electron is giving to the anode ($e\phi$)
- (ii) Kinetic energy of electron in the anode fall region ($I V_a$)
- (iii) Heat conduction and radiation from the column
- (iv) Joule heating of anode material

2.7.2.2 USED POWER

- (i) Energy lost by the vaporisation of metal atoms
- (ii) Radiation from hot spot
- (iii) Heat conducted away through the anode structure
- (iv) Energy lost due to ion emission, if any

1. Llewellyn Jones, F.
"Fundamental processes of electrical contact phenomena",
Her Majesty's Stationery Office, London, 1953.
2. Somerville, J.M.
"The electric arc",
Butler and Tanner Ltd., London, 1959.
3. Swinehart, M.R.
"Introduction to the theory of the arc",
Proceedings of the Engineering Seminar on Electrical Contacts,
1960, pp 107-115.
4. Farrell, G.A.
"Arcing phenomena at electrical contacts",
Proceedings of the Holm Seminar on Electrical Contacts, 1969,
pp 119-145.
5. Windred, G,
"Electrical contacts",
Macmillan and Co. Ltd., London, 1940.
6. Holm, R,
"Electric Contacts",
Fourth Edition, Springer Verlag, Berlin, 1967.

7. Llewellyn Jones, F.
"The Physics of Electrical Contacts",
Clarendon, London, 1957.
8. Greenwood, J.A.,
Brit. J. Appl. Phys., Vol. 17, 1966, p 1621.
9. Thomas T.M.,
PhD Thesis, 1970, University of Wales.
10. Hopkins, M.R. and Jenkins, A.V.
5th International Conference on Electrical Contact Phenomena,
Munich, 1970.
11. Slade P.G.
5th International Conference on Electrical Contact Phenomena,
Munich, 1970.
12. Llewellyn Jones, F. and Cowburn, M.C.
5th International Conference on Electrical Contact Phenomena,
Munich, 1970.
13. Llander J.J. and Bermer, L.H.
J. Appl. Phys., Vol. 19, 1948, p 910.
14. Utsumi, T.
IEEE Trans. Parts. Mater. Packaging, Vol. 5, 1969.
15. Nahemow, M.D. and Slade, P.G.

In Proceedings of the 4th International Research Symposium on
Electrical Contact Phenomena, 1968, p 102.

16. Koren, P.P., Nahemow, M.D. and Slade, P.G.
"The molten metal bridge stage of opening electric contacts",
Holm Conference on Electric Contacts, 1974, pp 81-88.
17. Jones, R.H.
PhD Thesis, 1953, University of Wales.
18. Slade, P.G.
PhD Thesis, 1966, University of Wales.
19. Thomas, B.R.
PhD Thesis, 1967, University of Wales.
20. Jenkins, A.V.,
PhD Thesis, 1970, University of Wales.
21. Cowburn, M.C.
PhD Thesis, 1969, University of Wales.
22. Thomas, B.R.
4th International Research Symposium on Electrical Contact
Phenomena, Swansea, 1968.
23. Price, M.J. and Llewellyn Jones, F.
Brit. J. Appl. Phys. Vol. 2, 1969, p 589.

24. Boddy, P.J. and Utsumi, T.
"Fluctuation of arc potential caused by metal vapour diffusion
in arcs in air",
J. Appl. Phys. Vol. 42, No. 9, Aug. 1971, pp 3369-3373.
25. Llewellyn Jones, F.
"Matter transfer in contacts and the microscopic molten metal
bridge",
Proc. of the Relay Conference, Section Three, 1964, pp 1-12.
26. Ayrton, H.
"The Electric Arc",
The Electrician, London, 1902.
27. Ives, H.E.
"Minimal length arc characteristics",
Journal of the Franklin Institute, Vol. 198, No. 4, 1924.
28. Nottingham, W.B.
"Normal arc characteristic curves",
Physical Review, Vol. 28, 1926, p 764.
29. Fink, H.P.
"Understanding the operation of moving contacts",
Wiss. Veroff. Siemens-Werk 17, 1938.
30. Aida, T.
"General formulas for arc duration in air",
Elec. Eng. Vol. 90, Japan, 1970, pp1-13

31. Sato, M., Hijikata, M. and Morimoto, I.
"Characteristics of the arc breaking a non-inductive circuit
in air",
Trans. Japan Inst. Metals, No. 2, 1974.
32. Sato, M.
"Studies on the silver base electrical contact materials",
Trans. Nat. Res. Inst. for Metals, Vol. 18, No. 2, 1976.
33. White, P.J.
PhD Thesis, 1979, Plymouth Polytechnic.
34. Gray, E.W., Uhrig, T.A. and Hohnstreiter, G.F.
"Arc durations as a function of contact metal and exposure
to organic contaminants",
Proceedings of the Holm Seminar on Electrical Contacts,
1976, pp 15-27.
35. Takagi, T. and Inoue, H.
"Distribution of arc duration and metal wear due to arc for
silver, copper and palladium contacts",
Proceedings of the Holm Conference on Electrical Contacts,
meeting jointly with the 9th International Research Conference
on Electric Contact Phenomena, Tokyo, Japan, 1978, pp 69-75.
36. Uhrig, T.A. and Gray, E.W.
"Effect of operating rate on the arc duration of activated
telephone relay contacts",
Proceedings of the 8th International Research Symposium on

Electric Contact Phenomena, Tokyo, Japan, 1976, pp 113-119.

37. Uhrig, T.A.

"Arc duration and erosion of protected palladium and palladium-silver contacts in telephone offices",
Proceedings of the 10th International Research Symposium on Electric Contact Phenomena, Budapest, Hungary, 1980, pp 1029-1039.

38. Germer, L.H. and Haworth, F.E.

"A low voltage discharge between very close electrodes",
Phys. Rev. Vol. 73, 1948, p 1121.

39. Haworth, F.E.

"Breakdown fields of activated electrical contacts",
J. Appl. Phys. Vol. 28, 1957, p 381.

40. Llewellyn Jones, F.

"Arcing phenomena at electrical contacts as used in communication engineering",
Proc. Inst. Electr. Engineers, Vol. 96, 1949, p 305.

41. Kisliuk, P.

"Electron emission at high fields due to positive ions",
J. Appl. Phys. Vol. 30, 1959, p 51.

42. Lawson, G.R.

"Generation of fast growing whiskers in the neighborhood of arcing metallic contacts"

Proc. of the 1st International Research Symposium on electric contact phenomena, Orono, University of Maine, U.S.A., 1961, pp 285-299.

43. Muniesa, J.

"Whiskers growth of silver surfaces",

Proceedings of the 11th International Research Symposium on Electric Contact Phenomena, West Berlin, Germany, 1982, pp 56-60.

44. Hueber, Bernard F.

"An oscilloscope study of the beginning of a floating arc",

Proceedings of the Engineering Seminar on Electrical Contacts, 1967, pp 141-153.

45. Hueber, B.F.

"Floating arcs in various atmospheres",

Proceedings of the 4th International Research Symposium on Electrical Contact Phenomena, Swansea, Wales, 1968, pp 107-112.

46. Pharney, J.R.

"Clarifications of arc initiation phenomena for closing contacts",

Holm Seminar on Electric Contact Phenomena, Chicago, 1969,

47. Germer, L.H.

"Physical processes in contact erosion",

Journal of Appl. Phys. Vol. 29, No. 7, 1958.

48. Kisliuk, P.
"Arcing of electrical contacts on closure; Part V, The cathode mechanisms of extremely short arcs",
Journal of Applied Physics, Vol. 25, No. 7, July 1954,
pp 897-900.
49. Germer, L.H., and Haworth, F.E.
"Erosion of electrical contacts on make",
Journal of Applied Physics, Vol. 20. Nov. 1949, pp 1085-1109.
50. Prutton, M.
"Surface Physics",
Second edition, Clarendon Press, Oxford, 1983.
51. Atalla, M.M.
"Arcing of electrical contacts in telephone switching circuits;
Part two, Characteristics of the short arc",
Bell System. Tech. J. Vol. 32, 1953, p 1493.
52. Newton, R.R.
Physics Review, Vol. 73, 1948, p 1122.
53. Boyle, W.S. and Germer, L.H.
J. Appl. Phys. Vol. 26, 1955, p 571.
54. Germer, L.H. and Boyle, W.S.
"Two distinct types of short arc",
Journal of Appl. Phys. Vol. 27, No. 1, 1956.

55. Smith, J.L. and Boyle, W.S.
"Fundamental Processes of the Short Arc",
Bell System Technical Journal, Vol. 38, Nos. 1-3, 1959,
pp 537-552.
56. Fujiwara, K. and Yamaguchi, Y.
"Adhesion characteristics of Ag-60 Pd alloy under extremely
short arc on closure",
Transaction on Components, Hybrids and Manufacturing
Technology, Vol. CMHT2, No. 3, Sept. 1979, pp 337-342.
57. Hopkins, M.R. and Jones, R.H.
"Transients, bridges, micro-arcs and metal transfer",
Holm Seminar on Electric Contact Phenomena, Chicago, Illinois,
1972, pp 399-407.
58. Slade, P.G.
"Current interruption in low voltage circuits",
Holm Seminar on Electric Contact Phenomena, Chicago, 1968,
59. Allen, A.L.
Proc. IEE, Vol. 100, 1953, p 158.
60. Curtis, A.M.
"Contact phenomena in telephone switching circuits",
Bell System Tech. J. Vol. 19, 1940, p 40.
61. Martin F.E. and Stauss, H.E.

"Contact transients in simple electrical circuits",
Trans. A. IEE, Vol. 70, 1951, p 304.

62. Mills, G.W.

"The mechanisms of the showering arc",
Proceedings of the Holm Seminar on Electrical Contacts,
1968, pp 107-121.

63. Germer, L.H.

"Erosion of separating electrical contacts",
Proc. Inter. Symposium on Electric Contact Phenomena,
University of Maine, 1961, p 239.

64. Sawa, K., Suhara, K., Ueki, T. and Miyachi, K.

"Influence of the atmospheric pressure on showing arc",
Proceedings of the 8th Inter. Research Symposium on Electric
Contact, Japan, 1976, pp 13-19.

65. Waymouth, J.F.

"Measurement of thermionic emission in arcs",
Proceedings of the Engineering Seminar on Electrical Contacts,
1960, p 115.

66. Fowler, R.H. and Nordheim, L.W.

Proc. Roy. Soc. London, N.119, 1928, p 173 and No. A124,
1929, p 699.

67. Froom, K.D.

Nature, No. 157, 1946, p 446.

68. Froom, K.D.
Nature, No. 159, 1947, p 129.
69. Froom, K.D.
Proc. Phys. Soc., No. 60, 1948, p 424.
70. Froom, K.D.
Proc. Phys. Soc., No. B62, 1949, p 805.
71. Froom, K.D.
Proc. Phys., Soc., No. B63, 1950, p 377
72. Cobine, J.D. and Gallagher, C.J.
Phys. Rev. Vol. 74, 1948, p 1524.
73. Secker, P.E. and George, I.A.
"Preliminary measurements of arc cathode current density",
Brit. J. Appl. Phys., (J. Phys. D), Ser. 2, Vol. 2, 1969,
pp 918-920.
74. Itoyama, K.
"The current density change of anode spot at breaking arc",
Inter. Conf. on Electric Contact Phenomena, Paris, 1974.
75. Djakov, B.E. and Holmes, R.
"Cathode spot division in vacuum arc with solid metal
cathodes",
J. Phys. D:Appl. Phys., Vol. 4, 1971, pp 504-509.

76. Lee, T.H.
"Theory of cathode spot mechanism",
Proceedings of the Engineering Seminar on Electric Contact,
1961, pp 114-128.
77. Djakov, B.E.
"Electron emission and energy balance in cold cathode arcs",
Proc. of the 8th Inter. Res. Symp. on Electric Contact
Phenomena, Tokyo, Japan, 1976, pp 1-6.
78. Langmuir, I.
"Positive ion currents in positive columns of a mercury arc",
General Elec. Rev. Vol. 26, 1923, pp 731-735.
79. Llewellyn Jones, F. and De La Perelle, E.T.
"Field emission of electrons in discharges",
Proc. of the Royal Society, Vol. A216, 1933, p 267.
80. Kisliuk, P.
"Electron emission at high fields due to positive ions",
Journal of Appl. Phys., Vol. 30, No. 1, 1959, pp 51-55.
81. Meyer, J.L. and Doan, G.E.
"Arc discharge not obtained in pure Argon gas",
Physics Review, Vol. 40, 1932, pp 36-39.
82. Robson, A.E. and Von Engel, A.
Nature, Vol. 175, 1955, p 646.

83. Cuile, A.E.
"Arc electrode phenomena",
Proc. IEE Reviews, Vol. 118, No. 9R, Sept. 1971.
84. Gambling, W.A. and Edels, H.
"Formation of the high pressure arc column in hydrogen",
Nature, Vol. 177, 1956, pp 1090-1091.
85. Gambling, W.A. and Edels, H.
"The properties of high pressure steady state discharges in
hydrogen",
Brit. J. Appl. Phys. Vol. 7, 1956, pp 376-379.
86. Petroff, W.
Rep. Acad. Chirurg. Med. Petersburg, 1803.
87. Mitkewicz, W.
Z. Russ. Phys. Ges., Vol. 35, 1903, p 507.
88. Stark, J.
Phys. Z., Vol. 5, 1904, p 750.
89. Davy, H.
Elements of Chemical Philosophy, Vol. 1, 1812, p 152.
90. Hagenbach, A.
Handbuch Der Physik, Vol. 14, Berlin Springer, 1927, p 324.
91. Seeliger, R.

- 92. Nottingham, W.B.
J. Franklin Inst., Vol. 207, 1929, p 299.

- 93. Mason, R.C.
Phys. Rev., Vol. 51, 1937, p 28.

- 94. Finkelburg, W. and Segal, S.M.
Phys. Rev., Vol. 80, 1950, p 258.

- 95. Lamer, E.S. and Compton, K.T.
Phys. Rev., Vol. 37, 1931, p 1069.

- 96. Kommnick, J. and Lubcke, E.
Phys. Z, Vol. 33, 1932, p 216.

- 97. Killian, T.J.
Phys. Rev., Vol. 35, 1930, p 1238.

- 98. Guntherschulze, A.
Z. Phys. Vol. 61, 1930, p 581.

- 99. Von Engel, A.
Wiss. Veroff, Siemens, Vol. 14, 1935, p 38.

- 100. Bauer, A. and Schulz, P.
Z. Phys., Vol. 139, 1954, p 197.

101. Froome, K.D.
Nature, Vol. 179, 1957, p 267.
102. Froome, K.D.
Nature, Vol. 184, 1959, p 808.
103. Dickson, D.J. and Von Engel, A.
"Resolving the electrode fall spaces of electric arcs",
Proc. Royal Soc. A, Vol. 300, 1967, pp 316-325.
104. Gray, E.W.
IEEE Trans. Plasma Sci., PS-1, 1973, p 30.
105. Bramhill, F.H.
Phil. Mag., Vol. 13, 1932, p 682.
106. Myer, J.L.
Z. Phys. Vol. 87, 1933, p 1.
107. Betz, P.L. and Karrer, S.
Phys. Rev. Vol. 49, 1936, p 860.
108. Boylett, F.D.A. and Maclean, I.G.
"Cathode fall in potential and space in mercury arcs",
J. Phys. D: Appl. Phys., Vol. 4, 1971, pp 677-679.
109. Zhu, S.L. and Von Engel, A.
"Fall regions and electrode effects in atmospheric arcs of
vanishing length",

J. Phys. D: Appl. Phys., Vol. 14, 1981, pp 2225-2235.

110. Von Engel, A. and Robson, A.E.
"The excitation theory of arcs with evaporating cathodes",
Proc. R. Soc. A, Vol. 243, 1957, pp 217-236.
111. Von Engel, A.
Ionised Gases, 2nd edn., Oxford University Press, Chapter 9,
1965.
112. Capp, B.
"The power balance in electrode dominated arcs with a tungsten
anode and a cadmium or zinc cathode in nitrogen",
J. Phys. D: Appl. Phys. Vol. 5, 1972, pp 2170-2178.
113. Vigh Ashok, K.
"The improved electrochemical theory for the quantitative
estimation of the magnitudes of cathode fall voltages in pure
metal arcs",
Journal de Chimie Physique, Vol. 73, No. 5, 1976, pp 566-568.
114. Bez, W. and Hocker, K.H.
Z.F. Naturforsch, Vol. 99, 1954, p 72.
115. Bez, W. and Hocker, K.H.
Z.F. Naturforsch, Vol. 10a, 1955, p 706.
116. Bez, W. and Hocker, K.H.
Z.F. Naturforsch, Vol. 10a, 1955, p 714.

117. Bez, W. and Hocker, K.H.
Z.F. Naturforsch, Vol. 11a, 1956, p 118.
118. Bez, W. and Hocker, K.H.
Z.F. Naturforsch, Vol. 11a, 1956, p 192.
119. Finkelburg, W.
Z. Phys., Vol. 116, 1940, p 214.
120. Busz Peuckert, G. and Finkelburg, W.
Z. Phys., Vol. 140, 1955, pp 540-546.
121. Busz Peuckert, G. and Finkelburg, W.
Z. Phys., Vol. 144, 1956, pp 244-251.
122. Sugawara, M.
"Anode melting caused by a d.c. arc discharge and its application to the determination of the anode fall",
Brit. J. Appl. Phys., Vol. 18, 1967, pp 1777-1781.
123. Dennerly, F.
"Les developements actuels de la physique des arc",
Soudages Tech. Connexes, Vol. 7/8, 1965, pp 269-287.
124. Cobine, J.D. and Burger, E.E.
J. Appl. Phys. Vol. 26, 1955, p 895.
125. Turner, C. and Turner, H.W.
"The erosion of heavy current contacts and material transfer

produced by arcing",

Proceedings of the 4th International Research Symposium on
Electric Contact Phenomena, Swansea, Wales, 1968, pp 196-199.

126. Turner, H.W. and Turner, C.
"Contact erosion and its implications",
Proceedings of the 1978 Holm Conference on Electrical
Contacts, Chicago, USA, pp 1-8.
127. Turner, H.W. and Turner, C.
"Material transfer between heavy current contact",
Proc. 10th Int. Research Symposium on Electric Contact
Phenomena, Budapest, Hungary, 1980, pp 61-70.
128. Kim, H.J. and Peters, T.
"A metallurgical model of arc erosion in Ag-Cd O contacts",
Proceedings of the 1978 Holm Conference on Electrical
Contacts, Chicago, USA, pp 89-97.
129. El Koshairy, M.A.B., Khalife, M. and Aboul Makarem, F.
"Erosion of contacts by arcing",
Proc. IEE, Feb. 1961.
130. Slade, P.G. and Holmes, F.A.
"Erosion characteristics of silver contacts",
IEEE Trans. Parts, Hybrids and Packaging, Vol. PHP13, No. 1,
March 1977.

131. Shaw, N.C.
"Investigations of contact bounce and contact welding",
Symposium on Electric Contact Phenomena, Graz, Austria, 1964.
132. Turner, C. and Turner, H.W.
"Minimum size of silver based contacts prone to dynamic welding",
Inter. Conf. on Electric Contact Phenomena, Paris, 1974.
133. Koepke, B.G. and George, R.I.
"Welding of medium energy electric contacts",
Holm Seminar on Electric Contact Phenomena, Chicago, Illinois, 1972.
134. Hewett, B.L.,
"Erosion of silver-palladium alloys in different gases",
Research Report of University of London, 1974.
135. Germer, L.H.
J. Appl. Phys. Vol. 22, 1952, p 1133.
136. Germer, L.H.
"Heat dissipation at the electrodes of a short electric arc",
The Bell System Technical Journal, Oct. 1951, pp 933-944.
137. Treguier, J.P., Ben Jemaa, N., Collobert, D., Prigent, H. and
Quéffelec, J.L.
"Electric and spectroscopic characterisation of arcing in
electrical contacts: study of erosion",

Holm Conf. 1976, p 179.

138. Eskin, S.G.
"Arc energy in a.c. switching",
General Electrics Review, Vol. 42, No. 2, 1939, p 81.
139. Tibolla, J.F.
"Average arc energy for random opening a.c. electrical
contacts",
MSc Thesis, University of Pennsylvania, May 1970.
140. Lesinski, S. and Glaba, M.
"Electric arc energy measuring device",
Inter. Conf. on Electric Contact Phenomena, Japan, 1976.
141. Lee, T.H.
"Energy distribution and cooling effect of electrons
emitted from an arc cathode",
J. Appl. Phys., Vol. 31, No. 5, 1960, p 924.
142. Somerville, J.M., Blevin, W.R. and Fletcher, N.H.
Proc. Phys. Soc., Vol. B65, 1952, p 963.
143. Blevin, W.R.
Aust. J. Sci. Vol. 6, 1953, p 203.
144. Bolanowski, B.
"Energy transfer between arc and electrodes in contactor",
5th Inter. Conf. on Electric Contact Phenomena, 1970,

pp 115-118.

145. Kubono, T.

"Theory of cathode erosion in the arc discharge",

8th Inter. Conf. on Electric Contact Phenomena, Japan, 1976.

146. Lee, T.H. and Greenwood, A.

"Theory for the cathode mechanism in metal vapour arcs",

Journal of Applied Physics, Vol. 32, No. 5, May 1961,

pp 916-923.

CHAPTER THREE THE DESIGN AND CONSTRUCTION OF EXPERIMENTAL APPARATUS

3.1 INTRODUCTION

This chapter comprises six interconnected sections, each concerned with a particular phase of the research. They are organised as follows:

- (i) The equipment
- (ii) Design of test rig
- (iii) Design of constant current source in conjunction with
timers
- (iv) Techniques of thermocouple probe construction
- (v) Thermocouple probe calibration system
- (vi) Computer control work station

Most emphasis is made on the tools which are directly relevant to the series of experiments that form the core of this investigation.

3.2 THE EQUIPMENT

The equipment which has been used for determining the speed of break and make operation of the test rig (Hyspeed camera), measurement of contact surface roughness due to the arc (Talysurf) and analysis of surface (scanning electron microscope) for study of contact erosion are similar to those used by White (1). The purpose of this section is not to describe this standard equipment.

However, these days, due to development of high technology, the burden of developing the hyspeed camera film can be replaced by more modern systems such as Kodak 1000⁽²⁾ which can capture 6000 pictures per second, the information being stored on a video tape which can be analysed more easily. Similarly, for

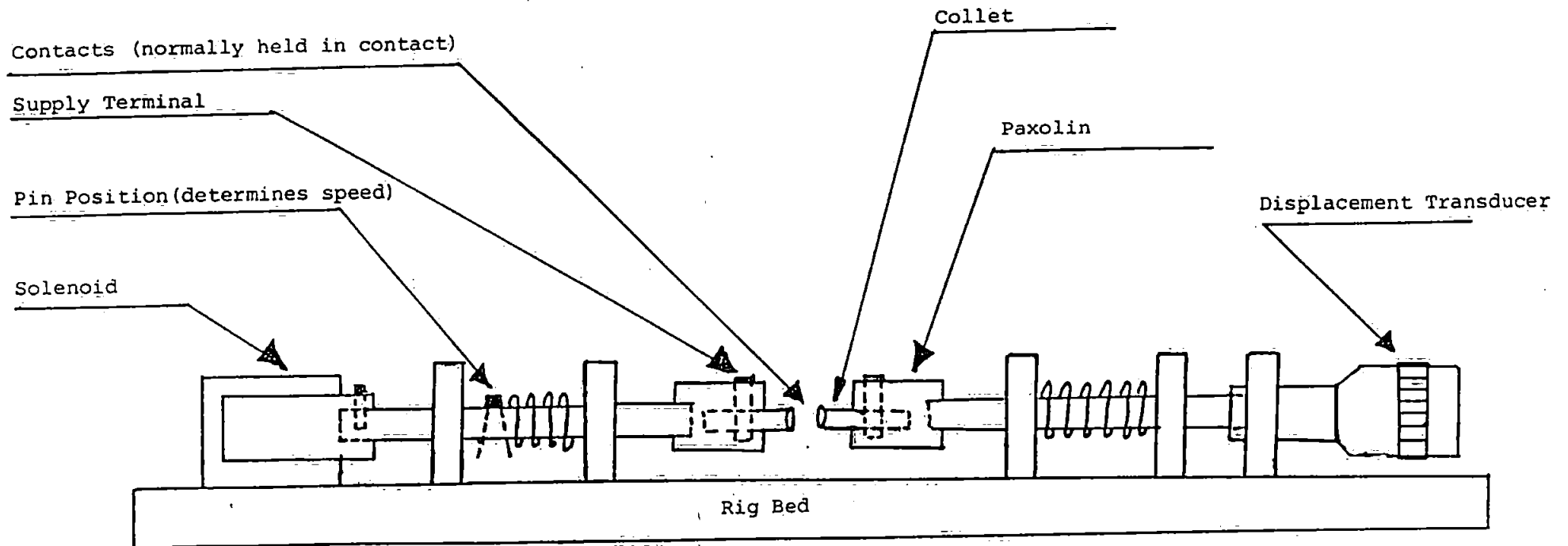


Figure 3.1: Schematic Diagram of the Test Rig

determining roughness and surface profile of small dimensions such as used in contacts in this research, which requires precision accuracy and low force diamond stylus, it can be replaced by SF220 computerised surface profiling⁽³⁾ in which the results are stored on the disc and displayed on VDU. Both of the above reduce the operating time and the potential damage to the sample respectively.

3.3 DESIGN OF TEST RIG

The test rig is shown in figure (3.1). The arc can be drawn horizontally between a fixed and a moveable contact. Both with diameter of 4 mm.

The contacts were mounted in a test jig in which they were held by collets which provided an adequate electrical connection, and also were designed to have a reasonably high thermal resistance to the contact. This ensures a fairly long time constant (~ 1 second) for the temperature fall of the contact.

The moveable rod was free to slide between supports and it is driven away from the fixed contact by a solenoid against a compressive spring with spring constant of 0.8 kg/cm.

The contacts are normally brought together when the spring has been released as the result of solenoid de-energisation. The end rod of the fixed contact was held against a compressed spring to absorb the impact force and so to reduce the number of bounces.

The contact spacing could be set accurately for the required value by means of a micrometer (displacement transducer) which is provided with the jig.

The test rig has been used throughout the investigations and it simulates functional aspects of switches.

3.4 DESIGN OF CONSTANT CURRENT SOURCE IN CONJUNCTION WITH TIMERS.

It is well known that the erosion of contacts is a function of current and is more severe under D.C. operating conditions compared to A.C. where the arc can only be sustained for a maximum of half the cycle of the waveform before a zero crossing point causes extinction.

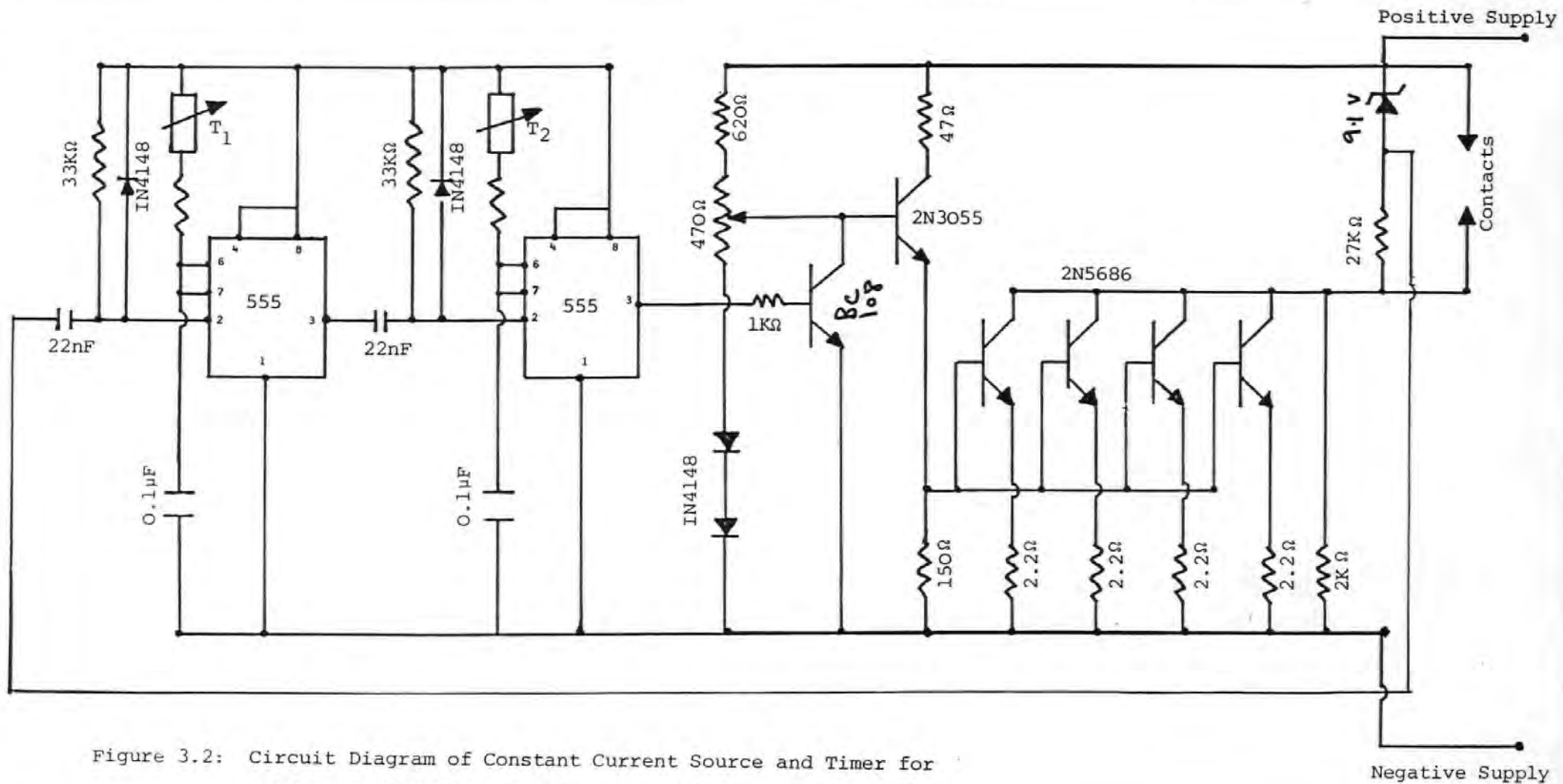
To obtain a full picture on the development of erosion the operating conditions must be extreme (D.C.) and the current should be kept constant, since at a known applied voltage the resistance of the arc increases as the gap increases and consequently the current decreases. To achieve this a constant current source device is designed for operating conditions in the range of 40 volts (d.c.) and current of 10 A, similar to the range used by Sato⁽⁴⁾ and White⁽¹⁾, in which they observed the change of phase in transfer at a current in the range of 6-8 A.

This device is based around four bipolar power transistors (2N5658) and all connected in parallel in which each carries a maximum current of 2.5 A.

To drive these transistors satisfactorily within the design range, it was necessary to design driving circuitry which could produce fast switching current pulse to the base of these transistors. The driving circuit is based on a 2N3055 bipolar power transistor with its base connected to a multi-turn resistor (470 ohms). This in turn is in series with 620 ohms resistor to determine the transistor (2N3055) switching time pulse and is also used to provide the arc current to the required value.

Another parameter which controls the development of arc erosion is the arc duration. This was controlled by a variable monostable circuit which interrupts the arc current after a pre-set period (typically 5-50 ms). This monostable circuit is connected to the constant current source via a BC108 transistor and it is triggered from the anode side of zener diode by the initial rise in voltage between the contacts when the arc is started.

The zener diode provides a fixed reference voltage and its breakdown region is



protected at breakdown voltage by a series of resistors which limit the current to a safe value.

Moreover, it is crucial that the electrical current pulse (trigger pulse) to the timer has the exact amplitude and width each time the contacts open. This ensures that there is simultaneous correlation between the start of the arc and the functioning of the monostable circuit (since this can be affected by the fluctuation of the arc voltage). It must also be emphasised that the duration of break and make must be much smaller than the set time on monostable 2 in order to avoid retriggering of monostable 1.

The details of the circuitry developed to produce constant current and to provide arc duration are shown in figure (3.2). The above system was used in all the tests where control of current and arc duration was required.

3.5 TECHNIQUES IN THERMOCOUPLE PROBE CONSTRUCTION

This section reports on temperature measuring techniques of contact surface due to transient heat dissipation of arcs in switches. Various methods for construction and mounting of the thermocouple sensor were investigated. It was found that for a very accurate measurement, the fastest heat transfer from contact surface to the sensor must be achieved. This requires the sensor to be placed as near as possible to the contact surface where the arc strikes.

The measuring equipment and the type of thermocouple used are described and the effect of each technique and the problems associated with it in mounting and methods of constructing sensors are detailed. Finally, the development of a technique for accurate temperature measurement is fully discussed. The transient heat defined as the time taken for contact body to reach steady state is much greater than the duration of the arc.

CODE	Conductor Combination		Approx. Working Temperature °C	British Standard	
	+ Leg	- Leg		+ Leg	- Leg
E	Nickel Chromium	Constantan or Copper Nickel	0-850	Brown	Yellow
J	Iron (Magnetic)	Constantan	0-850	Yellow	Blue
K	Nickel Chromium	Nickel Aluminium	-200-1100	Brown	Blue
T	Copper	Constantan	-250-400	White *	Blue **

American Standard { * - Blue (+ve)
 ** - Red (-ve)

Table 3.1: Typical family of standard thermocouples available on the market.

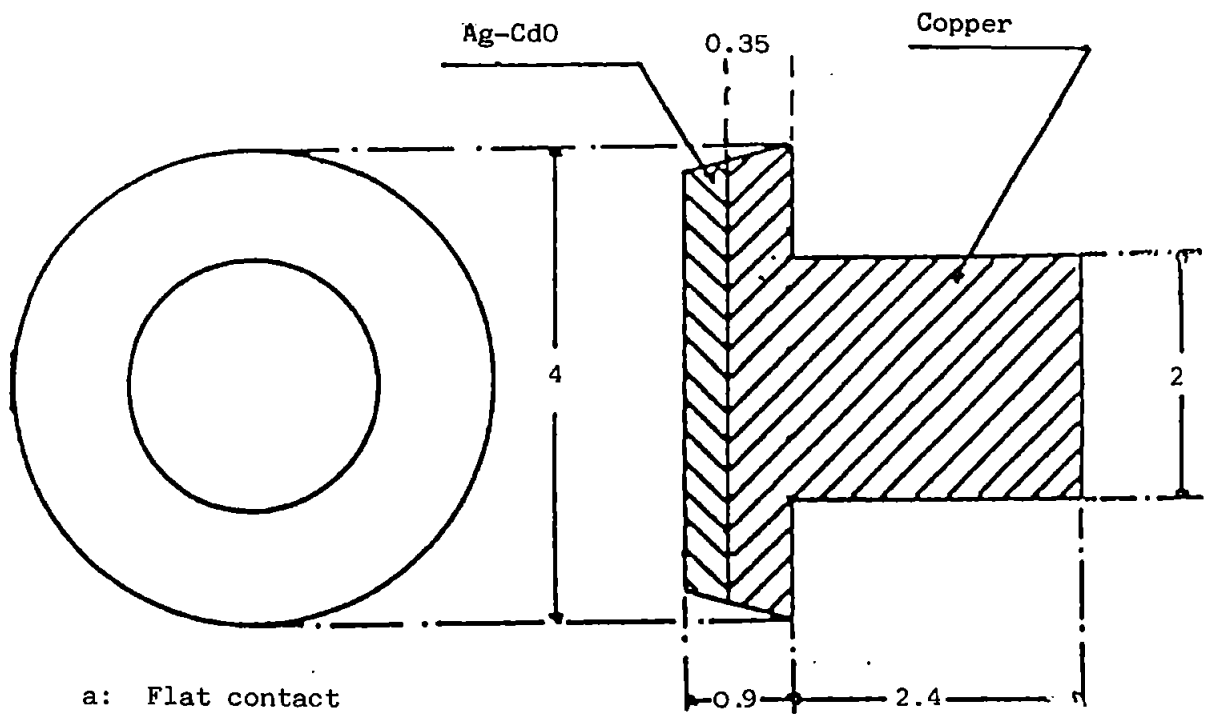
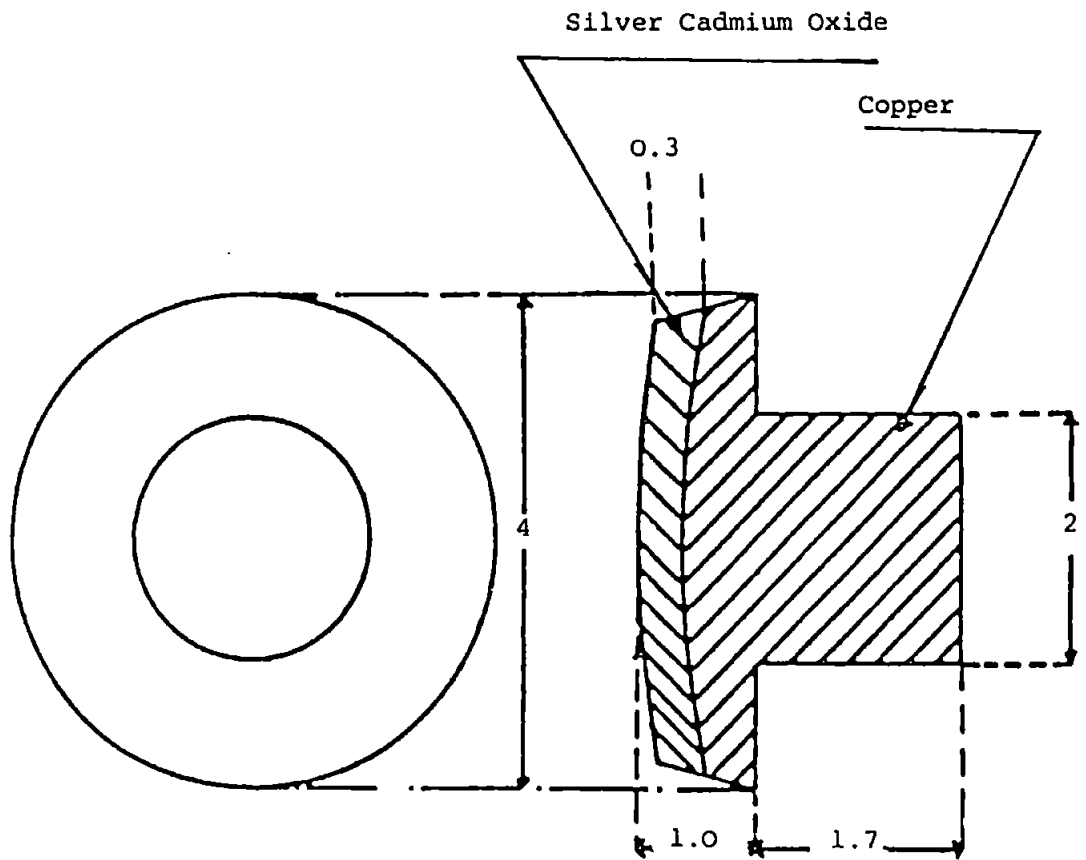


Figure 3.3: Physical Size of Contacts

- a: Flat
- b: Round

Dimensions in mm



b: Round Contact

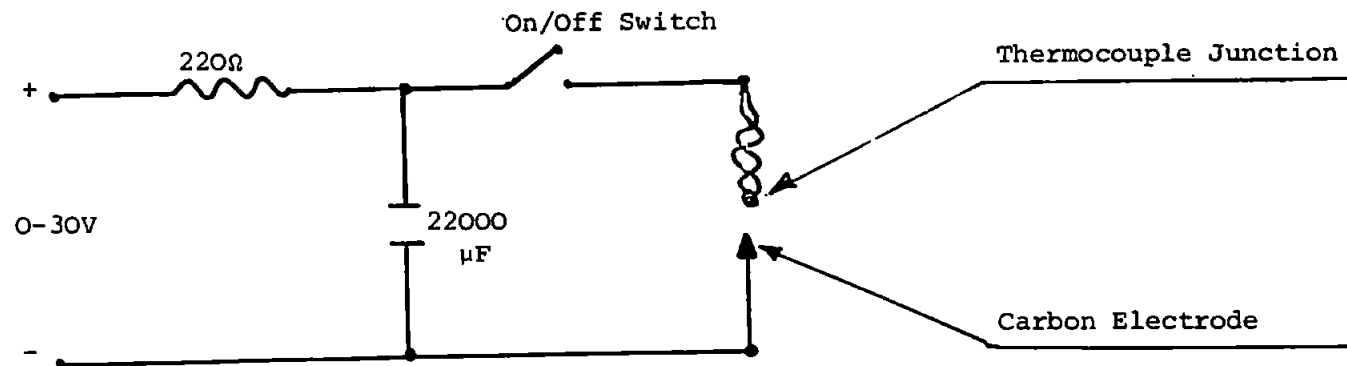


Figure 3.4: Circuit Diagram of Welding Rig

3.5.1 SENSOR CONSTRUCTION

A type 'T' thermocouple was chosen due to its high sensitivity, linearity of characteristics, negligible thermal mass and having adequate mechanical strength to withstand the break and make operation when it is connected to the contacts.

Table (3.1) shows family ^{of the} standard thermocouples available on the market.

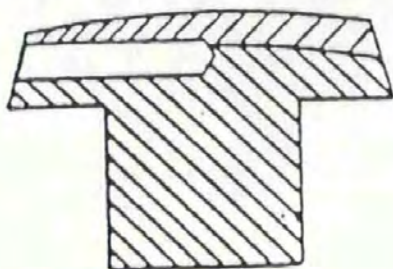
However, because of the small physical size of the contacts, as shown in figure (3.3), the diameter of the wires (Copper/Constantan) chosen was 0.075 mm and was insulated with a covering of P.T.F.E. (Teflon coated) and outer diameter of 0.25 mm. Thermocouple was calibrated with traditional Dewar flask method in terms of e.m.f. generated at the measuring junction relative to the reference junction which is kept at zero degree centigrade.

From the above calibration it was found that $40 \mu\text{V}$ is equivalent to 1°C . The thermocouple welded junction was achieved by twisting one centimeter (cm) of the bared wires together and discharging the capacitor momentarily between the carbon electrode and the twisted end of the thermocouple as shown in figure (3.4).

The twisted end must be placed vertically to form a ball weld subject to gravity. The ball weld diameter in general is in the range of 150 to 175 μm .

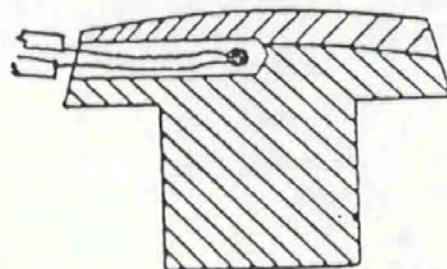
However, the welding processes should be carried out in an Argon gas to reduce oxidation and contamination, but this was dispersed during trial runs.

On completion of weld, the ^{bared} wires must be untwisted and insulated from each other to achieve a Spot thermocouple, since leaving the twist in, will cause temperature averaging over the whole one centimeter (cm) twisted length.



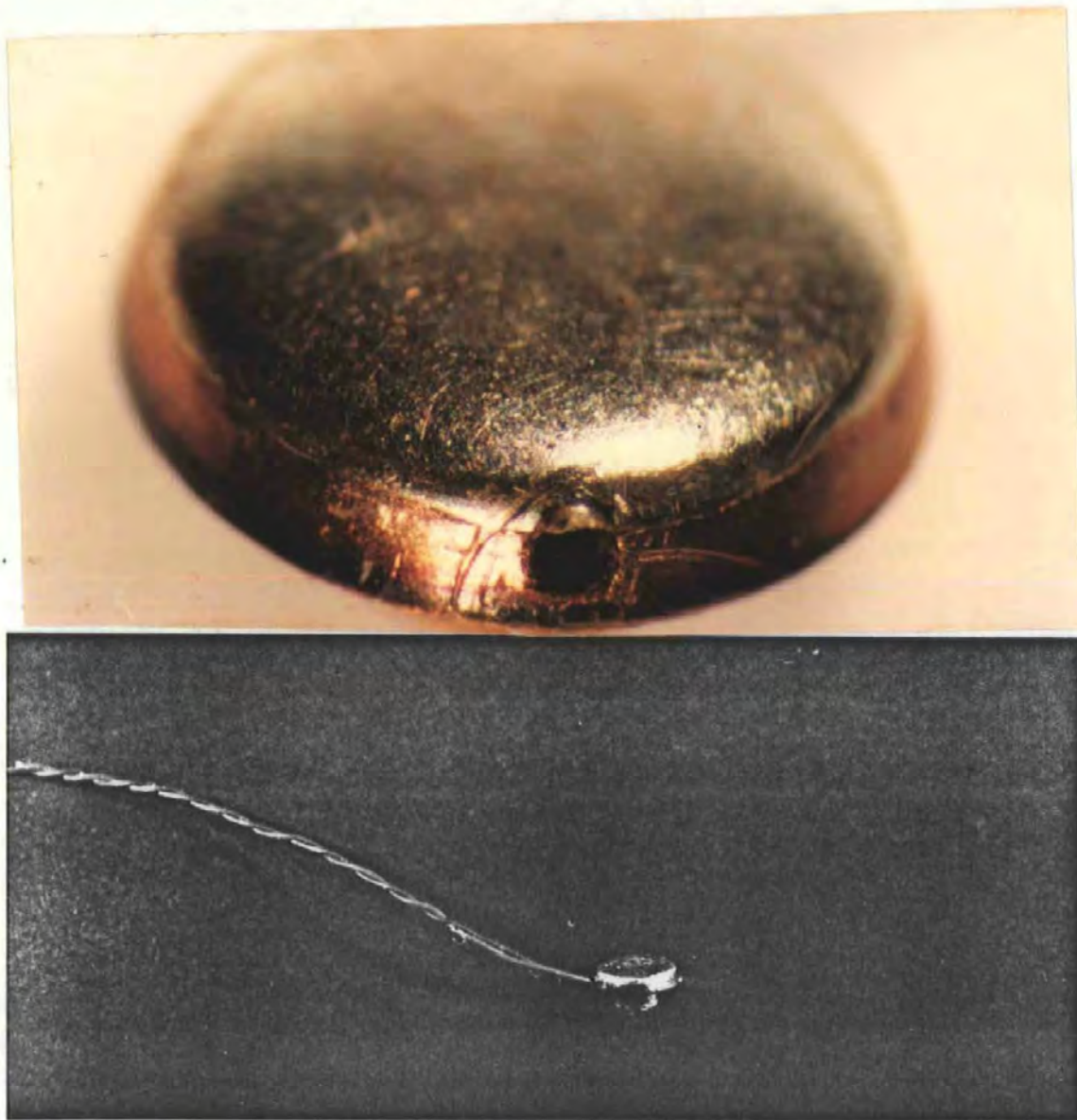
Half-way Drill

Thermocouple



Mounted Thermocouple

a: Schematic Diagram of Method I



b: Photograph of Method I

Figure 3.5: Complete Schematic Diagram and Photograph of Method I Sensor

3.5.2 SENSOR MOUNTING

Three methods have been used for sensor mounting and these are as follows:

METHOD I

A 0.4 mm diameter hole was drilled in the slit (side) of contact with 200 μ away from the surface. The hole was drilled half way and the weld end of thermocouple secured in the slit using various adhesive bonding agents, such as ceramic adhesive, nail varnish, laquer and super glue (cyano-acrylate CN). These insulators gave reasonable thermal contact, but unreliable electrical insulation.

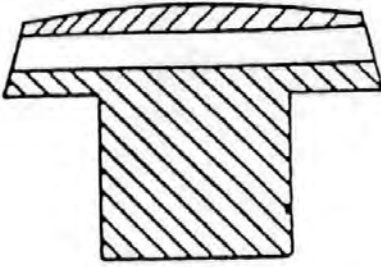
To improve electrical insulation, the welded end was placed in a capillary tube with epoxy resin around it and was placed in the slit of the contact with the heat sink compound, but it was found that the thermal conductivity was considerably reduced, despite the clearance distance between the capillary tube, thermocouple wires and the slit wall kept 0.1 mm to give very fast time response. The slit diameter (0.4 mm) affects the local loss distribution, but the effect on the results will be negligible since a very small amount of material is removed and this is constant throughout all such tests.

The poor thermal conduction may be due to air pockets in the slit and inconsistency of the temperature characteristics may be due to poor electrical insulation between sensor and contact body in the blind hole. Figure (3.5) shows the complete sensor with the contact.

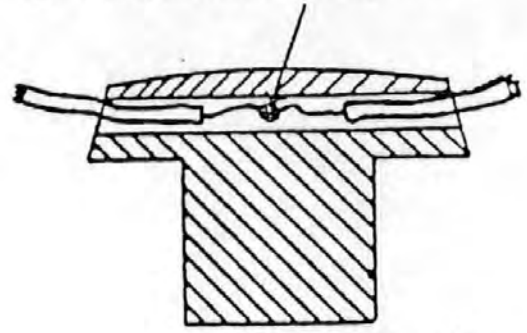
METHOD II

The thermocouple sensor was passed through the hole and secured in place in the centre with epoxy resin and then placed in a vacuum oven to cure and eliminate the air pocket or air bubble trapped.

in Position with Epoxy Resin

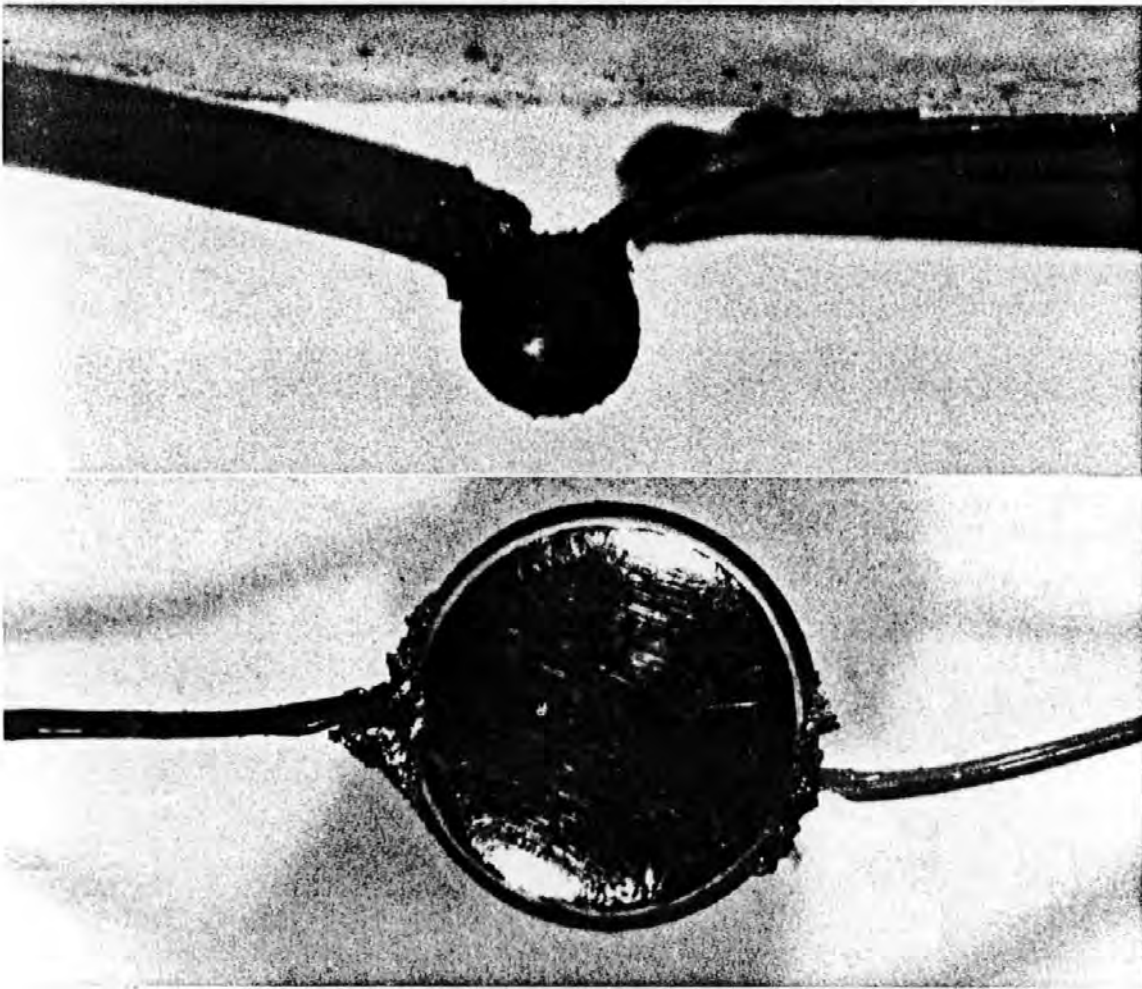


Full-way Drill



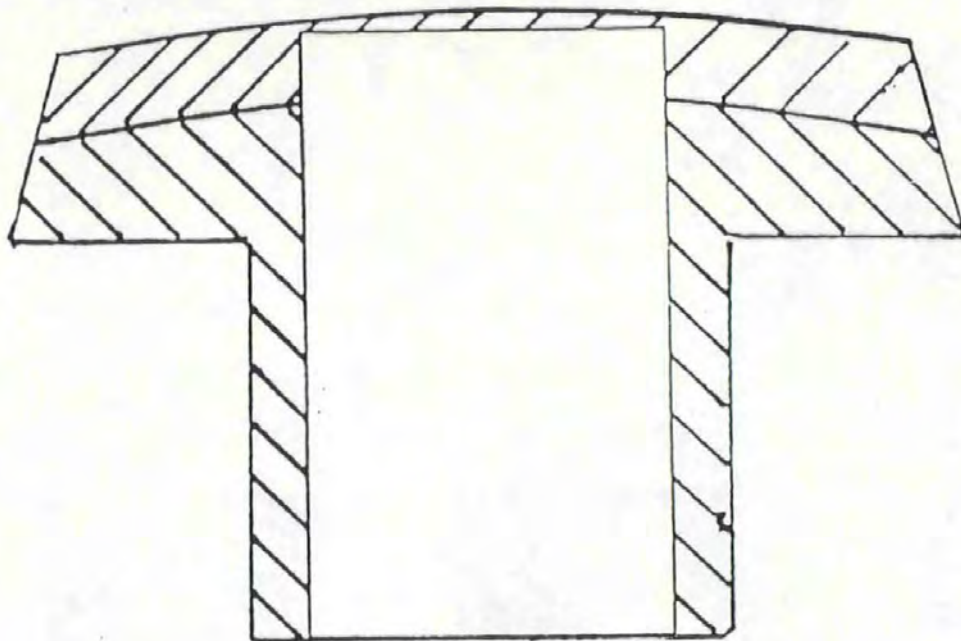
Mounted Thermocouple

a: Schematic Diagram of Method II Sensor

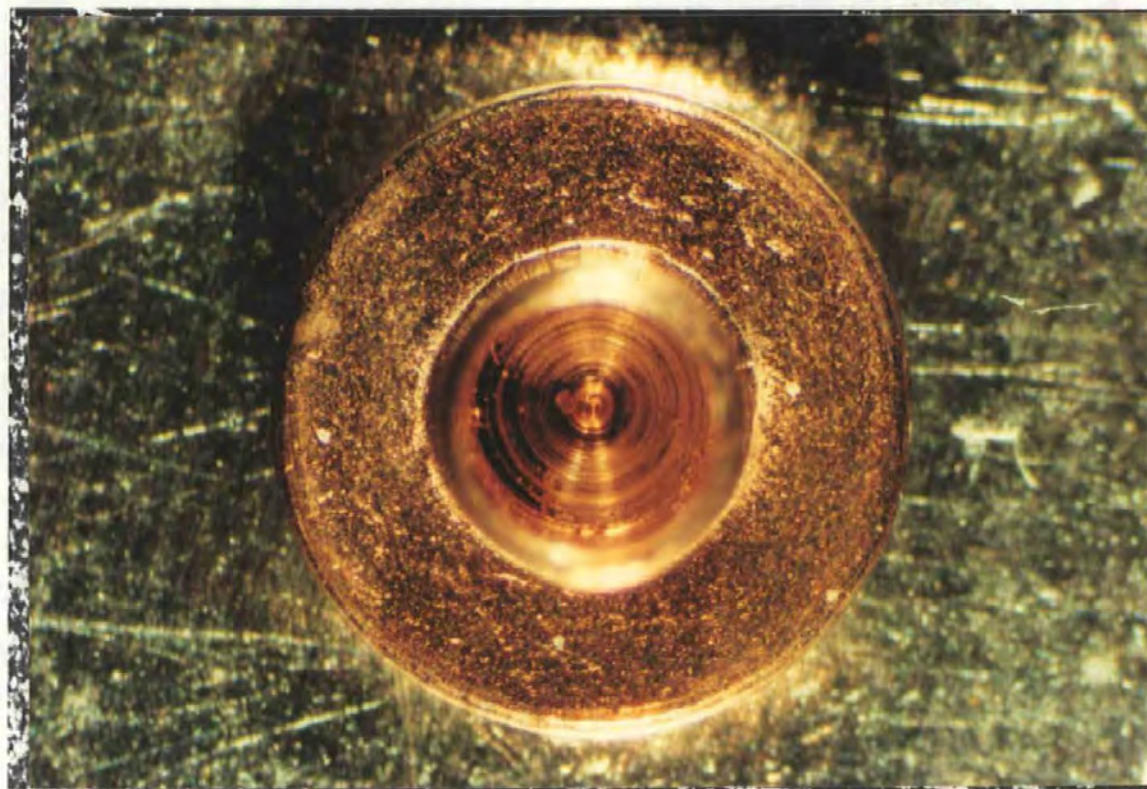


b: Photograph of Method II Sensor

Figure 3.6 : Complete Schematic and Photograph of Method II Sensor Construction

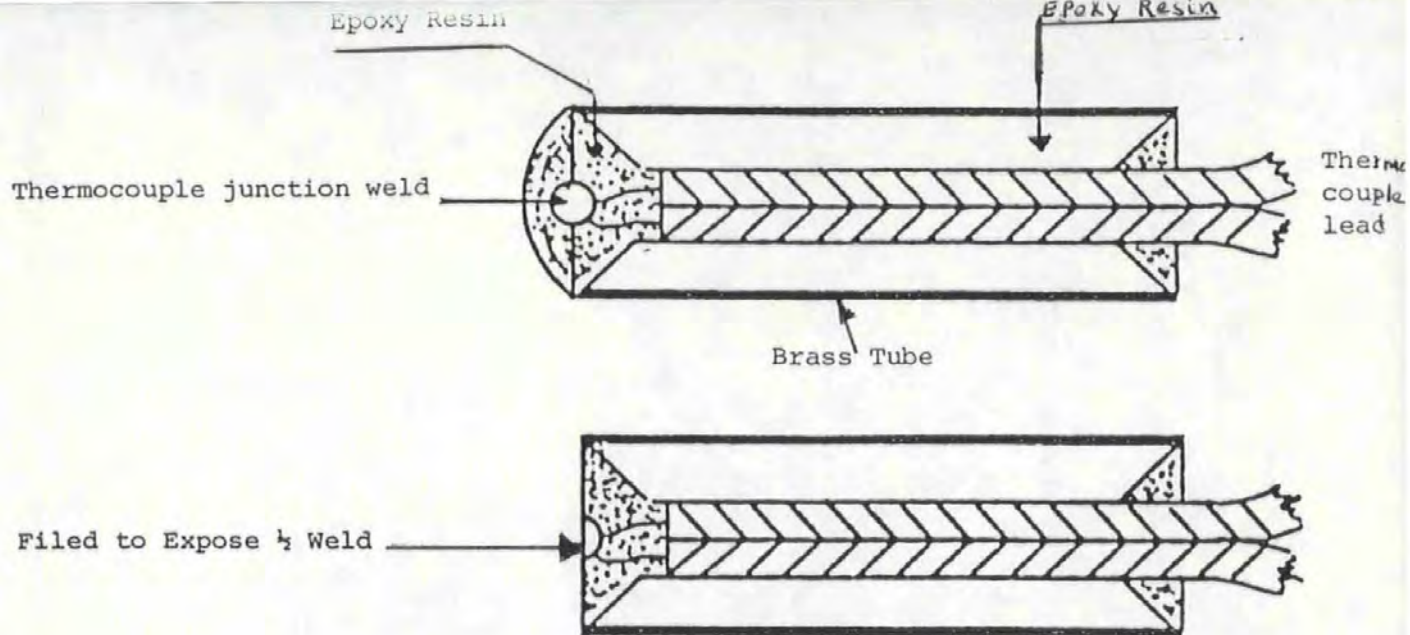


a: Schematic Diagram of Spill Construction

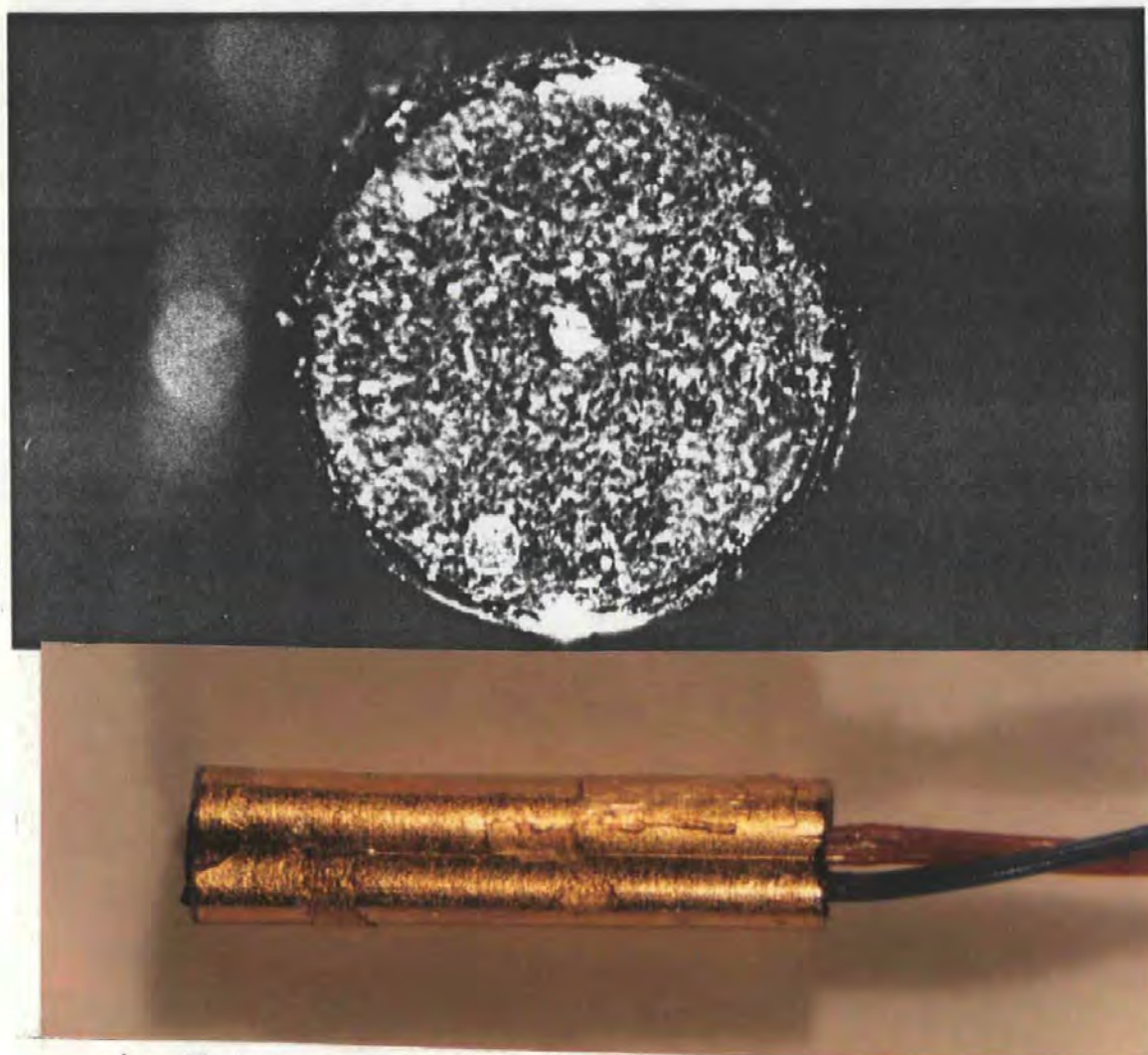


b: Photograph of Spill of Contact

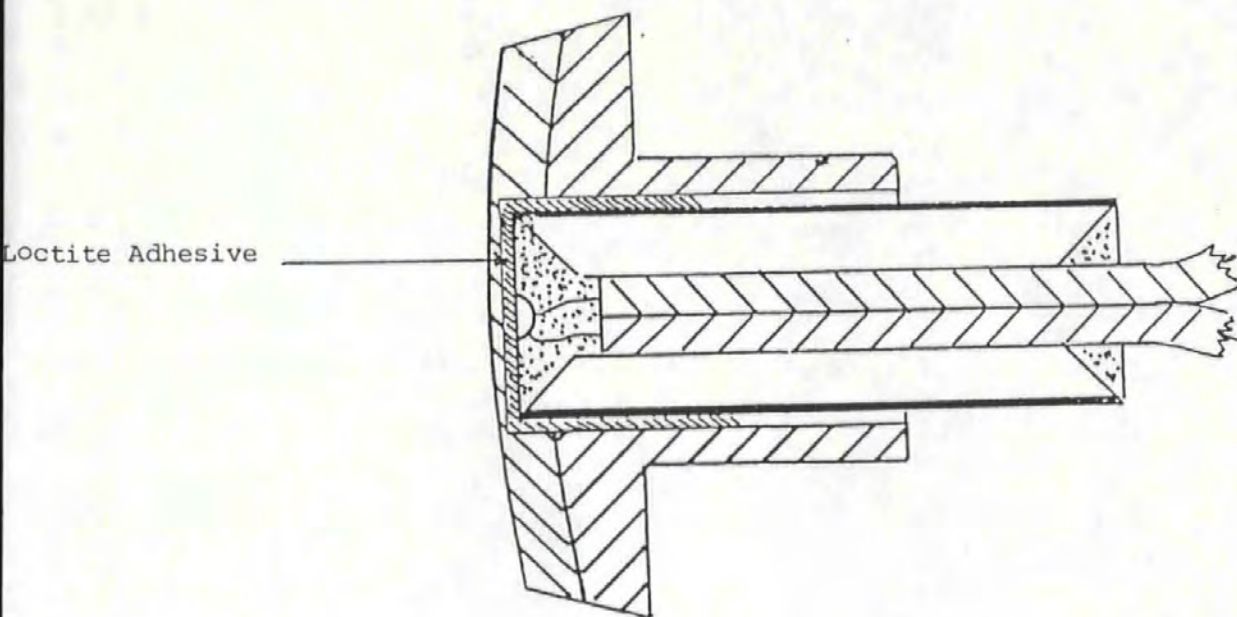
Figure 3.7: Shows Schematic and Photograph of Probe Position



a: Schematic Diagram of Probe Construction



b: Photograph of Probe of Method III



c: Complete Schematic Diagram of Method III Sensor



d: Photograph of Method III Sensor

Figure 3.8: Shows Complete Process in Construction and Mounting of Method III

This method in general also proved difficult to maintain good thermal conductivity and electrical insulation. A typical mounting of the sensor is shown in figure (3.6).

METHOD III

In this method, a hole was machined centrally through the spill (back) of the contact, and the end faced off. The depth of the hole could be accurately controlled and the distance from the surface set at 150–200 μm , as shown in figure (3.7). To ensure the thermocouple weld was centred in the hole and, to achieve maximum thermal conductivity, a jig was made from brass tube 4 mm in length with outer diameter 1.35 mm and inner diameter 1 mm.

Two thirds of this tube was filled with Araldite MY750, with hardener HY917 and accelerator DY070, which is usually used for laminating and impregnating the system. After its curing in a vacuum oven, it was drilled with a 0.5 mm drill.

The thermocouple was positioned centrally in the tube through the drilled hole and then the rest of the tube was filled with quick set epoxy resin. This ensures the thermocouple in the centre. The sensing end of the tube was filed down to expose the maximum area of the weld. The jig was bonded into the hole in the spill of contact, using Loctite 384 with thermal conductivity 0.815 watts/m⁰C and dielectric strength 23 KV/mm. To achieve good thermal conductivity for fast response before diffusion along the contact body takes place and electrical insulation, the jig was maintained under pressure until the adhesive cured. See figure (3.8).

However, the construction of the thermocouple probe proved far more difficult and time consuming than anticipated. The techniques of mounting a thermocouple in method I and II proved unreliable and inconsistent with respect to the electrical insulation and thermal path (conductivity) which resulted in the peak of the temperature characteristic not occurring at the time when the arc duration was terminated, despite thermocouple being very close to the surface. Method III performed far better than I and II, the only unknown variable being the thickness of

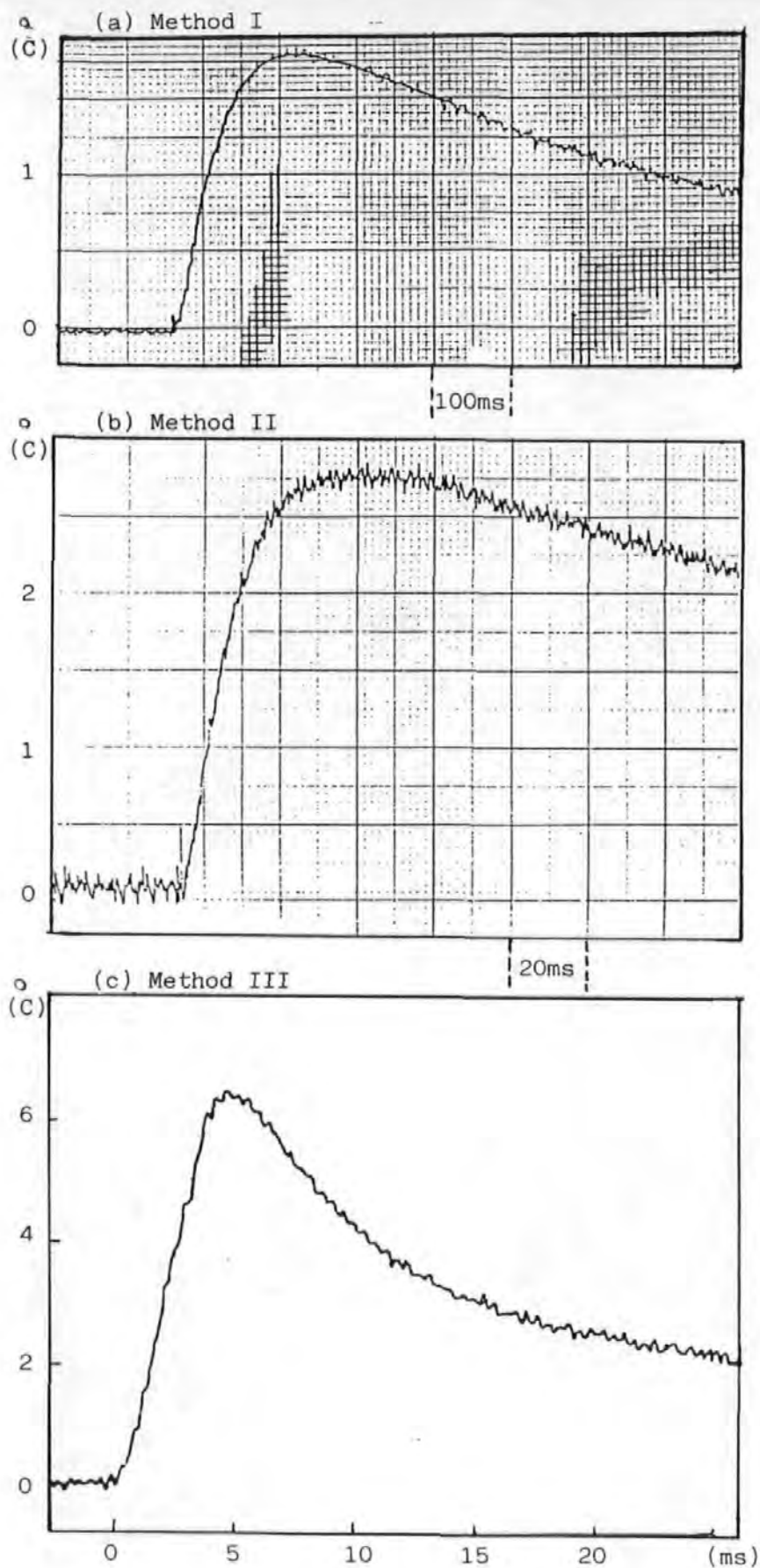


Figure 3.9: Typical characteristics of temperature-time curves obtained with Method I, II and III; at test conditions of 40 volts, current of 4A, gap-length of 1mm and arc duration of 4ms.

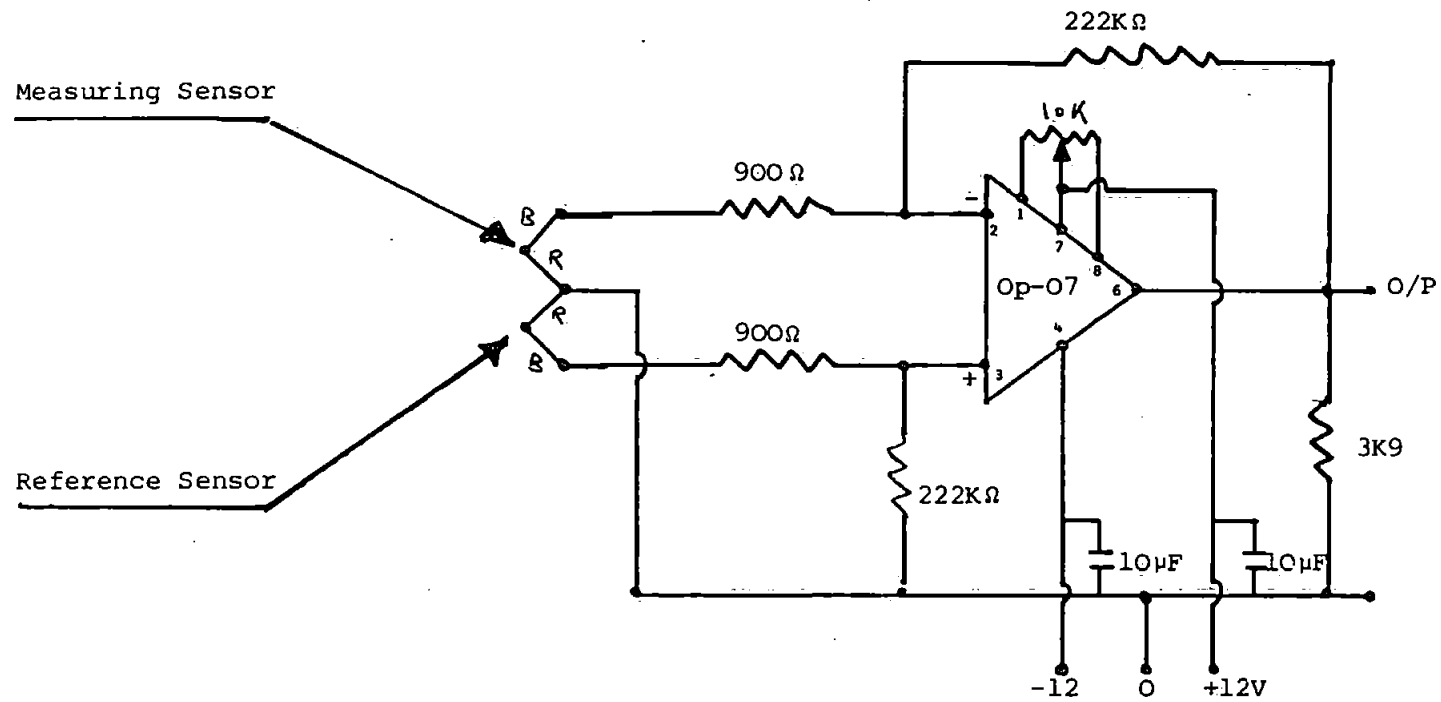


Figure 3.10: Circuit Diagram of Thermocouple Amplifier with Gain of 247.

the thermally conductive adhesive between the probe and the underside of the contact surface.

A typical characteristic of temperature-time obtained from each method at the same known parameters (current, voltage, speed of break and make and gap) is shown in figure (3.9).

The output of thermocouple is measured from thermocouple amplifier with gain of 246.48 and this is shown in figure (3.10). Finally, the leads had been twisted tightly together and a small adjustable loop included in the circuit to cancel any residual induction transient. The electrical insulation has been checked by measuring the resistance between thermocouple wire and contact body.

3.6 THERMOCOUPLE PROBE CALIBRATION SYSTEM

Although the procedure for the construction of the thermocouple probe and its mounting into the spill of the contact is the same, it was found that not necessarily all will have the same response at a fixed test condition due to the time constant of the probe. The differences may have been caused by the following:

- (i) Air pocket between probe and contact as a result of poor bonding between them.
- (ii) Variation in the thickness of adhesive used for bonding which was also used as good electrical insulator and thermal conductor.
- (iii) Variation in the centreness (position) of the weld junction in the brass tube and its diameter (size).

(i-iii)
However, some of the above reasons are unavoidable in the construction of the probe sensor.

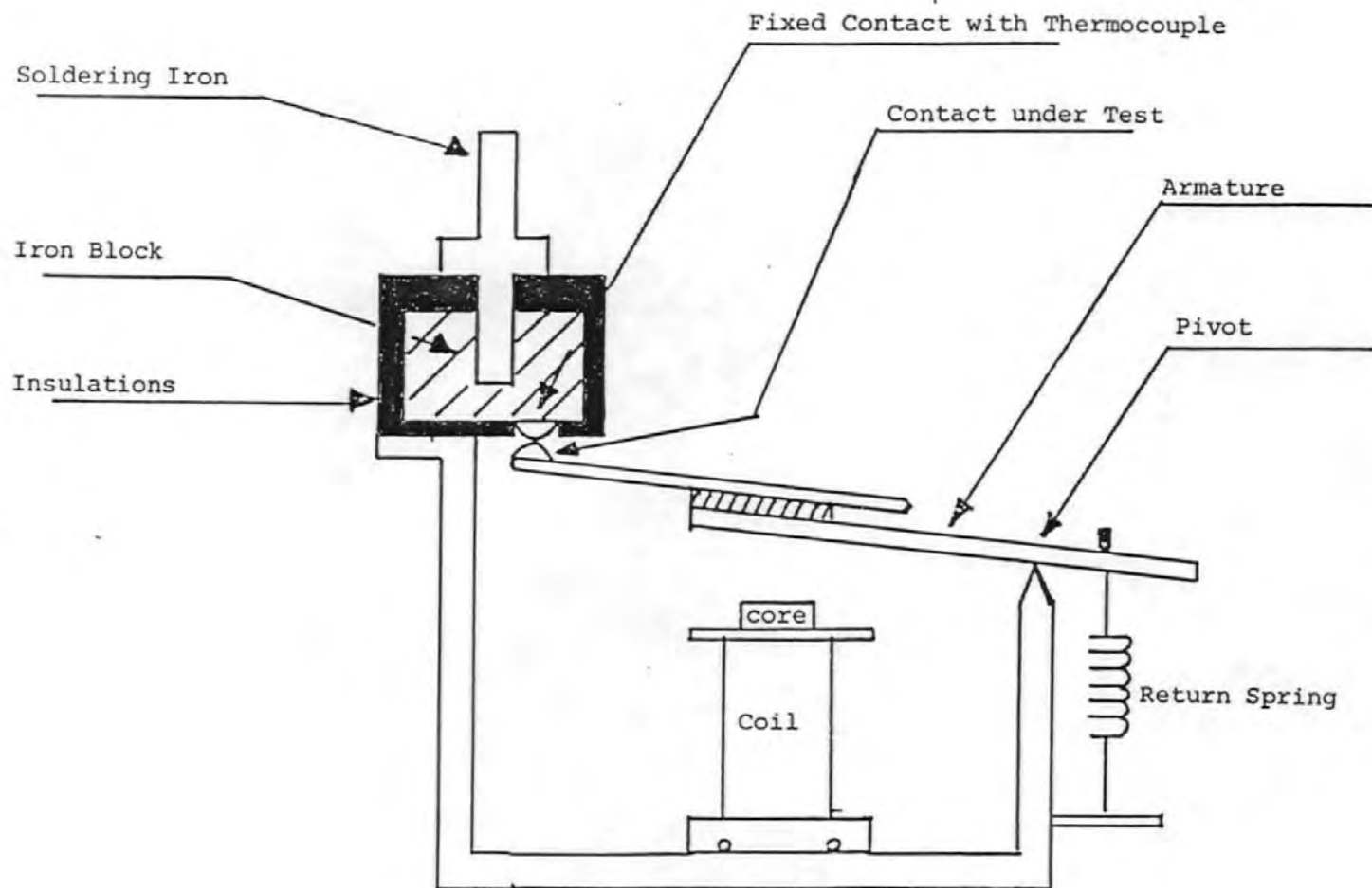


Figure 3.11: Calibration System

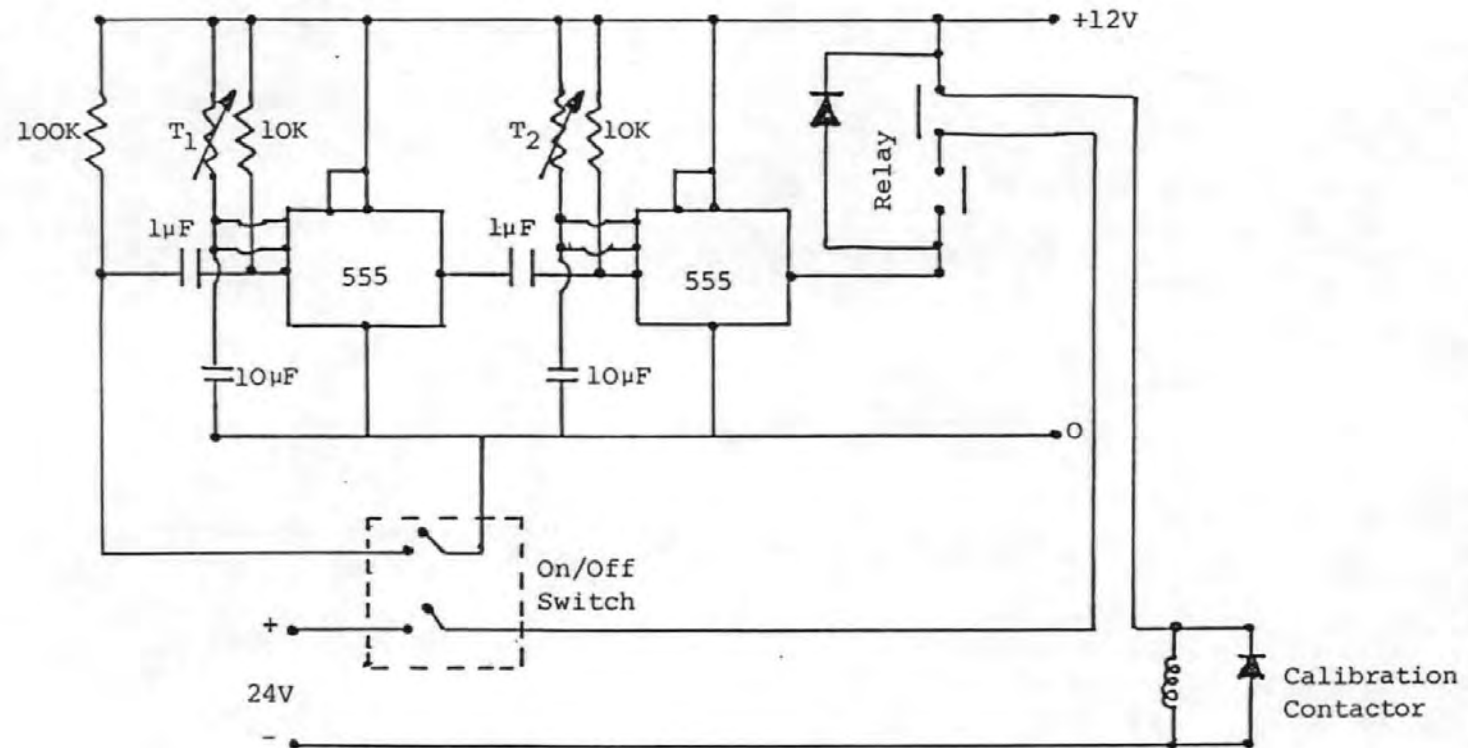


Figure 3.12: Shows Control Circuit of the Calibration System

For consistence comparison the characteristics (gradient and peak) of each pair of contacts with ^{the} thermocouple probe must be the same. Therefore, a system has been devised to ensure the above condition before test on the arc rig. This is called the calibration system which, in fact, simulates the test rig performance without actually arcing.

The above system comprises a contactor structure and a hot body. The hot body is made of iron with mass of 113.88 grams which is insulated by good insulating material all over except where the stationary contact is placed.

The heat input to the hot body is provided by a temperature control soldering iron which is placed inside the iron. The sensor (contact with thermocouple) under calibration is placed on the armature of contactor.

The calibration test is carried out when the hot body reaches ^a steady state temperature and this is observed from the output of ^{the} thermocouple which is fixed to the stationary contact.

The characteristic of the sensor under investigation is obtained from the thermocouple amplifier ^{output} on the oscilloscope. The details of calibration system and its control circuit are shown diagrammatically in figures (3.11) and (3.12).

However, the above system has a limited capacity, since the maximum operating range of ^{the} soldering iron is 400°C .

LED

3.7 COMPUTER CONTROL WORK STATION

To evaluate the degree of erosion after so many numbers of operations involved the operation of test rig and collection of data from numerous equipment (e.g. voltmeter, ammeter and thermocouple amplifier, etc.). This is obviously a very lengthy performance manually.

However, replacing manual with automatic operation reduces the test time. This procedure eliminates human errors, since the speed of break and make and time

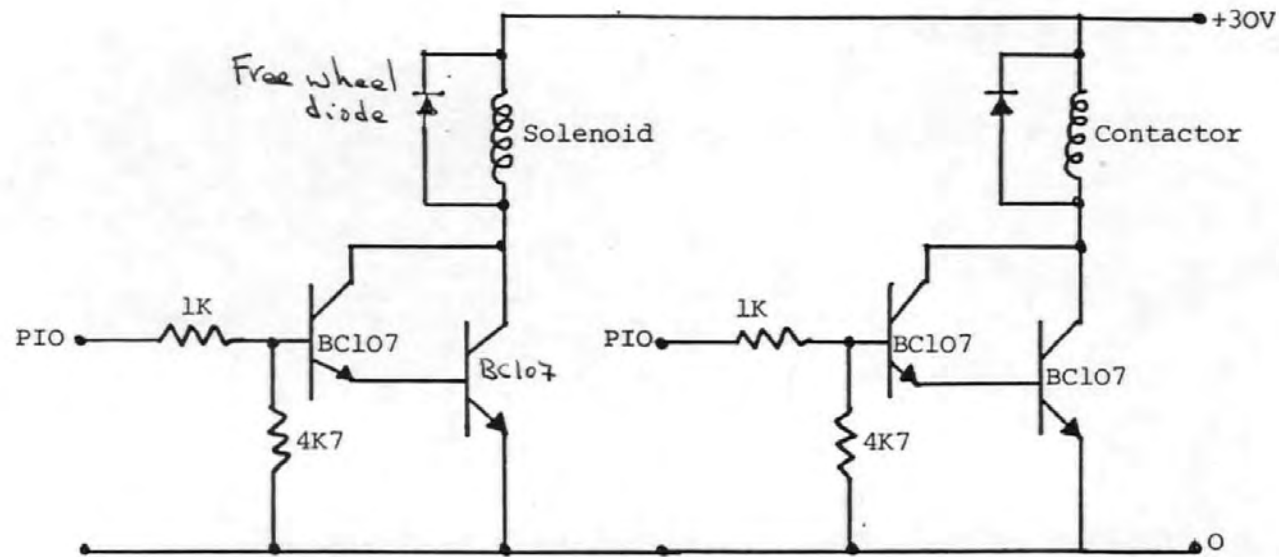


Figure 3.13: Interface Circuitry of Solenoid/Contactor with Micro-Computer

PIO: Parallel input/output interface

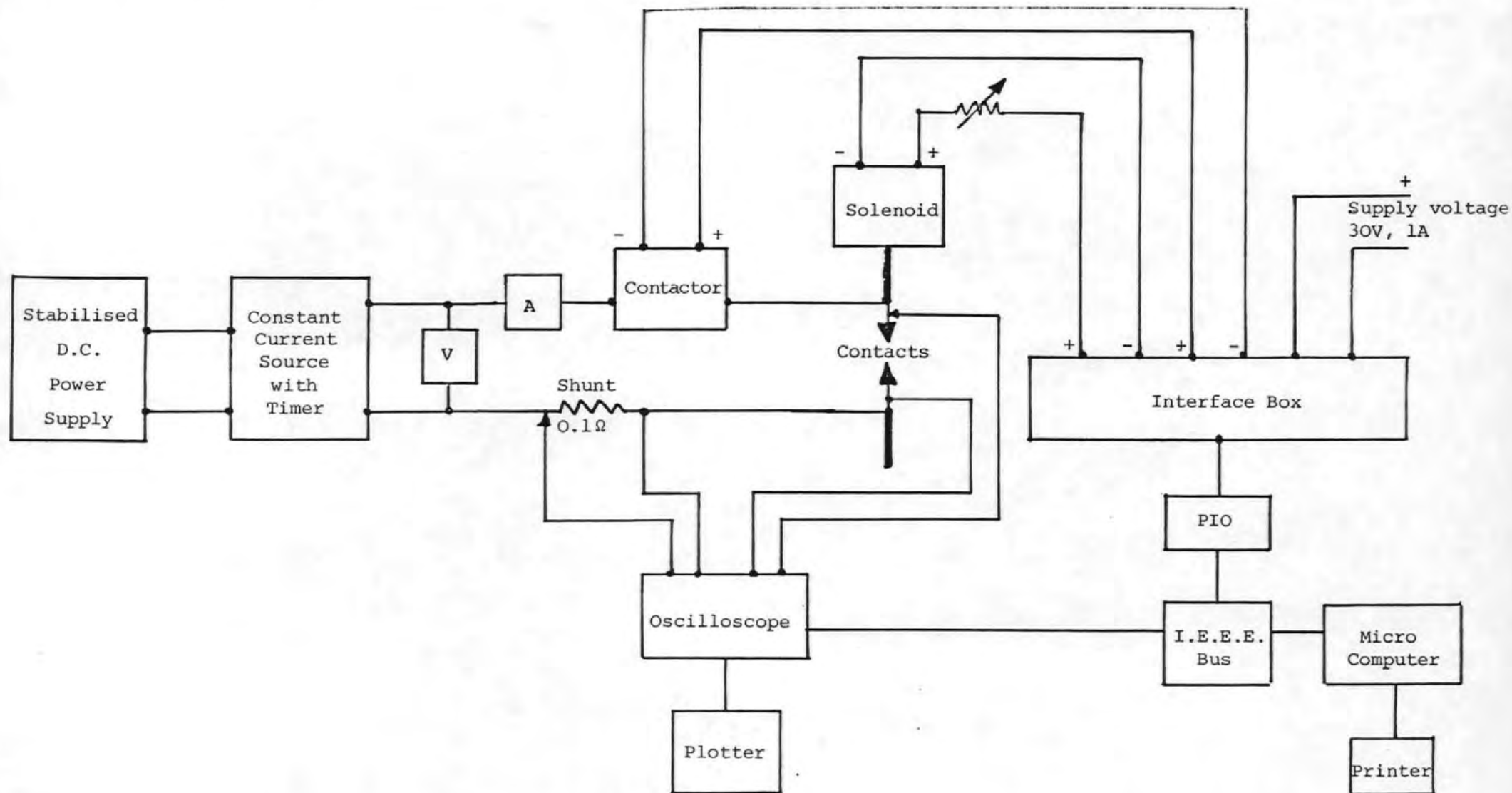


Figure 3.14 : Schematic Diagram of Complete Test Station

interval between successive operations also have important roles in the build up of erosion.

To achieve automation, a BBC microcomputer is employed as controller and IEEE 488 bus for communication. A disc drive is used to record the voltage, current and temperature waveform, and a printer and plotter to output the data stored on the floppy disc whenever needed.

As it has been mentioned previously, the test rig is driven by a solenoid and a contactor to provide the pre-switching. Both of these in turn are linked to the microcomputer through PIO. Figure (3.13) shows the interface circuitry.

The communication between oscilloscope and computer is through IEEE 488 bus and between controller, solenoid and contactor is through PIO interface box. The input resolution of high speed Philips storage scope (50 MHz) is ten bits (1024) per channel.

$$\text{resolution} = \text{full scale} \times 1/(\text{no of bits})$$

The oscilloscope is triggered externally when ^{the} contactor is active and the current is detected across a 0.1 ohms resistor. Figure (3.14) shows the complete test station schematically. However, in order to control, collect and process the data, the above hardware requires software. The main software is written in BASIC in a way that easily can be modified by anyone who wishes to use the existing program for sending instruction to the hardware and receiving, and processing the data into an acceptable form, since 1024 digital data values from each channel of ^{the} oscilloscope are stored in an array on the floppy disc.

Other options within the above program are for plotting the data stored on VDU and also sending the stored data directly to the main computer (PRIME) via RS232 since the floppy has maximum capacity of 640 K memory.

Finally, a check has been made on several waveforms in order to verify the computer generated values of the data with those on ^{the} oscilloscope. The overall accuracy of data redorded on the disc depends on the resolution of the oscilloscope and the power of the software. The block diagram of the program is illustrated in

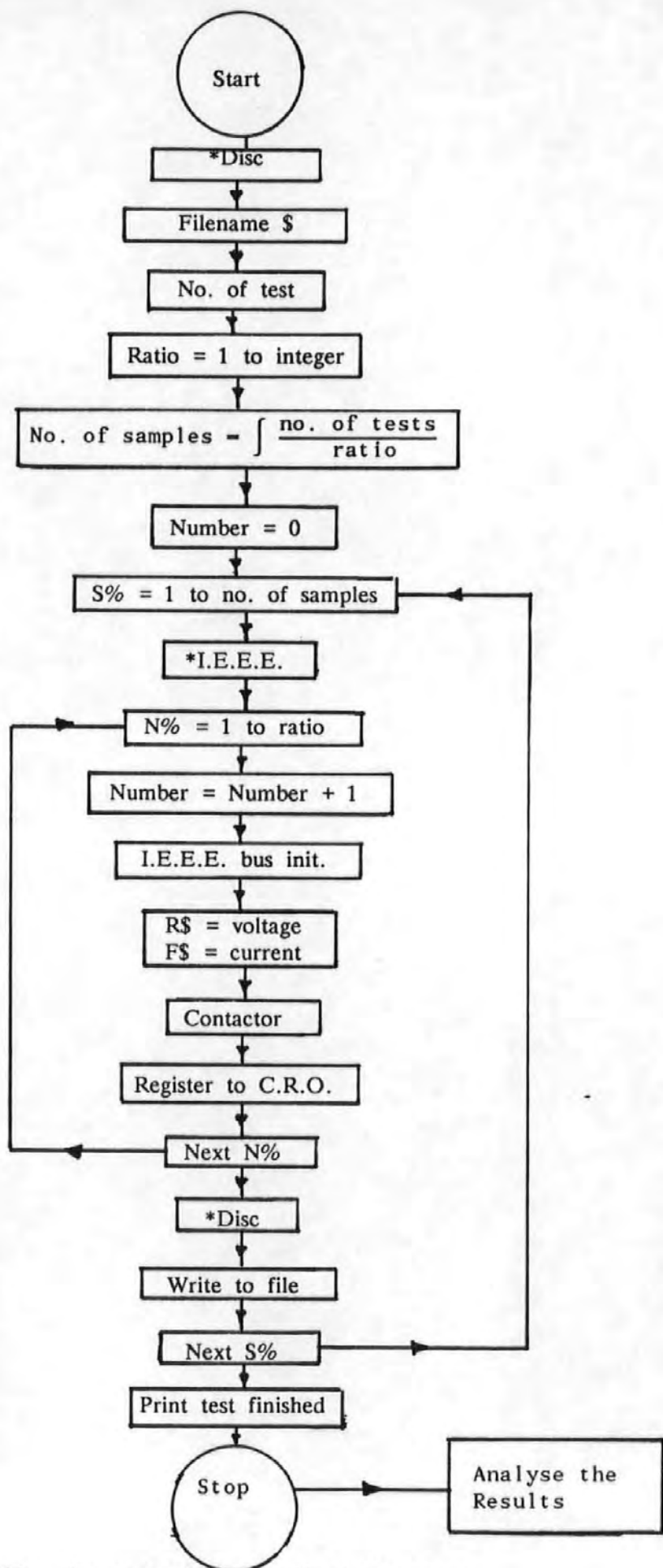


Figure 3.15: Computer Program Block Diagrams.

figure (3.15) and the program listing is in appendices I and II. The above development is used as a tool throughout investigation.

REFERENCES CHAPTER THREE

1. White, P.J.

PhD Thesis, 1979, Plymouth Polytechnic

2. The Engineer

Published 31 March 1988.

3. What's New in Electronics

Published April 1988.

4. Sato, M.

"Studies on the silver base electrical contact materials"

Trans. Nat. Res. Inst. for Metals, Vol. 18, No. 2, 1976.

CHAPTER FOUR EXPERIMENTAL INVESTIGATION

4.1 INTRODUCTION

This chapter covers mainly the experimental work which has been carried out to build up an understanding of the effect of arcing on the contact surface.

The experimental work, which is interdependent, comprises speed measurement on the test rig during closing and opening operations, electrode fall voltages, and contact temperature due to arcing, from which a correlation between electrical and thermal energy is obtained.

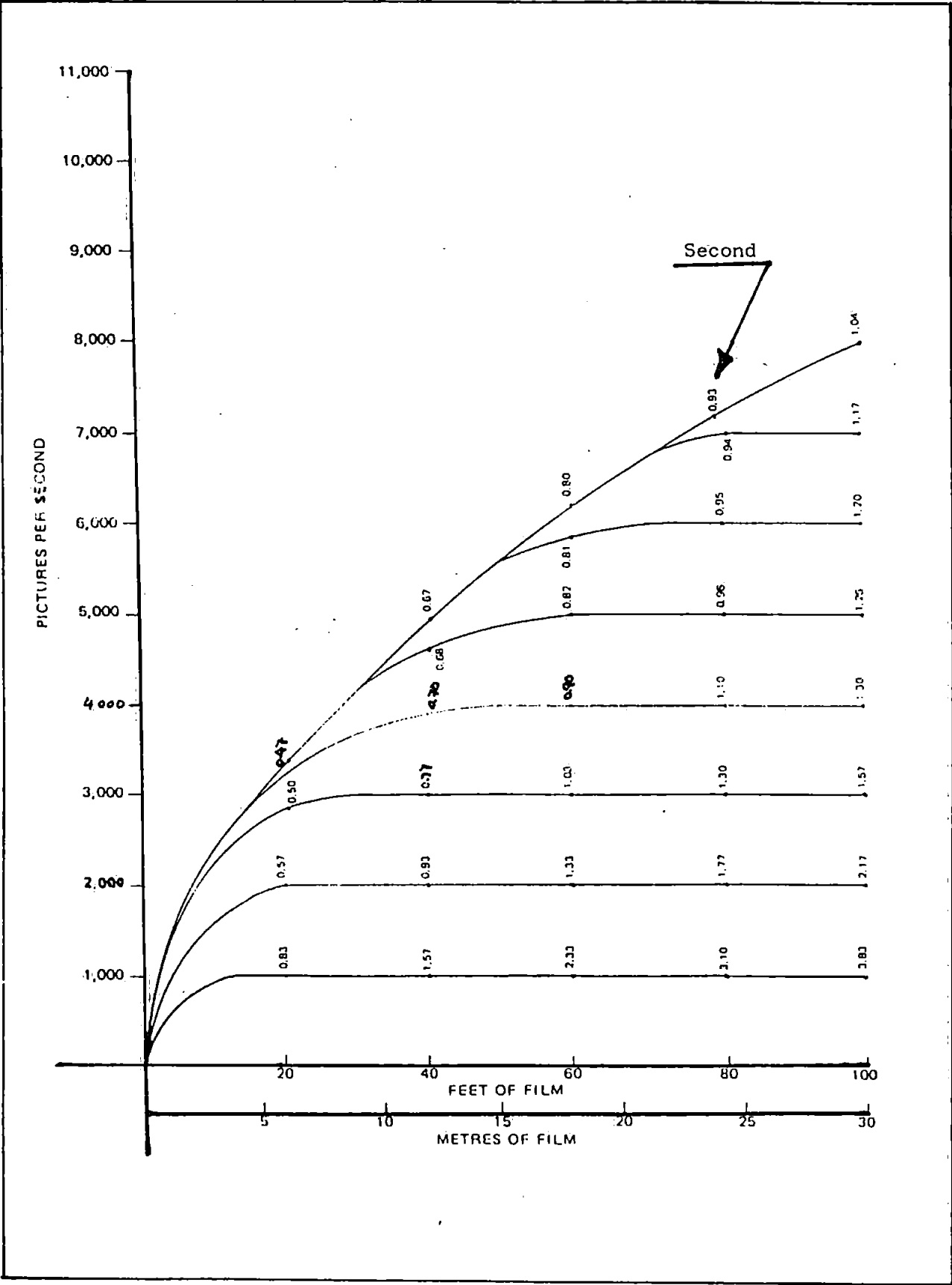
4.2 SPEED MEASUREMENTS

The mechanical characteristics of the test rig are shown on a separation versus time curve, which enables one to obtain a more complete understanding of its performance for a particular electrical duty and also explains the nature of the phenomena which occur during break or make operations, which is important for the analysis of the results obtained from the test rig.

The initial experimental work undertaken was on the earlier test rig which was similar to the present one shown in figure (3.1) of chapter three, but it had some limitations in other areas of research, therefore the present test rig has been especially designed and built. Its operational procedure is discussed in section (3.3).

The operating and closing characteristics of the test rigs are discussed in the following sections.

Figure 4.1: Shows the elapse time in seconds for 100 feet of Hyspeed camera film; extracted from John Hadland Photographic Instrumentation Ltd.



4.2.1 OPENING SPEED

The opening characteristics of the test rigs were measured using a Hyspeed camera.

To enable the contact motion to be filmed, the Hyspeed camera is focused within the distance in which the contact travels. The film used is Eastman 4x negative 72224, 100 foot long, black and white, and the picture is taken at a speed of 5000 p.p.s. (picture per second). From figure (4.1) one can see that a speed of 5000 p.p.s. is possible towards the middle of the film. Since this speed is reached in the last 50 feet, approximately 10 feet of the film is lost due to film backlash and exposure to daylight, and the test rig is operated automatically by a solenoid which in turn is triggered by the event control switch in the camera, thus allowing for the switch and solenoid movement. The event was set to start at 40 feet which allows approximately 50 feet for the event.

A time base for the films shot is provided by the camera system. This imposes an illuminated dot on the edge of the film frame at equal time intervals which enables one to analyse the film, frame by frame, on a microfilm reader in which the separation can be measured on each frame.

The information from Hyspeed film is plotted against time as ^{a typical example is} shown in figure (4.2) which represents the opening characteristics of the test rigs ^(500 mm/s). The gap is set by a micrometer which is coupled with the fixed contact.

Figure (4.2) indicates that the moving contact accelerates until it reaches the maximum separation between contact centres after 2.75 and 3.5 ms and then continues to oscillate, as a result of the transfer of the potential energy of the spring to kinetic energy, about the final rest position (this is the actual gap set by micrometer (1.3 mm)). Generally the results show that the earlier test rig has the larger acceleration, and hence oscillations, compared to the later one. The difference between them is sufficiently small that it can be assumed to be practically negligible.

Since the contact performs oscillations of a sinusoidal form and the amplitude

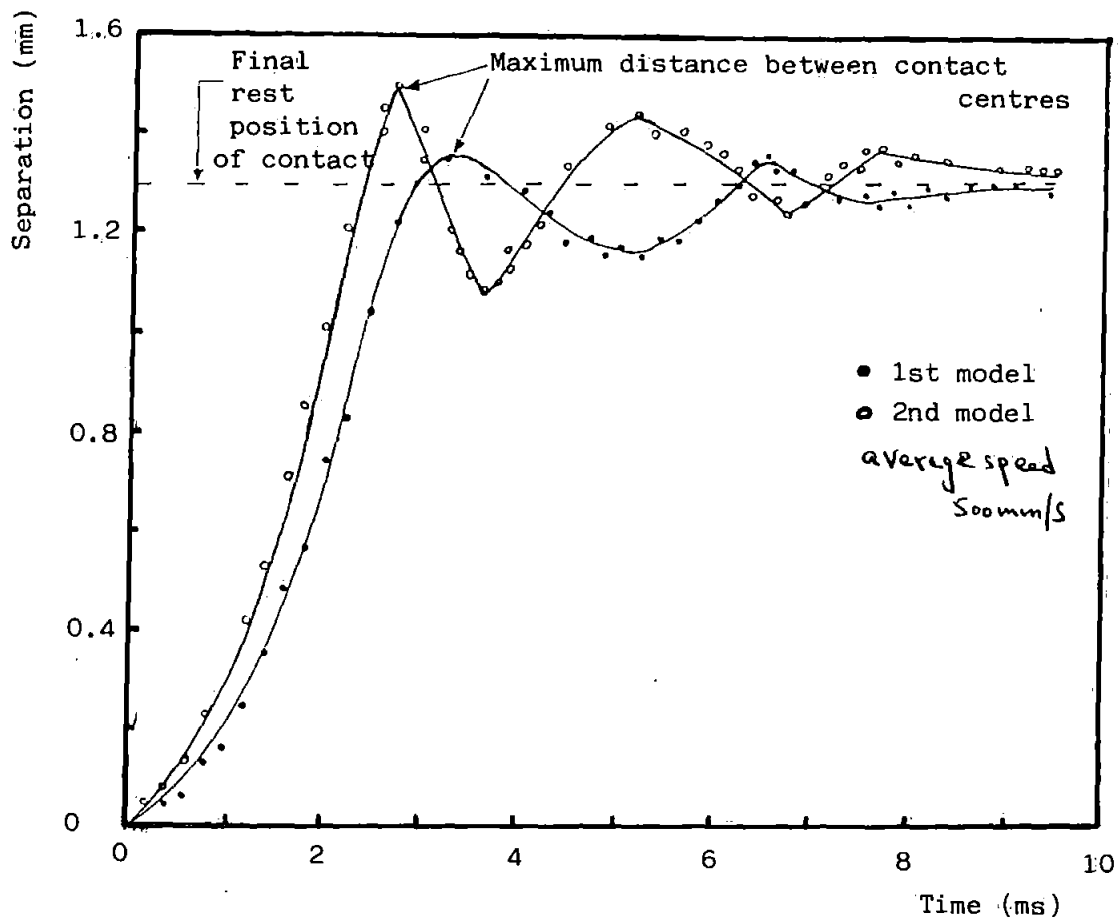


Figure 4.2: Shows the opening characteristics of the test models obtained by the Hyspeed camera.

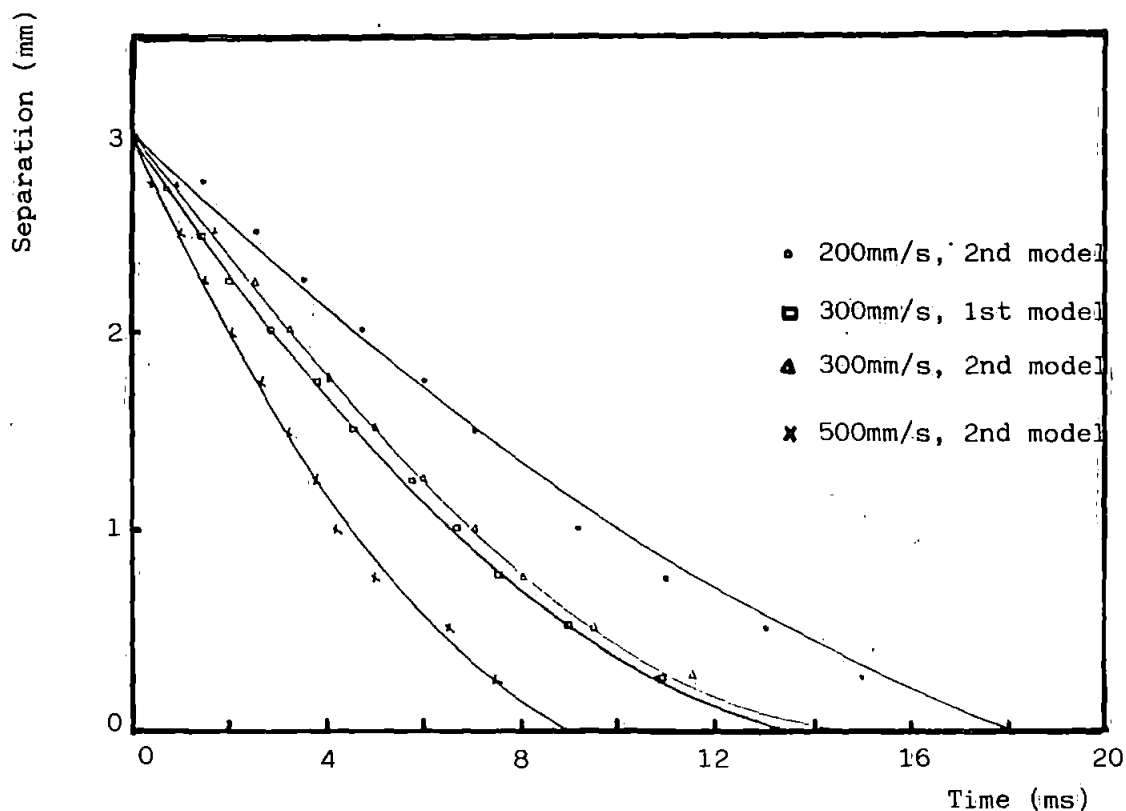


Figure 4.3: Closing characteristics of the test models measured on the oscilloscope

decay of these oscillations appears as exponential, White(1) used a computer programme to obtain a best fit of characteristics, where a general equation is obtained to define this sort of response.

4.2.2 CLOSING SPEED

The closing characteristics of the test rig are obtained by measuring on the oscilloscope screen time taken for the contacts to close from various separations. The separations are adjusted by moving the fixed electrode via the micrometer, leaving the driving mechanism and the moving electrode unaltered. The information for plotting separation against time is obtained by subtracting the time taken of each consecutive separation from the first separation (the largest chosen separation, (3mm)). The consecutive separations decrease. This approach approximately simulates the closing characteristic of the test rig from the information taken by the Hyspeed camera. Figure (4.3) shows the closing characteristics of the test rig at various speeds (200 mm/s to 500 mm/s), and the graph for each speed indicates that there is an initial acceleration period of the moving contact for the first 2.5 ms of travel, then it drops more gradually as separation decreases, and finally it comes to rest with the fixed contact.

4.3 ELECTRODE VOLTAGE FALL MEASUREMENT

It is known that the erosion of contact is due to the amount of power being dissipated at the contact surfaces from which contact material is boiled away and this amount is a function of the voltage drop near the electrodes. This suggests that for the study of erosion from the power balance relation, the voltage drop for various test conditions must be obtained.

The theory of electrode voltage fall and the techniques used to measure these falls are described in chapter two, sections (2.5) and (2.5.1). The present work is confined to arcs between solid electrodes (Ag-Cd O) in air using the Moving

Electrode Method in conjunction with a fast oscilloscope. In the moving electrode method the magnitude of the last sudden voltage step which occurs when the electrodes are brought together is measured; this takes place just before the approaching electrode makes contact with the fixed one(2).

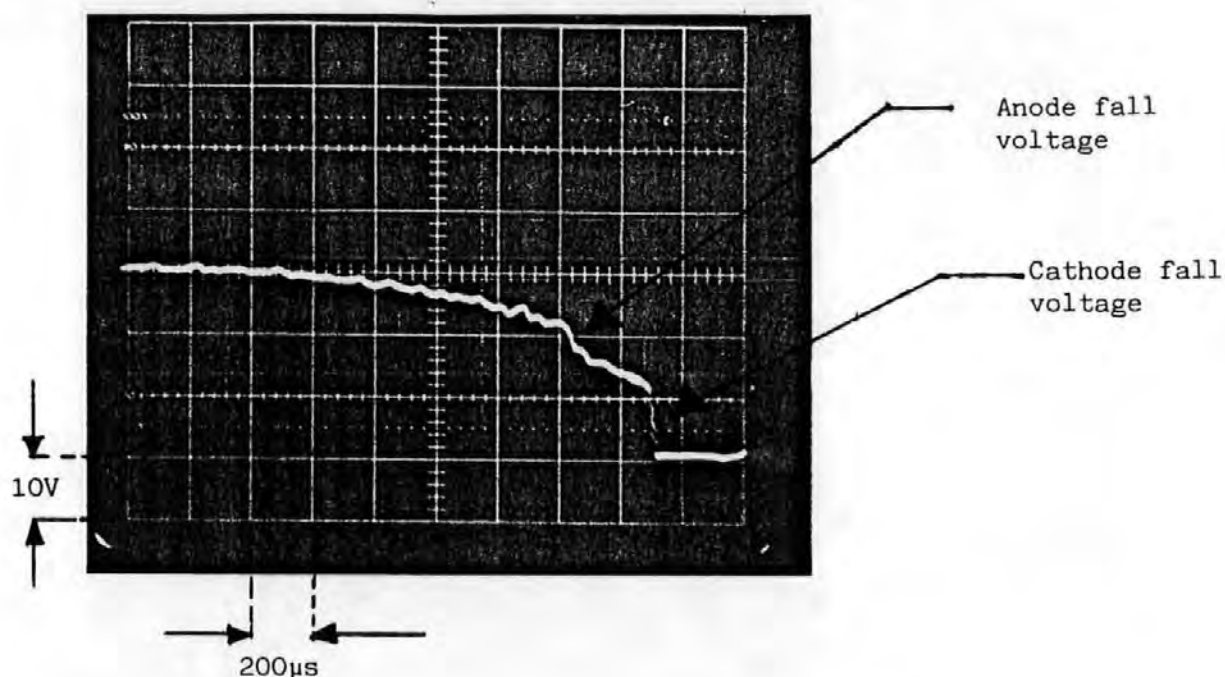
Here the effect of various parameters, such as speed of closure, operating voltage and the number of operations, on the magnitude of the voltage falls and over the distances which these steps occur have been investigated. Therefore the anode and cathode fall and arc voltages have been measured under the test conditions of 40 Volts d.c., 4 to 10 Amperes and gap-length of 0.05 and 1 mm, with opening speed of 300 mm/s.

4.3.1 EXPERIMENTAL DETAILS

The experimental apparatus used to determine the voltage drop is shown schematically in figure (3.1) of chapter three. The cathode and anode electrodes both have a diameter of 4 mm and rounded shape. They are held by a collet to the shaft; both are mounted horizontally. The fixed contact is the cathode.

The gap was set when an energised solenoid held the anode against a compressed spring, and the current was adjusted to a suitable value with electrodes in contact. The event was started by energising the solenoid which travelled up to the previously set gap. An arc was drawn across the gap, and after a predetermined delay of a second, set up by computer programme, the current into the solenoid was interrupted, the anode was released towards the cathode, and the characteristics of voltage versus time were recorded on the oscilloscope. The oscilloscope used was a 50 MHz Philips PM3055, and it was triggered externally. Each test was carried out on the new pair of contacts.

- (a) For a current of 3A, gap-length 3mm and speed of closure at 75mm/s.



- (b) For a current of 4 amperes, gap-length of 3mm and speed of closure at 75mm/s.

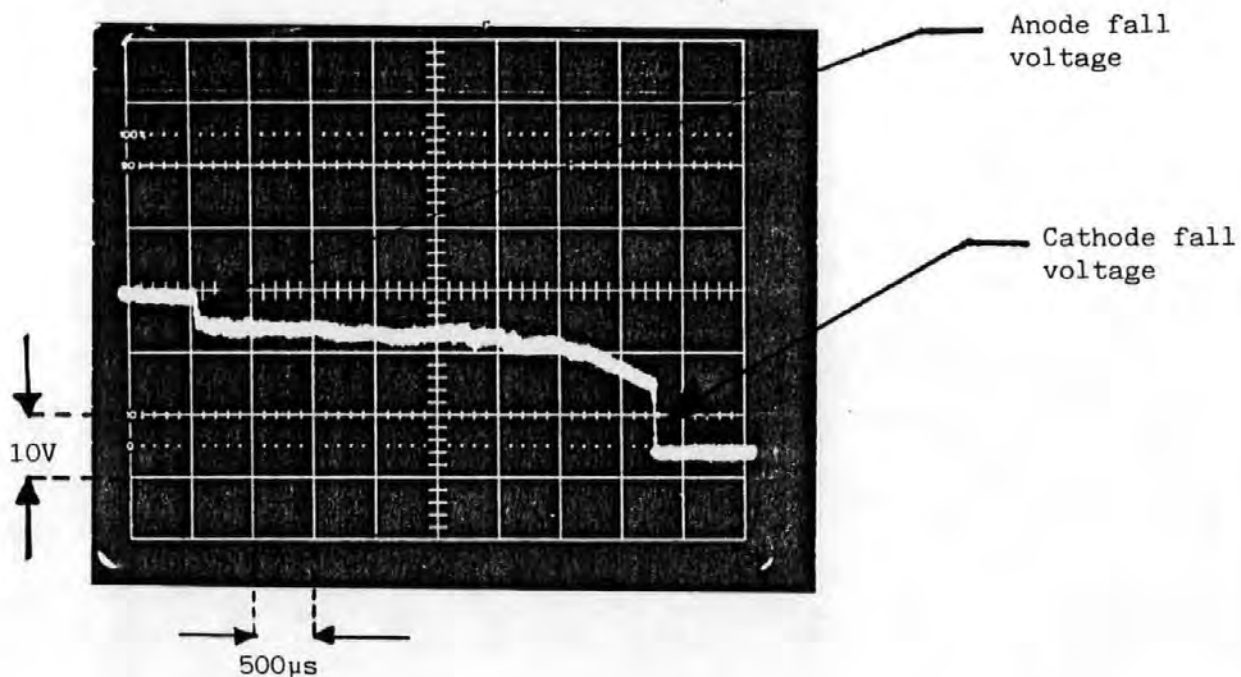
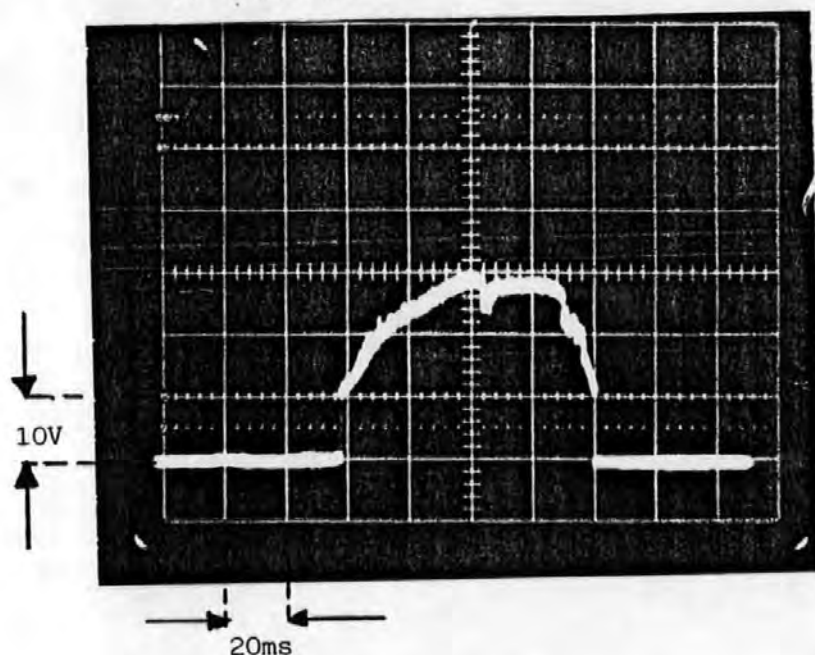


Figure 4.4: Photographs (a) and (b) represent the anode and the cathode fall voltages between Ag-Cd O electrodes, when contacts are closed after first establishing an arc between them at a fixed operating voltage of 40 volts.

- (a) The full event of the arc from initiation to extinction.



- (b) Portion of the above arc with expanded time scale

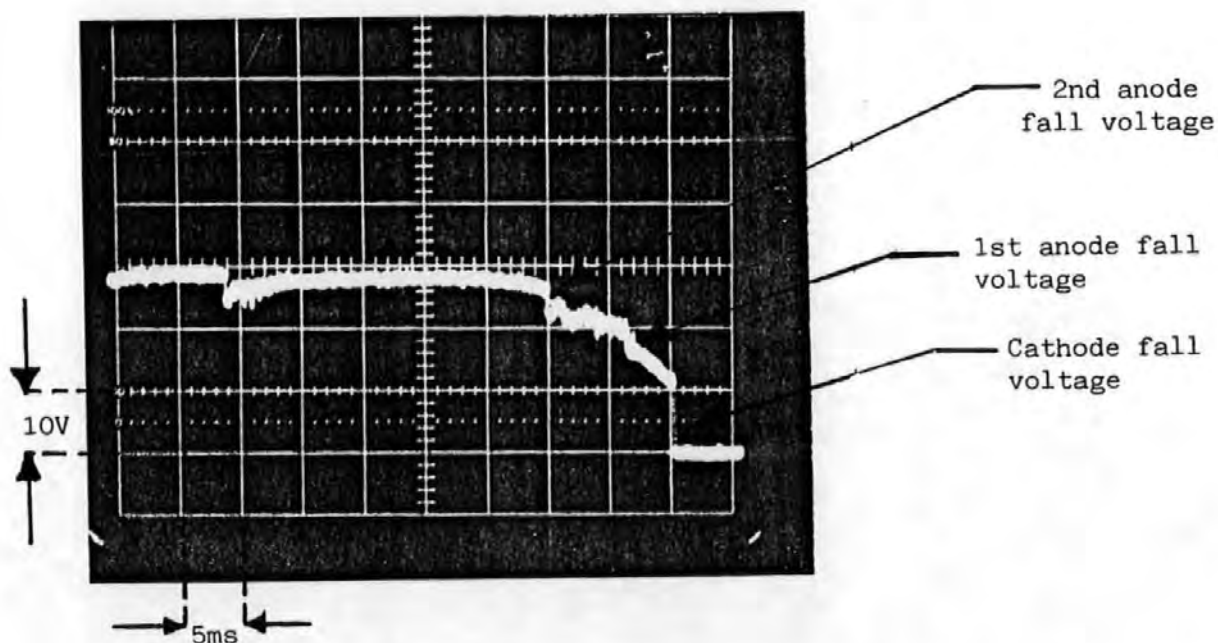
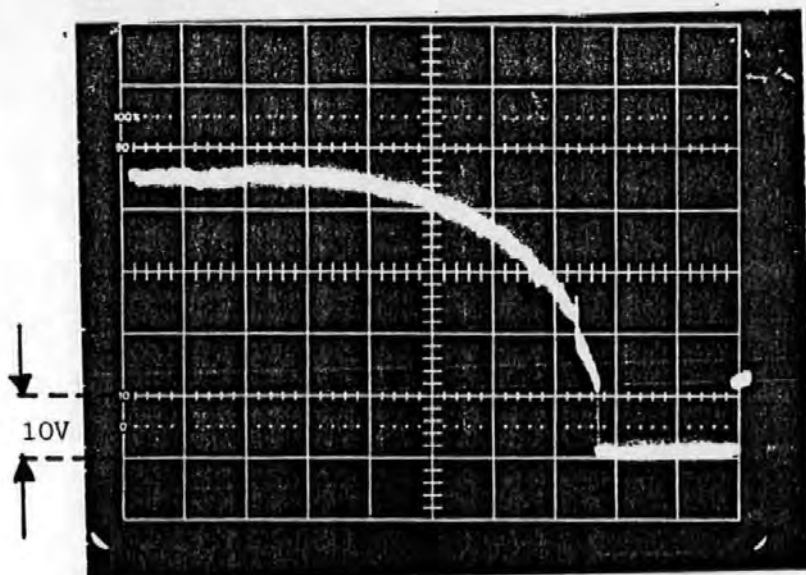
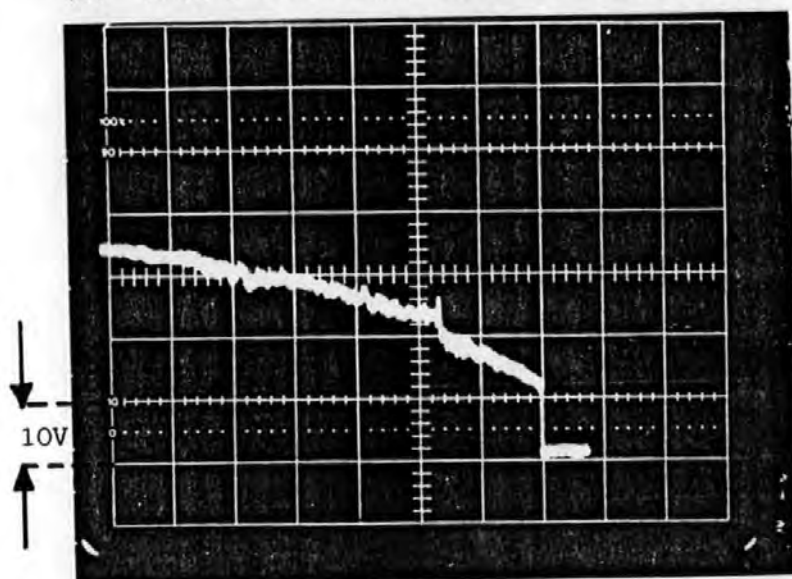


Figure 4.5: The oscilloscope record of the electrodes fall voltage measurement between Ag-Cd O contacts, as the anode is separated from the cathode and then driven back; at test conditions of 3mm gap-length, closure speed of 75mm/s, in atmospheric pressure and operating voltage of 40 volts.

(a) With a time scale of $500\mu\text{s}/\text{Div.}$



(b) With a five times faster time scale ($100\mu\text{s}/\text{Div.}$)



(c) With a ten times faster time scale ($50\mu\text{s}/\text{Div.}$)

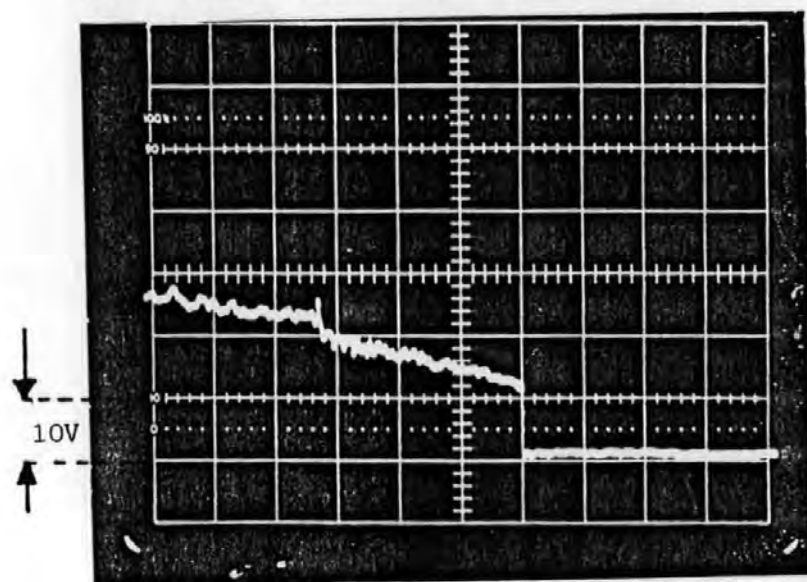


Figure 4.6: The anode and the cathode fall voltages versus time for the test condition of 50V, current of 4A, gap-length of 3mm and with a closing speed of 75mm/sec.

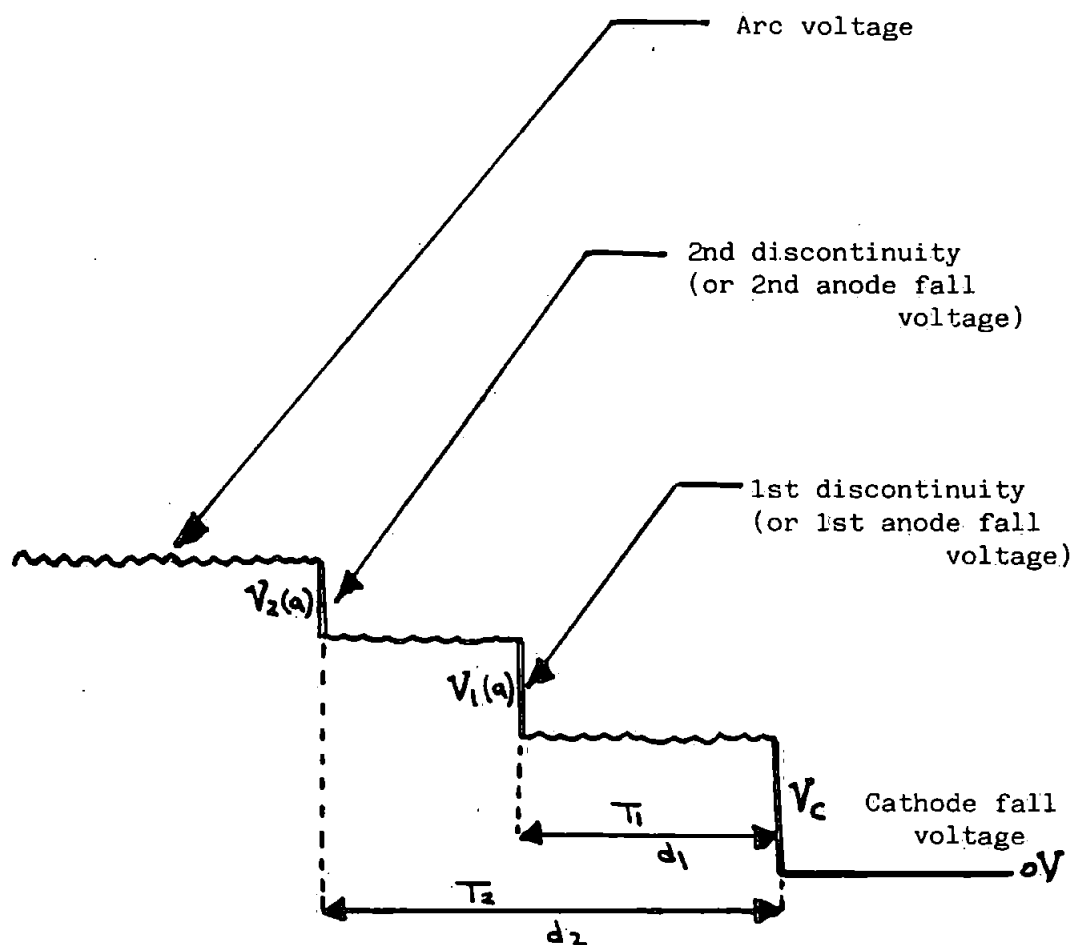


Figure 4.7: This represents diagrammatically the anode falls, the cathode fall and the distance in which the anode fall occurs from the cathode.

4.3.2 RESULTS, OBSERVATIONS AND DISCUSSION

A typical oscillogram of voltage when the anode is accelerated towards the cathode is shown in figure (4.4), in which the arc length decreases with diminishing electrode separation and discontinuity takes place in two steps. They occur very close to the electrodes and hence at a very short time from each other. The first is ascribed by Dickson et al⁽²⁾ to the anode fall and the second to the cathode fall. The above confirms the earlier workers' observation.

The oscillograms of figure (4.4) are for the test conditions of 40 V volts, current of 3-4 A and gap-length of 3 mm with speed of closure 75mm/s. It was observed that at this speed (75 mm/s) the occurrence of discontinuity becomes more regular when contacts have already performed over 1000 operations. This may be related to surface conditions, or conditions within the arc.

From careful observations of the photograph (figures 4.4-4.6) one can conclude that the amplitudes of cathode and anode fall voltages decrease slightly with increases in the currents for the same test conditions, but variations in amplitude of the falls were not detected at the above operating voltages.

The photograph of figure (4.5) illustrates the oscillogram of a full event of opening and closing, which reveals that at the moment the anode (moving contact) changes its direction, moving towards the cathode, the arc voltage decreases and then curves, and the two discontinuities occur away from the cathode fall. The first (nearer to the cathode) occurs at a distance of 180 μm from the cathode and the second at 750 μm .

The anode fall voltage, the cathode fall voltage and the distance in which anode fall occurs from the cathode are shown in figure 4.7.

Research into the effect of speed (75 and 300 mm/s) on the occurrence of these discontinuities has also been considered, and the results are shown graphically in figure (4.8a), for the test condition of 40 Volts, 4 A and 1 mm gap-length, with over 30 tests at each speed.

Figure (4.8a) shows that speed has no influence on the distance of the first step

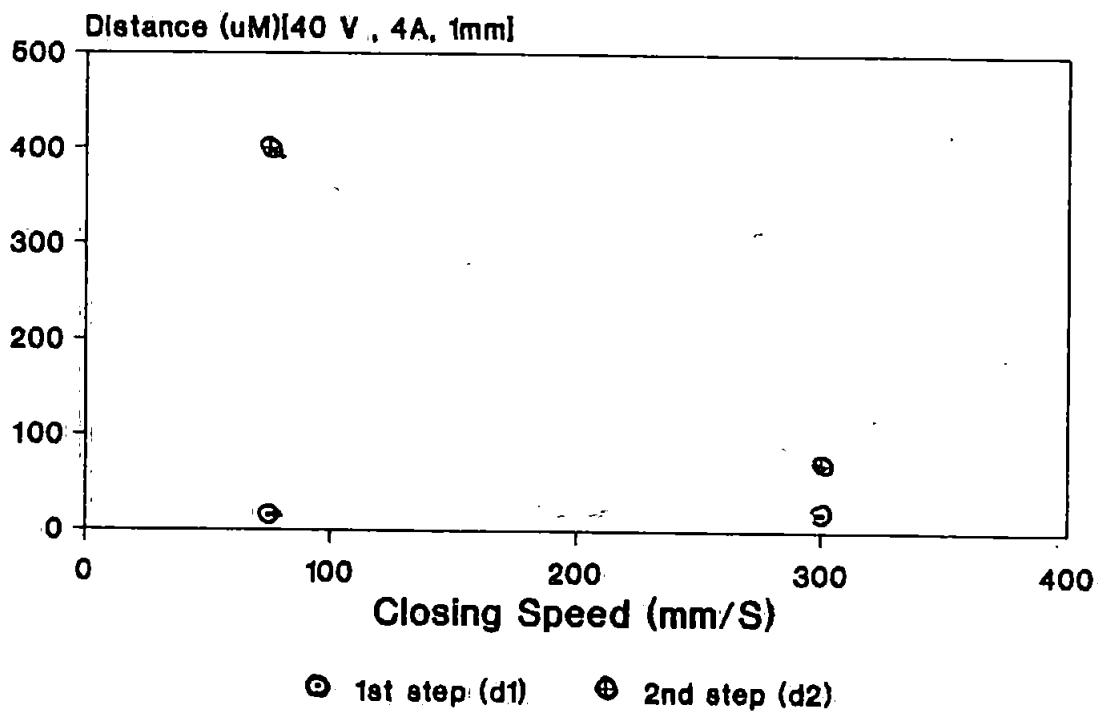


Figure 4.8a: Shows the average value of d_1 and d_2 taken from 30 operations for each speed; all on the same contact. (d_1 and d_2 are the distance from the cathode.)

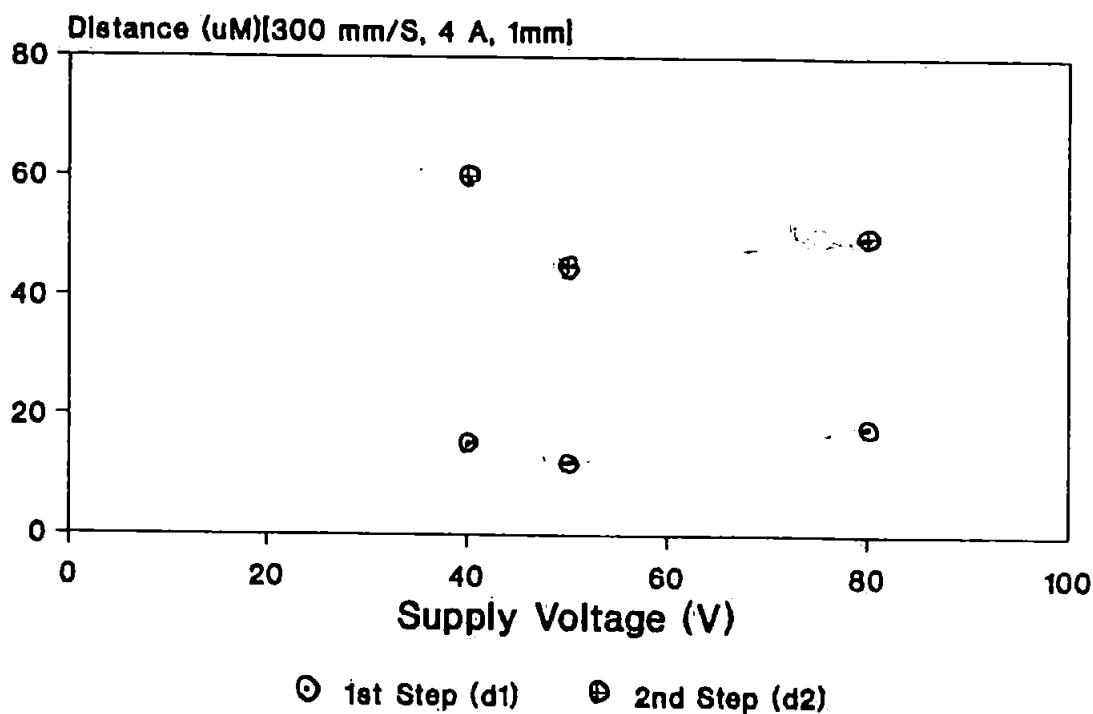
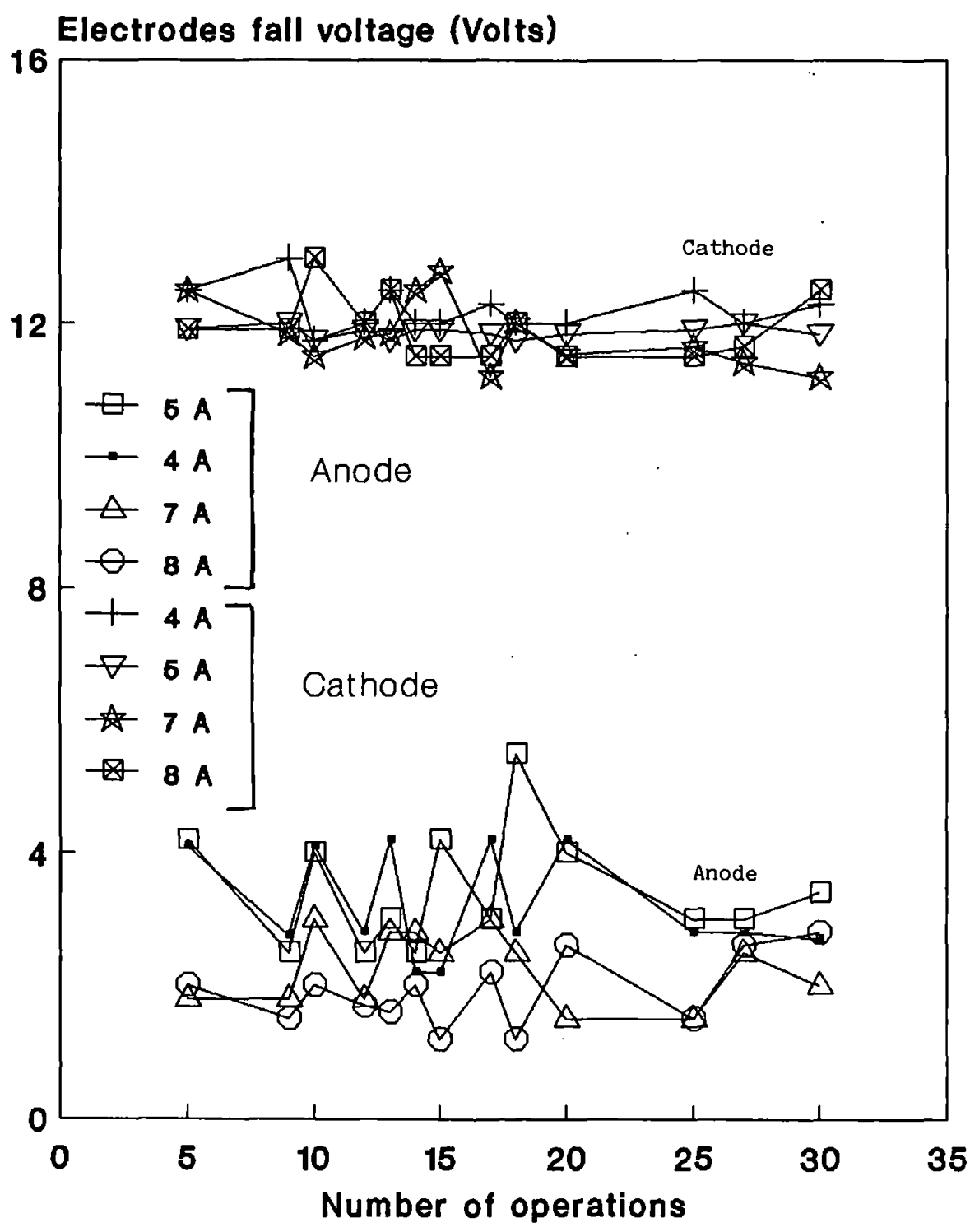


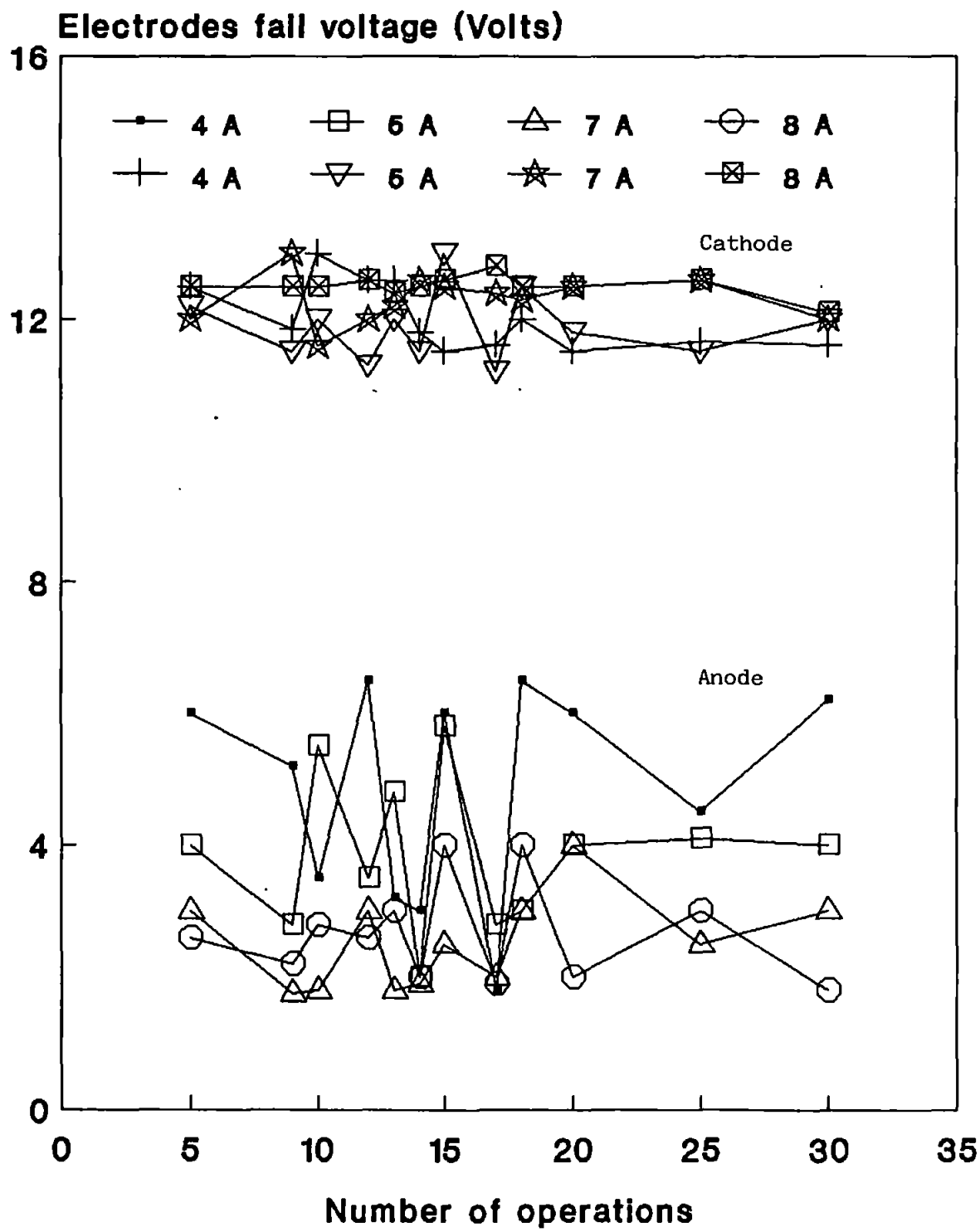
Figure 4.8b: Shows the average value of the 1st and 2nd steps, taken from 30 tests for each voltage; all on the same contact. (d_1 and d_2 are the distance from the cathode.)

Figure (4.10): Graphs of (a-d) show variation of anode and cathode fall voltages with number of operations at a test condition of 80 volts, current of 4-8A, and gap-length of 1-2mm.

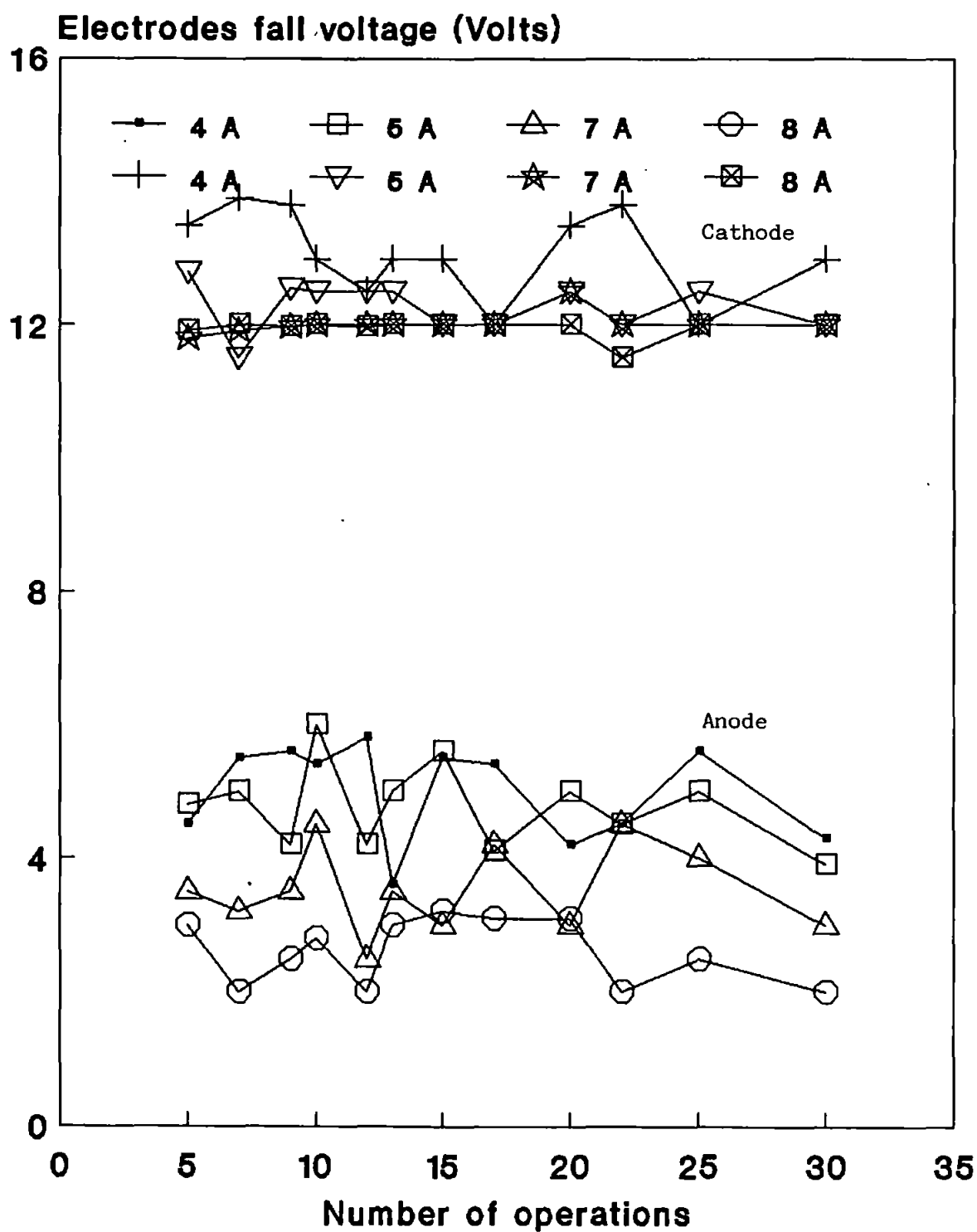
4.10a : Electrodes fall voltage versus the number of operations at a gap-length of 1mm and a current of 4-8A.



4.10b : Electrodes fall voltage versus the number of operations at a gap-length of 1.25mm and a current of 4-8A



4.10c : Electrodes fall voltage versus number of operations for gap-length of 1.5 mm.



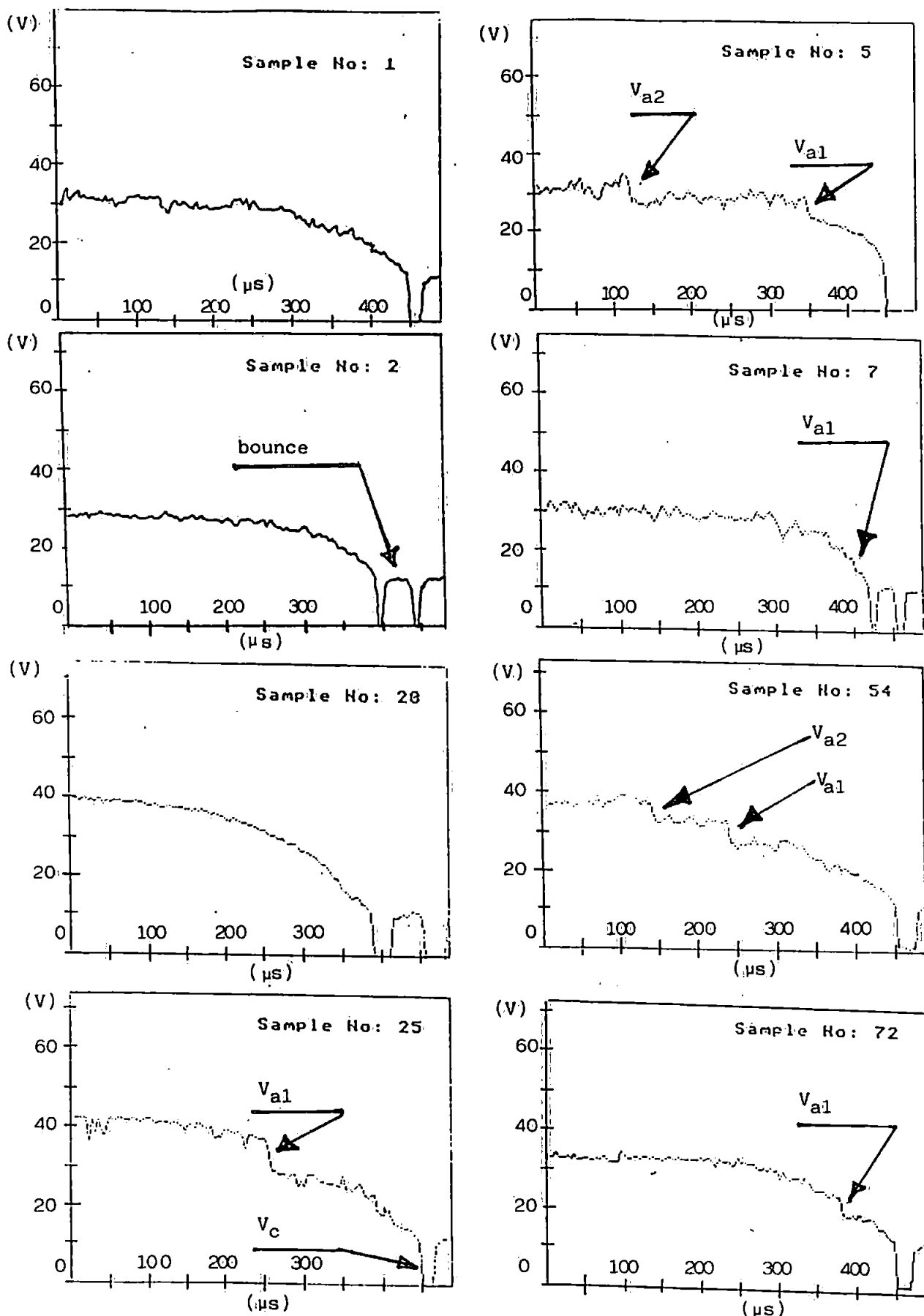
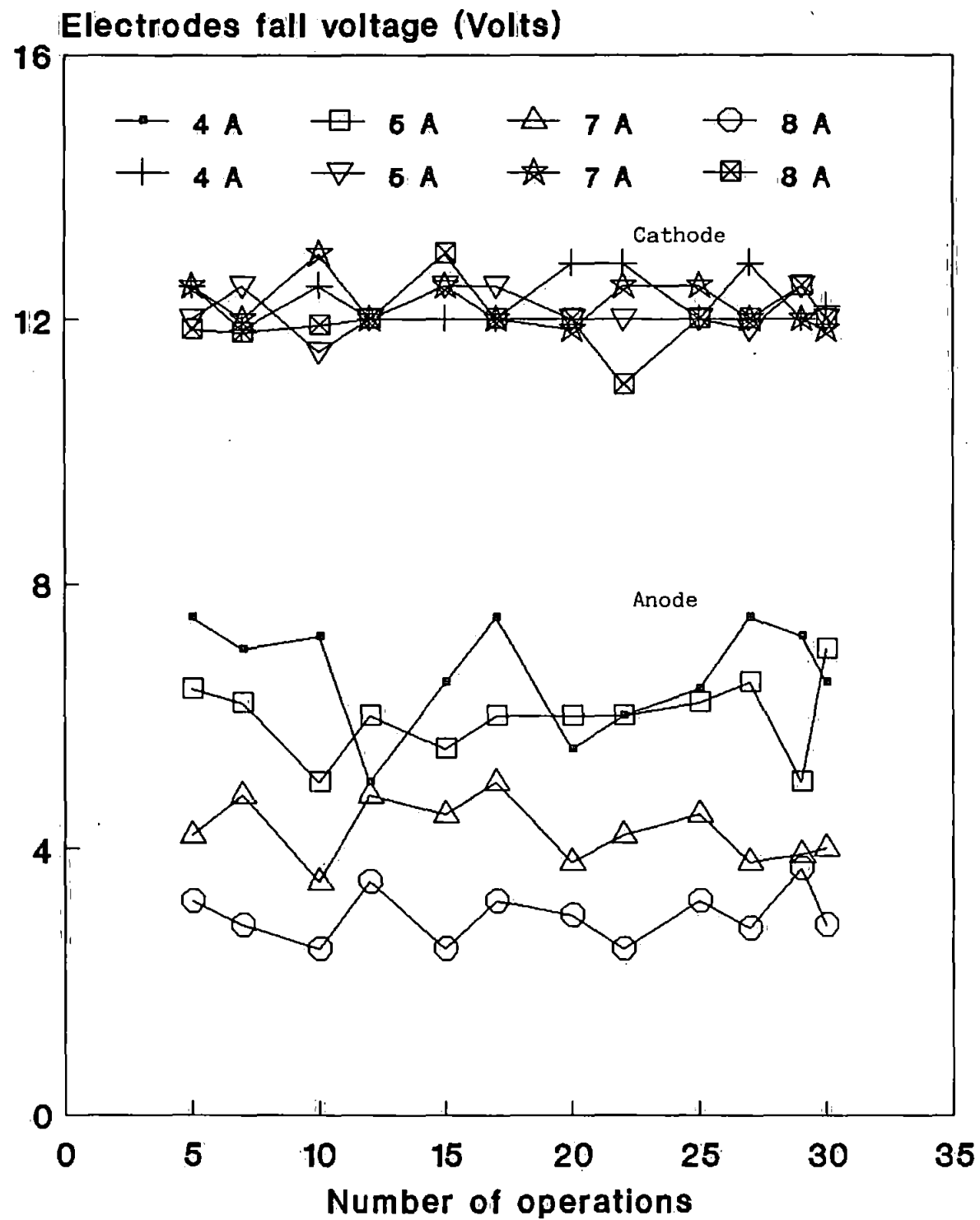


Figure 4.9: Shows the amplitude and the number of occurrences of the anode falls against the number of operations at test conditions of 80 volts, current of 4A, gap-length of 1.7mm, with a speed of closure of 300mm/s. Samples 1, 2 and 20 show the anode fall is absent. Samples 5, 25 and 54 show the anode fall can occur in 2-steps. Sample 72 shows small potential drop at the moment electrodes touch.

4.10d : Electrodes fall voltage versus the number of operations for a gap-length of 2mm and a current of 4-8 A



(i.e. d1) from the cathode; but the second discontinuity (2nd anode fall) at the faster speed (300 mm/s) occurs within a few tens of microns, as opposed to a few hundreds of microns, for slower (75 mm/s) closing speed. So this suggests that the speed determines where the second discontinuity should occur. Also, observations on the large number of oscillograms revealed that speed has no effect on the magnitude of the falls.

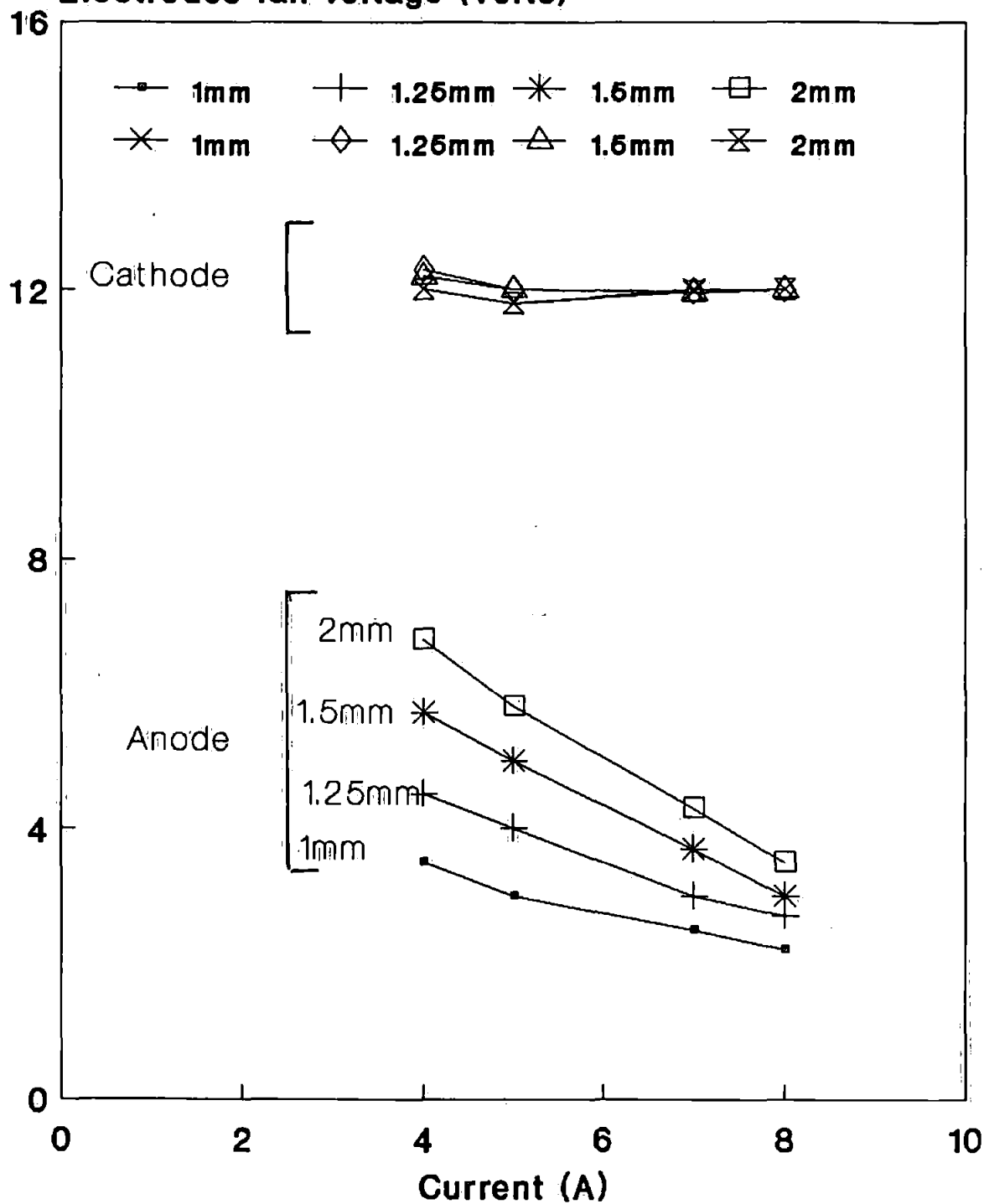
The effect of higher operating voltages on the distance over which these discontinuities occur has been considered for the test conditions of 40, 50 and 80 Volts, 300 mm/s, 4 A and 1 mm gap-length. The average distance from 30 tests for each operating voltage on the same contacts is shown graphically in figure (4.8b). These graphs suggest that different operating voltages have no influence on the occurrence of these discontinuities.

To study the effect of the number of operations on the fall values, a series of tests at 80 V, 4 A, 1.7 mm with speed of 300 mm/s was carried out. The results are shown in figure (4.9). They are interesting in that anode fall in some cases is absent or occurs in the form of single or double discontinuities. Therefore it was decided that for the test conditions of 80 Volts, 4 to 8 A and gap-length of 1 to 2 mm, the readings of the anode fall and the cathode fall be taken over 30 samples (tests). This information was then plotted against the number of operations (tests) from which the average values are obtained. The spread of values is small enough for the average value to be taken as representative. These results are shown in figure (4.10). The same method is used for every test condition. Figures (4.11-4.12) show the plots of the medians value of electrodes fall against current and gap-length, for operating voltage of 80 volts.

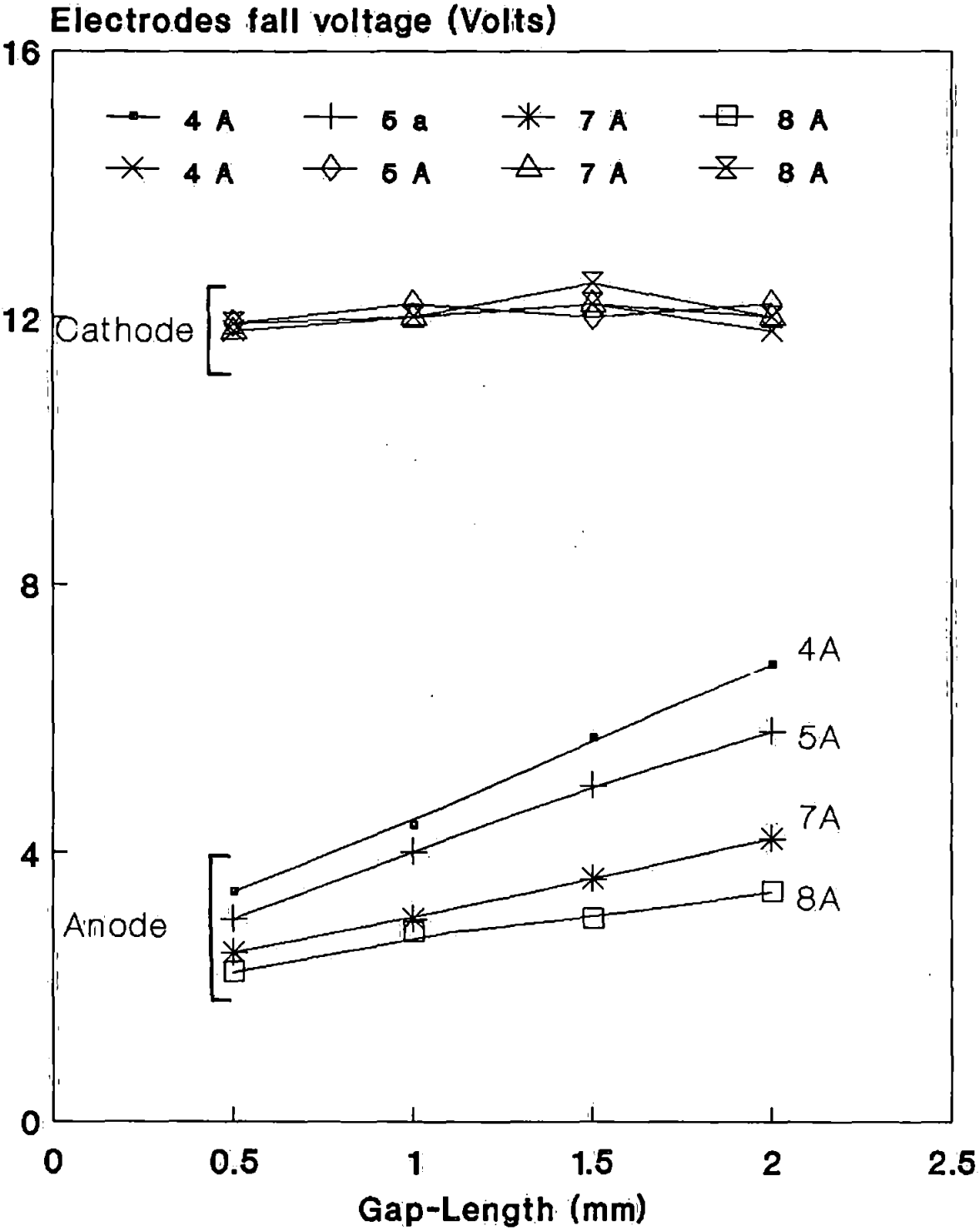
Observations of figures (4.11-4.12) suggest that the anode and cathode falls are increasing with gap-length and decreasing with currents, but the increase of the cathode fall is slight compared to the anode, in fact one can assume it is negligible.

Finally, a series of tests similar to the above have been carried out to measure anode fall, cathode fall and arc voltage for 40 V, 4 to 10 A and 0.05 to 1 mm,

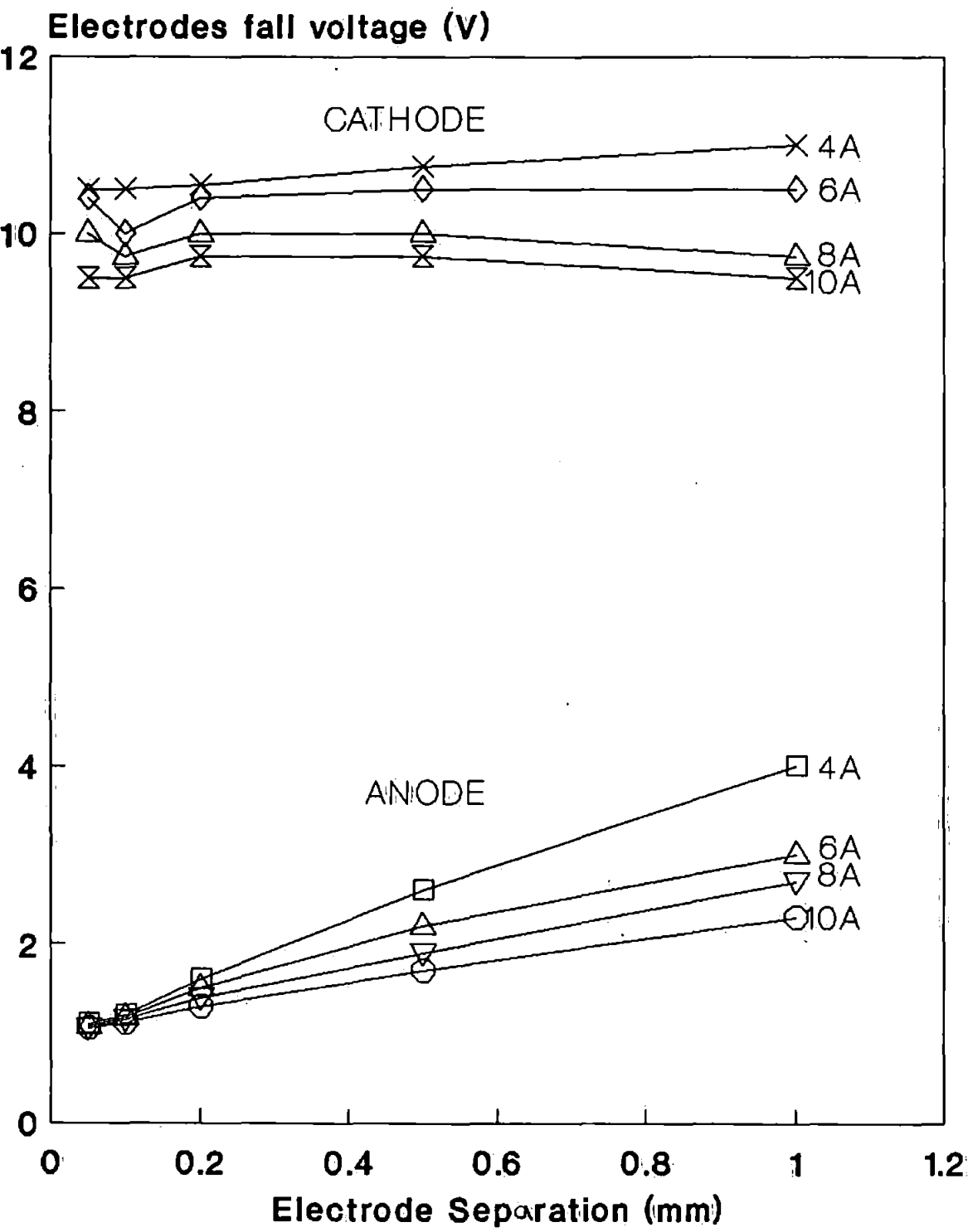
Figure (4.11) : Represents electrodes fall voltage versus currents for 80 volts supply and a gap-length of 1-2mm
Electrodes fall voltage (Volts)



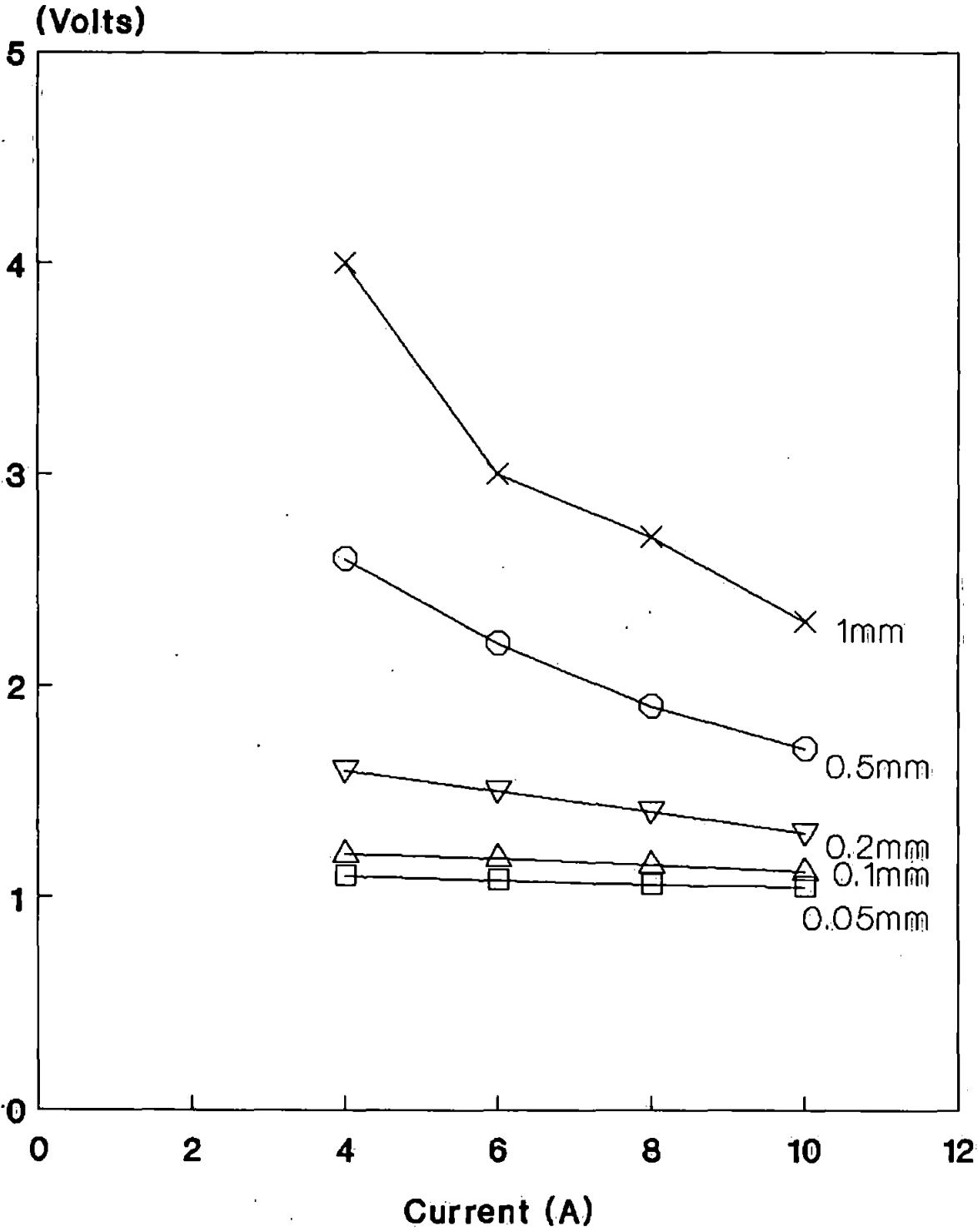
Figure(4.12) : Shows electrodes fall voltage against gap-lengths for a supply voltage of 80 and a current of 4-8A



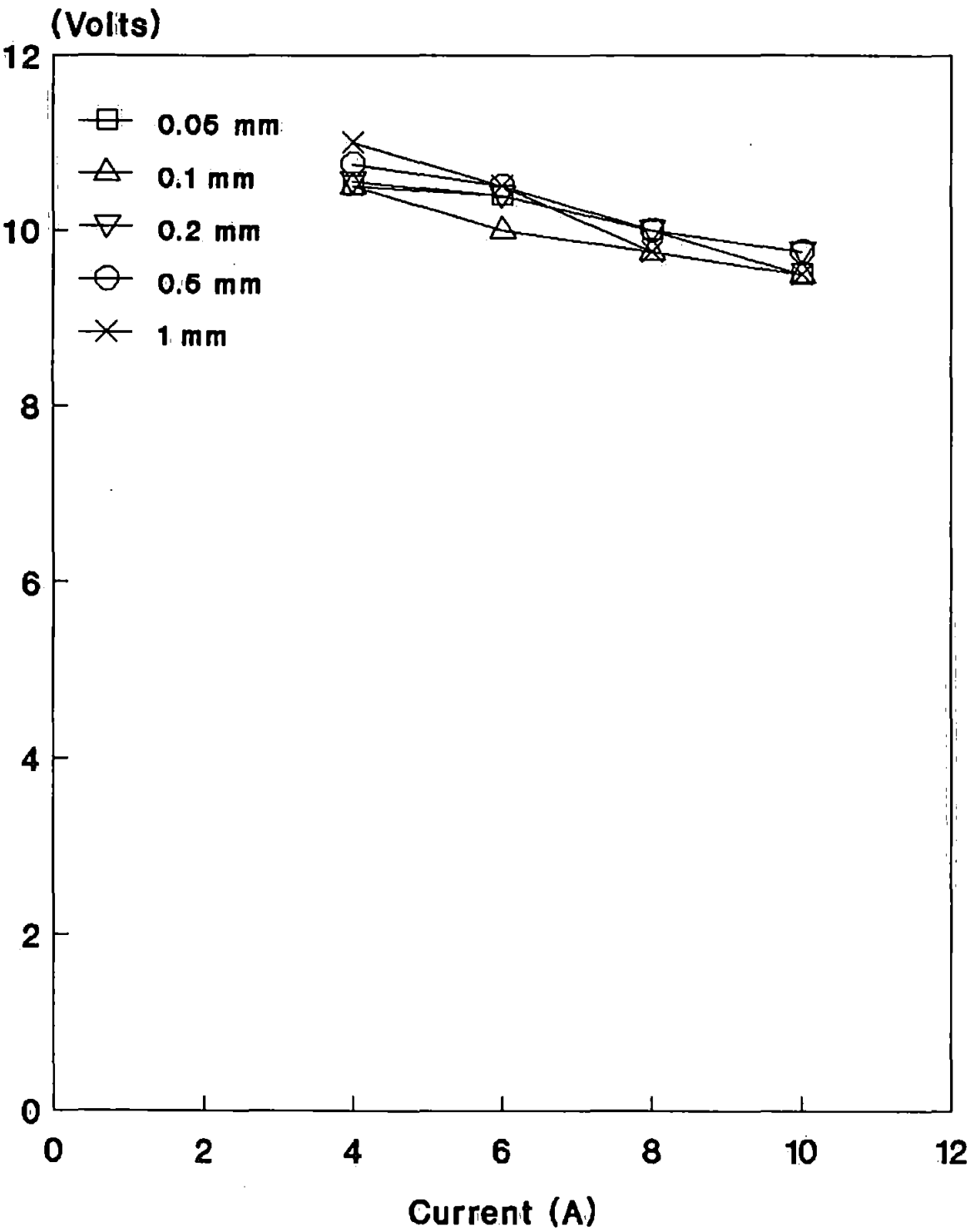
Figure(4.13) : Electrodes fall voltage versus gap-lengths for a supply voltage of 40V and a current of 4-10A.



Figure(4.14) : Shows the anode fall voltage versus currents for a supply voltage of 40V and a gap-length of 0.05-1mm.



Figure(4.15) :Shows the cathode fall voltage versus currents for a supply voltage of 40V and gap-length of 0.05-1mm.



with speed of 300 mm/s. This is the condition used for temperature measurements from which, in the power balance relation, the electrical power for each gap-length has been evaluated. The results are shown graphically in figures (4.13-4.17).

Figures (4.13-4.15) exhibit similarities to figures (4.11 and 4.12); the anode and cathode fall voltage increasing with the gap-length and decreasing with the current. But, the values of cathode and anode fall are less at 40 Volts compared to at 80 Volts. This may be due to a difference in the number of positive and negative charges in the transition regions.

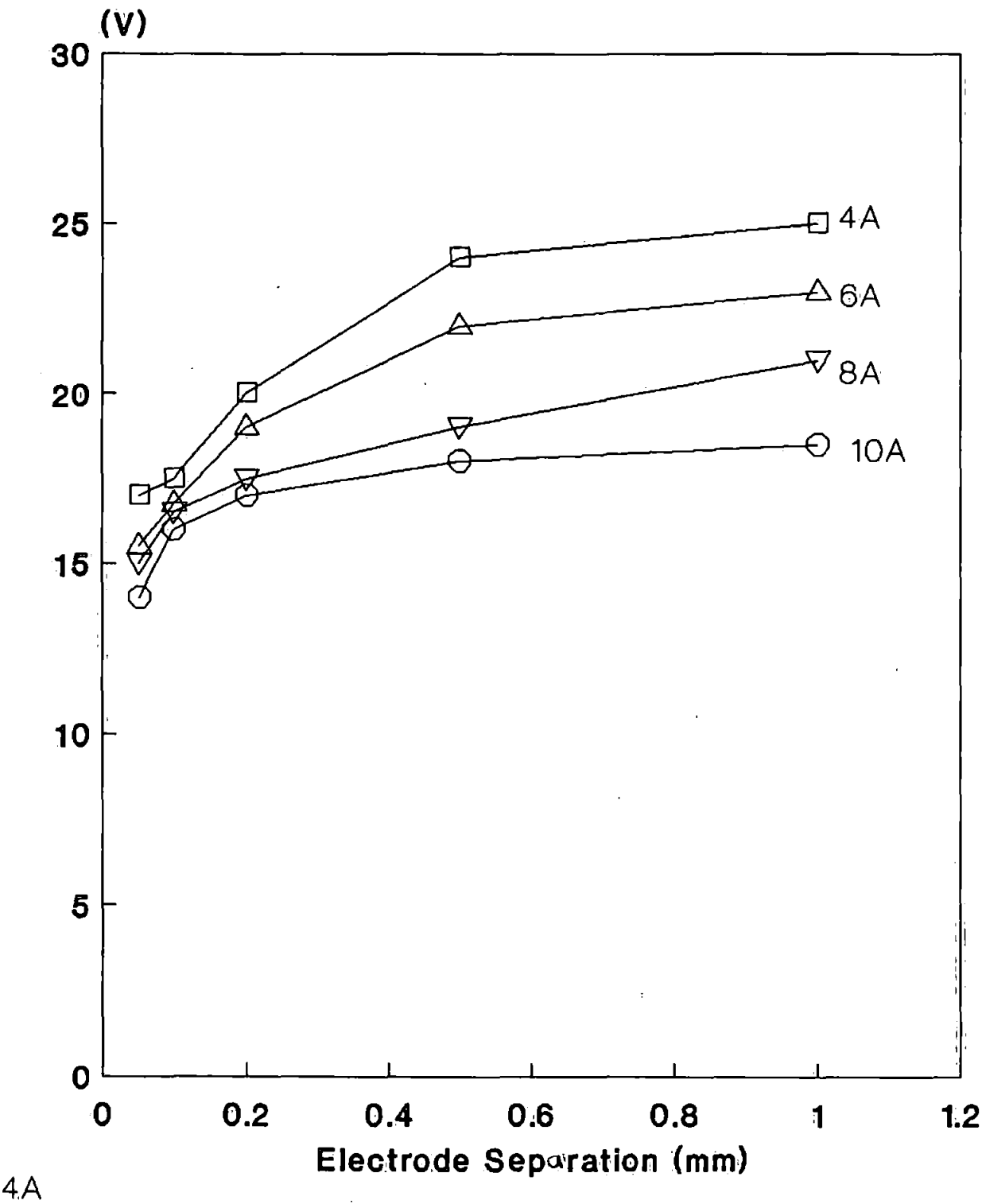
Why the electrode fall increases with the gap and decreases with the current may be due to the following explanation: at larger gaps, charges between the electrodes tend to have a wide distribution in the transition regions, as a result there are higher differences between the numbers of these charges in those regions, which consequently leads to higher voltage drops across these transition regions (this process is shown schematically in figure 2.4, and discussed in section 2.5.1 of chapter two).

The decrease of fall voltages with increase of current for a fixed test condition may be due to that at higher current the current density on the cathode is high, so that less cathode fall voltage is essential for maintenance and initiation of the arc. Similarly, less anode fall voltage may be required for the continuity of the arc. If this is the case that may be the reason why at higher current the anode fall in most cases occurs in one step or is totally absent. Therefore, at lower current, V_a has a more important role to play for continuity of the arc than at higher currents.

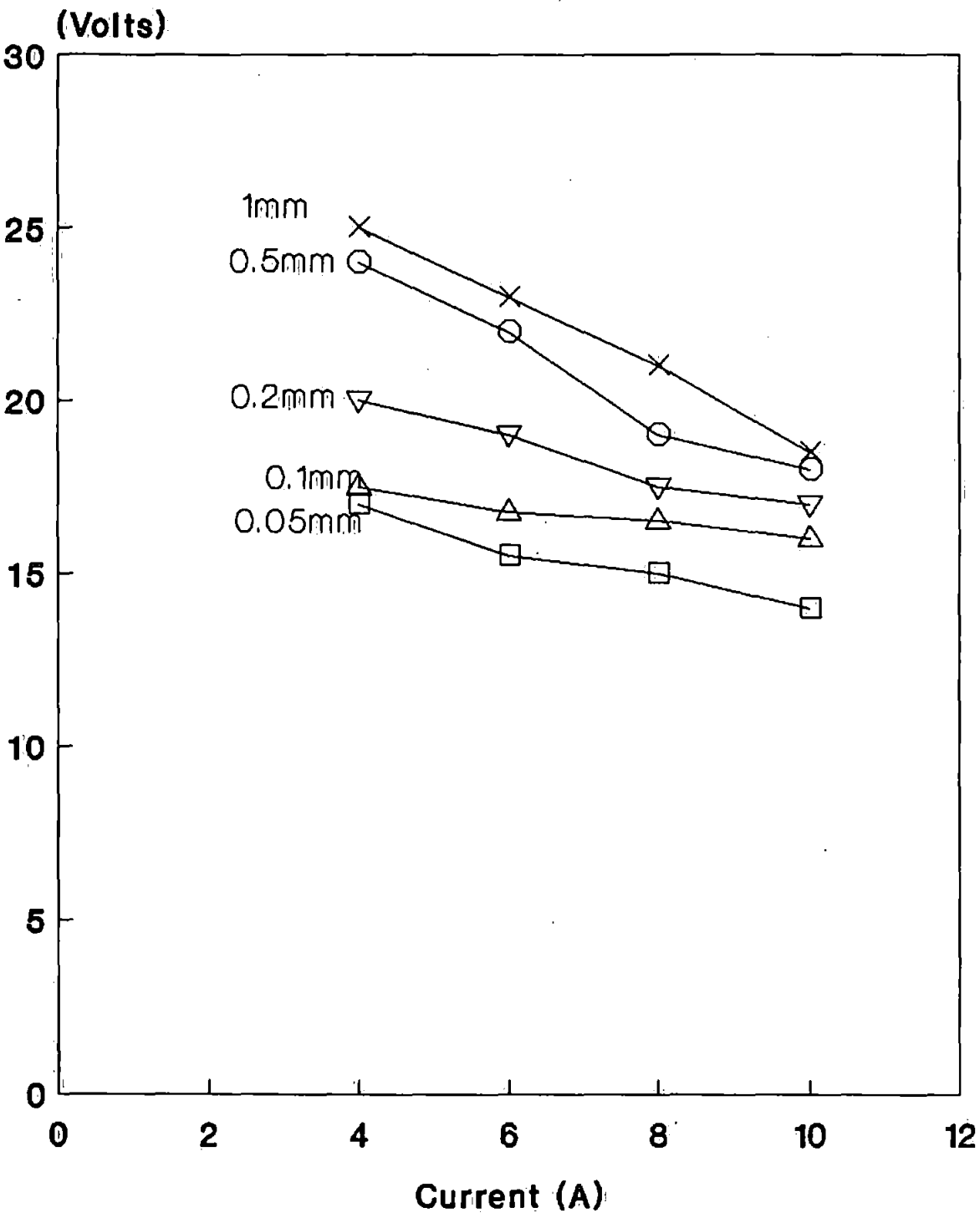
Maecker⁽³⁾ suggests that at larger currents an intense jet from the cathode develops, which has a high velocity, to retard the positive ions moving towards the cathode. Hence, because of neutralisation of the electron space charge by slowed-down positive ions, the development of anode fall may become limited, or not take place at all.

Zhu and Von Engel⁽⁴⁾ suggest that the reason anode fall is small is possibly due to the presence of high vapour density close to the cathode which limits its development and range.

Figure(4.16) : Arc voltage versus electrodes separations for a circuit voltage of 40 volts and a current of 4-10A.



Figure(4.17) : Arc voltage versus currents for a circuit voltage of 40V and a speed of opening of 300mm/s.



A close inspection of samples 1, 2 and 20, figure (4.9), reveal that the anode fall is absent, or it is so small that it is not possible to detect it (in the order of fluctuation voltage magnitude). Dickson et al⁽²⁾ have suggested that, when the electrode separation becomes so small the electron carrying the arc current can reach the anode, without positive ions being repelled from its surface, this is due to the electrons very close to the anode not having a sufficiently large uniform axial velocity component. The magnitude of the anode fall depends on the energy used for repelling ions, therefore anode fall cannot be developed.

Zhu and Von Engle⁽⁴⁾ also related the absence of the anode fall to variations occurring on the electrode surfaces. Figure (4.9), which represents typical characteristics of the fall measurements, shows that the anode fall can occur in two steps. In general those occurring very close to each other are from 10 to a few tens of microns from the cathode, and in those which are not very close to each other the first step is about 15 μm , and the second about 100 μm , from the cathode surface. So, it may be possible to classify them in a way that those occurring at a few tens of microns from the cathode surface belong to the second step. The first may have taken place within 15 μm , but because its value is similar to the fluctuation voltage, it is difficult to distinguish it.

Another observation is that since for a particular gap or current the anode fall is constant, if it occurs in the form of two discontinuities, its total value is the sum of those two discontinuities. Typical examples are shown in samples 5, 25 and 54, of figure (4.9).

The reason why anode fall voltage occurs in one or two distances from the cathode may be explained as follows: since the value of the anode fall voltage depends upon the energy required to repel the ions from the anode, and the existence of ions ensures the continuity of the arc, one may assume that where the above condition prevails, in which there is lack of ions, the anode fall voltage will occur.

So, according to the above hypothesis, the anode fall can occur in many steps if it is required by the condition of the arc; but the maximum discontinuities observed

were two. Finally, observations on all sets of graphs at different current and gap-length confirmed that at speeds of 300 mm/s the first anode fall voltage occurs at a distance of about $15\mu\text{m}$ and the second at a distance of a few tens of microns, which is in complete agreement with the earlier statement that speed determines the distance at which the anode fall occurs from the cathode surface.

Zhu et al⁽⁴⁾, in their experiments, found that the cathode fall voltage, and its space value, are independent of the velocity of the moving anode.

During the course of fall measurements, voltage fluctuation has also been observed in some voltage traces with magnitude of 2 to 3 Volts. A typical example can be seen clearly in figures (4.6) to (4.9).

Dickson et al⁽²⁾ have suggested since the fluctuations are absent with arcs between carbon electrodes but present in metal vapour arcs, therefore they are due to cathode processes such as erratic spot movements or ejected lumps of metal crossing the cathode fall space. Boddy and Utsumi⁽⁵⁾ suggested that the fluctuations of arc potential are caused by metal vapour diffusion in arcs. Boylett and Maclean⁽⁶⁾, in their work on mercury arcs, suggested that the small fluctuations, which were found to persist up to the instant of electrical contact between the electrodes, were about 0.3 Volts in magnitude, and were believed to have been caused by small movements of the cathode spot, or variations in the rate of evaporation of mercury from the cathode surface.

A closer inspection of the voltage traces of figure (4.9), samples 7, 25 and 72, indicate that a small potential drop persists at the moment when the electrodes touch. Dickson et al⁽²⁾ related this to a constriction resistance of the microscopic points making the contact. The findings of the other researchers about the present investigation are discussed in chapter two, sections 2.5.1.1 and 2.5.1.2.

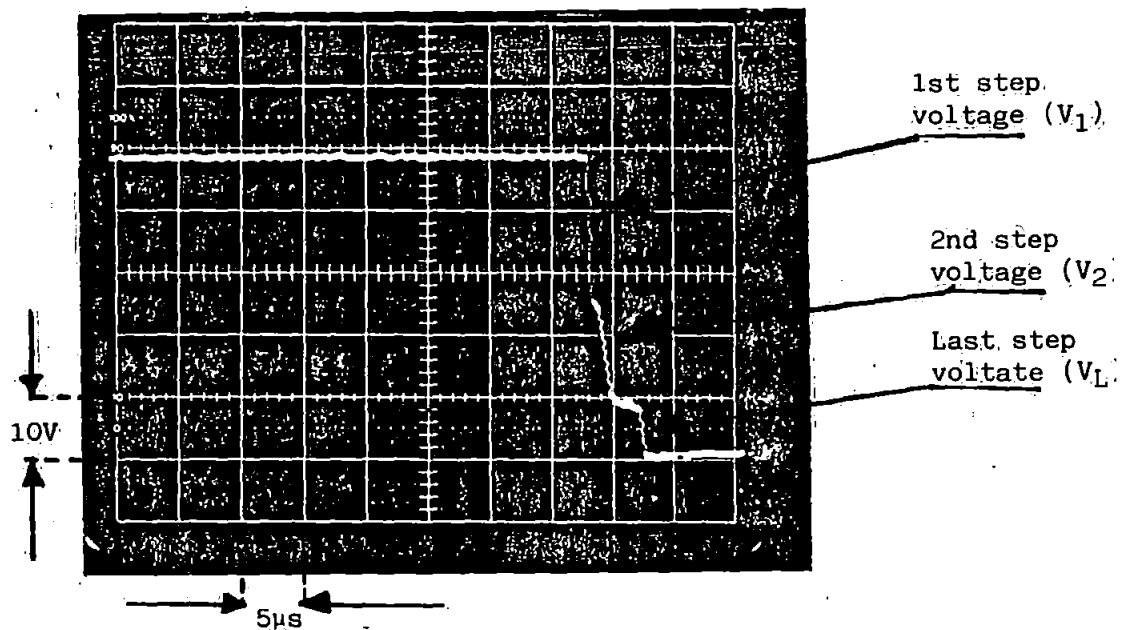


Figure 4.18: Shows a photograph of a typical voltage step observed at closure for an operating voltage of 50 volts, a current of 5A and a speed of 500mm/s.

4.4 ARCING AT CONTACTS ON SNAP-ACTION SWITCHES

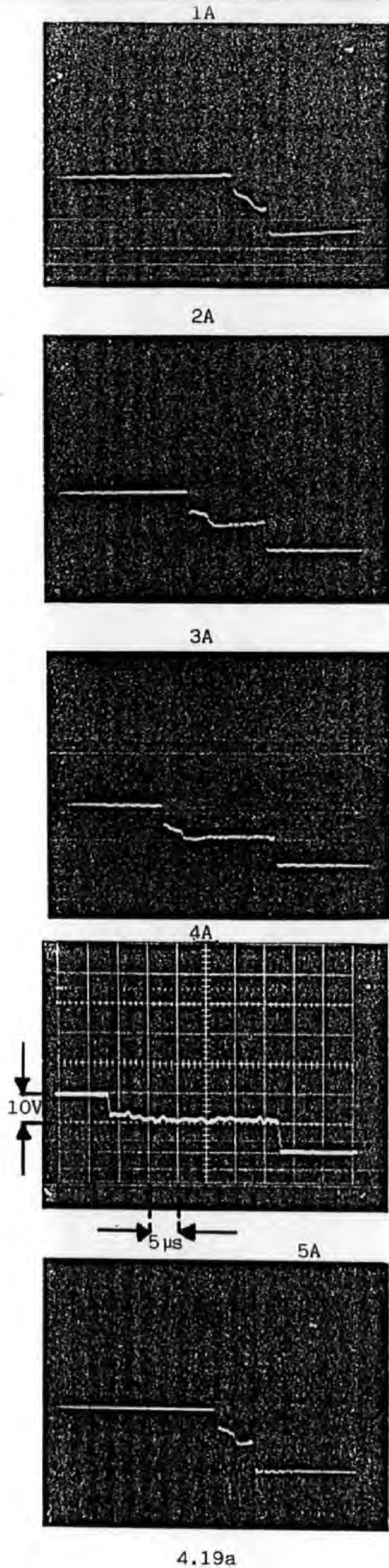
ON CLOSURE: VOLTAGE STEP PHENOMENA

Oscilloscope records of the potential across the contacts of a model switch used in this reasearch, on closure, have yielded a phenomenon in which discontinuity is observed within the drop voltage before closure, and this is named as the Voltage Step phenomenon. Figure (4.18) shows a typical voltage step. The above phenomenon was observed during measurments of anode and cathode fall voltages at operating voltage of 40 Volts, and a gap-length which was greater than ^{the} arc length, in which case the fall measurements when the contacts break is not possible. However arcing on closure of electric contacts has been known since the beinginning of this century and it is recognized that this is the main cause of material transfer from one electrode to the other, but, despite its catastrophic effect, the nature of this arcing is not yet fully explained.

Various arguments have been put forward, for example Earhart⁽⁷⁾, Shaw⁽⁸⁾ and Pearson⁽⁹⁾ have suggested that arcing over a very short gap on closure is not due to voltage breakdown.

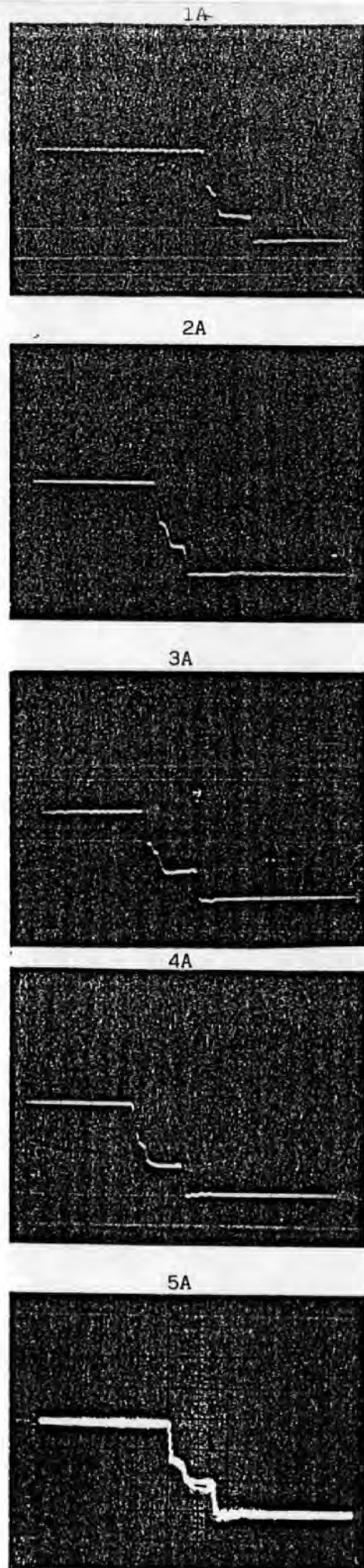
Compton⁽¹⁰⁾ and Mackeown⁽¹¹⁾ from a series of tests have suggested that for mercury arc and for arcs of low boiling point metals the discharge occurs by field emission.

In 1949 Bell Laboratories' Germer and Hawarth⁽¹²⁾, in the study of erosion on make in low voltage relay contacts used in the telephone system, observed the effect of a capacitor which had been connected across the relay for the purpose of minimising the voltage rise when they separate. They found that when the contacts are brought together, the capacitor across them is discharged and this is the main cause of erosion in telephone switching systems. Since these arcs occurred in air at potentials as low as 30 Volts, which is far below values of minimum sparking potential, their attention was directed to find out the nature of this discharge. They use crossed wires of the contact metal under investigation as their tool of research,



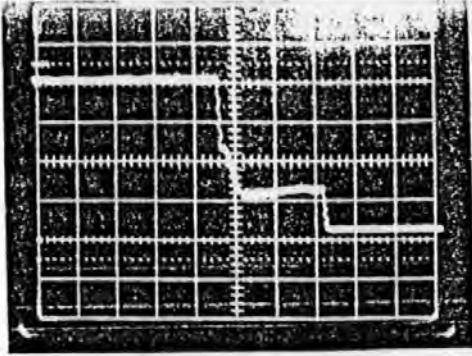
4.19a

Figure 4.19: (a-d) show the effect of different operating voltages and currents on the step phenomena observed on closure at a fixed test condition of 500mm/s and a gap-length of 3mm. (a): for 20 volts, current of 1-5A. (c): 40V, 1-5A.

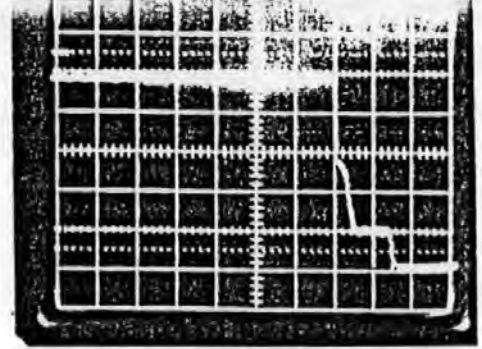


4.19b

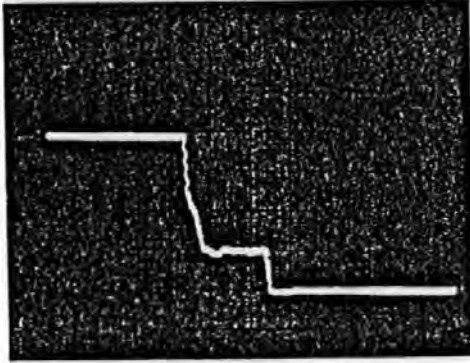
1A



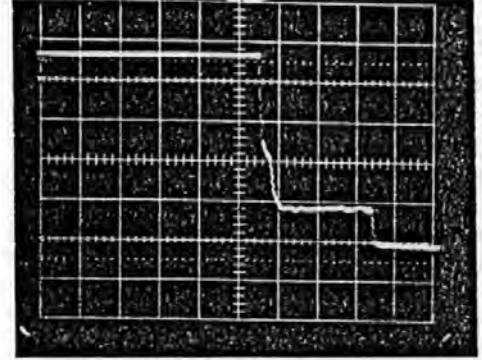
1A



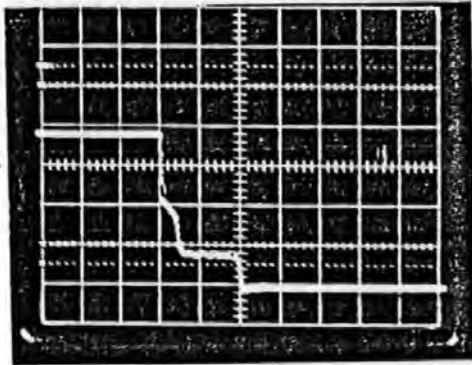
2A



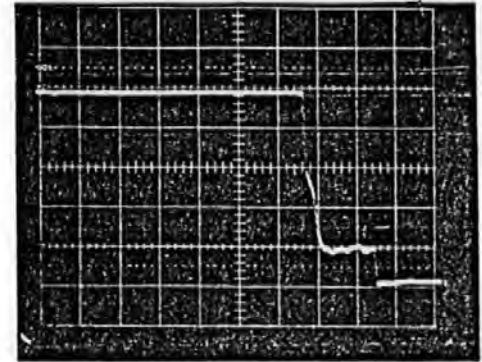
2A



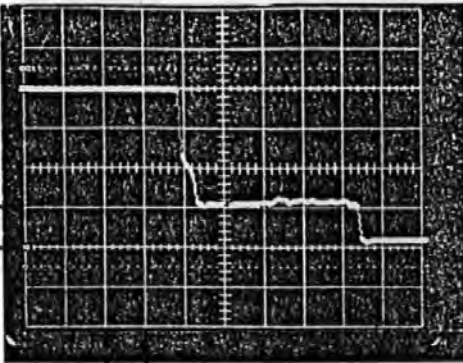
3A



3A

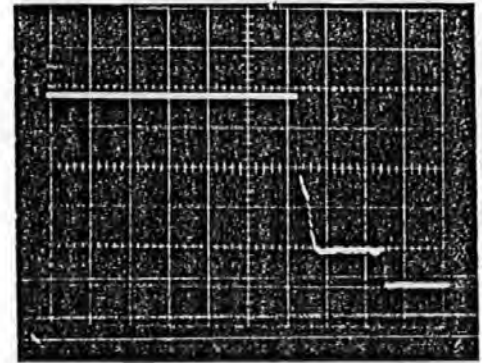


10V



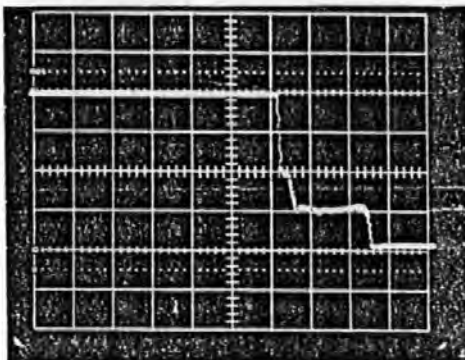
4A

4A

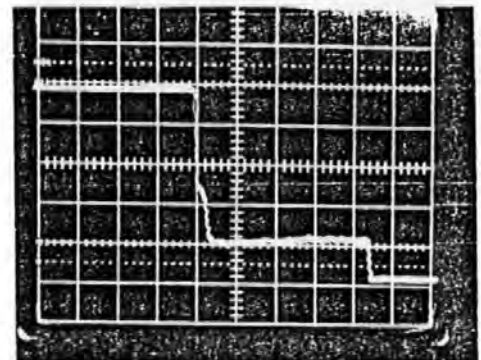


5μs

5A



5A



4.19c

4.19d

which were separated and brought together about 60 times per second by means of a magnetic loudspeaker unit. In the first approach⁽¹³⁾ the effect of various circuit parameters such as capacitor, inductor and resistor were investigated.

They describe that the effect of inductance is to limit the discharge current from the capacitor and the discharge time is determined solely by fixed circuit parameters.

They observed that in some cases several discharges took place before final closure. They related this to the capacitor being repeatedly recharged from the voltage source and the successive discharges depend on the values of capacitance, inductance, and resistance in the circuit, and the voltage source. Their view was supported by use of a camera from which photographs showed drop and opening in voltage traces. They also suggest that the natural capacity of wires may be sufficient for the above occurrence.

Since these discharges take place at separation of $1000 - 2000 \text{ \AA}$ ($0.1 \mu\text{m} - 0.2 \mu\text{m}$) ($1 \text{ \AA} = 10^{-10} \text{ m} = 10^{-4} \mu\text{m}$), and corresponding fields of $10.16 \times 10^6 \text{ V/cm} - 5.1 \times 10^6 \text{ V/cm}$ which showed that a progressively higher field was required for successive discharges. They related this to smoothing out or roughness on the cathode by each discharge which requires a different field in which case the discharge may be initiated by field emission of electron from the cathode due to the high field at the cathode. On the other hand, because of successive discharges these fields are 6 - 200 times smaller than known values for field emission to occur. So they decided to investigate the concept of the metal thrown up from the anode pit bridging completely across to the other electrode. This led to a new interpretation that if the metal bridge is so narrow, the flow of current through it promptly burns out this bridge, and as a result an arc of brief duration will follow and therefore the successive discharges may be due to more than one closure taking place and the bridge being burned out by the current flowing through them. In the AC case they observed that if a closure lasts more than $1/2$ cycle it becomes permanent; but most burn out within a $1/2$ of the $1/2$ cycle.

They concluded that the concept of thrown up metal is not the usual way for a

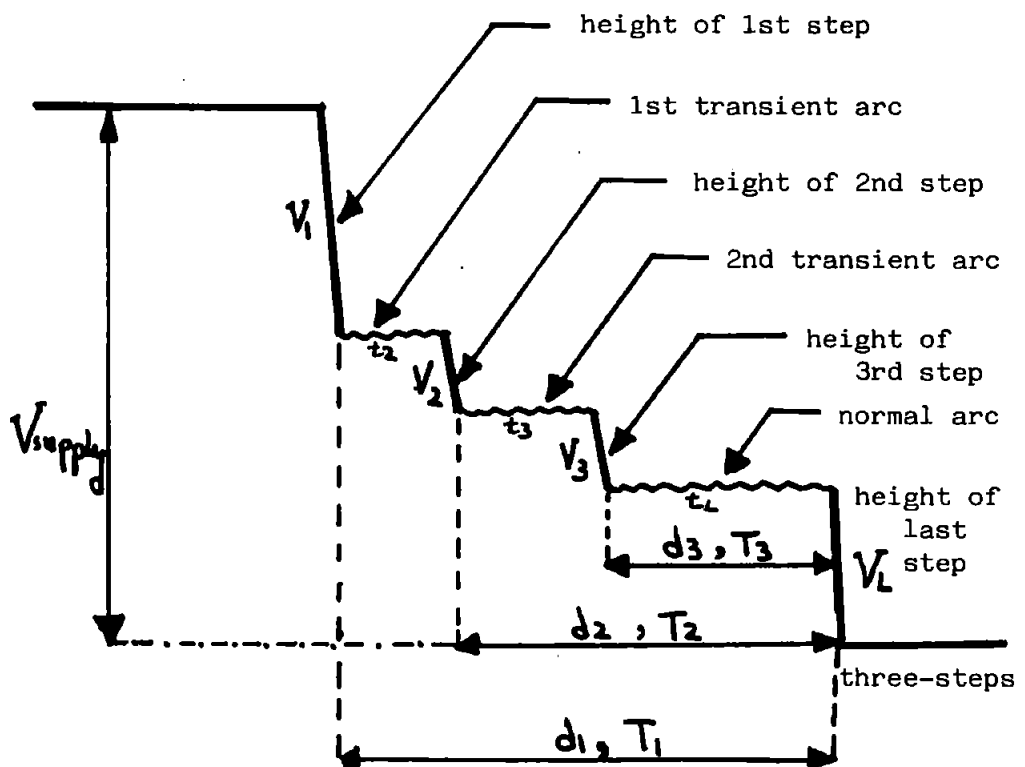
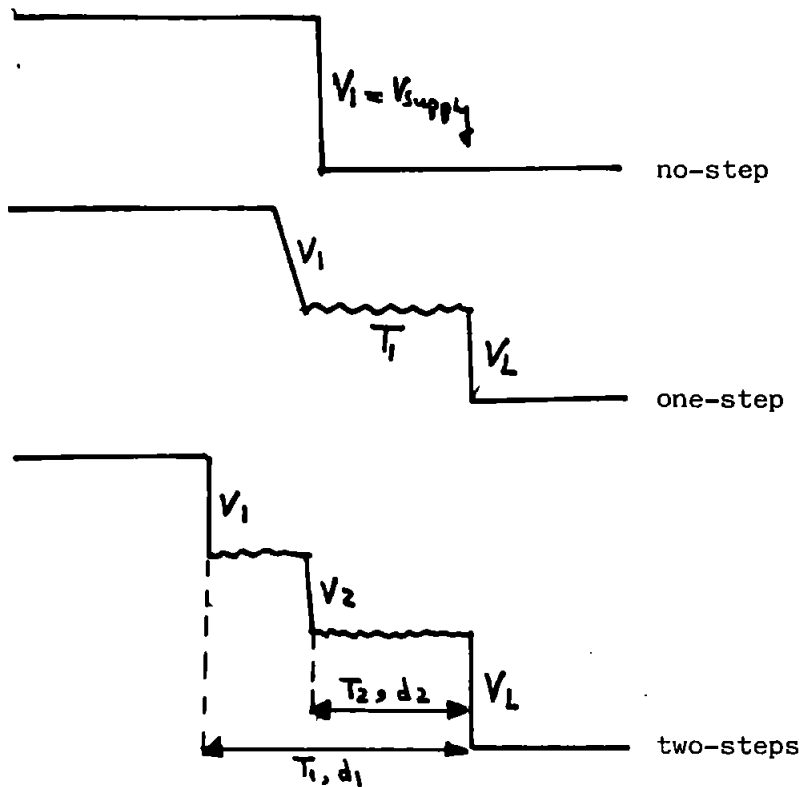


Figure 4.20: Represents diagrammatically the typical steps observed on closure.

closure arc to start, at least at the voltage they were experimenting with.

In most cases the arc is initiated by field emission current when electrodes are still relatively far apart. Often the arc is over before the contacts touch first time.

However, this view supports the early work of Germer⁽¹⁴⁾ in which he observed that most of the energy is dissipated upon the anode, by measuring heat dissipation on each contact, with the aid of a thermocouple, in which he concluded that the capacitor is discharged before physical contact of the electrodes by an electron current which bombards the anode (field emission current due to high field).

This energy is dissipated upon the anode in an extremely short time, of the order of 10^{-7} second or less.

In other investigations^(15,16), they decided to consider the concept of Active and Inactive surface. Active surface is defined when the surface is covered by foreign substances which are like an insulating film. The outer surface of this film becomes charged by +ions which creates a high field at the cathode across the insulating film, and its addition with the electric field is effective in drawing out electrons from the cathode:

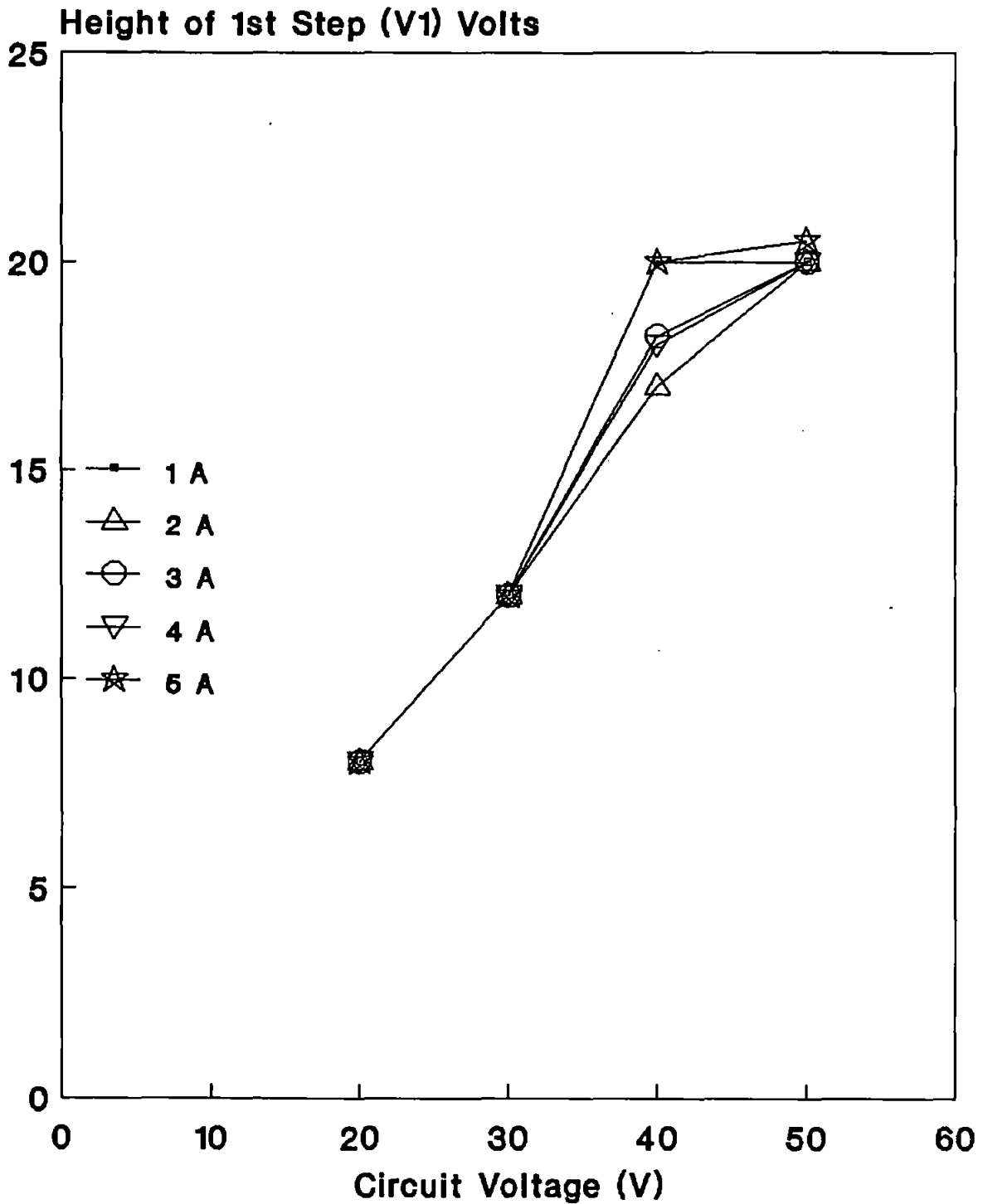
This view has been supported by Kisliuk in a series of papers^(17,18), in which he says that the initiating field is strongly dependent on surface contamination, which in addition to affecting the emission of electrons from the cathode, supplies the initial atoms for ionisation when the contacts are in open air and at high fields. Electrons may be liberated by tunnelling through rather than passing over the potential barrier, or, when a single ion in approaching the cathode surface creates a "pass" by decreasing (thinning) the width of the potential barrier.

In the investigation of Active surface they also considered the concept of greasy surface due to finger grease in which case for the first few break operations a quantity of soot is created on the surface and this sooty material, which may be oxide on the surface, causes arcing on every closure. Or, in other words, they make the surface active.

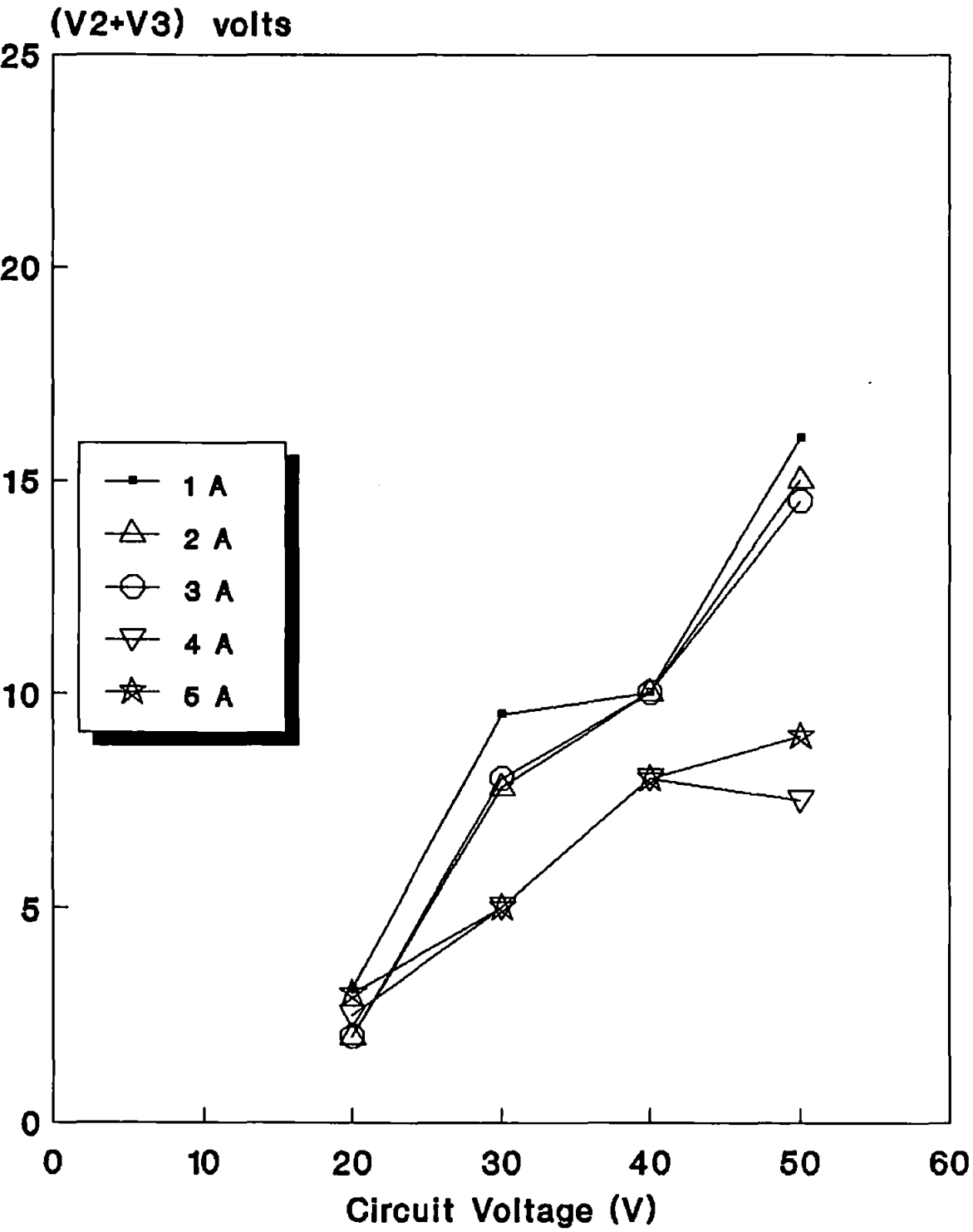
They found that the electrode separation at which an arc strikes is much greater

Figure (4.21): (a-g) shows the effect of operating voltages ranging 20-50 volts on various parameters, such as height, over the distance from the cathode which they occur, the electric field for a fixed speed of closure 500mm/s and various currents ranging 1-5A.

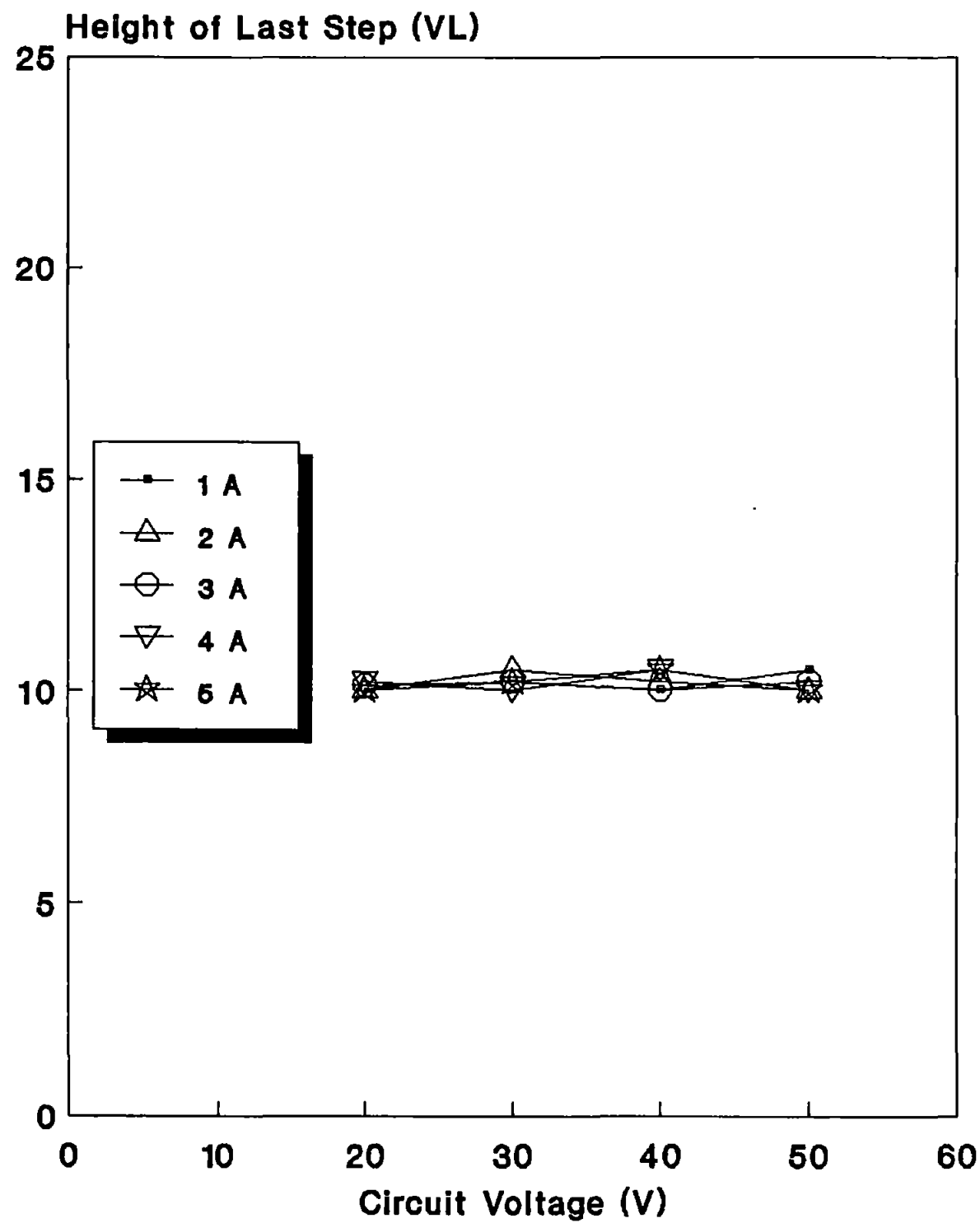
4.21a : Shows dependency of height of the 1st step(v1) on circuit voltages for currents ranging from 1 to 5 A.



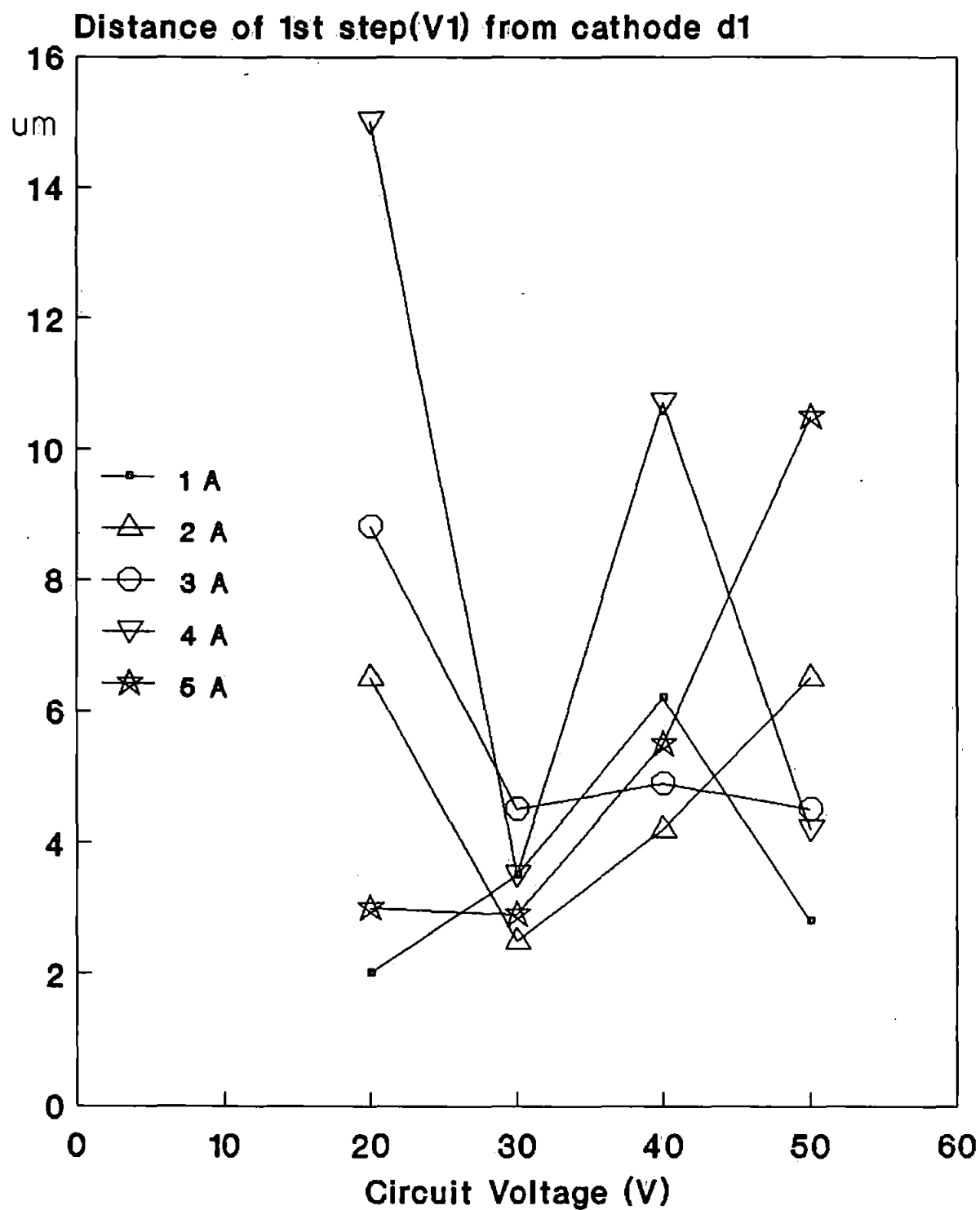
4.21b : Shows the height of 2nd (or sum of 2nd and 3rd) step versus circuit voltages for a current of 1-5 A.



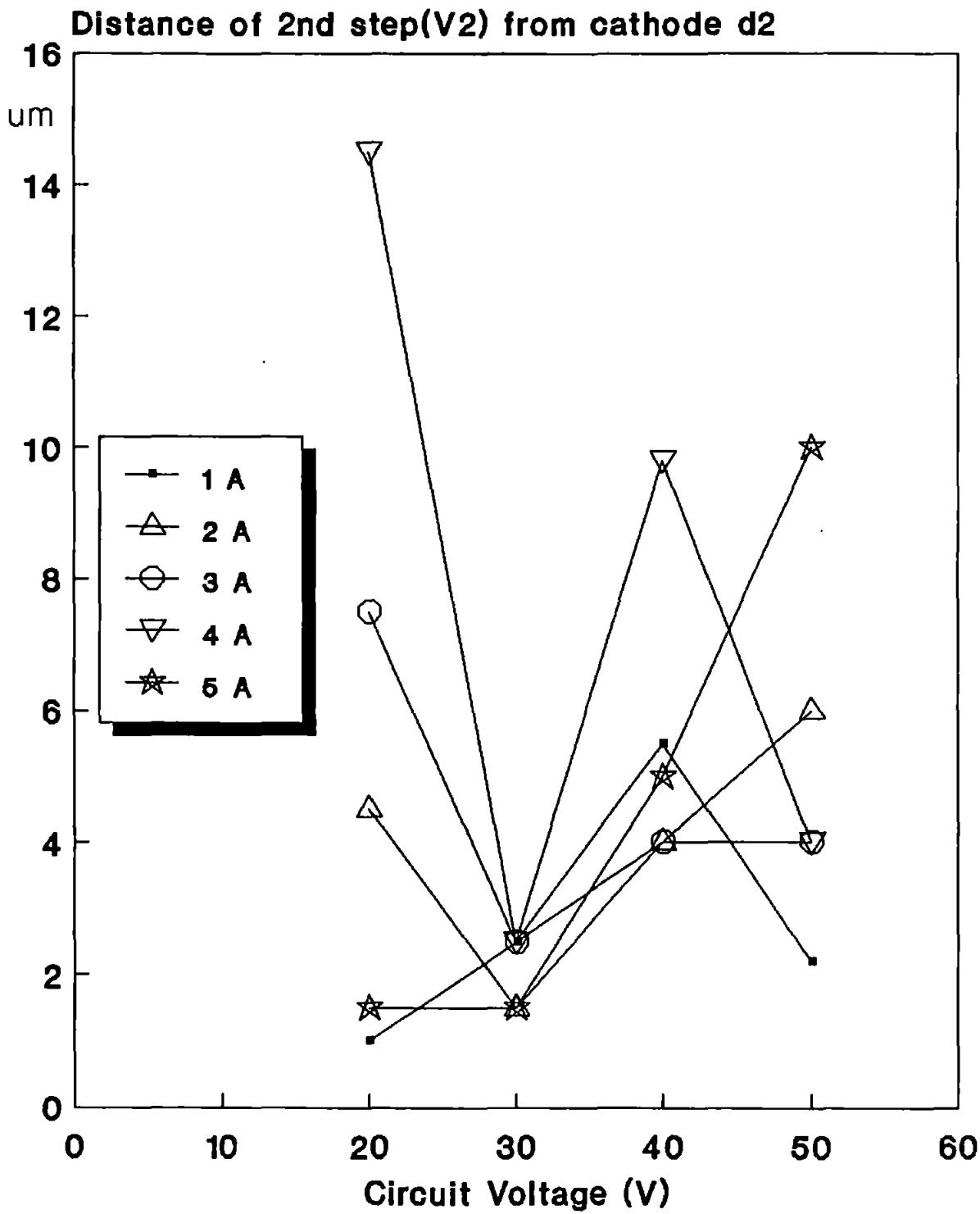
4.21c : The height of the last step(VL) versus various circuit voltages for a current of 1 to 5 A.



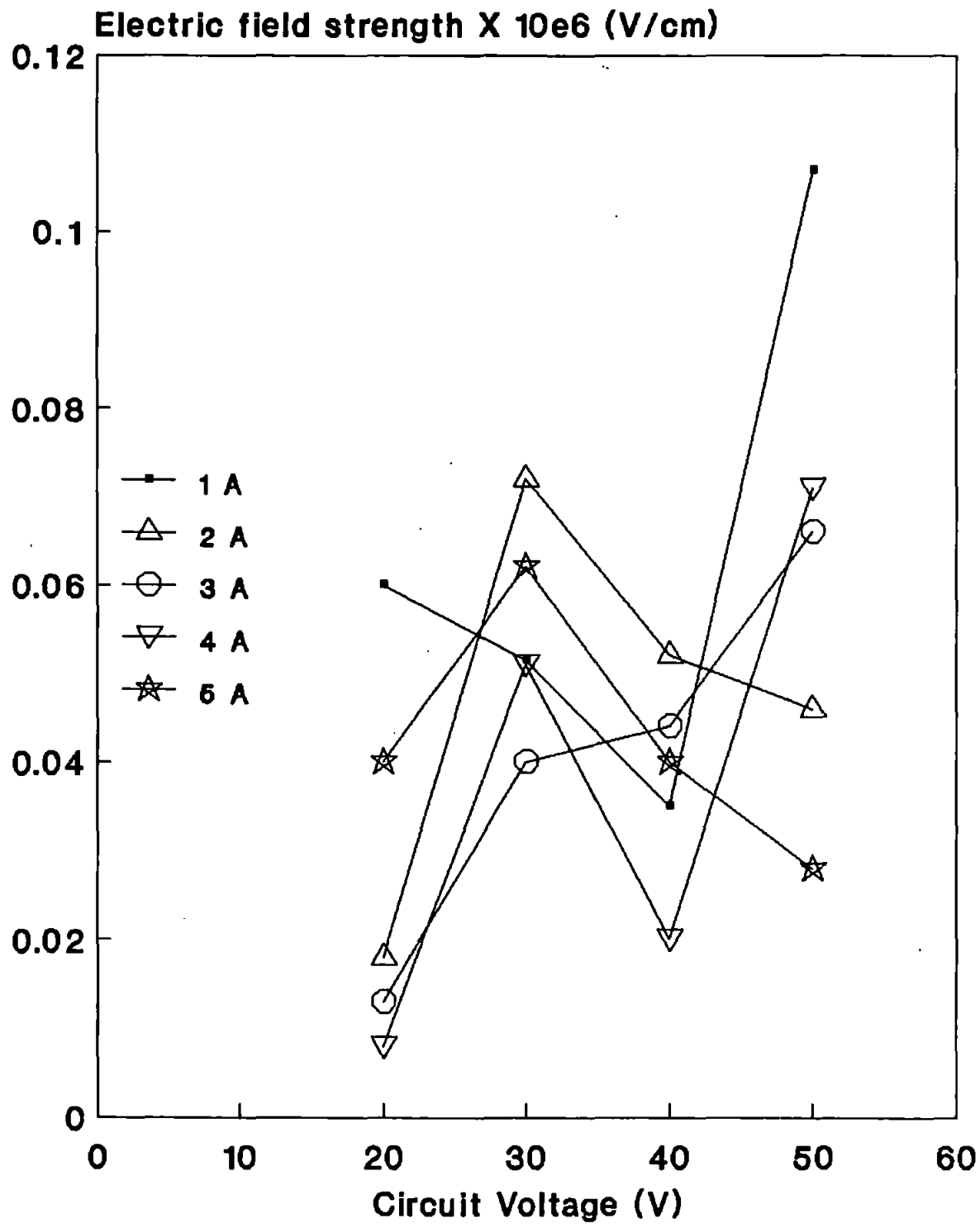
4.21d : Shows the distance of the 1st step from the cathode versus circuit voltages for a current of 1-5 A.



4.21e : Shows the distance in which the 2nd step occurs from the cathode versus circuit voltages for a current of 1-5A.

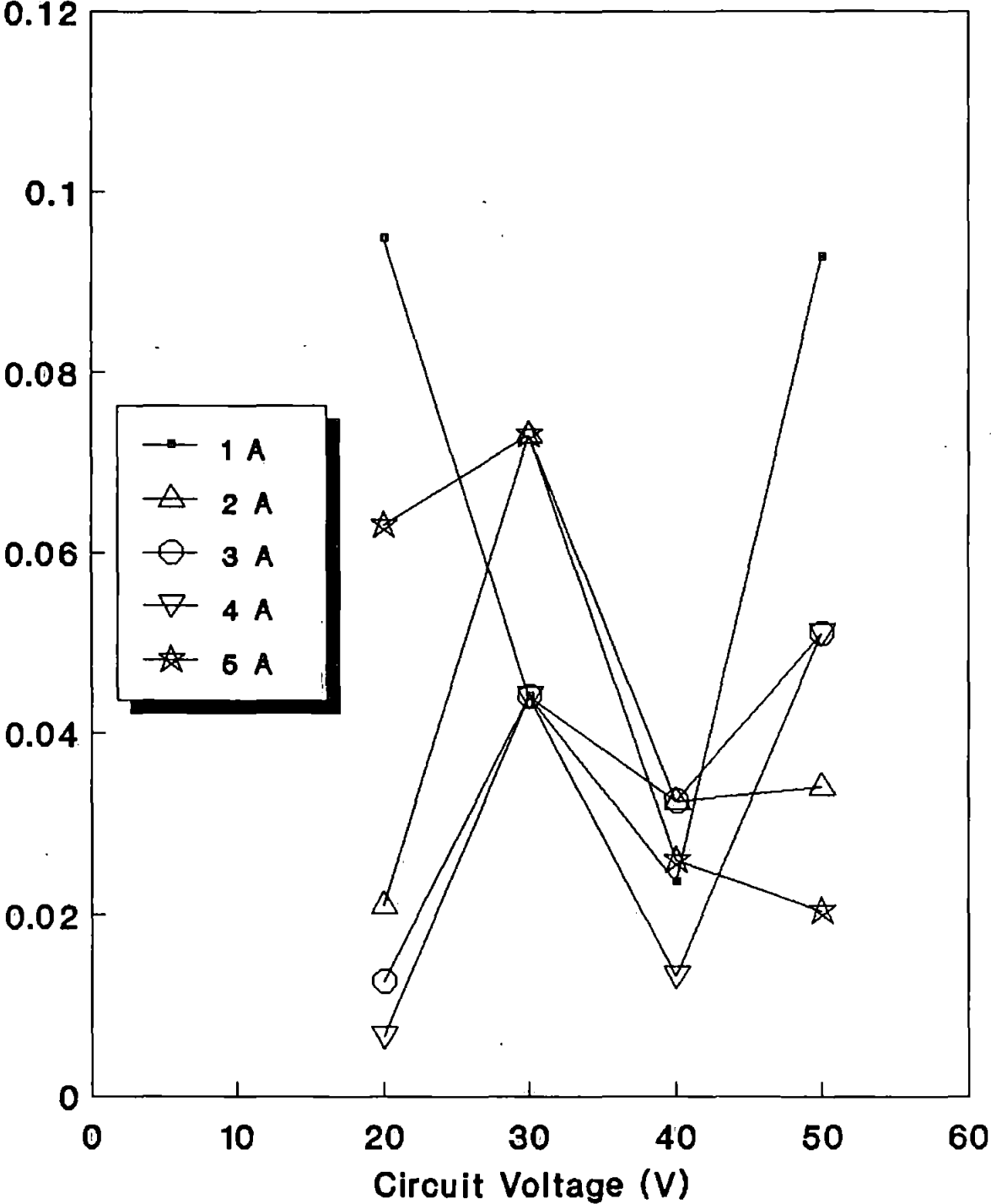


4.21f : Represents the electric field strength of the 1st step against circuit voltages for a current of 1 to 5 A.



4.21g : The graph shows the electric field strength of the 2nd step versus circuit voltages for a current of 1 to 5 A with speed of closure at 500mm/s.

Electric field strength X 10e6 (V/cm)



for active electrodes than for inactive. For example, for active silver or rough surfaces, the separation is about 6000 \AA , and for inactive 1600 \AA . The corresponding fields for active is $0.58 \times 10^6 \text{ V/cm}$ and inactive $0.67 - 2.2 \times 10^6 \text{ V/cm}$. Finally they concluded that at lower inductance the repeated discharge and charge are in the form of an oscillation which they related to partial discharge of the oscilloscope plate capacity, and after a number of oscillations the discharge ends up as an arc of constant value which is characteristic of the metal electrode, and they called it the normal arc or metal arc. However, as inductance is increased the number of oscillations decreased; for example for inductance of 12 Henrys they observed discontinuity similar to that shown in figure (4.18).

Arcing on closure has been discussed in chapter two, section 2.2.2. Here attention has been drawn to the conditions where no capacitor is connected across the switch model and the only capacitance and inductance is the natural capacitance and inductance of the leads and oscilloscope probes; also in general the first arc strikes (step voltage) at a separation which is 50 times greater than the separation observed by Germer and his co-workers^(33,36). To find out the cause of the formation of these steps and their nature, a series of experiments are carried out at various values of the parameters of voltage, current, impact velocity, number of operations, change of polarity and surface roughness, which eventually may lead to a fundamental insight into the understanding of this phenomenon.

4.4.1 THE EXPERIMENT

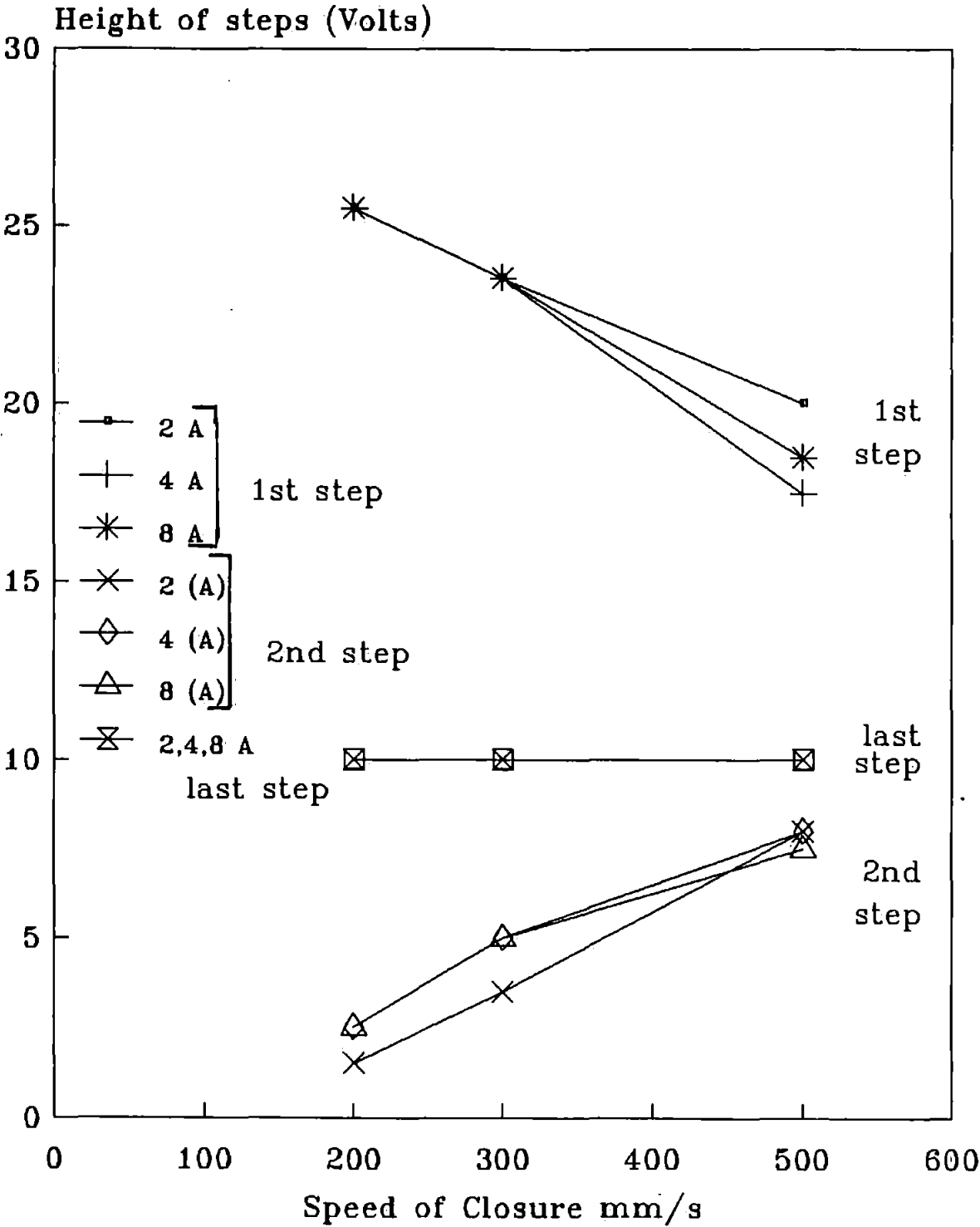
The experimental apparatus used here and its procedure is similar to the one discussed in section 4.3.1.

4.4.1.1 Dependence of the steps on supply voltage and current

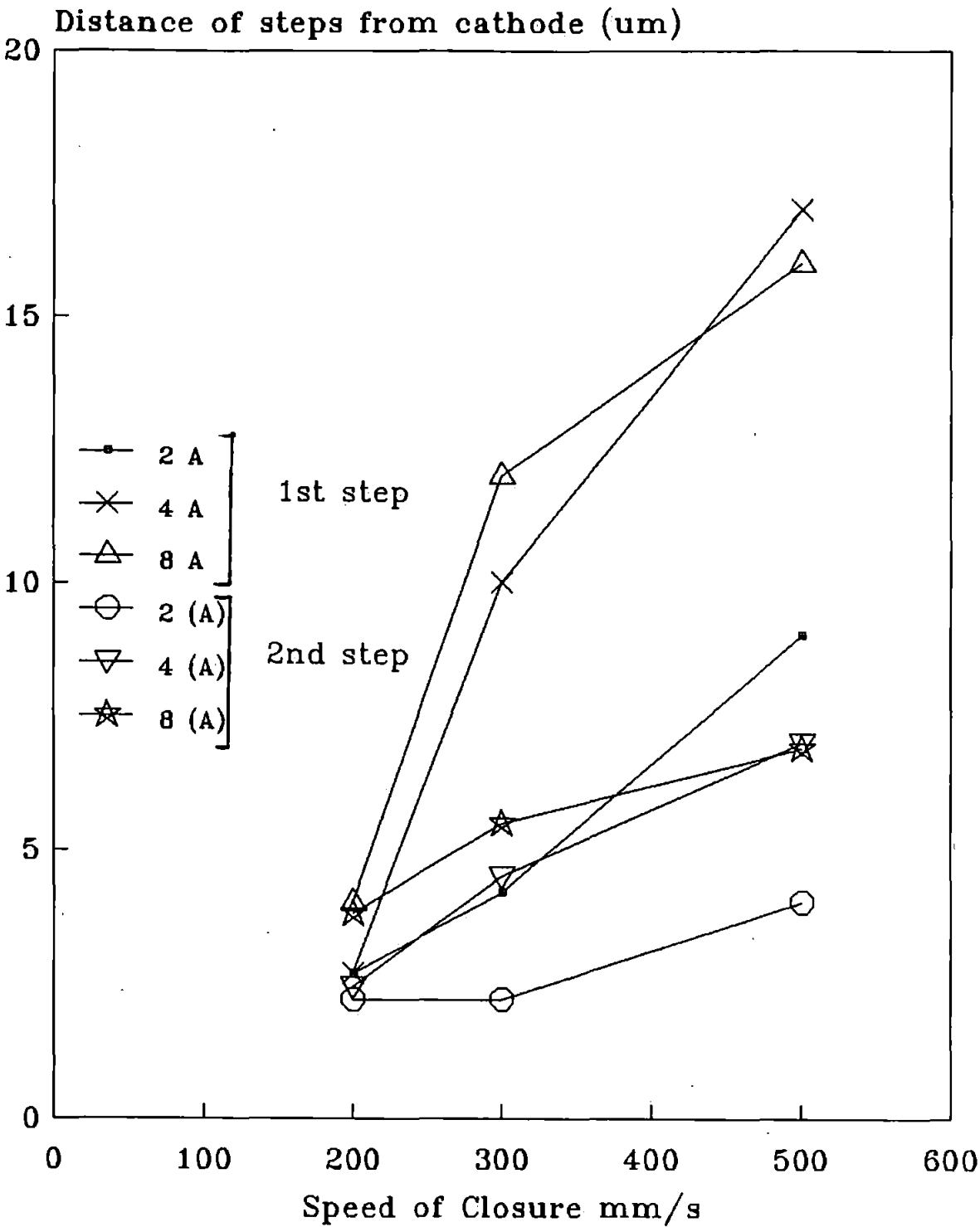
To study the effect of voltage and current on the occurrence of these steps, a series of 500 tests was carried out with oscilloscope at each supply

Figure (4.22): (a-e) show effect of various speeds of closure 200-500mm/s on height, over the distance which they occur from the cathode, electric field and percentage occurrence of steps for a test condition of 40V, and currents of 2-8A. (Readings are median values of 500 tests).

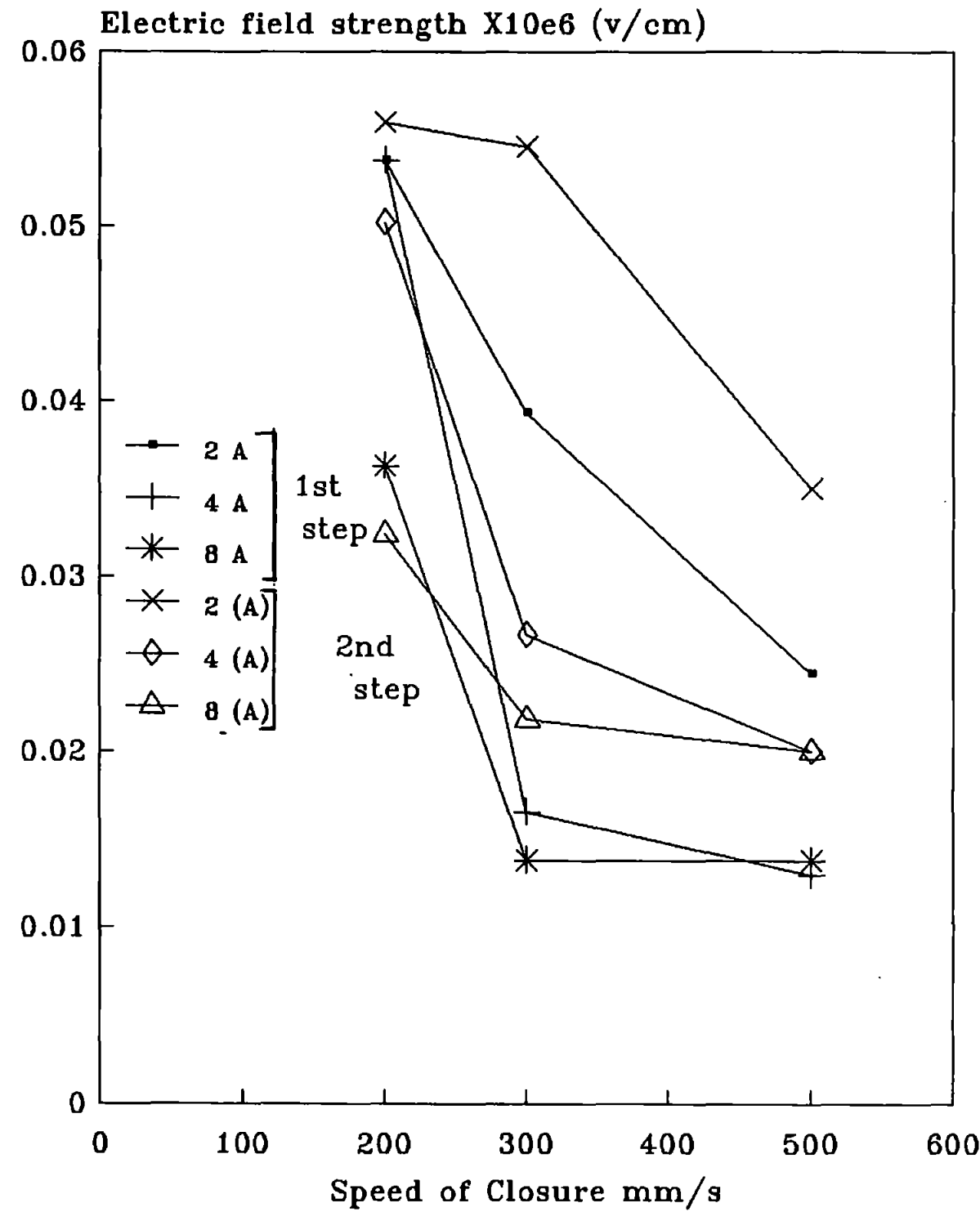
4.22a : Shows the height of the steps against various speeds of closure for a current of 2-8A.



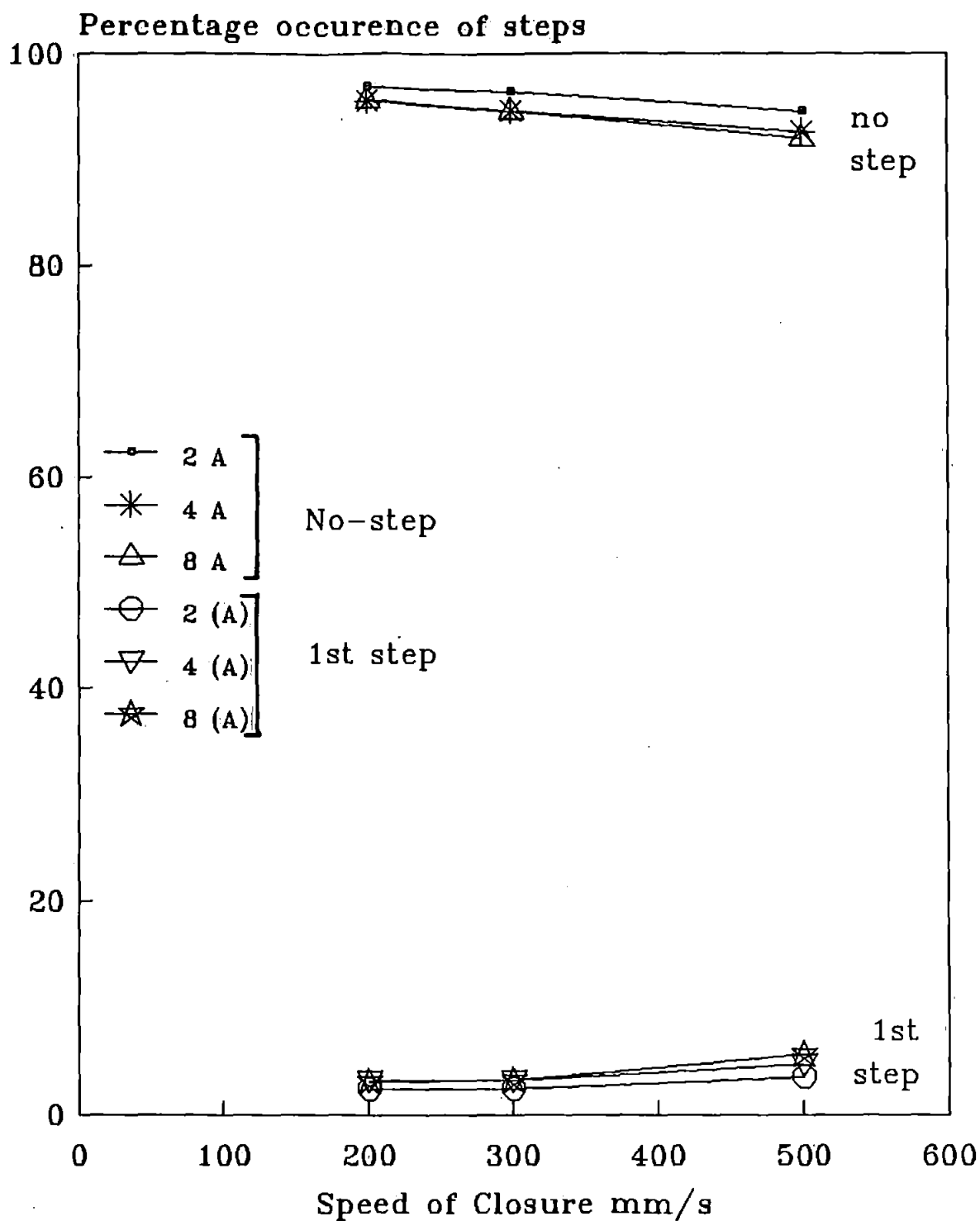
4.22b: Shows the distance in which the steps occur from the cathode surface against speeds of closure for a current of 2 to 8 A.



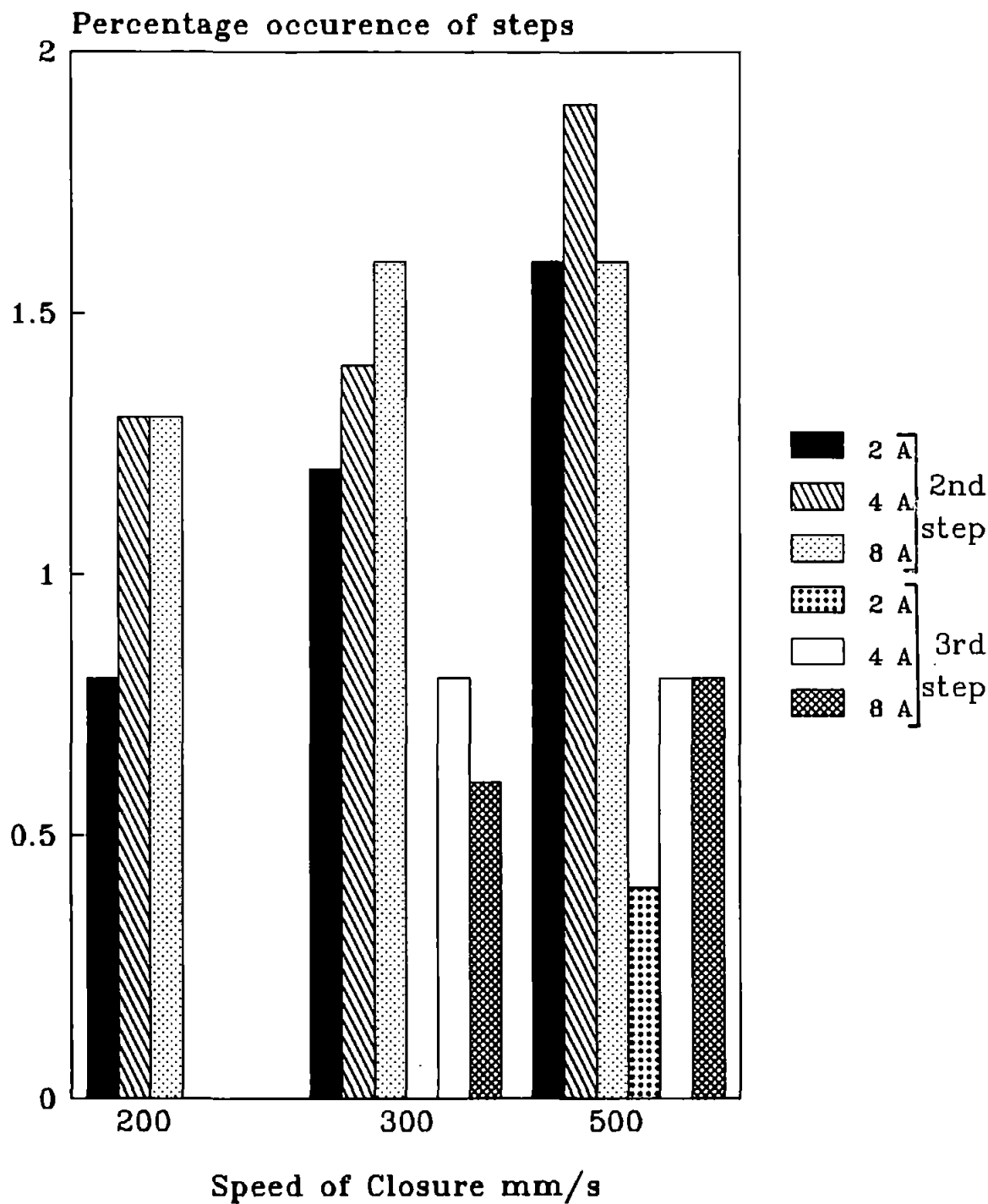
4.22c : The electric field strength of the 1st and the 2nd steps versus speeds of closure for a current of 2-8A.



4.22d : Shows the percentage at which the steps occur at various speeds of closure for a current of 2 to 8 A.



4.22e : Shows the percentage occurrence of the steps against various speeds of closure for currents of 2 to 8 A.



voltage of 20, 30, 40 and 50 Volts, and currents of 1 to 5 Amperes. The operating velocity and gap-length were respectively 500 mm/s and 3 mm. A typical sample of results at each supply voltage and current is represented in figure (4.19). From inspection of figure (4.19) one can see the discontinuity within the arc before closure. However, these discontinuities in most cases are occurring in two steps and occasionally in three steps: the voltage drops associated with these are labelled V1, V2, V3 and VL. They are shown diagrammatically in figure (4.20).

Close examinations of the above photographs revealed that at higher voltages the magnitude of V1 and V2, or the sum of V2 + V3 (where three steps occurred) is increased, by VL at each supply voltage and current remained constant, typically 10 Volts. Also the current in general has no influence on the magnitude of V1 but at higher currents, when supply voltage is high, V2 (or sum of V2 + V3 when V3 occurs) is slightly decreased. This probably is due to the slope of the first or second step, or a combination of them.

Figure (4.21) which is representative of Figure (4.19) shows graphically the variations in magnitude of V1 and V2 (or V2 + V3), over the distance they occur, and their electric field with respect to current for different operating voltages. Figure (4.21) shows that at lower voltage in general the steps occur at larger distances, typically 2 to 16 μm from the cathode, and the average electric field is $0.03 \times 10^6 \text{ V/cm}$, compared to $0.05 \times 10^6 \text{ V/cm}$ at higher voltages.

4.4.1.2 Dependency of steps on speed

A series of 500 tests have been undertaken at speeds of 200, 300 and 500 mm/s, and currents of 2 to 8 Amperes, with fixed operating voltage of 40 Volts. The median values of the amplitude of steps, over the distance that they occur from the cathode, the electric field, and the percentage occurrence of the steps, have been plotted against current, as shown graphically in figure (4.22). The results suggest that the magnitude of V1 (i.e. the first step) remains constant for various currents at a fixed speed but increases at lower speed. However, VL (last step)

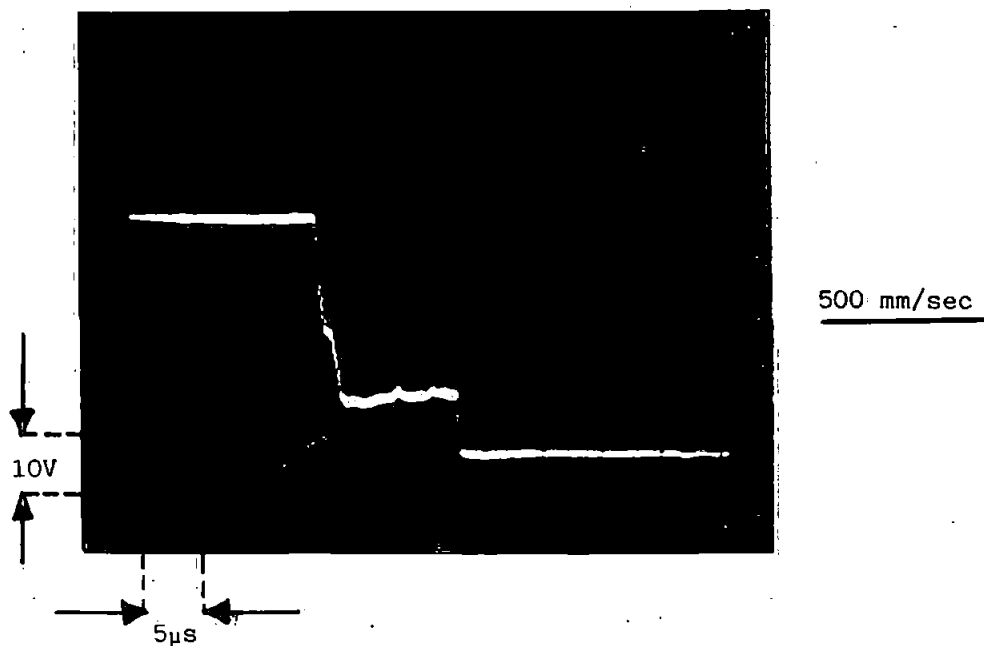
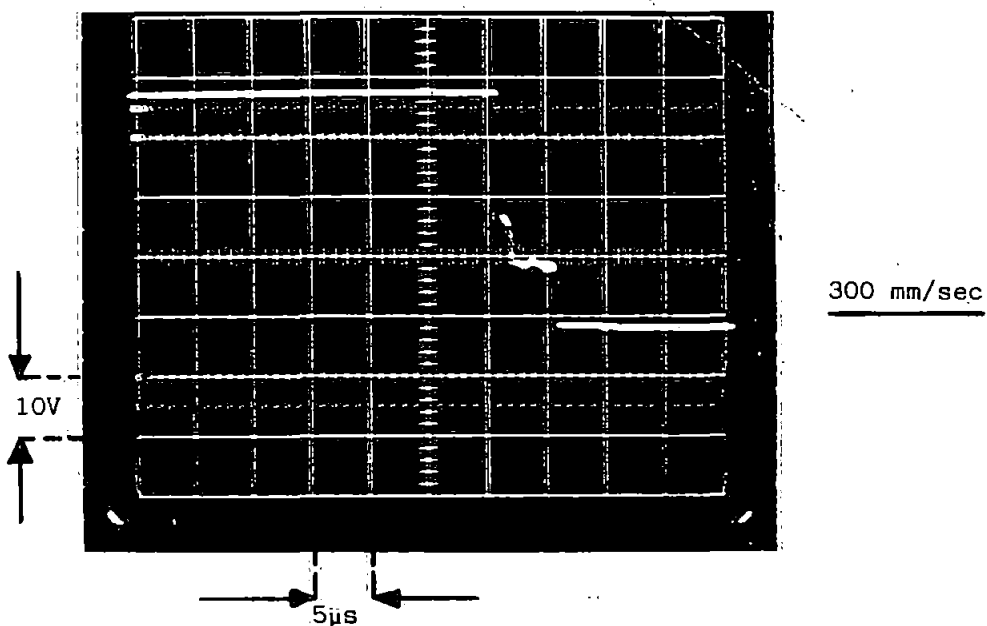
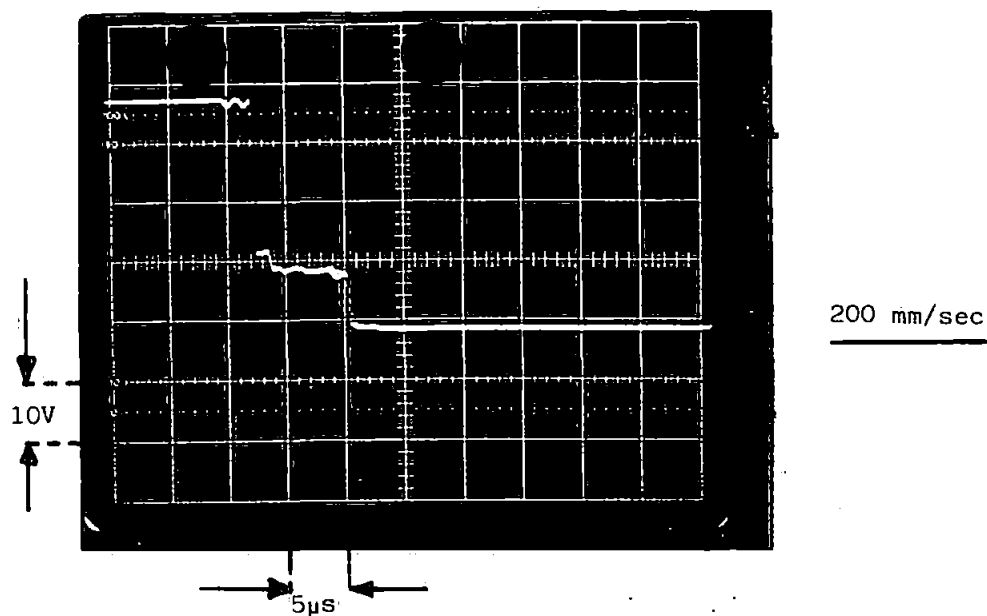


Figure 4.23: Shows the effect of an unroughened (new) surface of electrodes on the steps for a test condition of 4 amperes, gap-lengths of 3mm and voltage 40 volts at various speeds of closure.

always remains constant.

Observations from 500 tests at each speed and current confirmed that at lower speed the duration of the last arc (t_L) is longer than at higher speed. However, at higher speed of closure the duration of the transient arcs (t_2 or t_3) is longer compared to lower speed.

Figure (4.22c) reveals that the average electric field for the steps lies in the range of 0.01 to 0.06×10^6 V/cm. This is far below breakdown voltage.

Also, it was observed that at faster speeds and higher currents the occurrence of two or three steps is more frequent compared to slower speeds and lower currents; it seems at lower speeds and lower currents many tests are required before they occur. This suggests that speed and current have a great role in affecting their occurrence, and hence numbers. This is clearly shown, in figure (4.22d), as a percentage occurrence of steps against speed of closure, over 500 tests, for various currents. However, at higher speeds and currents the two steps in general are more numerous than three; but still over 90% closure-without-arc (NO STEP) was observed. This is thought to be due to absence of a foreign layer on the cathode surface, or probably the point of contact is covered by a good insulator, so that there was no arc.

4.4.1.3. Dependence of steps on surface conditions

Disfigurements of the contact's surface is the result of the amount of power being dissipated between the electrodes, and this amount is a function of the operating current and voltage. In the previous section it was observed that at a higher current and voltage the steps become apparent earlier, as the number of tests increased, than at lower speed and lower current. This may suggest that the occurrence of steps is dependent on the state of the surface.

For this reason, experiments have been carried out from higher current to lower and from faster to slower speed. For each test the surface of a new pair of contacts has been roughened manually (contacts roughened using abrasive paper in two

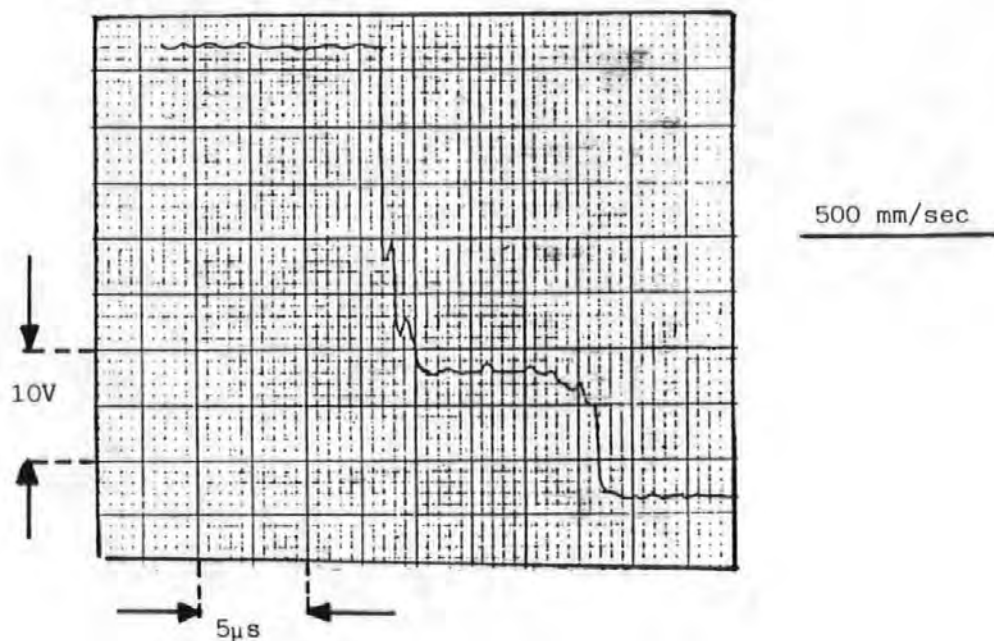
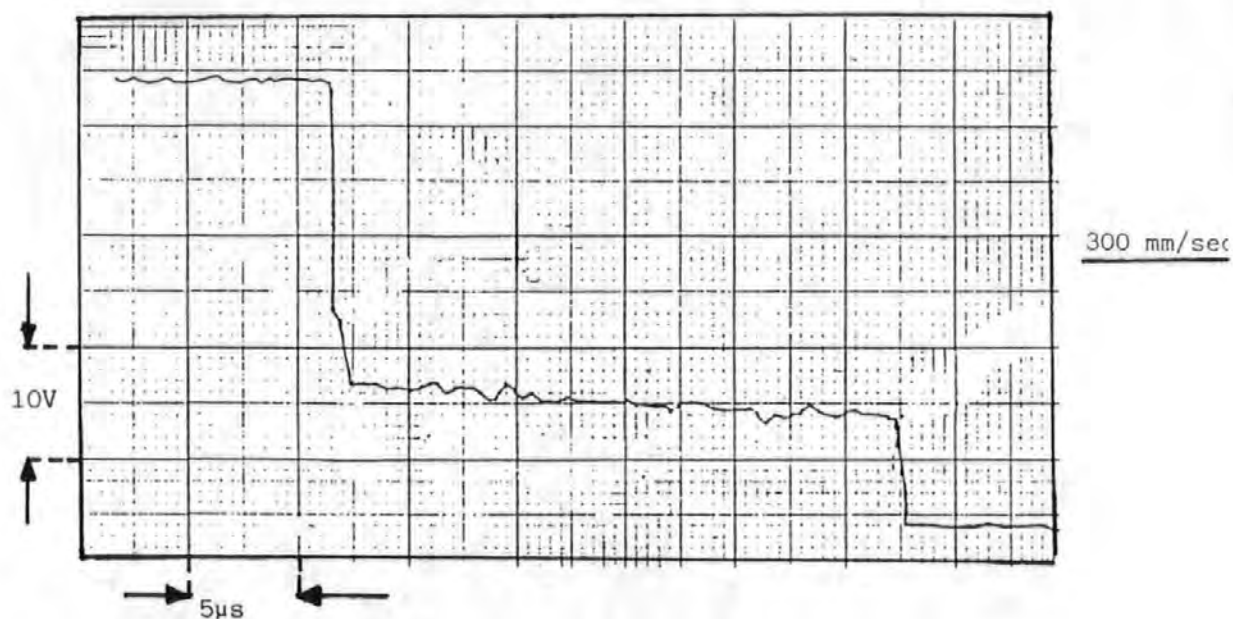
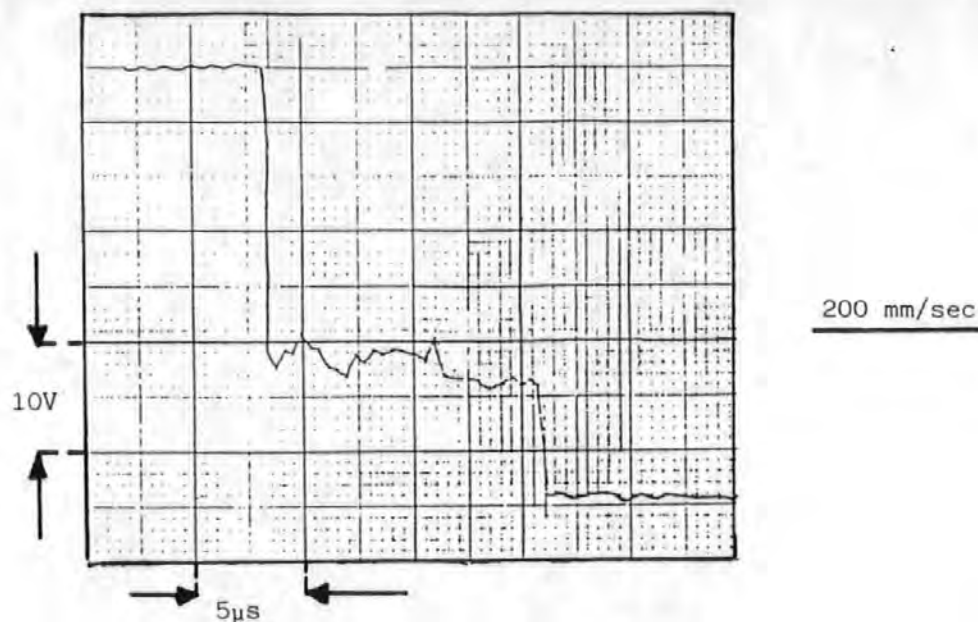
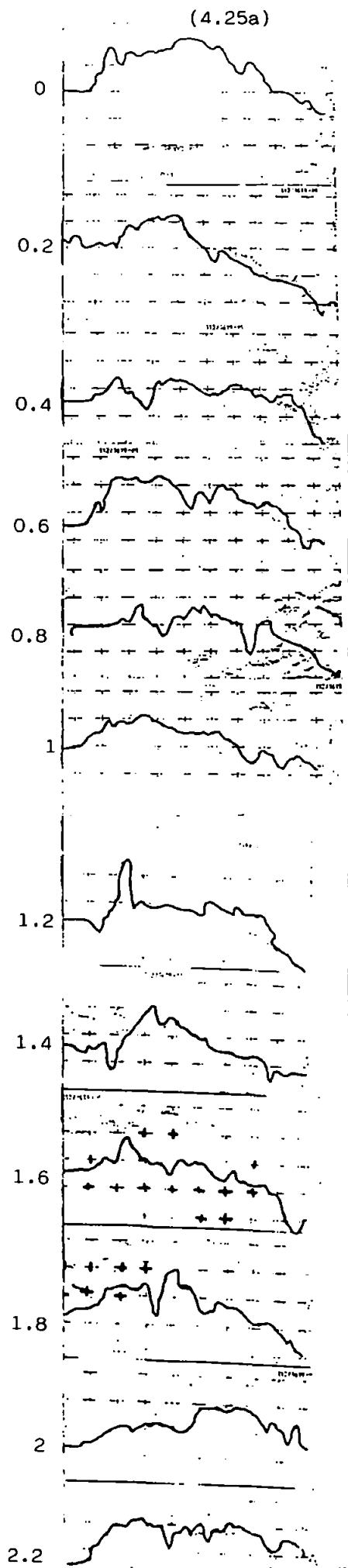
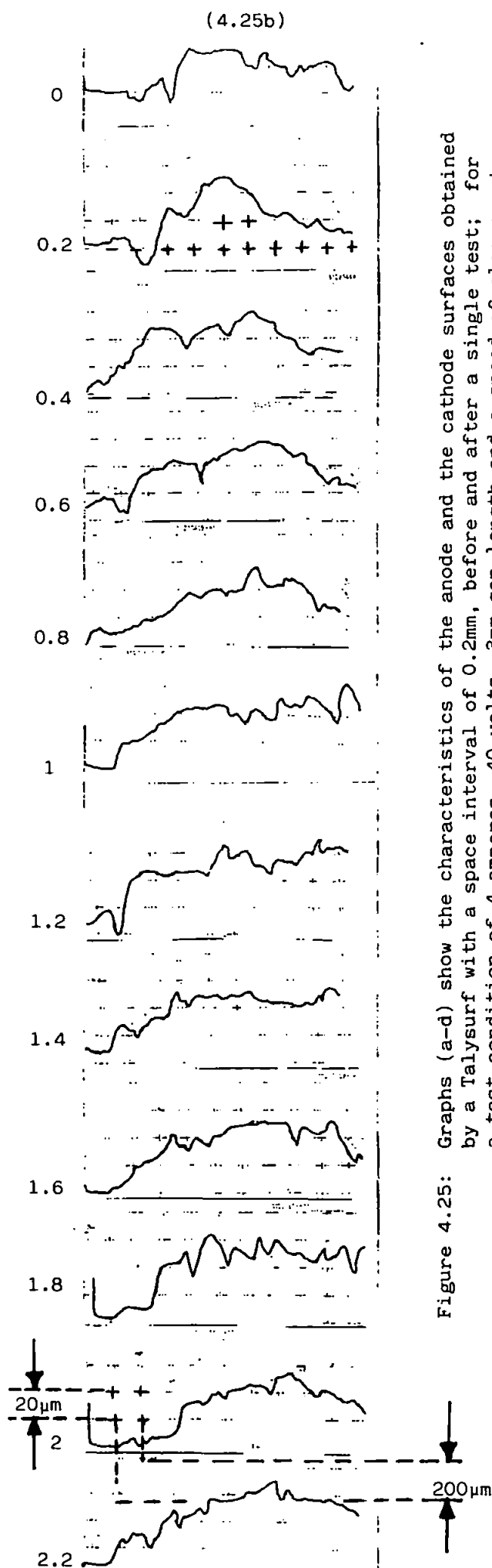


Figure 4.24: Shows the effect of a roughened surface of the electrodes on the steps voltage, after a single operation; at a test condition of 4 amperes, gap-length of 3mm and at a speed of 200-500mm/s.



Anode round before test

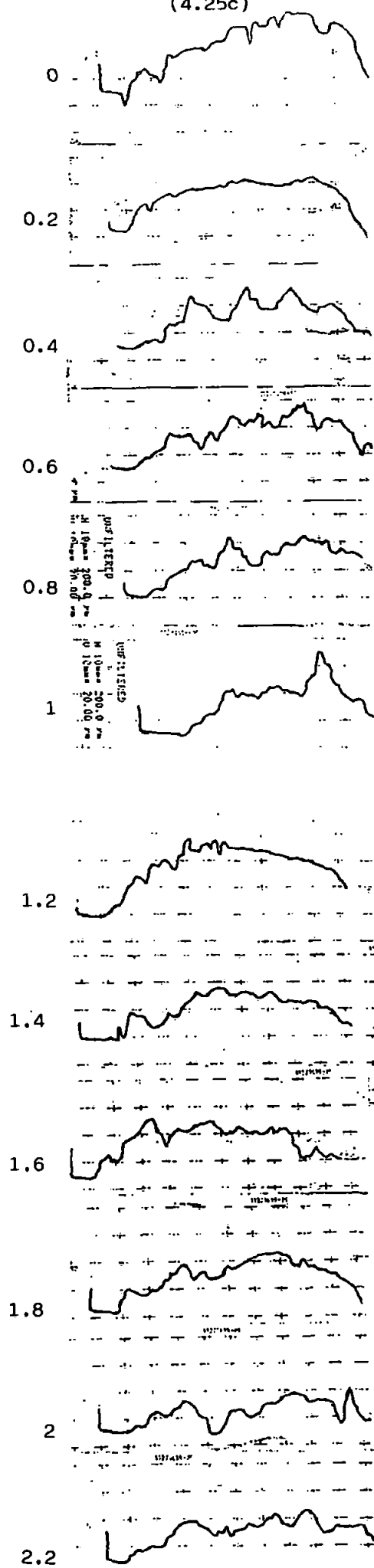


Anode round after test

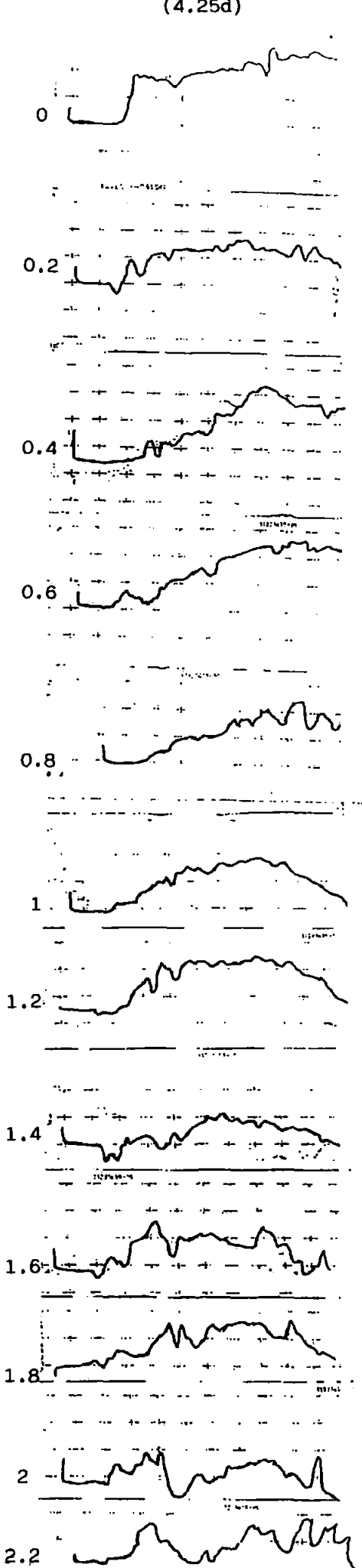
Figure 4.25: Graphs (a-d) show the characteristics of the anode and the cathode surfaces obtained by a Talysurf with a space interval of 0.2mm, before and after a single test; for a test condition of 4 amperes, 40 volts, 3mm gap-length and a speed of closure at 300mm/s.

(4.25c)

(4.25d)



Cathode round after test



Cathode round before test

directions at right angles) in order to test the above statement and also to observe its effect on the number of steps, of which up to now a maximum of three have been observed.

The results from 3000 tests, for operating condition of 40 Volts, 2 and 8 Amperes and speeds of 200 to 500 mm/s, revealed that the steps occurred from the first operation, and in most cases occurred in twos and occasionally threes, similar to those observed earlier, where V_1 , for a fixed speed and voltage, remained constant. A sample of results obtained at current of 4 Amperes and speeds of 200 - 500 mm/s, using unroughened and roughened contacts, are shown in figures (4.23) and (4.24) respectively.

Also for a current of 4 Amperes and a speed of 300 mm/s, before and after a single operation tests, the Talysurf has been used to compare the peak obtained with the distance obtained from the oscilloscope. This approach has not revealed much information. This is shown in figure (4.25).

The observations of the voltage characteristic on closure, on the oscilloscope, also revealed that the cathode fall is slightly less when the surface is roughened compared to previous tests (unroughened), where it was 10 Volts. This may be due to a reduced work function for the emission of the electrons because the surface state is changed. This can also be seen from figure (4.24). The most interesting conclusion obtained from the above tests is that the roughness increases the number of occurrences, but not the number of steps.

4.4.1.4 Dependence of steps on change of polarity

From the above section it can be understood that the surface roughness has a great influence on the occurrence of the steps.

However, in this section the investigation is to find out whether the occurrence of steps is due to the surface condition of the positive electrode or negative electrode in order that the cause of the initiation of the arc becomes clearer. The change of polarity on a pair of contacts which already have performed 1000 operations revealed

that it can occur in both cases with the same arcing time. This suggests that the surface condition of either electrode contributes to the occurrence of steps.

The above conclusion has been proved by two sets of experiments; in the first, the positive electrode has been roughened, and, in the second, the negative electrode. In each case for the same test condition no change in arcing time and number of steps has been observed.

It is known that the surface of an electrode which has performed a large number of operations, or has been roughened, is usually covered with spikes. The formation of spikes is described in the next section.

4.4.2 DEVELOPMENT AND FORMATION OF SPIKES

The spikes are usually known to be the first point of contact (microscopic point area of contact) during closure before the metallic contacts take place. These spikes can be created by roughening the electrodes' surface or they can develop as the result of arcing during break and make after a single or many operations, depending on the working circuit condition.

At break, after termination of the arc, or during arcing, the rim which surrounded the pit on the anode or the mound of metal which is thrown about the pit, or the mound of metal which has been sputtered over the cathode becomes solid and forms the microscopic points of contact (spikes).

However at make the contacts get in touch at these microscopic point areas of contact. There is an elastic and plastic relaxation of the area of contact and as contact pressure is increased, heating first softens these areas and then the contacts sink together. These processes may increase the area of the contact and also create a situation for new microscopic points.

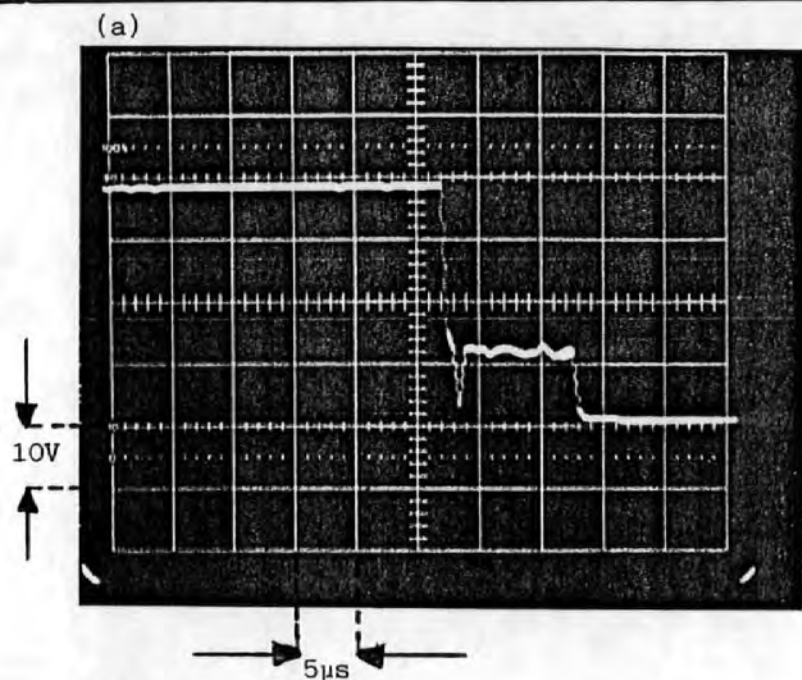


Figure 4.26: The photograph and sketches (a-d) are typical of a voltage drop during closure, and show the evidence of the point of contact.

4.4.3 THEORY OF THE ARC AT CLOSURE

Here the theory of the arc on closure has been developed from the tentative conclusions derived from the observations on the oscilloscope and the recorded output. From observations and the results obtained, one may postulate that the steps and the initiation of the arc are due to momentary points of contact, or they are as the result of field break-down due to the state of the electrodes surfaces.

The momentary points of contact take place when these microscopic points (spikes) are covered by a layer of insulating material. In these circumstances, since the contact area is small, contact pressure is light and current density is high, the rush (surge) of current through these points will vaporise them and then the arc is established.

Each point of contact will produce a traverse to zero voltage so quickly that it may be beyond the speed of resolution of the oscilloscope, and therefore it may not be noticeable on the oscilloscope trace. Holm⁽¹⁹⁾ states that there can be no closure arc at a low voltage and if the first point of contact is so substantial that it is not burned out. The photograph of figure (4.26) shows that the voltage dropped from 40 Volts to zero and then rose to a certain value. This also shows the evidence of point of contact.

The field breakdown takes place when an intense field builds up between two electrode surfaces as they get closer (probably between spikes). But whichever causes the initiation of the arc, after initiation (first arc) both have the same characteristics until the two contacts come to rest on each other. That is voltage collapses suddenly to a value named here as V_1 (defined in figure 4.20), and as the arc starts, the potential across the electrodes decreases in steps from voltage V_1 to a steady value, which is characteristic of the metal electrode, and is called the Normal arc. The Normal arc has a steady value in the order of 10-11 Volts, and it is also known as the final arc or the arc before closure.

The first arc has a duration typically in the range of 0.5 - 2 μ s, it is named

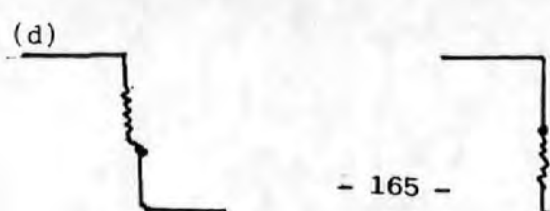
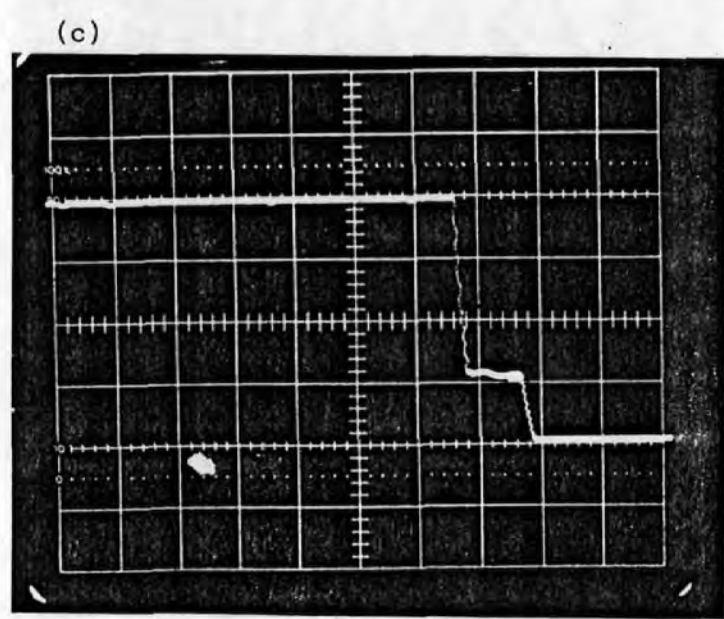
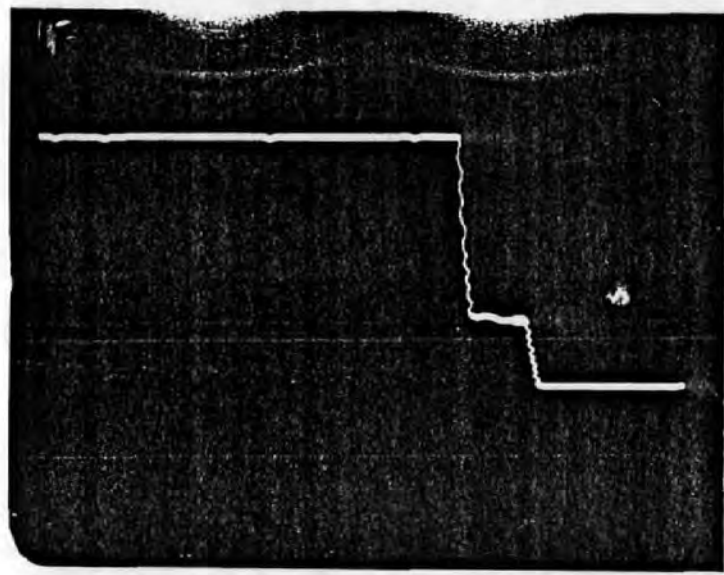
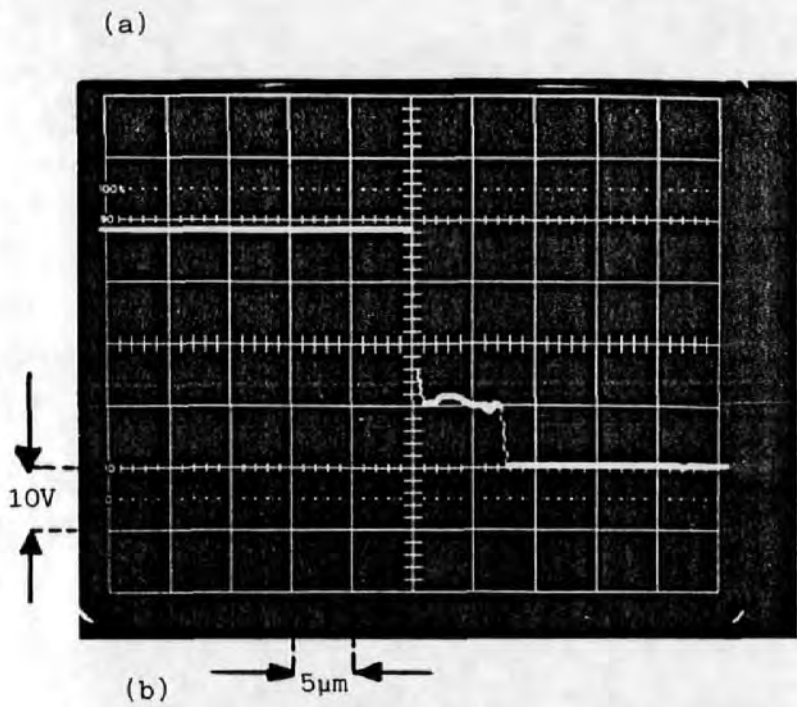


Figure 4.27: Photographs (a-c) and the sketch below (d), show examples of a step phenomenon with a brief duration of T_1 , T_2 and T_L which are scarcely detectable (T_1 , T_2 and T_L are defined in figure 4.20); for a test condition of 40 volts, a current of 8A, gap-length of 3mm and a speed of closure of 300mm/s.

here as the transient arc.

Since the Normal arc voltage value (V_L , defined in figure 4.20) in any test condition remains constant at about 10 to 11 volts, which is characteristic of the metal electrode, this suggests that its mechanism is unique. In most cases the Normal arc follows after a transient arc, the transition period between them is extremely short, and the whole process becomes continuous. This indicates that there is inter-relation between V_2 , V_3 and V_L . V_L exists whenever there is an arc.

The parameter required for the continuity of the arc is known to be Anode Fall. The voltage drop across the anode vaporises metal from the anode in sufficient amounts to provide ions. The ions charge the outer surface of the cathode and as a result create an intense field. Its addition with the electric field, when the electrodes come closer together, is sufficient to drag out electrons from the cathode for the maintenance of the arc. So the Normal arc is due to the field emission of electrons.

4.4.4 RESULTS AND DISCUSSION

Investigations into the effect of various parameters, such as current, voltage, speed, roughness and number of operations may have opened an explanation into the cause of these steps and provided further insight into the mechanism of the arc.

The parameters which determine the nature of the arc are the separation at which these discontinuities take place, and their electric field. The data on separations and the electric fields are obtained solely from the oscilloscope and the speed of closure.

The separation at which the first discharge takes place is variable and depends on the height of spikes. These spikes too depend on the condition of the surface. The surface condition is dependent on current, voltage, gap-length, speed, arcing at break and number of operations.

Data on the distance separations of the steps from the cathode, and their corresponding fields, for various test conditions are shown in figures (4.21) and (4.22).

From examinations of a large number of oscilloscope traces, it is found that the time between the first transient discharge and the final closure varies considerably, and hence also their separations from the cathode surface.

It was found that the initiation of the arc is strongly dependent on the state of the electrode's surface. For example, on clean contacts, arc will not occur at least for the first few operations. However, if it takes place it may be as one step and this is thought to be due to the presence of foreign layers on the surface. Foreign layers can be contamination, by finger grease, or some organic substance which has been deposited on the electrodes from the air. When the surface is roughed manually or after a large number of operations, the steps occur regularly. This may be due to spikes or build-up or asperities on one or both electrodes which short-circuits to the other, or creates a situation for field breakdown to occur.

Speed is another parameter which effects the duration of the arc, and the magnitude of V_2 (or $V_2 + V_3$), second and third steps. For example, at lower speed, the duration of the ^{Transient} arc is longer and V_2 (or $V_2 + V_3$) is smaller, but V_1 remains constant for the same test conditions. So, if V_2 is recognised as anode fall, this suggests that at lower speed the erosion rate is less on the anode.

At lower speed it was also observed that it takes a longer time to build up a situation where two steps can be seen. But at the same speed when the surface is roughened the two steps phenomenon occurs immediately, and also the duration of the last arc ^(t_L) is longer. It was observed that at higher currents the number of ^{no-} steps reduces and the number of one and two steps increases.

At various operating voltages, and fixed speed, the magnitude of V_1 increases with the voltage and so does V_2 (or $V_2 + V_3$). The normal arc voltage (V_L) seems to be independent of current, speed and applied voltage, but not roughness, and occurs within a few μm from the cathode.

The duration of the last arc in general is greater than the duration of the first

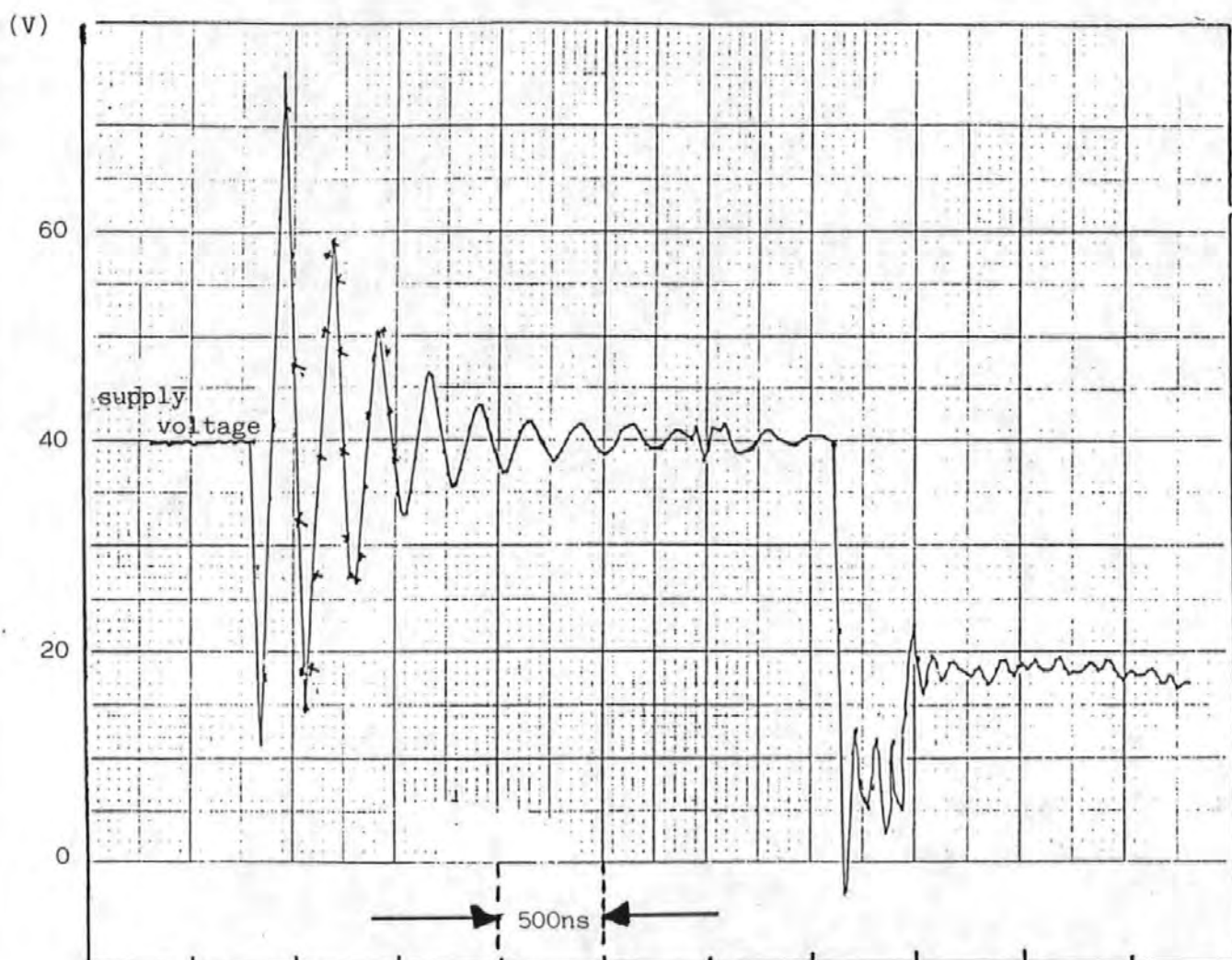


Figure 4.28: The supply voltage shows the oscillation during closure before it drops to zero; at a test condition of 40 volts, gap-length of 3mm, a current of 4A and a speed of closure at 300mm/s.

(t2) or second (t3) arc. In some cases it was observed that the duration of the first or the last arc, or the second arc, is so brief that it escapes detection on the oscilloscope, with such a time scale as has usually been used here ($5 \mu\text{s}/\text{DIV}$). A sample of such phenomena is shown in figure (4.27). It must be noted that whenever the first transient arc occurs, the Normal arc also occurs. The Normal arc is characteristic of metal electrodes.

Sometimes it is observed that there is just Normal arc. Here one could interpret this as being due to field emission before a metallic contact takes place, due to surface impurities as Germer and co-worker⁽¹⁶⁾ suggested. This arc occurs when the electrodes are still relatively far apart.

In some cases closure without arc (closures which are not preceded by an arc) was observed. One can assume that the first point of contact is covered by a good insulator, so that it did not arc. Or it was due to absence of a foreign layer on the cathode surface. It has been observed in some cases that it takes about $1 \mu\text{s}$ for the current to vaporise the first point of contact and then the voltage rises, and then drops back to a value which is characteristic of the metal electrodes. It was also observed that within the last step, the arc voltage sometimes goes to zero. This might be as a result of metal which has been thrown out shorting the circuit, which then vaporises and arcing continues.

Another pattern observed was oscillation before the drop of supply voltage to V1. This is observed when a faster time base has been used ($500 \text{ ns}/\text{DIV}$) and it is shown in figure (4.28). The cause of this oscillation may be due to the oscilloscope probe leads, or natural capacity and inductance of wires in the circuit. This oscillation has not always been observed, and has not been investigated here.

Throughout the tests, the maximum number of steps observed was three, and the transient arc is always followed by the Normal arc, and V2 (or $V2 + V3$) decreases with current. This is especially noticeable at higher voltages. What happens between the first and the last arc is recognised as anode fall, because anode fall is necessary to the continuity of the arc. The values of V2 (or $V2 + V3$), second and

third steps respectively, are consistant with the previous measurements, the only difference is the distance the 2nd step occurs from the cathode. For example, for a speed of 300 mm/s, it occurs at 90 μm , as opposed to 10 to 20 μm in previous tests (see section 4.3), but the first step for both cases is the same, about 15 μm . The difference may be due to the way the arc is established.

All the experiments reported here have been made on Ag-Cd O electrodes. The uniform progression of the tests was important for the understanding of these voltage steps. The above finding, that V_2 (or V_2+V_3) (second step) is equivalent to the anode fall voltage, may introduce a new way for the measurement of cathode and anode fall voltages.

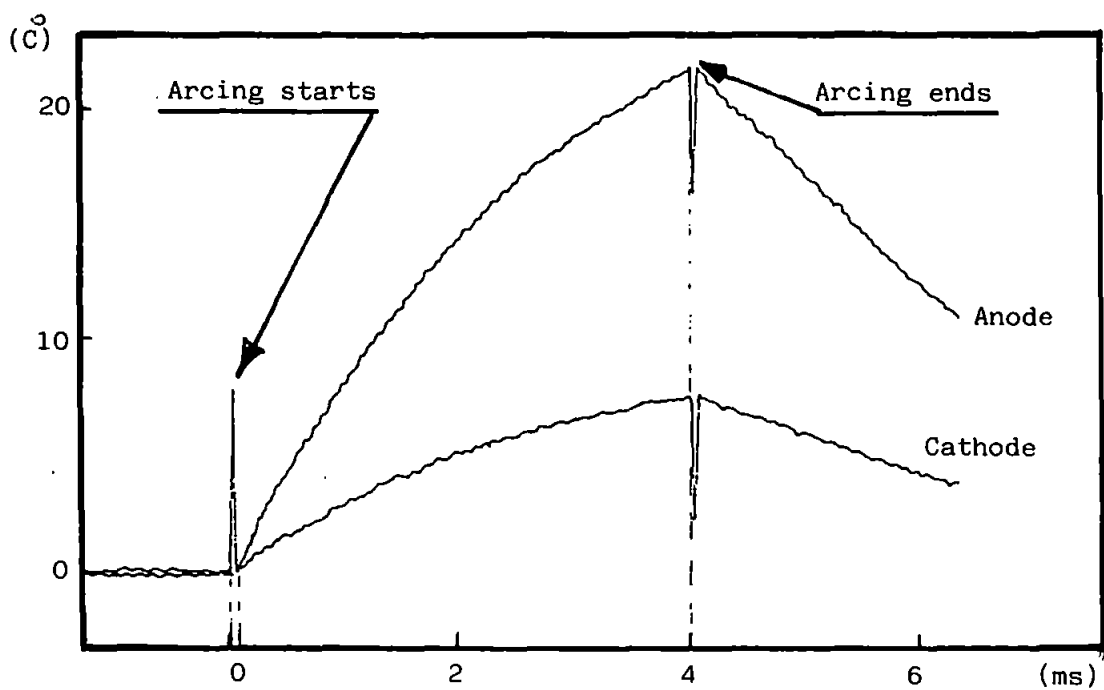


Figure 4.29: Shows a typical temperature-time curve of the electrodes (anode and cathode) due to arcing; at a test condition of 40 volts, current of 10A, gap-length of 0.5mm and arc duration of 4ms.

4.5 TEMPERATURE-TIME CURVES OF THE ELECTRODES

These are defined as the means of measuring the amount of arc power being dissipated on the surface of the electrodes for various parameters such as current, gap-length and arc duration, and are recorded from the thermocouple output.

Since the duration of the arc in snap-action switches at break is usually short (typically 3 ms, depending on opening speed), and within these periods the contact body does not reach to a steady state, these measurements have been taken immediately after the contacts have opened in order to prevent appreciable heat diffusion to its surroundings. This has been achieved by placing the thermocouple in the centre of the contact, where in most cases this is seen to be the active area of the arc, and as close as possible to the surface in order to obtain the correct temperature measurement.

4.5.1 PROCEDURE IN TESTING

The experiments were performed on the test rig shown in figure (3.1). The current was adjusted with the constant current source, the arc duration with the timer and the gap-length with a micrometer, and the rig operated by the computer. All these are explained fully in sections 3.3.

For each parameter such as current, gap-length and arc duration the temperature rise at the contact due to joule heating has been measured with the aid of a T-type thermocouple using technique III as has been described in section 3.5.2.

The e.m.f. generated in the thermocouple is fed to an amplifier with gain of 246.47. In temperature measurements it is customary to refer the thermo-e.m.f. of the hot junction to a cold junction which is kept at a known temperature (reference junction). Here the known temperature has been chosen to be room temperature. Before the start of the tests the thermocouple differential amplifier output has been aligned with the ground level of the oscilloscope, and after each test the signal was

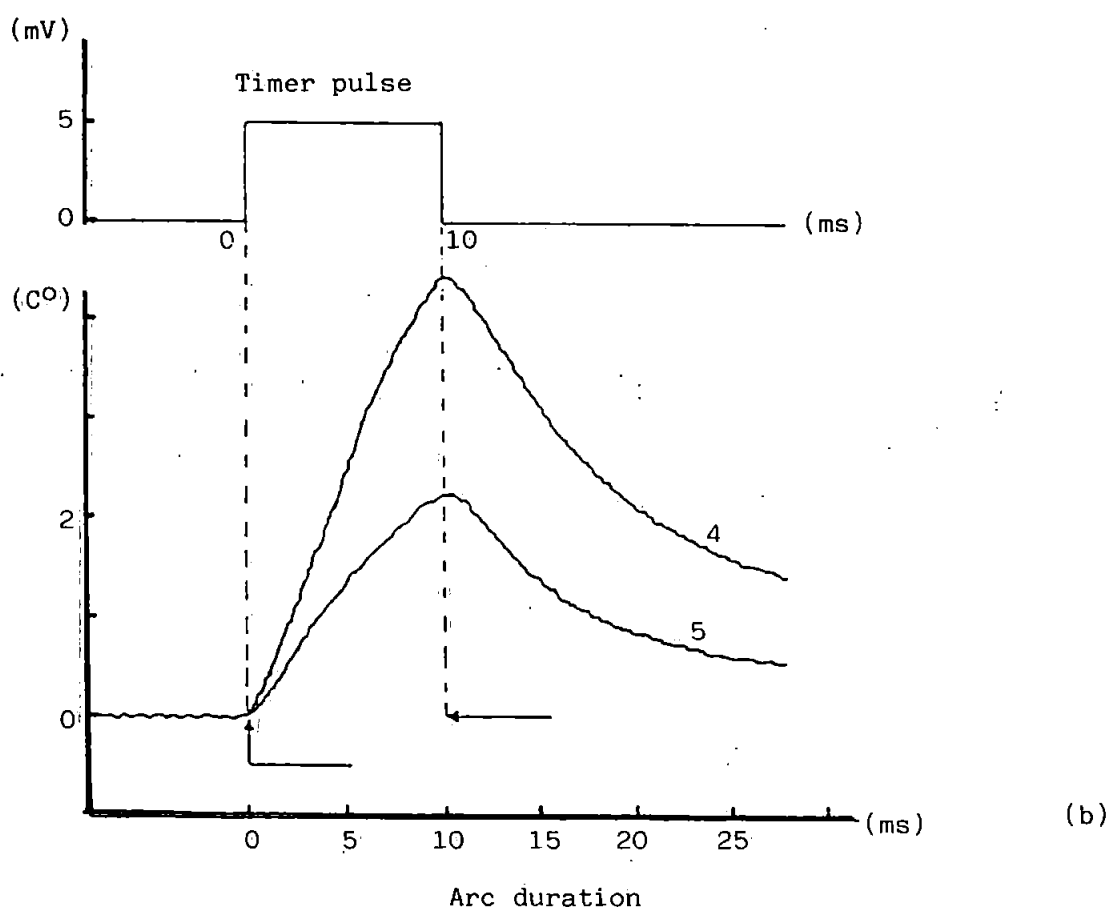
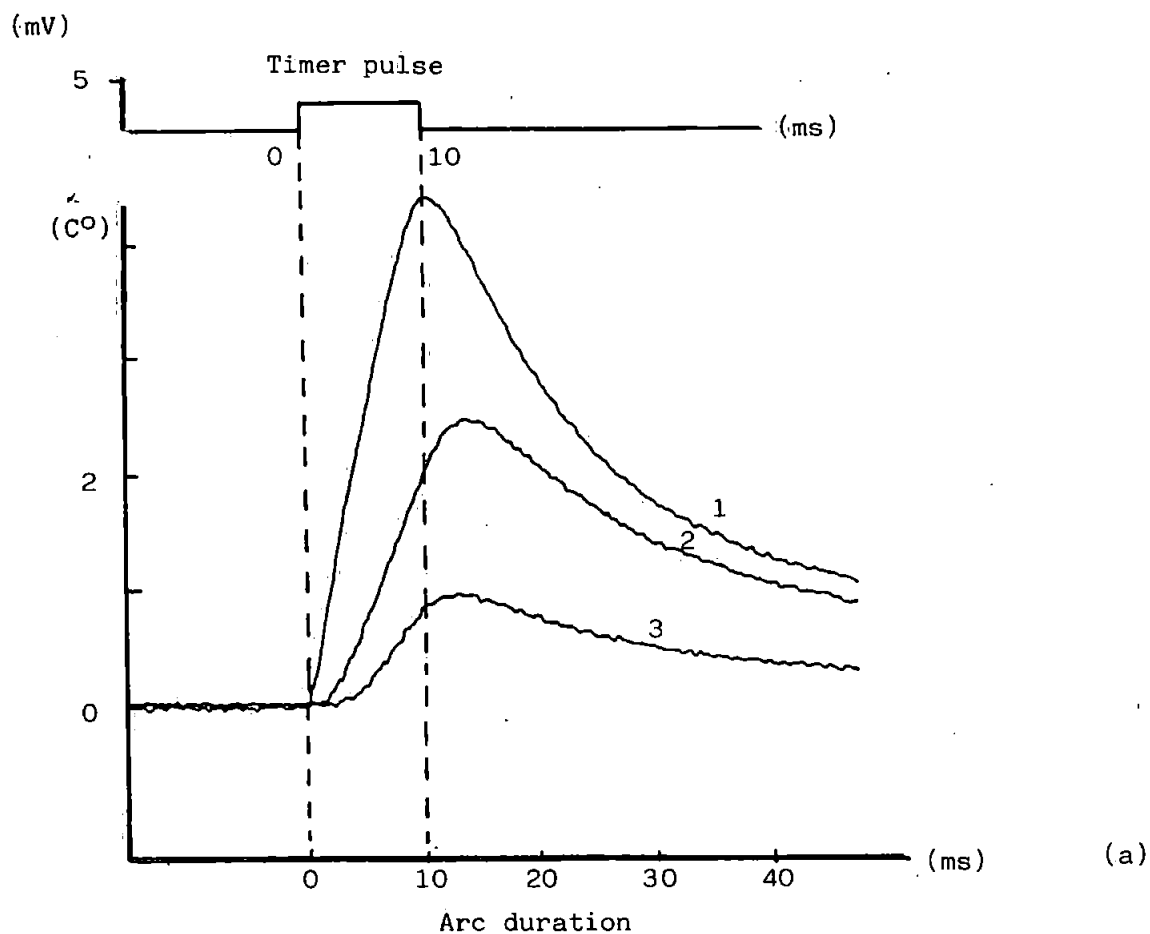


Figure 4.30: (a & b) show that differences exist between the output response of the thermocouple probes (1-5), - 173 - which have the same method of construction; for a fixed test condition. (The timer pulse determines the duration of the arc.)

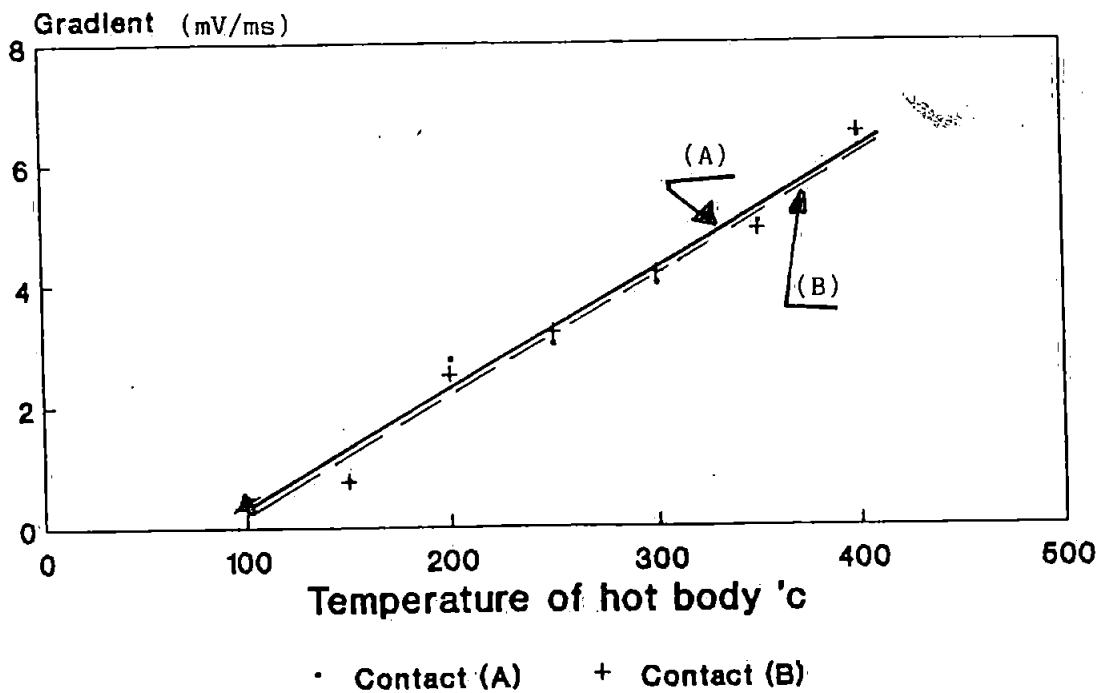


Figure 4.31: Shows the characteristics of the probes A and B obtained from the calibration system; for a fixed test condition.
(These two probes have been used for all the temperature-time experiments here.)

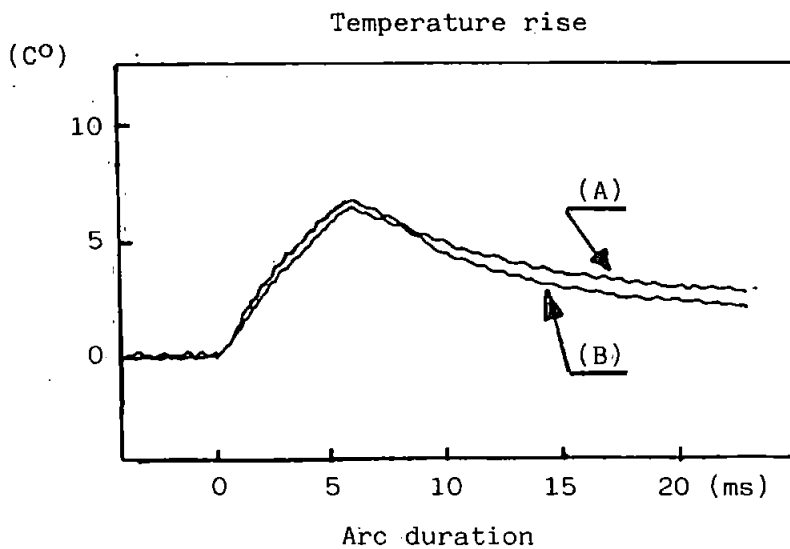


Figure 4.32: Shows the characteristics of the probes A and B on the test rig, in which each has been used as the anode for a fixed test condition.

allowed to settle to its original position. This enables one to detect accurately a small temperature rise of the contact body which otherwise would not be detected. A typical temperature-time curve is shown in figure (4.29) for test conditions of 40 V, 10 A, 0.5 mm, and arc duration of 4 ms.

4.5.2 CALIBRATION OF THE SENSOR

Temperature-time characteristics of several tens of sensors have shown that although the method of their construction and the materials used for each are the same, the response of each for a fixed test condition is different. Typical examples are shown in figures (4.30). These figures reveal that the gradient of the curve, the amplitude of the peak and its timing are different from each other.

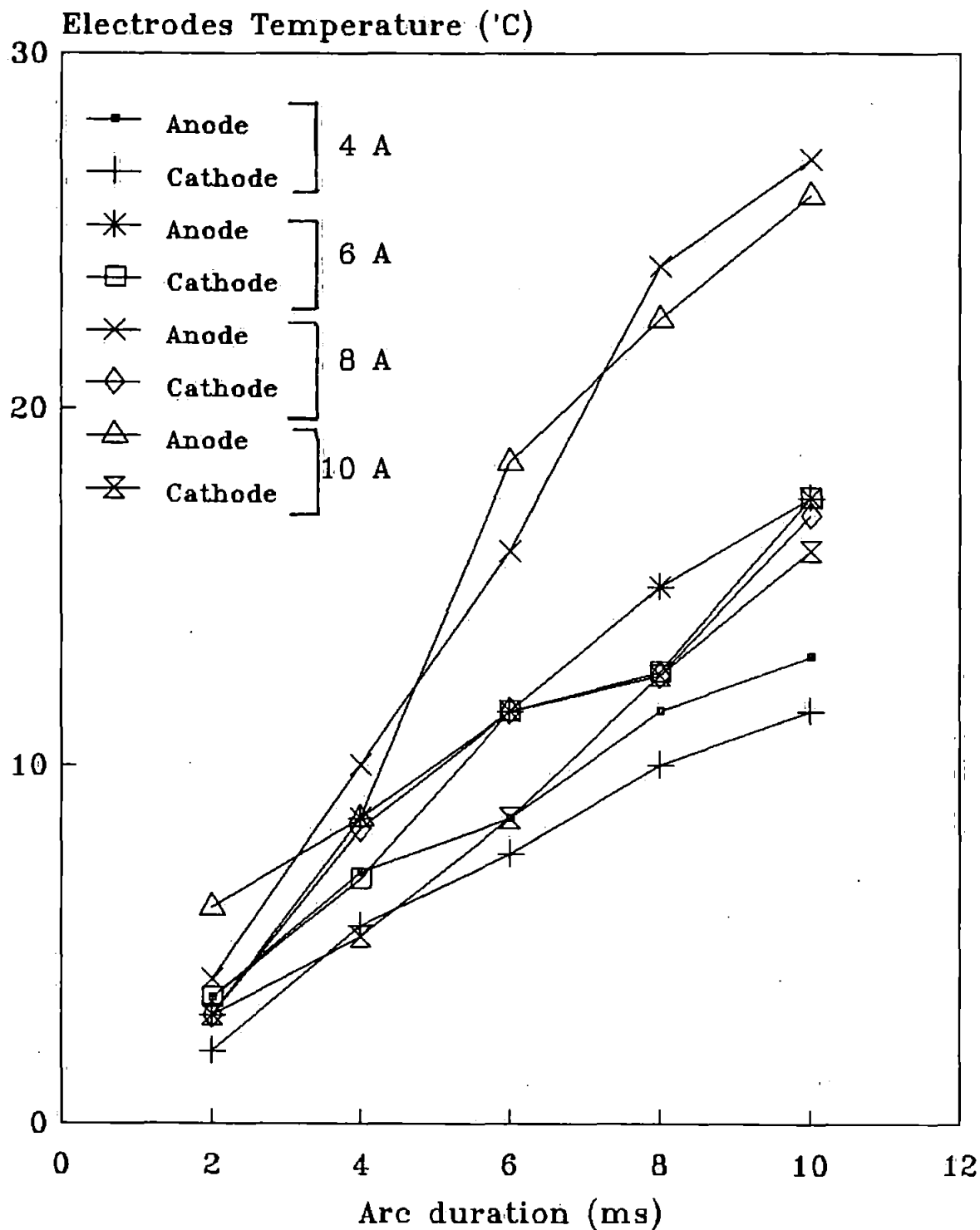
Use of any pair of these sensors will mislead one as to the interpretation of the results and hence a meaningless relation between thermal and electrical power. For this reason the probes (contact with thermocouple) under investigation for fixed test conditions must be identical in every aspect, such as time constant, amplitude and timing of peak.

To ensure the above conditions before the test, a number of probes have been calibrated on the calibration system designed and constructed here. (This facilitates testing and reduces damage to the contacts before the actual test.) Two probes, named here as A and B, which had identical characteristics, as shown in figure (4.31) have been chosen. Their performance has also been checked on the Test Rig, in which each has been used as anode for a fixed test condition. This is shown in figure (4.32).

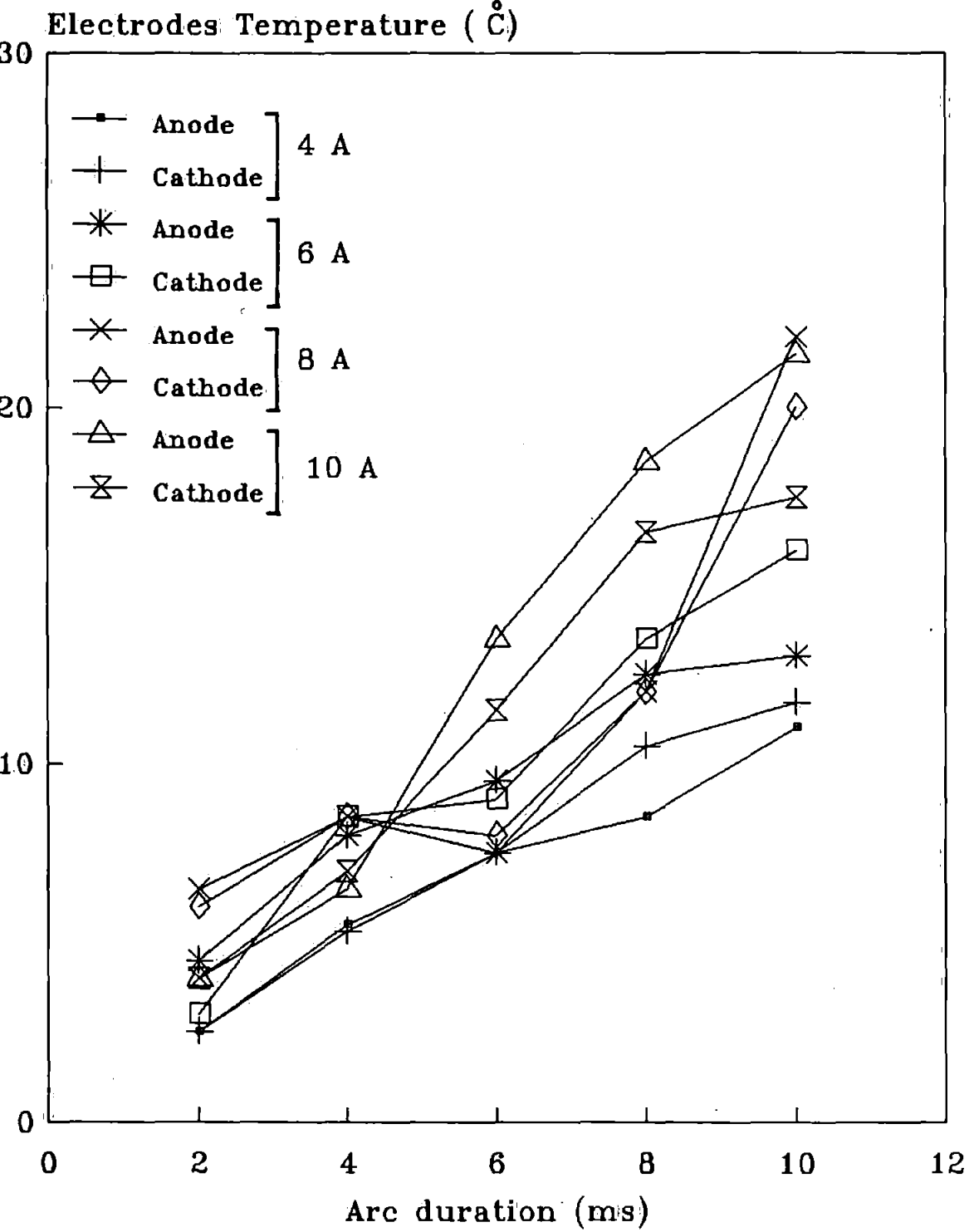
All temperature-time experiments for various test conditions and parameters have been carried out on these two probes.

Figure (4.33): Graphs of (a-e) show variation of electrode temperatures with arc duration at a test condition of 0.05-mm gap-length, 40 volts supply, 300mm/s speed of opening and currents ranging 4-10A.

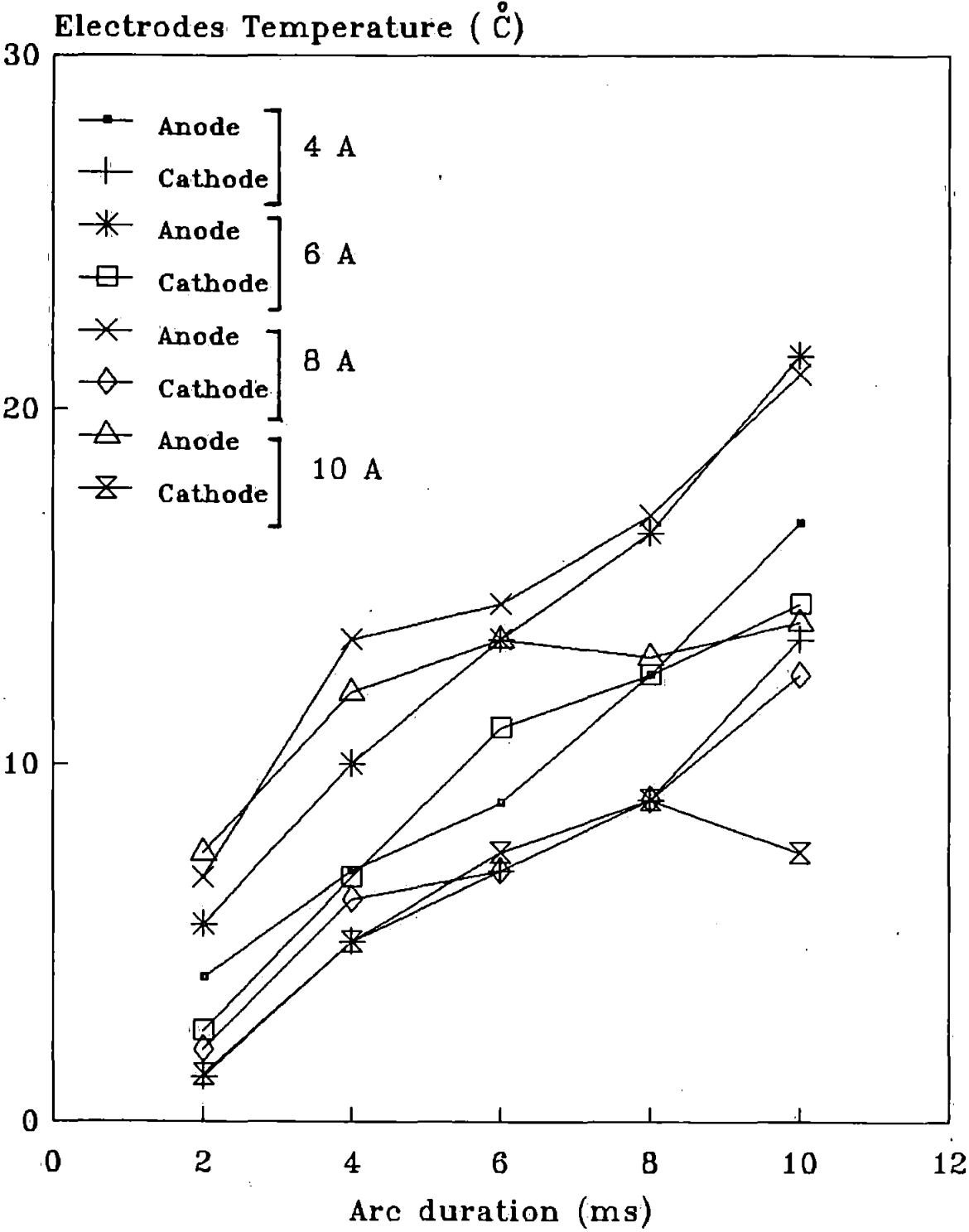
4.33a : Electrodes temperature versus arc duration for a gap-length of 0.05 mm and a current of 4-10 A.



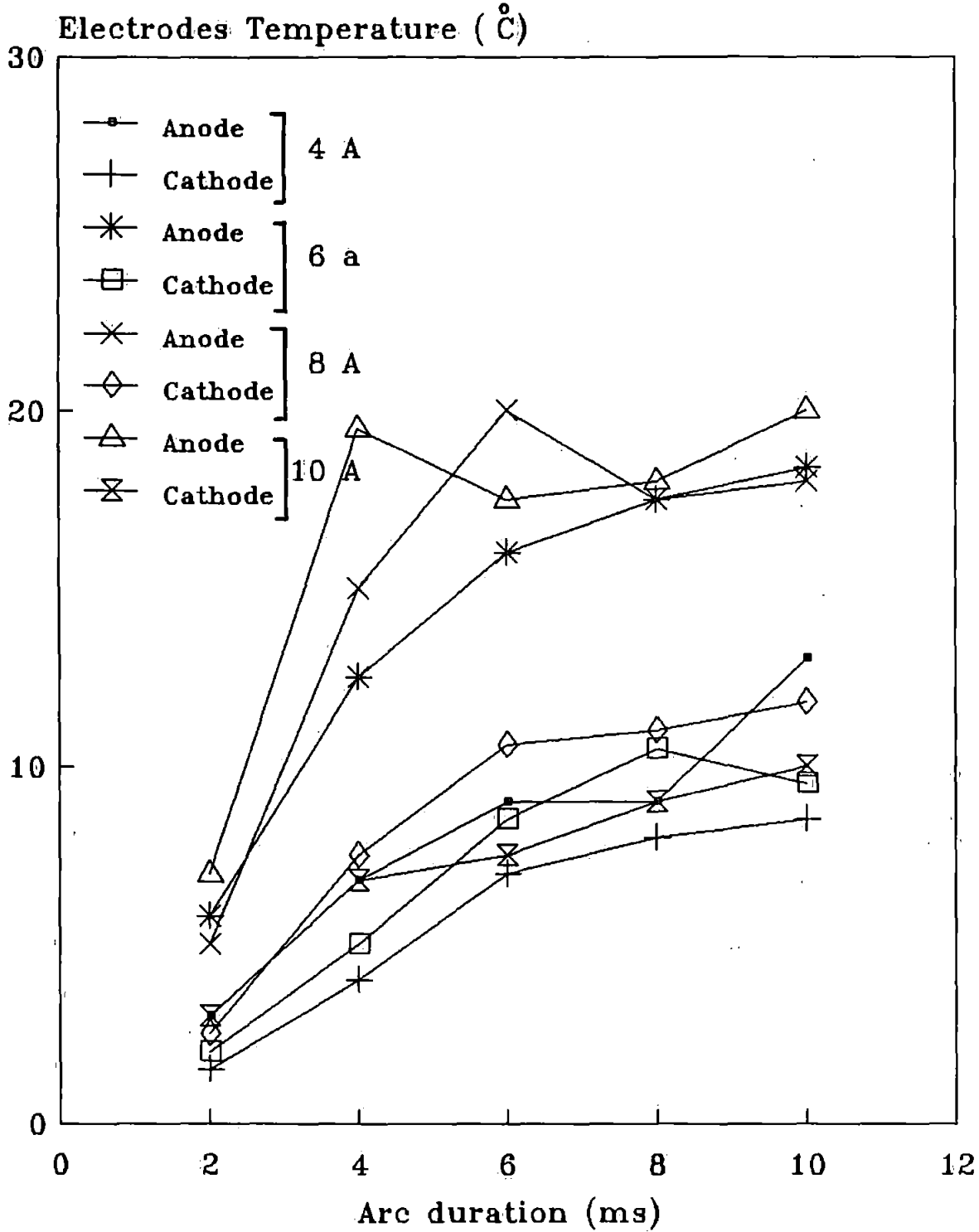
4.33b : Electrodes temperature versus arc duration for a gap-length of 0.1 mm and a current of 4-10 A.



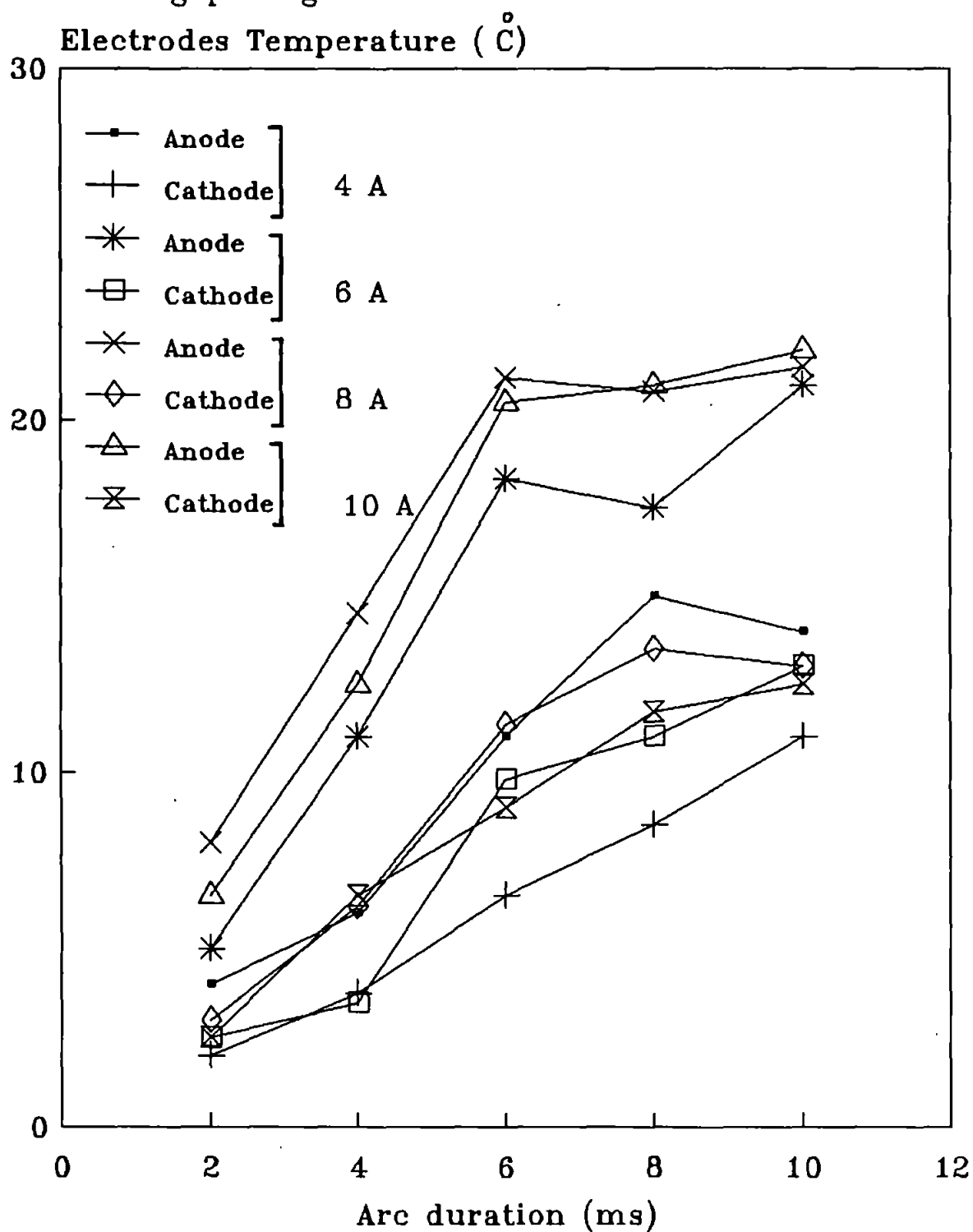
4.33c : Electrodes temperature versus arc duration for a gap-length of 0.2 mm and a current of 4-10 A.



4.33d : Electrodes temperature versus arc duration for a gap-length of 0.5 mm and a current of 4-10 A.



4.33e : Electrodes temperature versus arc duration for a gap-length of 1 mm and a current of 4–10 A.



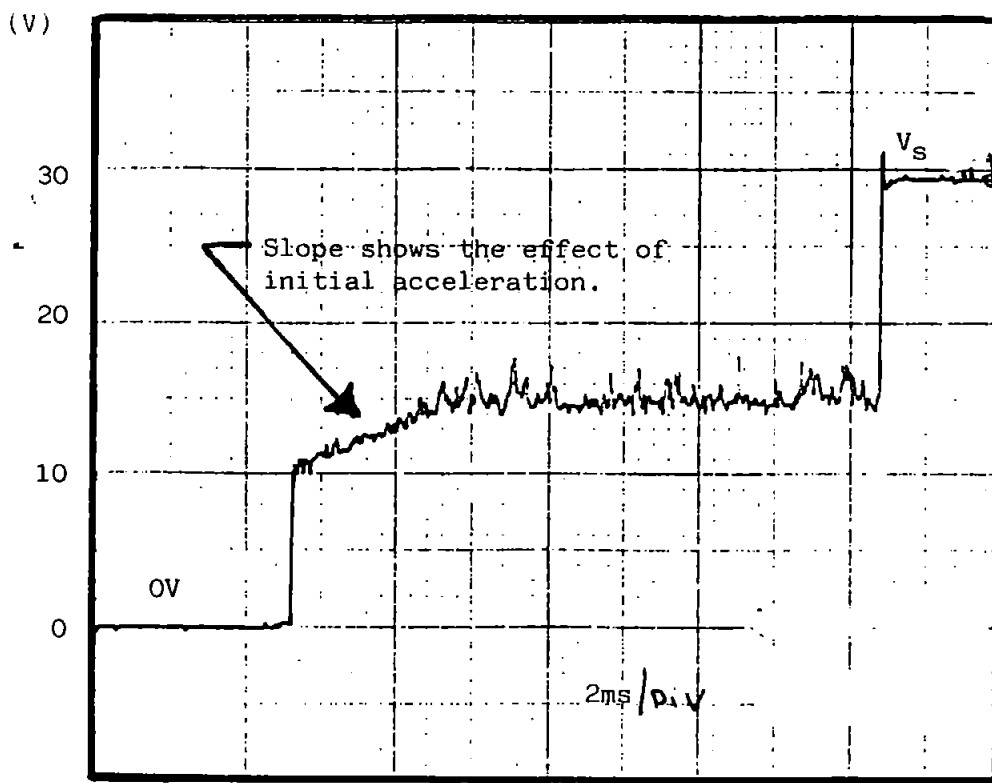


Figure 4.34: Shows the effect of a slower initial acceleration of the solenoid on the arc voltage waveform; for a test condition of 30 volts, current of 8A, speed of opening 300mm/s and gap-lengths of 0.1mm.

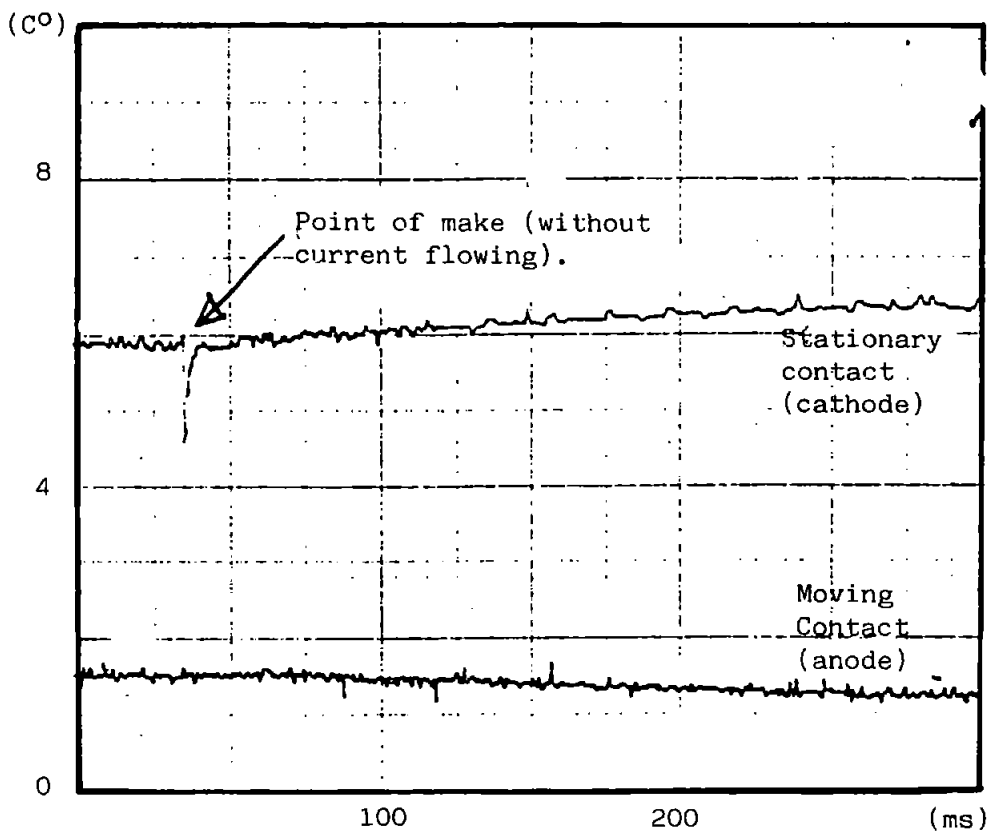


Figure 4.35: Show that from the moment the contacts come to rest, the cathode temperature rises by the same amount as the anode temperature decreases; for this condition the supply voltage is off.

Using the two calibrated probes A and B, the temperature of the electrodes (cathode and anode) for various test conditions such as current, gap-length and arc duration for an operating voltage of 40 Volts and speed of 300 mm/s at break has been measured. A sample of characteristics of these electrodes for various parameters can be seen in appendix III. However, the responses of these electrodes (which are representative of the actual temperature) for current of 4-8A and gap-length of 0.05-1mm are plotted against arc duration and are shown in figure (4.33).

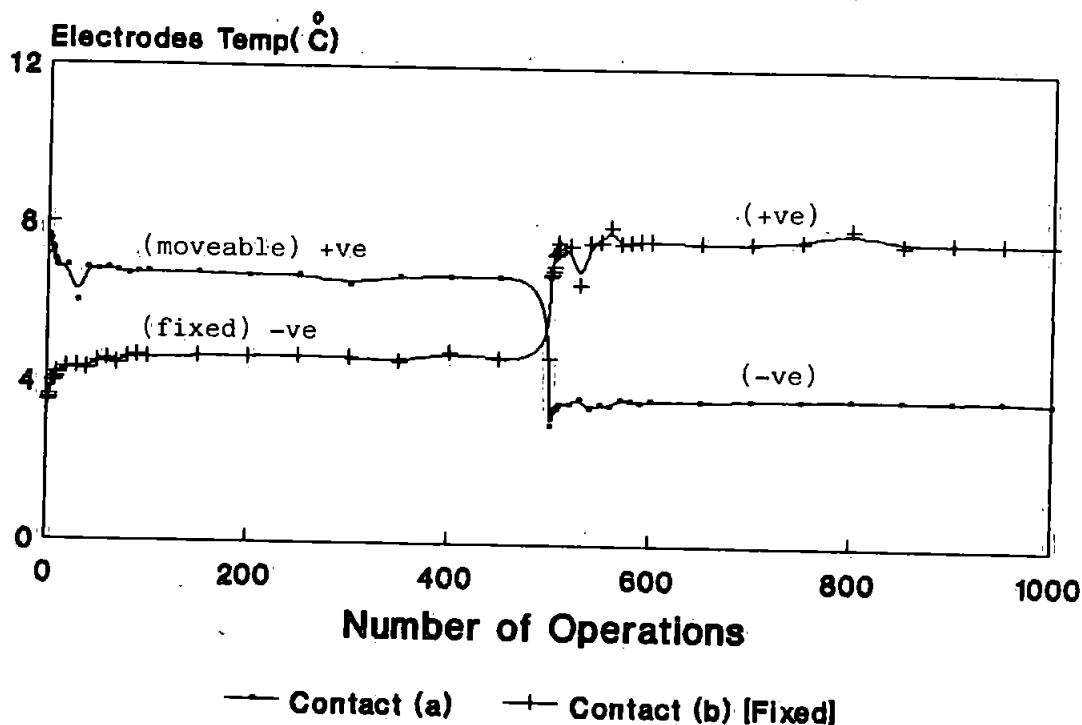
From figure (4.33), one can observe that the temperature difference between the electrodes for a gap of below 0.2 mm is insignificant compared to that for a higher gap-length. This is especially true for current below 8 A and arc duration below 6 ms.

Also the temperature of the electrodes at different current and gap-length has a linear relation to the arc duration and increases from room temperature to approximately 30° C over a range of current, gap-length and arc duration extending from 4-10 A, 0.05-1 mm and 2-10 ms respectively.

From figure (4.33), one could also observe that in some cases the temperature of anode, or cathode, or both, at higher current are smaller than that at lower. One can relate this to non-uniform movement of the arc, or the arc not occurring at the same place where the previous arc occurred (i.e. the arc occurred at a place remote from the thermocouple), or a change in the initial acceleration of the solenoid (slower compared to previous), which affects the arc voltage waveform. A typical example obtained for an operating voltage of 30 V, current of 6 A and gap-length of 0.1 mm is shown in figure (4.34).

The graphs in appendix III show that for gap-length greater than 0.2 mm the anode temperature is higher than the cathode temperature. This can also be observed from figure (4.35) which shows that when the contacts come together (the

4.36(i): 4A, 0.5mm, 4ms.



4.36(ii): 4A, 0.5mm, 8ms.

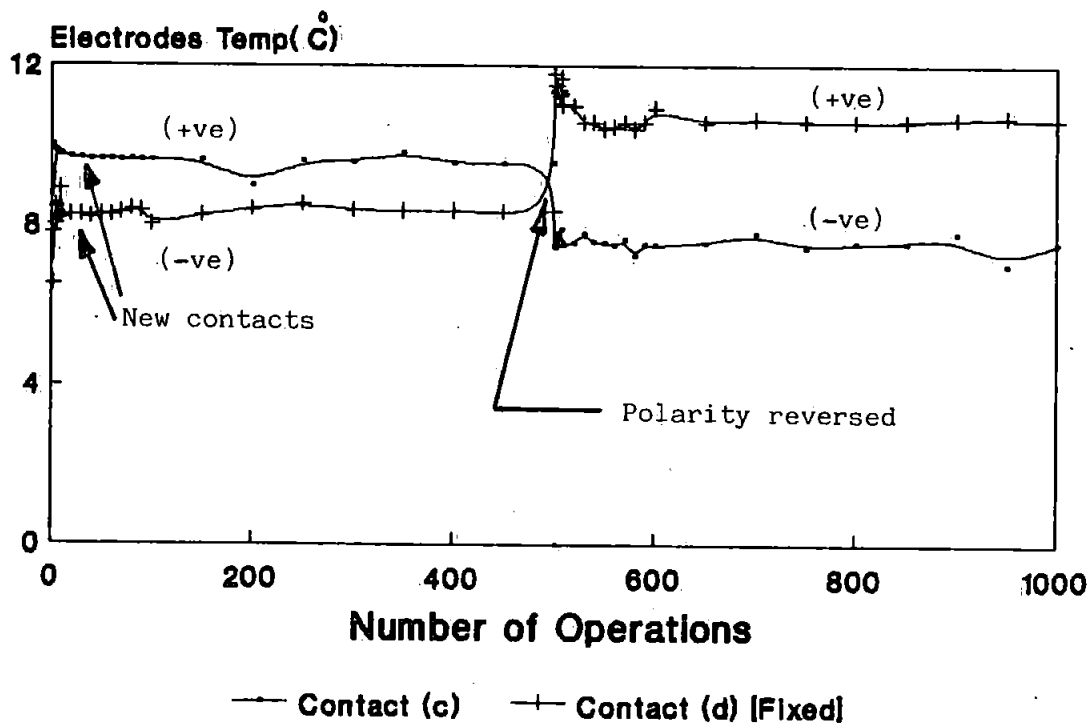
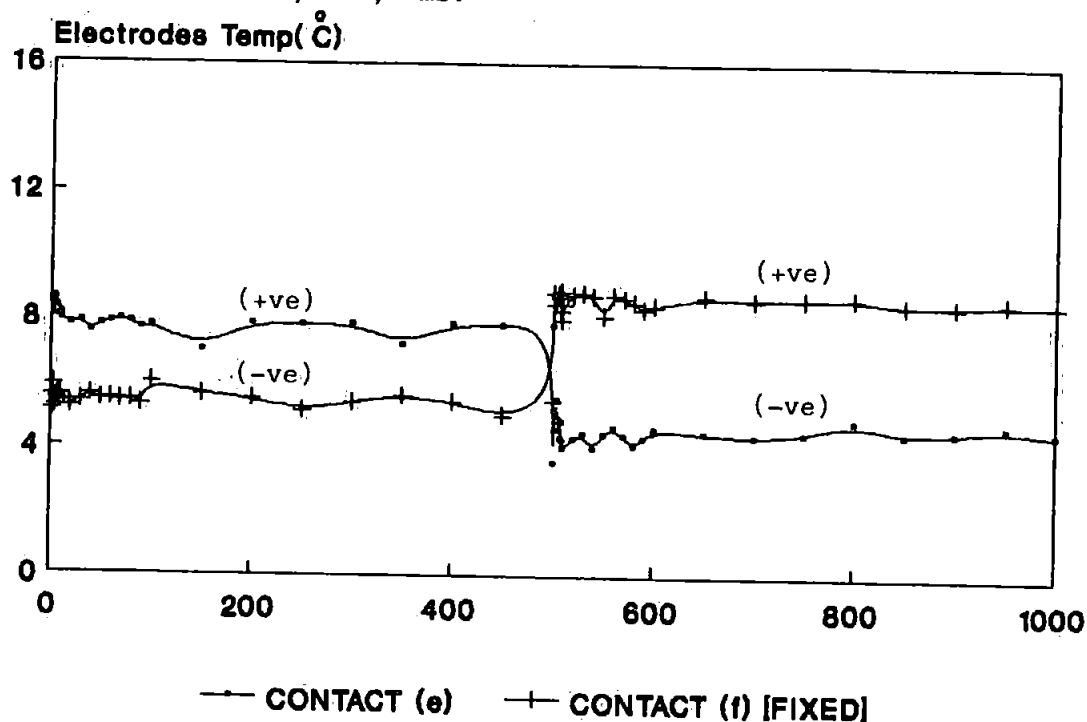


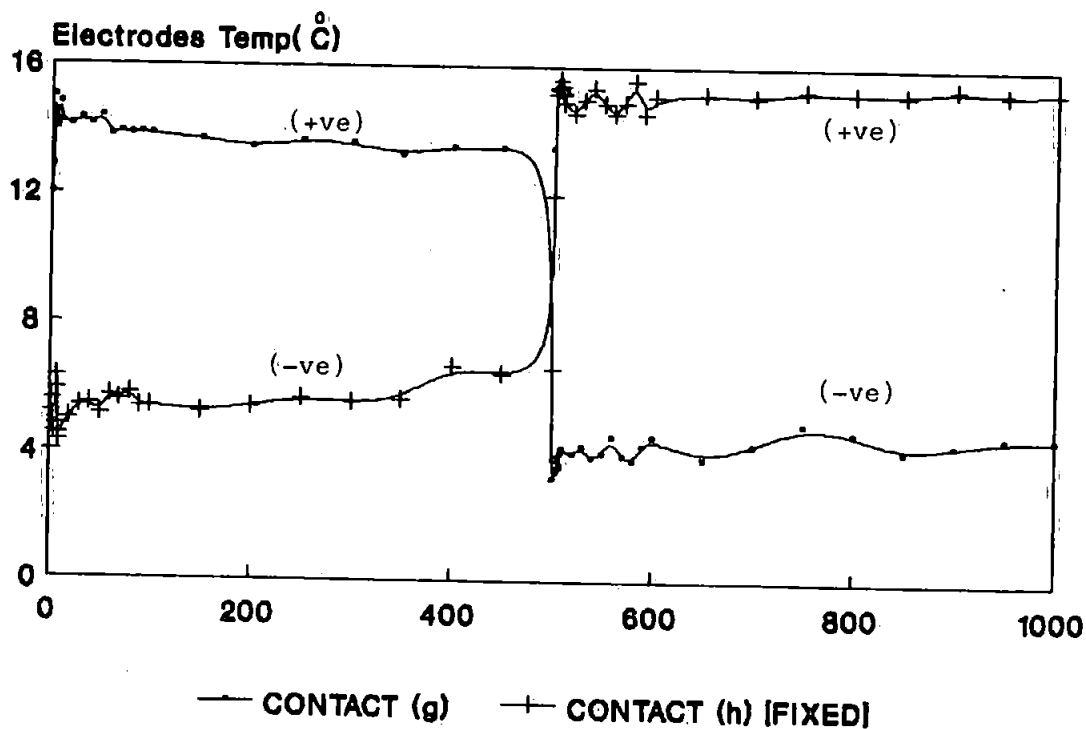
Figure 4.36: Graphs of (i-iv) show the effects of contact newness and polarity change for four pairs of contacts against the number of operations at the following test conditions:

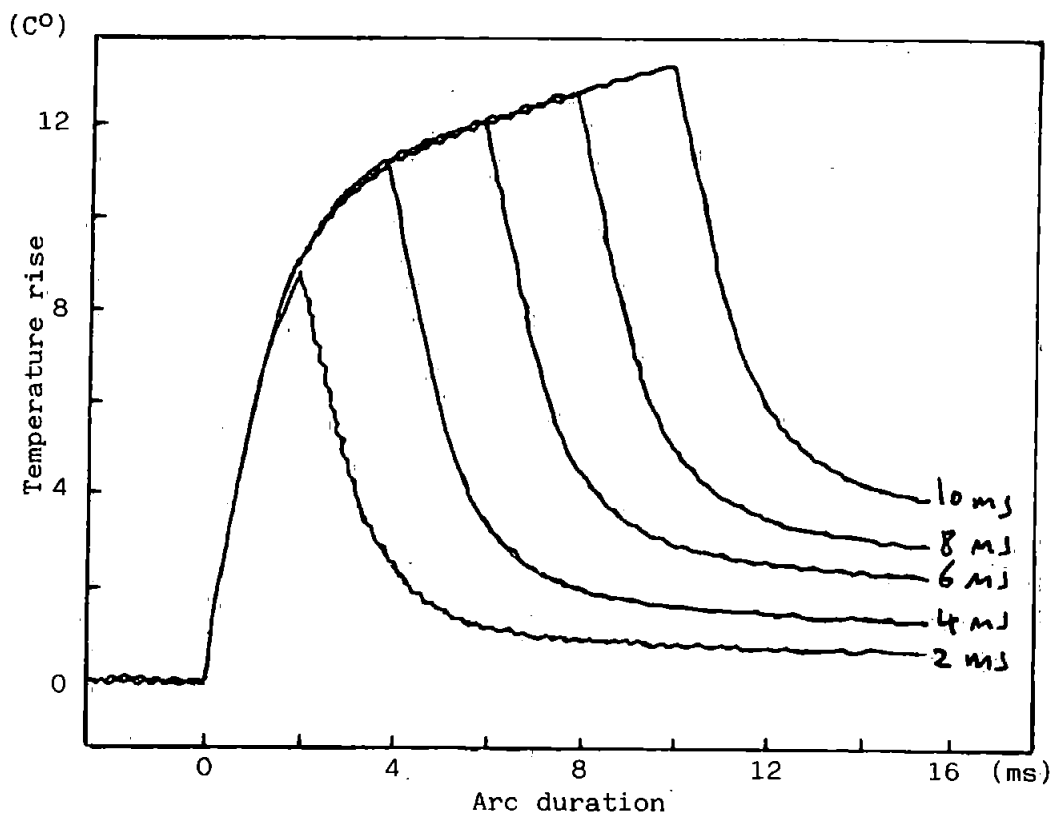
- (i) Current 4A, gap-length of 0.5mm and arc duration 4ms.
 - (ii) Current 4A, gap-length of 0.5mm and arc duration 8ms.
 - (iii) Current 4A, gap-length of 1mm and arc duration 4ms.
 - (iv) Current 6A, gap-length of 1mm and arc duration 4ms.
- Observed operations are 1-10 step 1, 11-100 step 10, 101-500 step 50 and then polarity has reversed.

4.36(iii): 4A, 1mm, 4ms.



4.36:(iv): 6A, 1mm, 4ms.

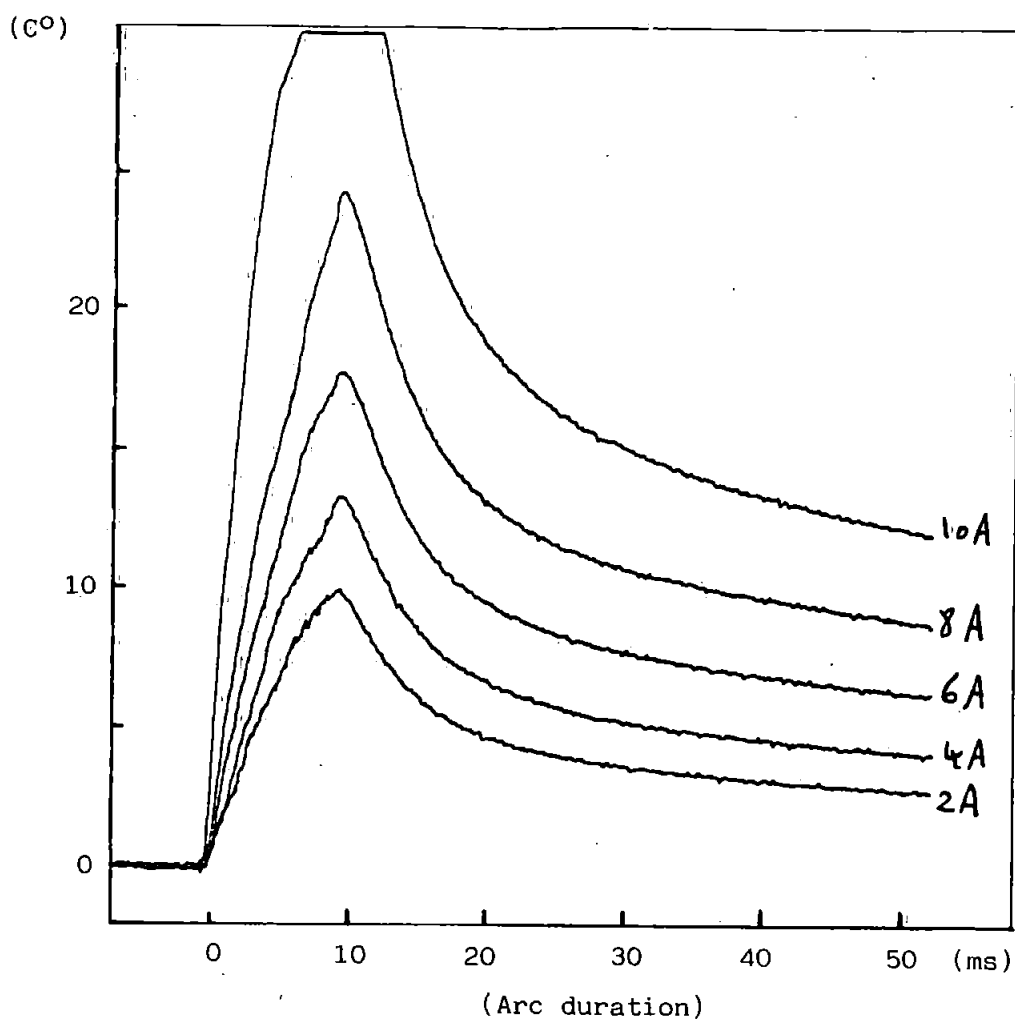




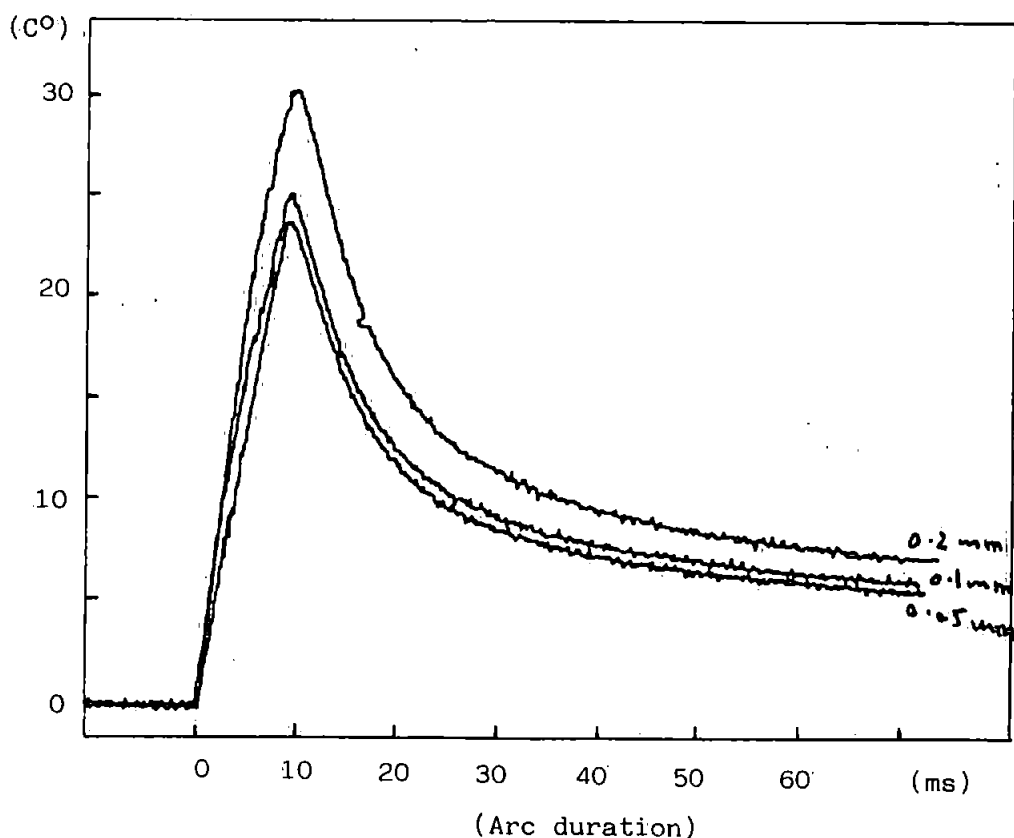
4.37(i): For an arc duration of 2-10ms, gap-length of 0.1mm, current of 5A and operating voltage of 40V.

Figure 4.37: (i-iii) show the temperature-time response of probe (A) which is the same as probe (B) at the following test conditions:

- (i) Current 2-10A
- (ii) Gap-length 0.05-0.2mm
- (iii) Arc duration 2-10ms



4.37(ii): For a current of 2-10A, gap-length of 0.1mm, arc duration of 10ms and supply voltage of 40V.



4.37(iii): For a gap-length of 0.05-0.2mm, arc duration of 10ms, current of 5A and operating voltage of 40V.

supply being off) the cathode temperature rises by the same amount that the anode temperature decreases.

The effects of contact newness and polarity change for four pairs of contacts have been studied at various current, arc duration and gap-length. The results obtained are plotted against the number of operations and are shown in figure (4.36). These results also suggest that when the contacts are new there is inconsistency in the value of electrode temperatures and after about 50-100 operations, depending on circuit conditions, the electrode temperatures reach to steady values. This may be the reason why where these contacts are used in switches for the temperature control of electrical appliances such as refrigerators, before their employment a high level D.C. arc is drawn between them, probably to burn off poorly-conducting surface deposits which are often found on metal components, which would otherwise adversely affect the temperature-control function of the switch.

Figure (4.36) also shows that where the change of polarity occurs after 500 operations, the contact which now acts as anode (fixed contact) has a higher temperature than previously and the situation is reversed for the contact which now acts as cathode (moving contact), its temperature now being lower than previously. This may be due to the moving contact causing a flow of air over its surface.

If the above argument is true, one can conclude that in D.C. operating conditions, making the cathode the moving contact may reduce the life expectancy of the switches.

Finally, in order to complete the set of temperature-time characteristics of the above used electrodes, in relation to the development of thermal power modelling, the responses of the probe (A), which is the same as probe (B), for various currents, gap-length and arc duration are represented graphically in figure (4.37).

4.6 POWER BALANCE AT THE ELECTRODES

The performance and the reliability of the switches depends upon the erosion of their contacts. Contact erosion is caused by joule heating on the contact surface. In order to understand the mechanism of the contact erosion, it is important to know the distribution of the arc power to the contacts. This can be assessed from a comparison of electrical and thermal power.

The electrical power which is the input power, is the product of current and voltage drop in front of the contact surface which then raises the electrode temperature. The thermal power consists of some of the power absorbed by the contact and power used in the melting and evaporation of contact material.

In section (2.7) the models for the power balance relation at the electrodes of several workers are explained and their derived equations are shown in table (2.6).

Here the power balance relation has been derived from temperature-time characteristics of the electrodes, measurements of cathode and anode fall voltage, Capp's⁽²⁰⁾ derived expression and network response technique.

It is assumed that the power to the electrodes is transferred by the ion and electron current in the fall regions.

4.6.1 ELECTRICAL MODEL

Since the duty of each electrode is different from each other, the power balance at the cathode and anode electrodes have been considered separately.

4.6.1.1 Power balance at cathode

Due to electric field or thermal excitation, electrons in the atoms on the cathode surface become excited and they move to higher shells. The force of attraction between nucleus and electrons reduces, and as a result the electrons are liberated.

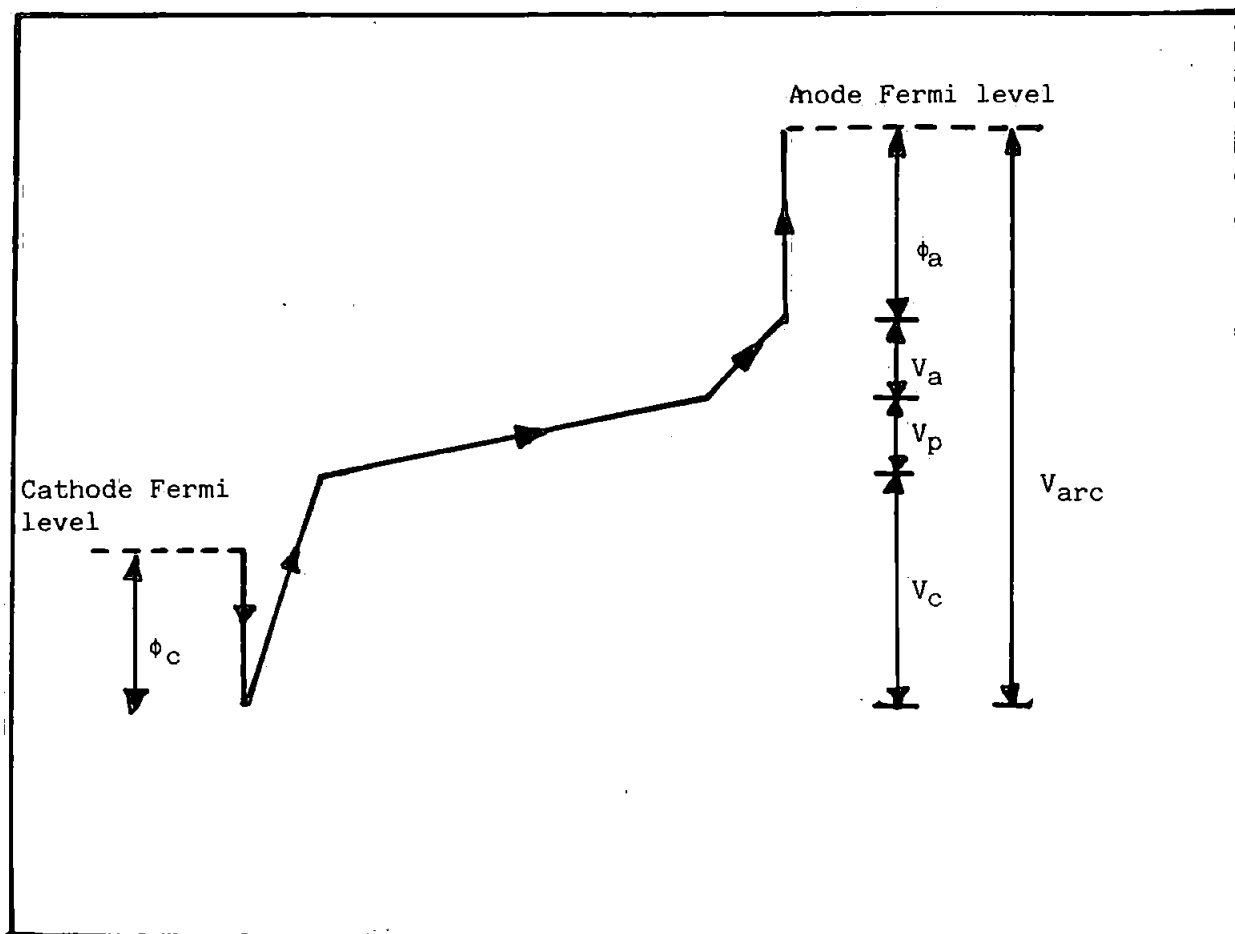


Figure 4.38: Capps' Electron Potential in the Arc.

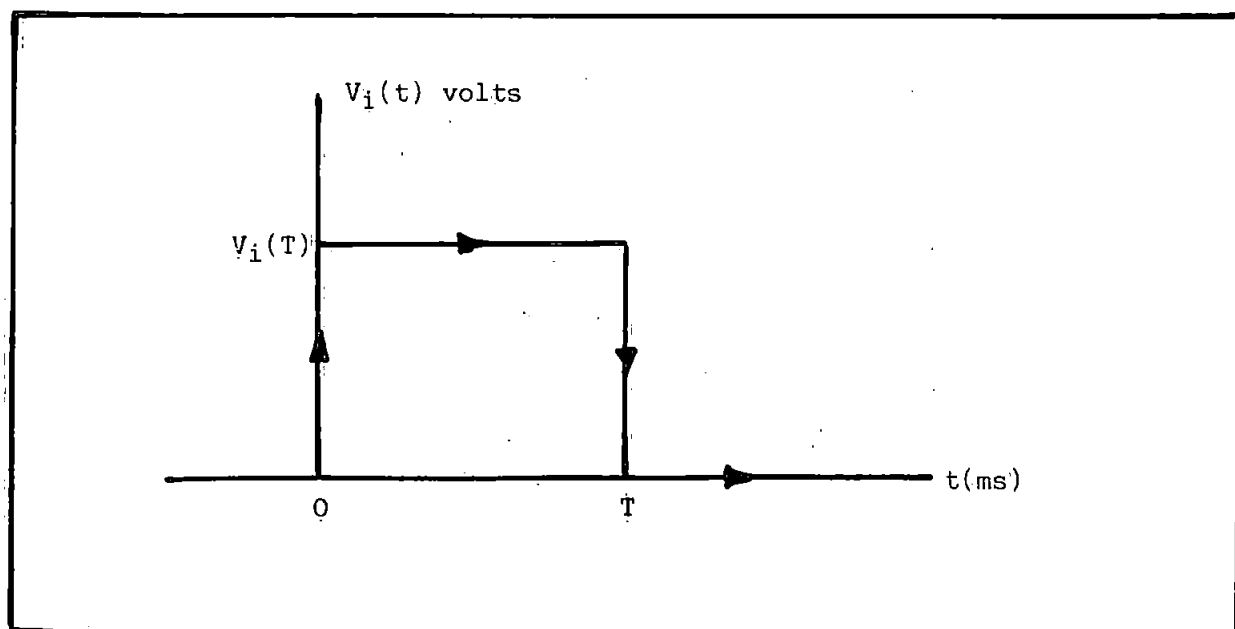


Figure 4.39: The d.c pulse, of width T and amplitude $V_i(T)$ to the RC network.

These electrons in the cathode fall region ionise the excited and uncharged atoms (neutral atom), as described by Capp⁽²⁰⁾. This region is also described by Von Engel and Robson⁽²⁾ as a source of positive ions, due to multiple collisions of excited atoms.

Considering that the dominant mechanism of energy transfer to the cathode is positive ion bombardment and the energy loss from collision of these +ve ions with atoms in the ionisation region is negligible⁽²⁰⁾ and using the simple outline of the potential in the different regions of the arc as shown in figure (4.38), it can be proposed that the cathode is heated up by the power from the voltage drop across the cathode fall ($I_p.V_c$); power from the ionisation region ($I_p.V_i$), which is assumed to be thin with a small voltage drop across it; and power from the hot column by thermal transfer.

In the plasma column, the power generated is $I.V_p$, since electrodes separations are small compared with the diameter of the electrodes and the diameters of the electrodes are much greater than the diameter of the column, and the plasma is a good conductor, it can be assumed that half of its heat is conducted to each electrode. Thus radiation, convection and conduction losses through the plasma to the exterior surroundings are ignored.

The power losses from the cathode surface are: the conduction power (P_{ch}); evaporation power (P_{ev}); convection power (P_{cov}); and the power loss to the escaping electrons ($I\phi_c$) moving out from the cathode (which is known as the Work-Function). In view of the above assumptions, the power balance equation for the cathode is as follows:

$$I_p.V_c + I_p.V_i + I.(0.5).V_p = I.\phi_c + P_{ch} + P_{ev} + P_{cov} \quad (1)$$

Let $\gamma = I_p/I$... ratio of positive ion current to total current.

Therefore (1) can be written as

$$I(\gamma.V_c + \gamma.V_i + 0.5.V_p - \varphi_c) = P_{ch} + \text{other losses} \quad (2)$$

Let $VCE = \gamma V_c + \gamma V_i + 0.5 V_p - \varphi_c$ ^{total} (voltage drop in front of cathode).

4.6.1.2 Power Balance at Anode

The electron current is assumed to be the dominant mechanism of the heat transfer to the anode, and $I_e \approx I$ (approx.). The heat received by the anode is from: the fall region ($I.V_a$); thermal power of the electrons ($I.V_e$); the power conducted from the hot gas (column) ($0.5 V_p.I$); and power given off by the electrons absorbed by the anode.

The heat losses from the anode surface are: the conduction heat flow; evaporation power; and convection power. The power balance for the anode is then:

$$I.V_a + I.V_e + I(0.5 V_p) + I.\varphi_a = P_{ah} + P_{ev} + p_{cov} \quad (3)$$

or

$$I(V_a + V_e + 0.5.V_p + \varphi_a) = P_{ah} + \text{other losses} \quad (4)$$

Let $VAE = V_a + V_e + 0.5 V_p + \varphi_a$ (total voltage drop in front of anode).

4.6.2 THERMAL MODEL

For the purpose of calculating the amount of power being dissipated on the surface of each electrode from the thermocouple output which is placed approximately $200\mu m$ away from the centre of the electrode, the response of the thermocouple in the contact with respect to constant heat flow is simulated by the response of an RC circuit to a d.c. pulse.

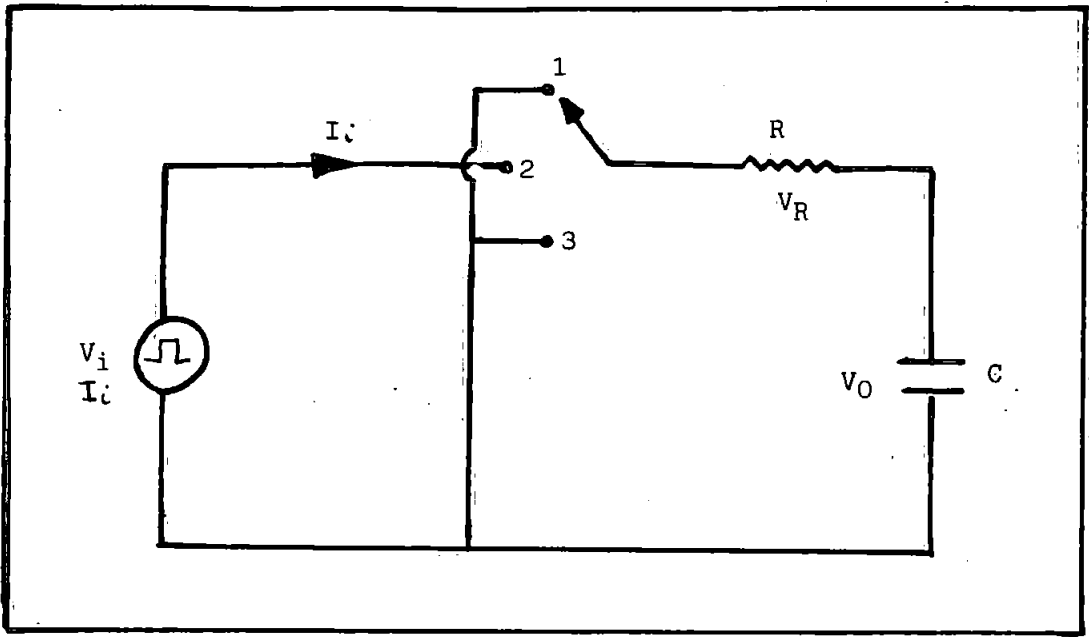


Figure 4.40: A simple RC circuit, which simulates the response of the thermocouple in the contact with respect to a constant heat flow.

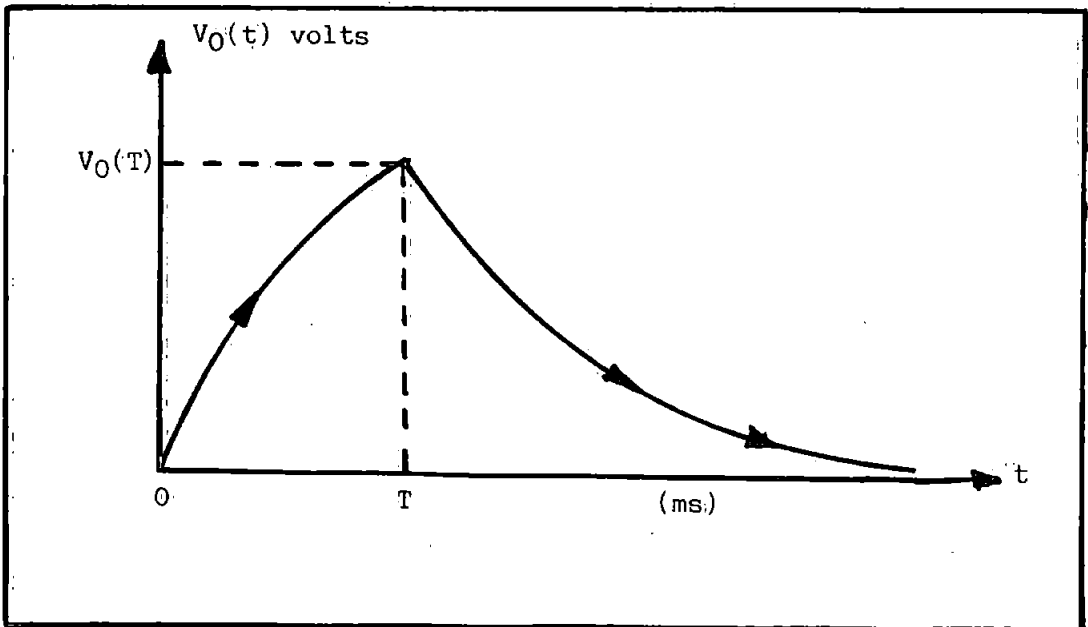


Figure 4.41: The charging and discharging characteristics of the figure 4.40.

Consider a pulse of width T and amplitude V_i as shown in figure (4.39) generated by the circuit of figure (4.40).

Initially the switch sweeper is in position 1, which is open-circuit and no current is flowing. To start the sequence the sweeper is switched to position 2. It is assumed that at the instant at which the switch is closed the capacitor is initially uncharged.

Applying Kirchhoff's voltage law to the circuit (4.40) for $t = T$ the charging voltage is as follows:

$$V_o = V_i \left[1 - e^{-\frac{T}{CR}} \right] \quad (5)$$

The CR is known as time constant of the circuit and is denoted by α . If $T = \alpha$, equation (5) becomes as $V_o = V_i(1 - e^{-1}) = 0.63V_i$, so that the time constant of the circuit can be defined as the time for the capacitor voltage to increase approximately 63% of its final value.

For $t > T$, when switch is turned to position 3, the new time origin becomes $t = T$; that is $t' = t - T$, in which case, the charged capacitor is discharged through a resistor, R . The discharge equation is as follows:

$$V_o = V_i \left[e^{-\frac{t}{CR}} \right] \left[e^{\frac{T}{CR}} - 1 \right] \quad (6)$$

From equation (6) one can say that for $t > T$ the voltage decays exponentially to zero from a value V_o . The charge and discharge characteristics are shown in figure (4.41).

The different electric circuit parameters and their analogue in the thermal system are:

Current flow i (A)

Heat flow \dot{Q} (J/s or W)

Electrical capacity C_e (F)

Thermal capacity $C_A = \rho v(J/k)$

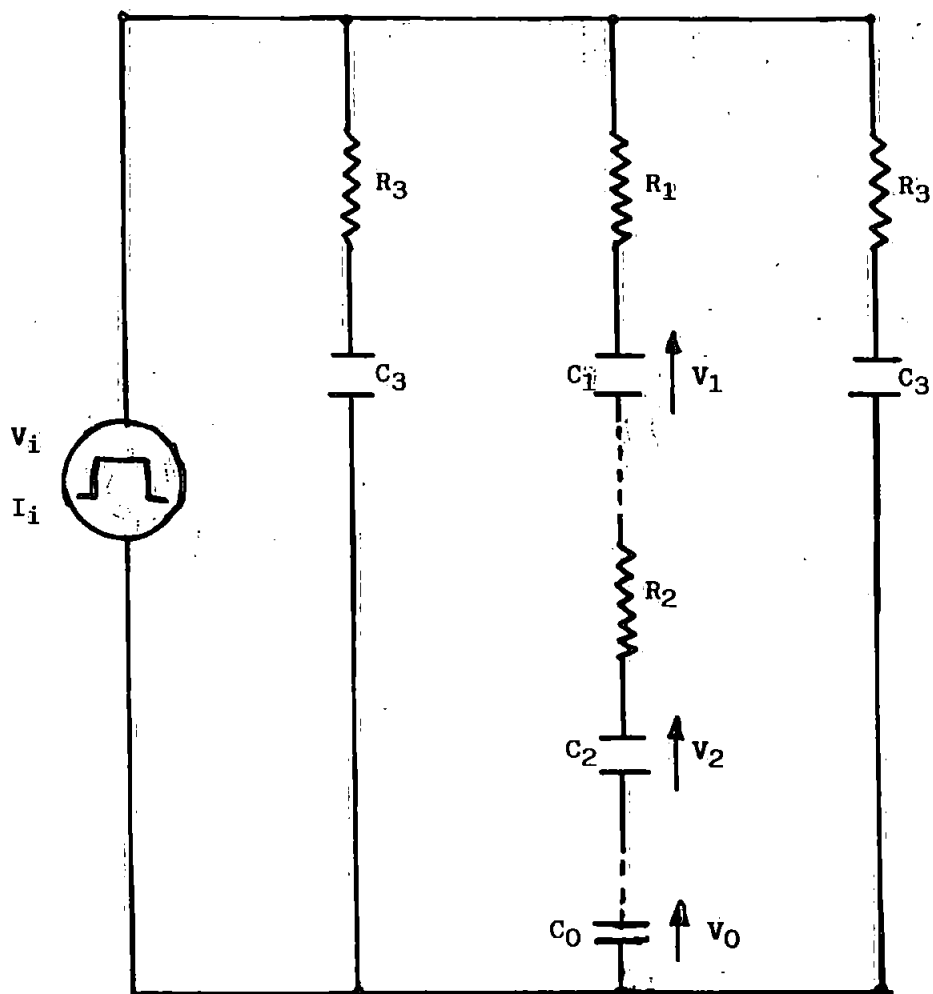


Figure 4.43b: Shows equivalent circuit of figure 4.43a.

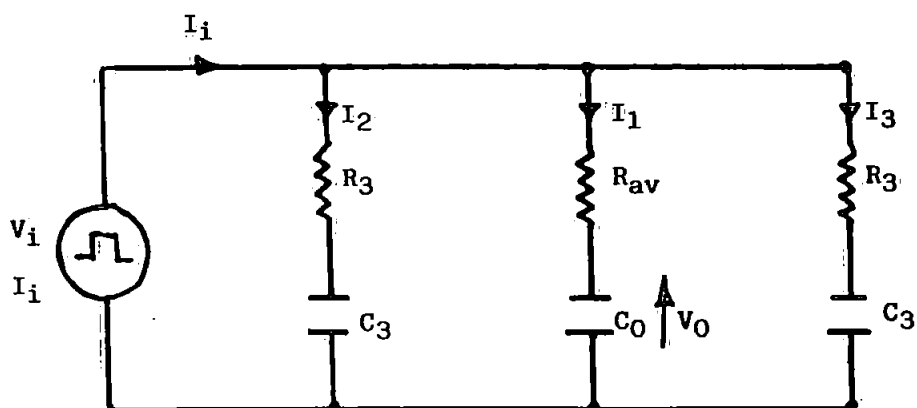


Figure 4.43c: Represents the simplified equivalent circuit of figure 4.43b.

$$\text{Electrical resistance } R (\Omega) \quad \text{Thermal resistance } R_{th} = \frac{\Delta X}{KA_s} \quad (\frac{^\circ K}{W})$$

$$\text{Electrical potential } (V_2 - V_1) (V) \quad \text{Thermal potential } (\theta_2 - \theta_1) (^\circ K)$$

where C_p = specific heat of contact $J/Kg \text{ } ^\circ K$
 ρ = density of contact kg/m^3
 V = volume of contact m^3
 θ = average temperature of contact $^\circ K$
 K = thermal conductivity $W/m/^\circ K$
 A_s = surface area of contact m^2

To apply equations (5) or (6) to the thermal system (contact containing thermocouple), the potential field of the thermal system must be fully understood in terms of equal flux lines and equal voltage lines.

The analogue of equal current flow line is heat flow line and equal voltage line is isotherm. the isotherm and heat flow lines are perpendicular to each other at any point.

It is assumed that, since the diameter of the contact is much greater than the gap-length, during heating (arcing) heat lost to the surroundings is negligible and once the intermediate layer of the contact surface (arc seat) is heated to an equilibrium temperature, most of the heat entering the contact flows from one cell (curvilinear square) into the next cell and is received by the thermocouple. The isotherms and heat flow lines for the contact with the thermocouple are shown in figure (4.42).

The electrical analogue of figure (4.42) is shown in figure (4.43a), in which each isotherm is represented by an equivalent series of resistance and capacitance. These equivalent resistances and capacitances are the electrical analogue of the cells.

In figure (4.43a), R_1 and R_2 are the thermal resistances of the Silver and the Loctite adhesive respectively, C_1 and C_2 their thermal capacitances, C_0 the thermal capacitance of the thermocouple, R_3 and C_3 the thermal resistance and thermal capacitance of those parts of the contact which do not contribute to heating up of the thermocouple.

Figure (4.43a) could be simplified further by considering its equivalent circuit as

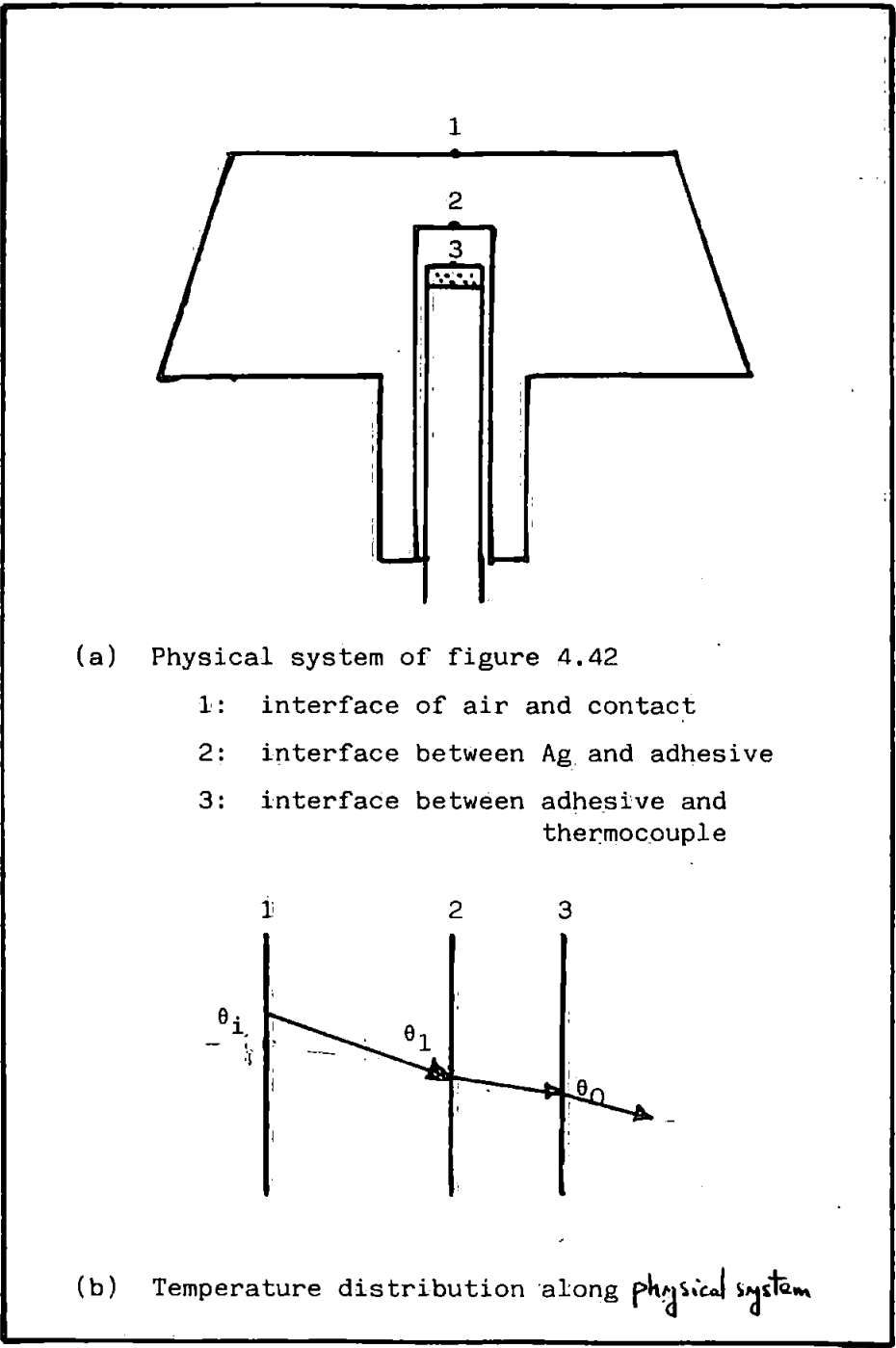


Figure 4.44: (a) and (b) show the physical system of the thermal model and its temperature distribution.

The time constant of the probe (contact with thermocouple) is calculated from the following relations:

$$\begin{aligned}
 \alpha &= C_{th} \cdot r_{th} \\
 &= (C_{th} \cdot r_{th})_{Ag} + (C_{th} \cdot r_{th})_{Loctite} \\
 &= \left[(p \cdot C_p \cdot V) \cdot \left(\frac{\Delta X}{K \cdot A_s} \right) \right] + \left[(p \cdot C_p \cdot V) \cdot \left(\frac{\Delta X}{K \cdot A_s} \right) \right]_{Loctite} \quad (9)
 \end{aligned}$$

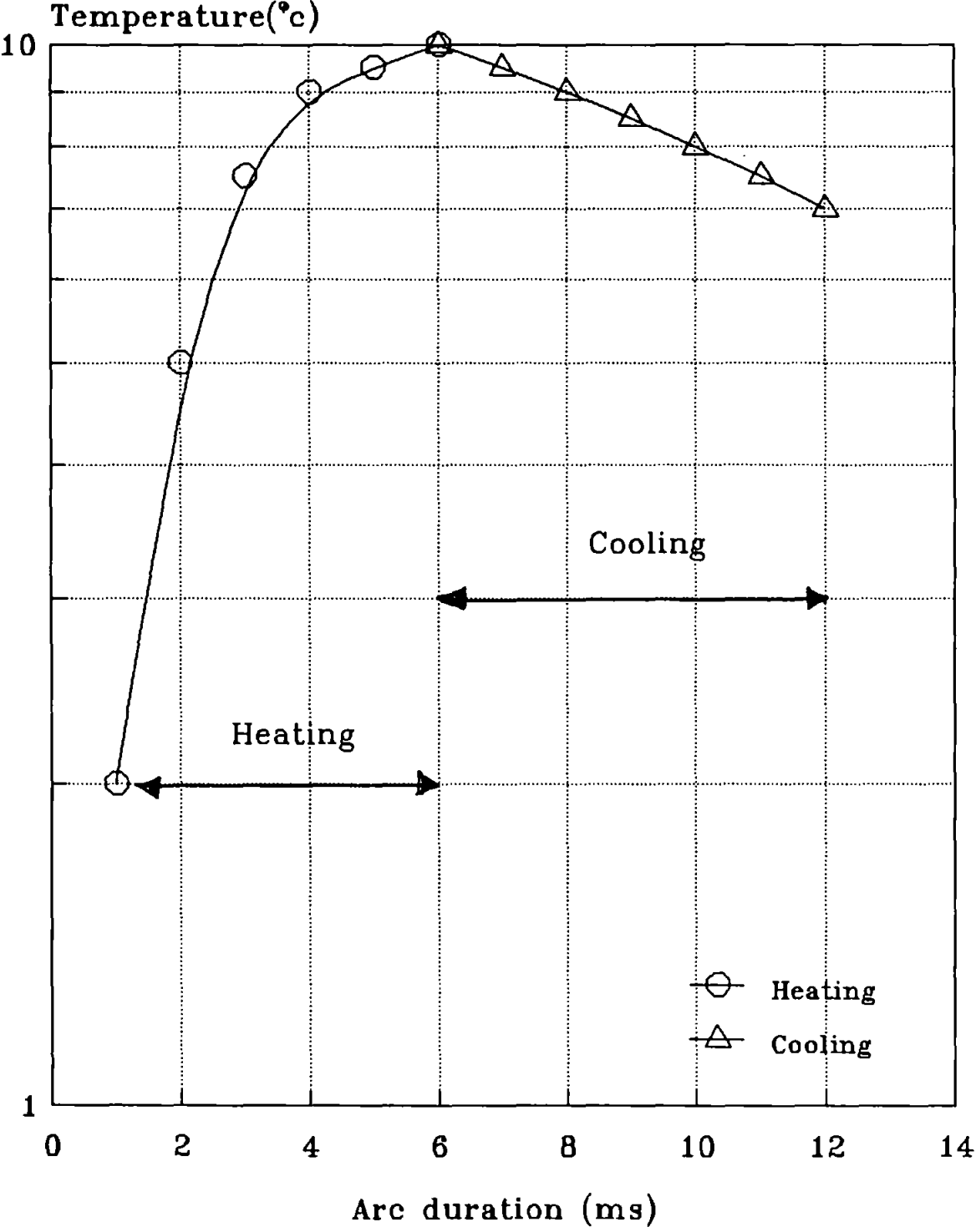
$$\left[\text{where } V = \frac{\Delta X}{2} A_s \right]$$

The thermal conductivities, heat capacities, densities and the thickness of Silver and Loctite adhesive are as follows:

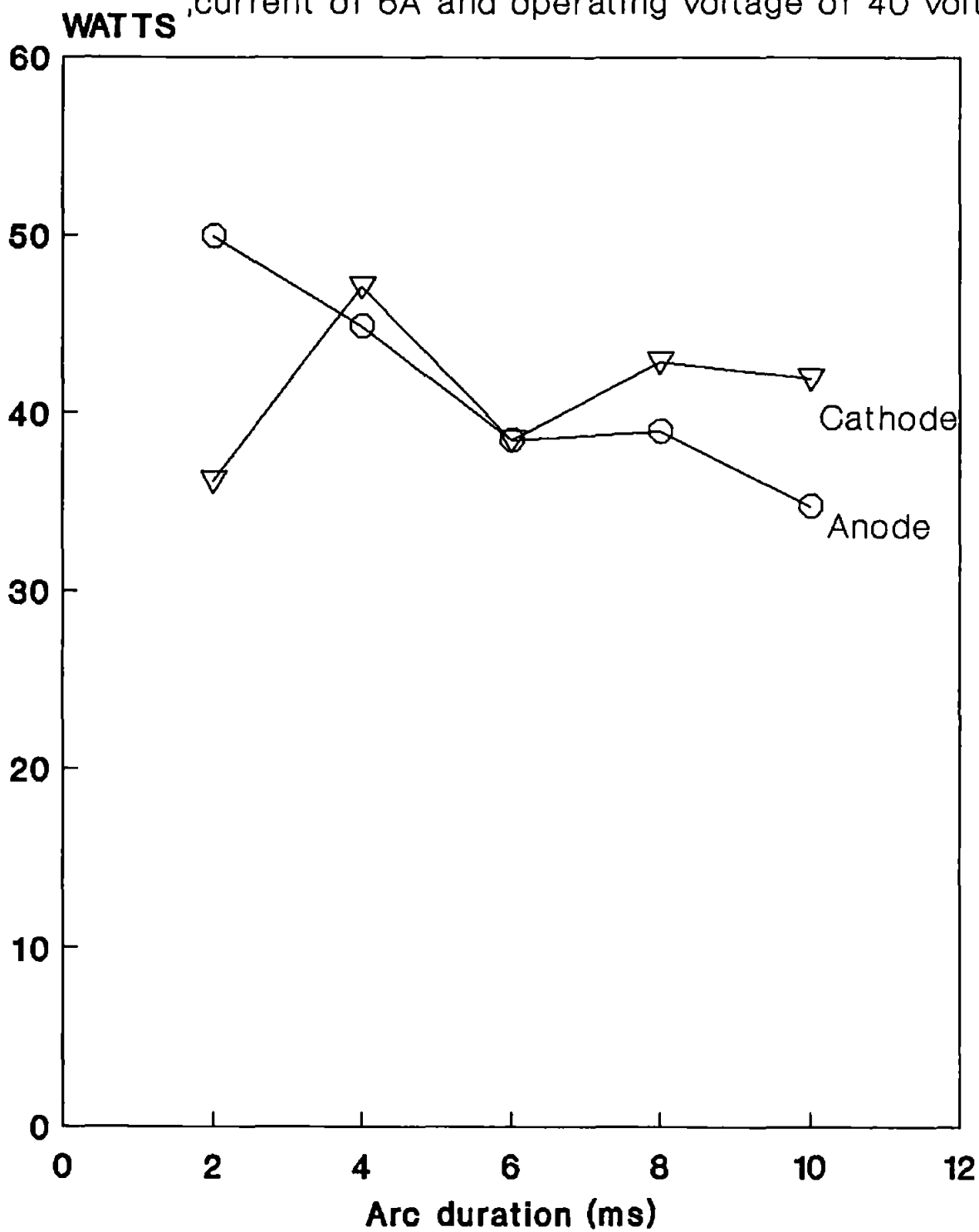
Ag	$ \left[\begin{array}{lcl} K & = & 419 \text{ W/M/K} \\ C_p & = & 236 \text{ J/Kg/K} \\ p & = & 10500 \text{ Kg/M}^3 \\ \Delta X & = & 200 \mu m \end{array} \right. $	$Loctite$	$ \left[\begin{array}{lcl} K & = & 0.815 \text{ W/M/K} \\ C_p & = & 970 \text{ J/Kg/K} \\ p & = & 1640 \text{ Kg/M}^3 \\ \Delta X & = & 120 \mu m \end{array} \right. $
------	--	-----------	---

Substituting the above data into equation (9) gives the time constant for Silver 118 μs and for Loctite 14ms which is in good agreement with the measured one (18ms). ΔX , thickness of Silver and Loctite are obtained from figure (a) page A20.

Figure(4.45): Semi-log plot of heating and cooling curve
for current of 6A, Voltage of 40V, arc duration of 6 ms
and gap-length of 0.1mm.



Figure(4.46): Shows variation of electrodes power with arc durement for a test condition of 0.1mm of gap-length ,current of 6A and operating voltage of 40 volts.



4.6.3 RESULTS AND DISCUSSION

To calculate the power dissipated on the contact surface by the arc one could use equation (7) or (8) derived from the thermal model. The log-linear (semi-log) plot of the heating curve, a typical example is shown in figure (4.45), reveals that it is not truly exponential, but in the semi-log plot of the cooling curve, as shown in figure (4.45), although at some point there is a kink (perhaps due to extra heat loss to the surrounding air at that time) in the graph, one could assume that it satisfies the requirement for using equation (8).

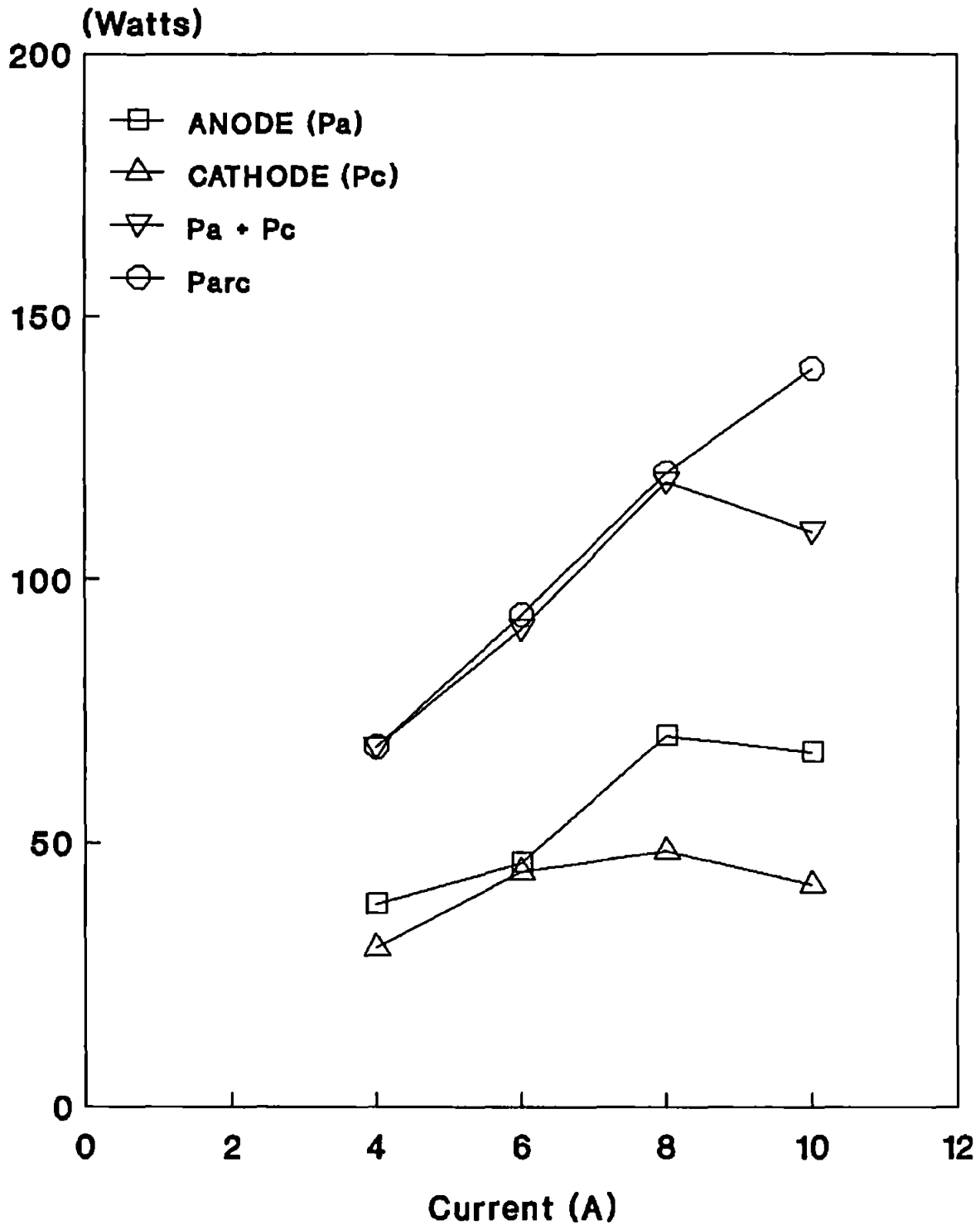
The kink in the semi-log of the cooling curve shows that heat is lost not only to the contact body but also to the air. This occurs in most cases at the mid-point of cooling, just for a few ms. In reality one should be able to use the temperature of cooling curve at any time in order to calculate the input power, but that for the above reason when the temperatures at the beginning and at the end, before the cooling curve reaches steady state, have been put into equation (8), it was found that the highest heat-flow rate was obtained using the temperature right at the start of cooling.

This has been followed in all the calculations of input power to the electrodes for various current, gap-length and arc duration using their temperature-time curves obtained from thermocouple output. The results show that for a fixed gap and current with different arc durations, there are differences in the value of input power obtained from each curve, when one would expect them to be the same. A typical result is shown in figure (4.46).

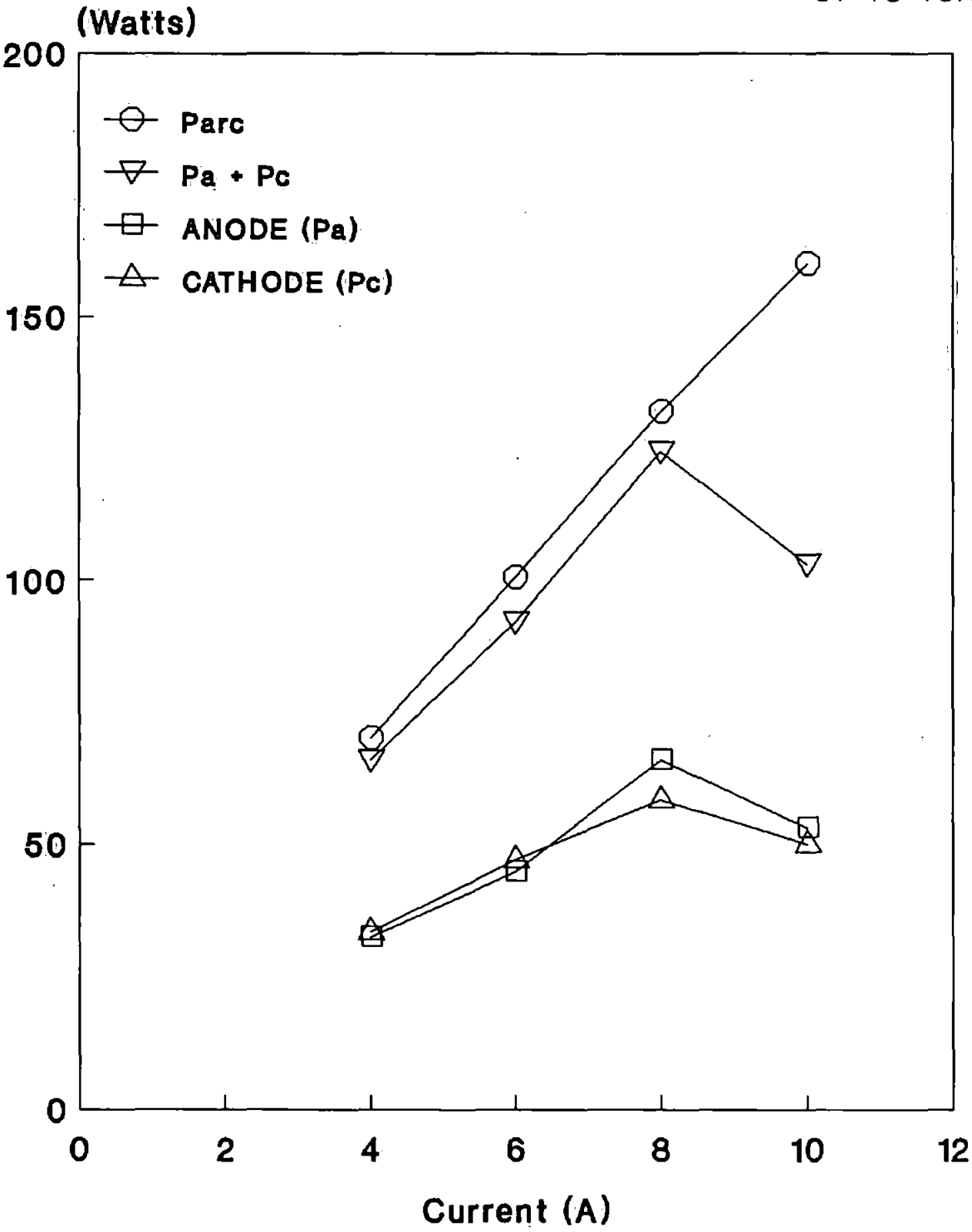
The differences are thought to be caused by variations in the mechanical parameters of the switch model (initial acceleration of opening contacts as shown in section 4.2.1 speed has non-linear characteristics) which affects the shape of the arc voltage waveform; two such typical waveforms are shown in figure (4.34). Or they may be caused by the arc occurring remote from the thermocouple position on one or both electrodes which would change the time constant of the thermal system.

Figure (4.47): (a-e) show variation of power transfer to the electrodes with current, for a gap-length of 0.05-mm and supply voltage of 40 volts.

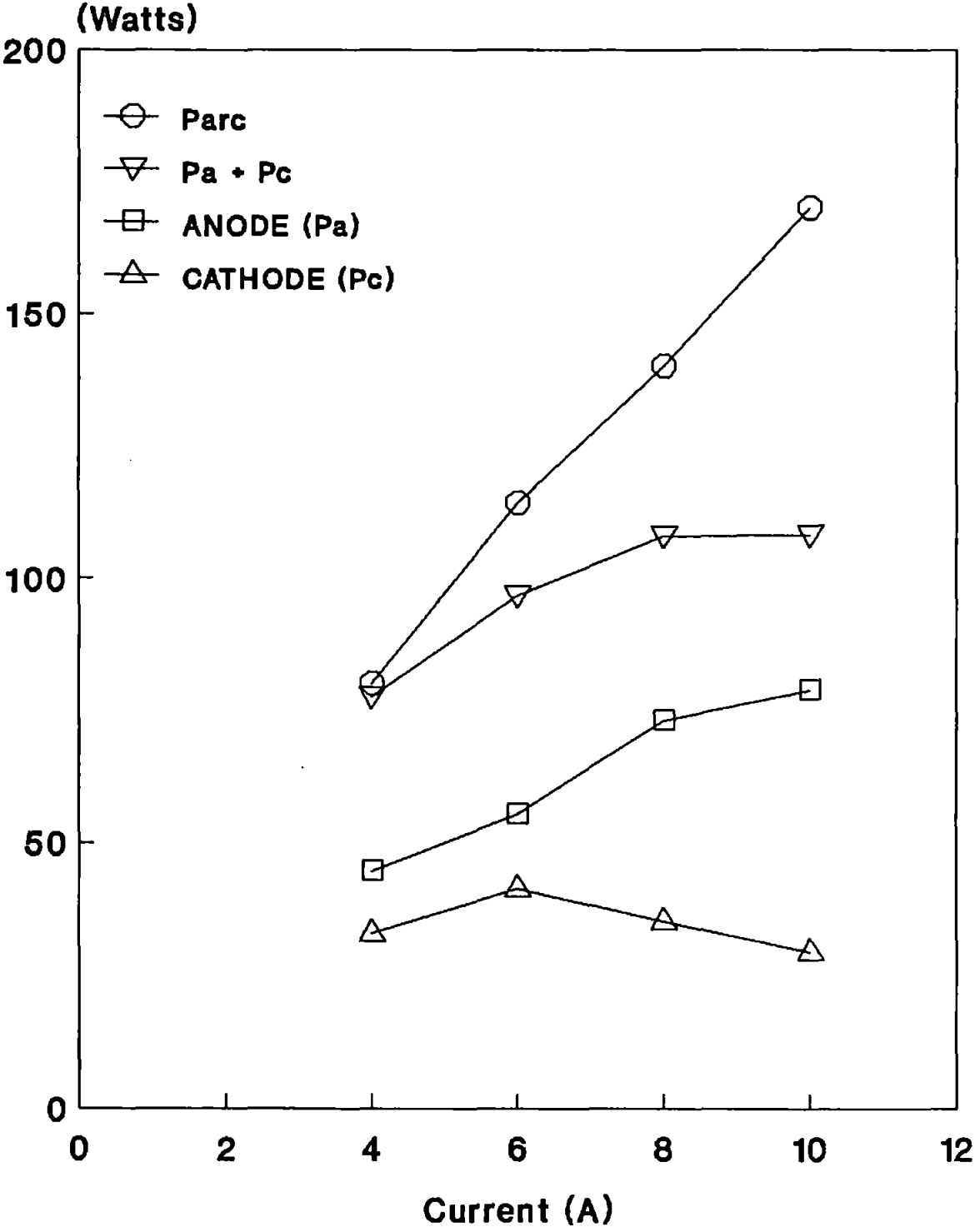
4.47a : Shows variation of power transfer to the electrodes with current for a gap-length of 0.05mm and supply voltage of 40 volts.



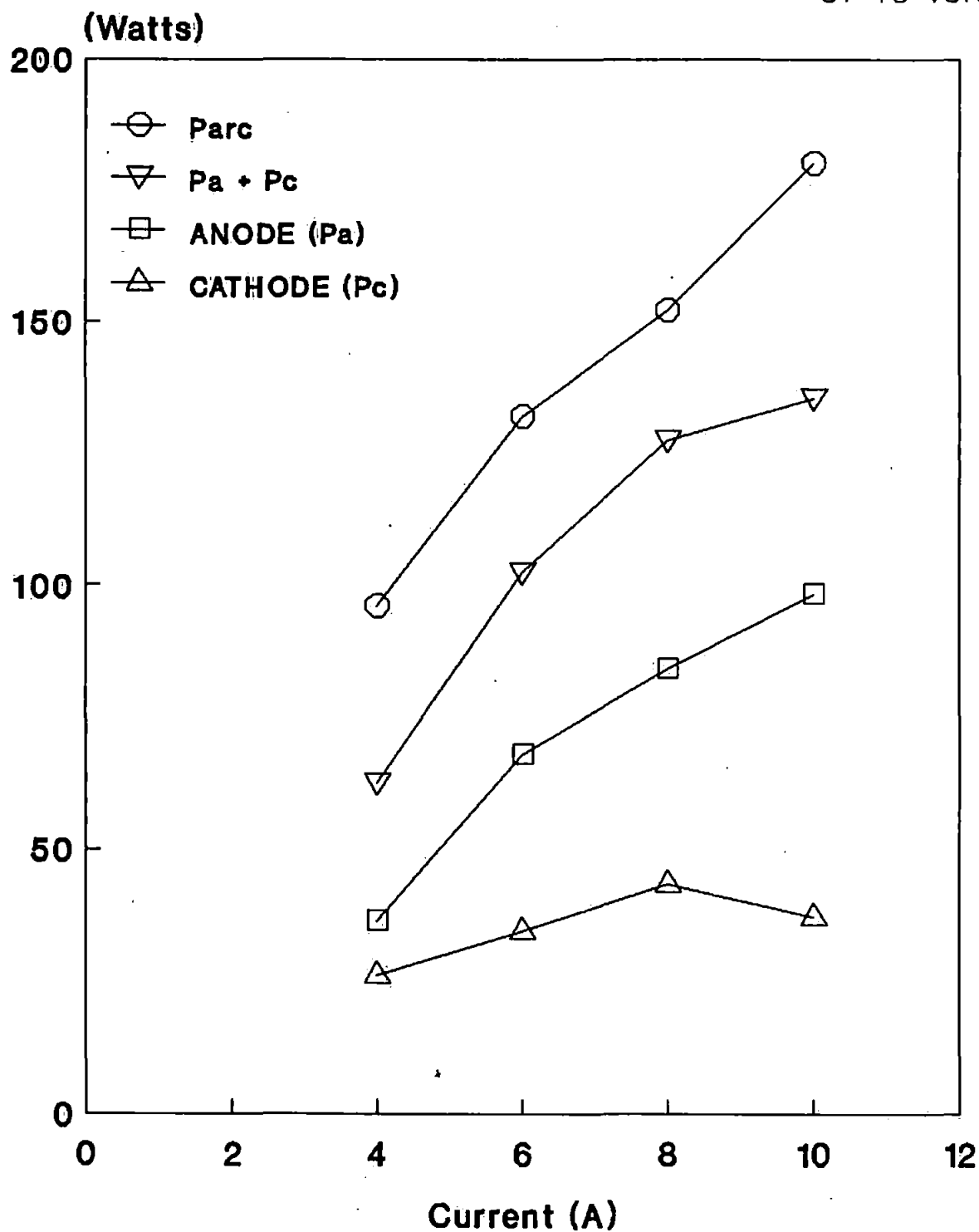
4.4/b: Shows variation of power transfer to the electrodes with current for a gap-length of 0.1 mm and supply voltage of 40 volts.



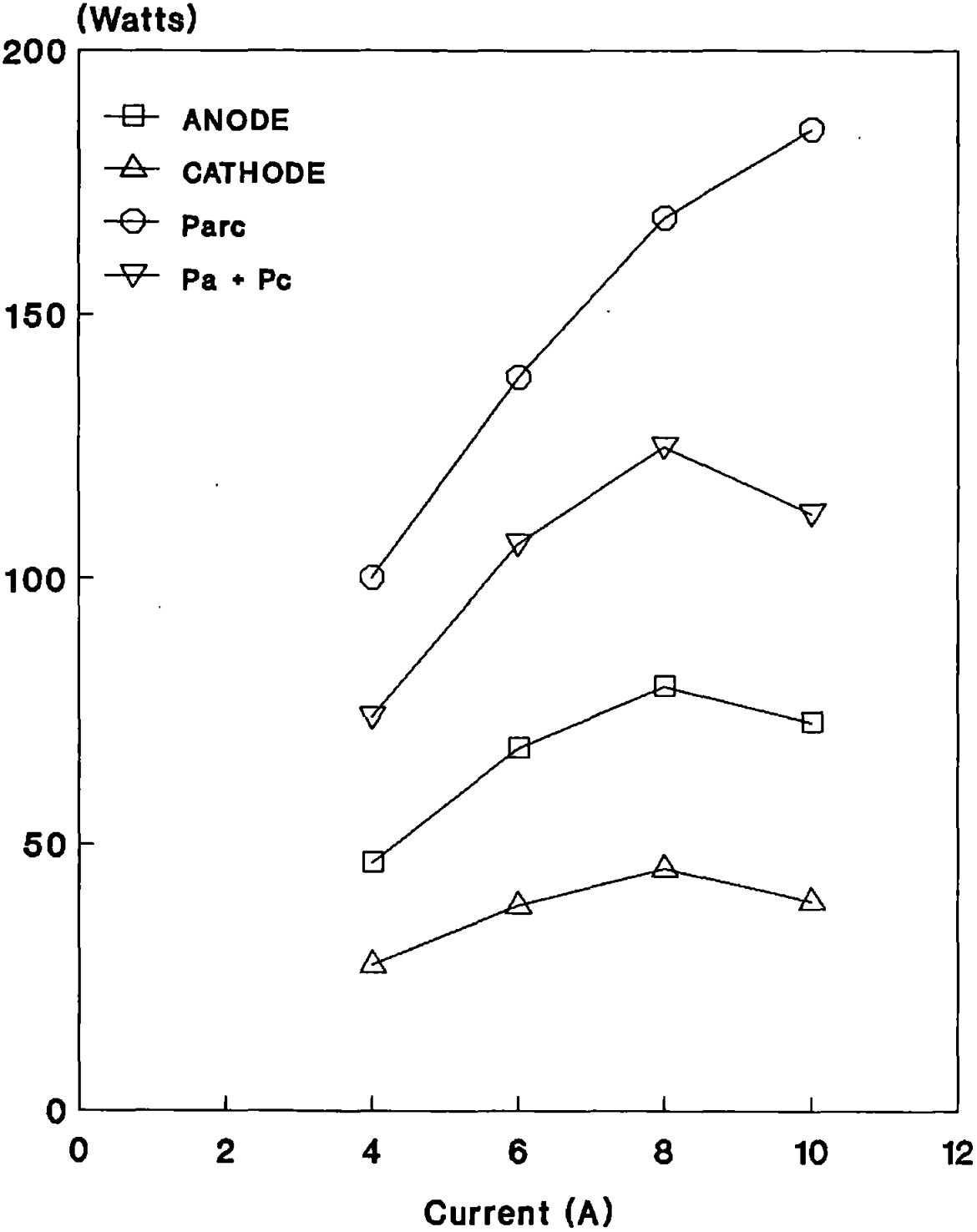
4.47c: Shows variation of power transfer to the electrodes with current for a gap-length of 0.2mm and supply voltage of 40 volts.



4.47d: Shows variation of power transfer to the electrodes with current for a gap-length of 0.5 mm and supply voltage of 40 volts.



4.47e: Shows variation of power transfer to the electrodes with current for a gap-length of 1 mm and supply voltage of 40 volts.



Another cause could be the arc being of longer period, which would change the surface condition of the electrodes and hence the time constant. Spurious triggering of the first timer, which controls the arc duration, may provide a duration slightly greater than its preset time.

These differences lie within 5 to 10% of the highest value calculated, and for this reason at each gap, for a constant current, the highest value of the input power to the electrodes has been chosen.

These values, their sum and arc power, are plotted against current and gap-length as shown in figures (4.47-4.48)

Figures (4.47) suggest that for gaps of 0.05 and 0.1 mm, and for current from 4 A to 8 A, the sum of cathode and anode power are equal to the arc power. For 0.2 mm this is only true for current of 4A.

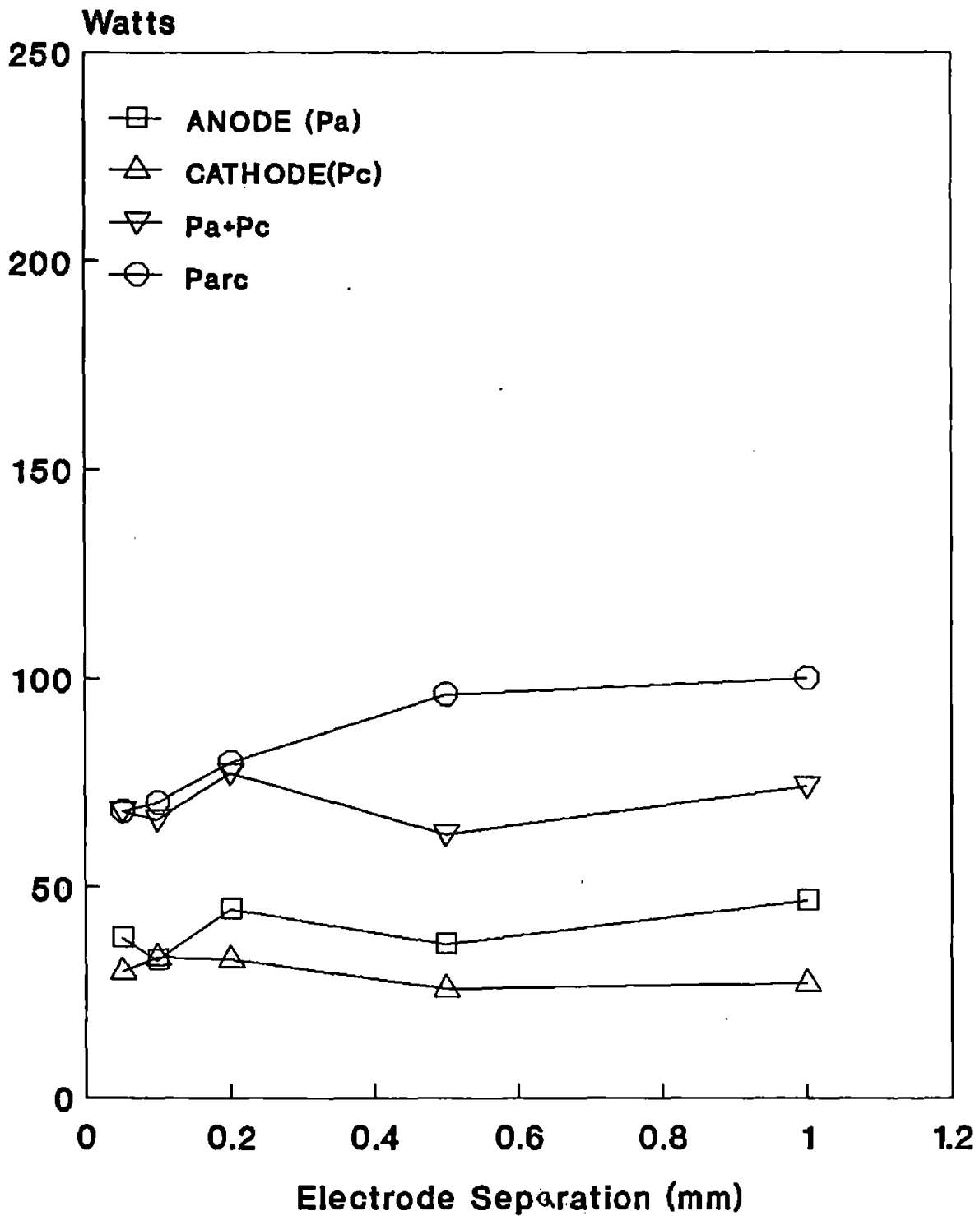
For 0.05 mm at 6 A the anode and cathode power are nearly the same. For 0.1 mm, below 6 A the cathode power is higher than anode power, and then the curves cross over each other at 6.5 A. If one extends the curves of anode and cathode power at 0.1 mm beyond 10 A, one can notice that they cross each other again around 11 to 12 A. For any other gap the anode power for every current is higher than the cathode power.

The above results agree with White's⁽¹⁾ suggestion that below 0.2 mm the net power causing erosion is virtually the same as the net arc power. Sato⁽²³⁾ and White⁽¹⁾ from experiments on switches with Ag Cd-O contacts and with electrical test conditions similar to here (i.e. 40 V d.c., currents of 2-10 A) but with different speeds of opening of 63 mm/sec and 1500 mm/sec respectively, by using Talysurf and weighing techniques have defined a transition region in which material transfers from the electrodes change their direction.

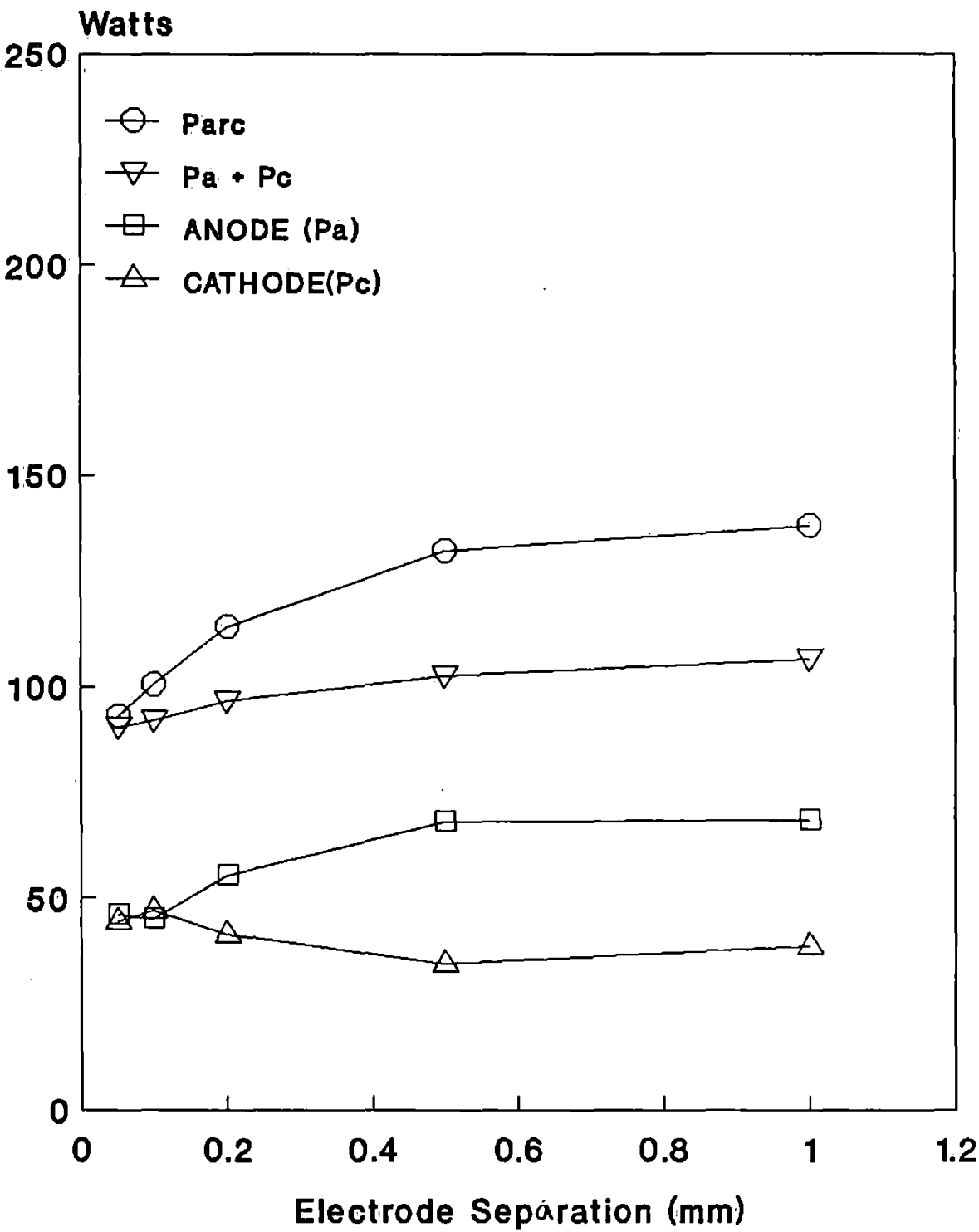
White's⁽¹⁾ transition region is at 8 A. Material transfer direction below 8 A is cathodic loss, anodic gain and above 8 A is cathodic gain, anodic loss. With

Figure (4.48): Graphs of (a-d) show power transfer to the electrodes versus gap-length for a current of 4-10A and circuit voltage of 40 volts.

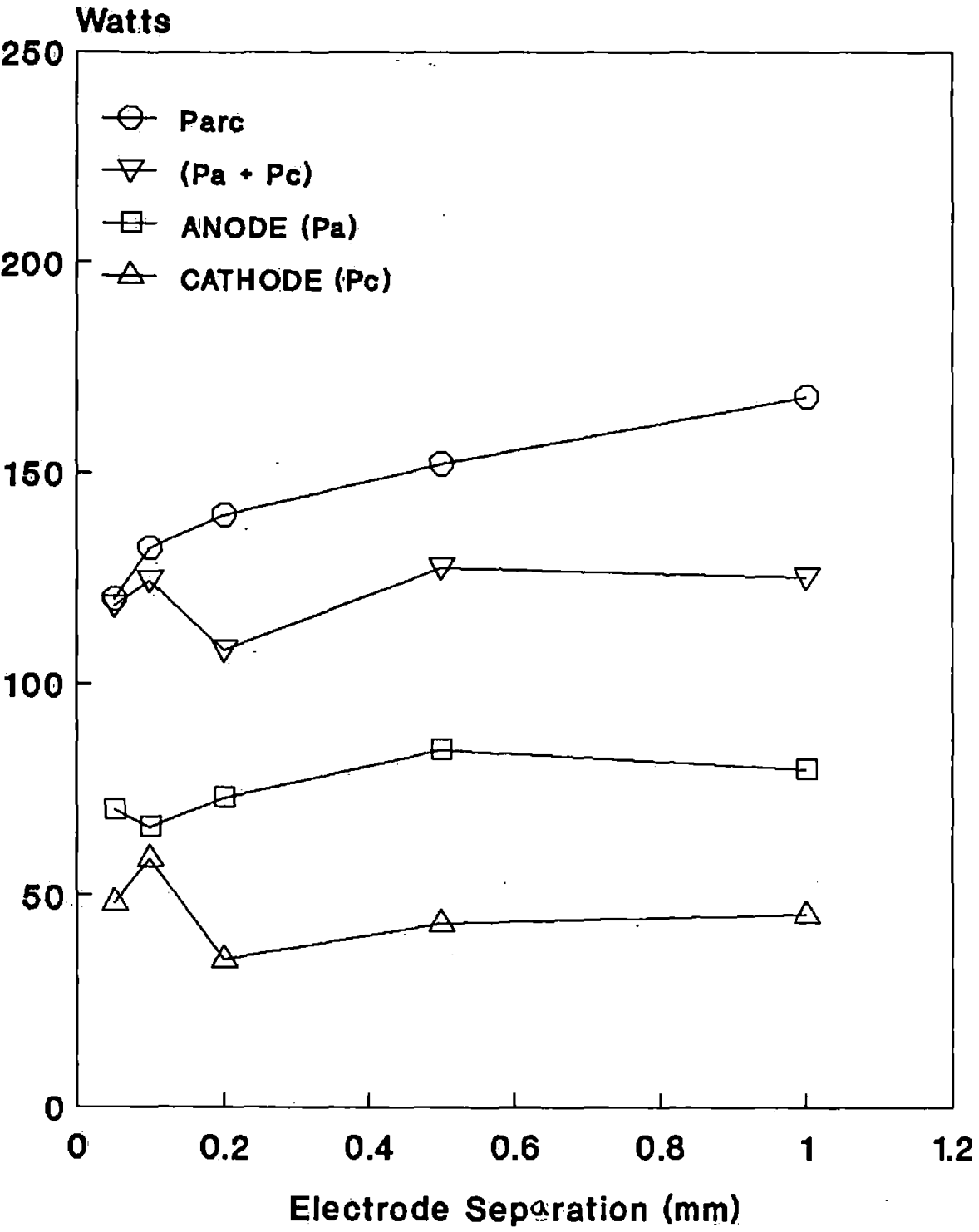
4.48a: Power transfer to the electrodes versus gap-length for a current of 4A and circuit voltage of 40 volts.



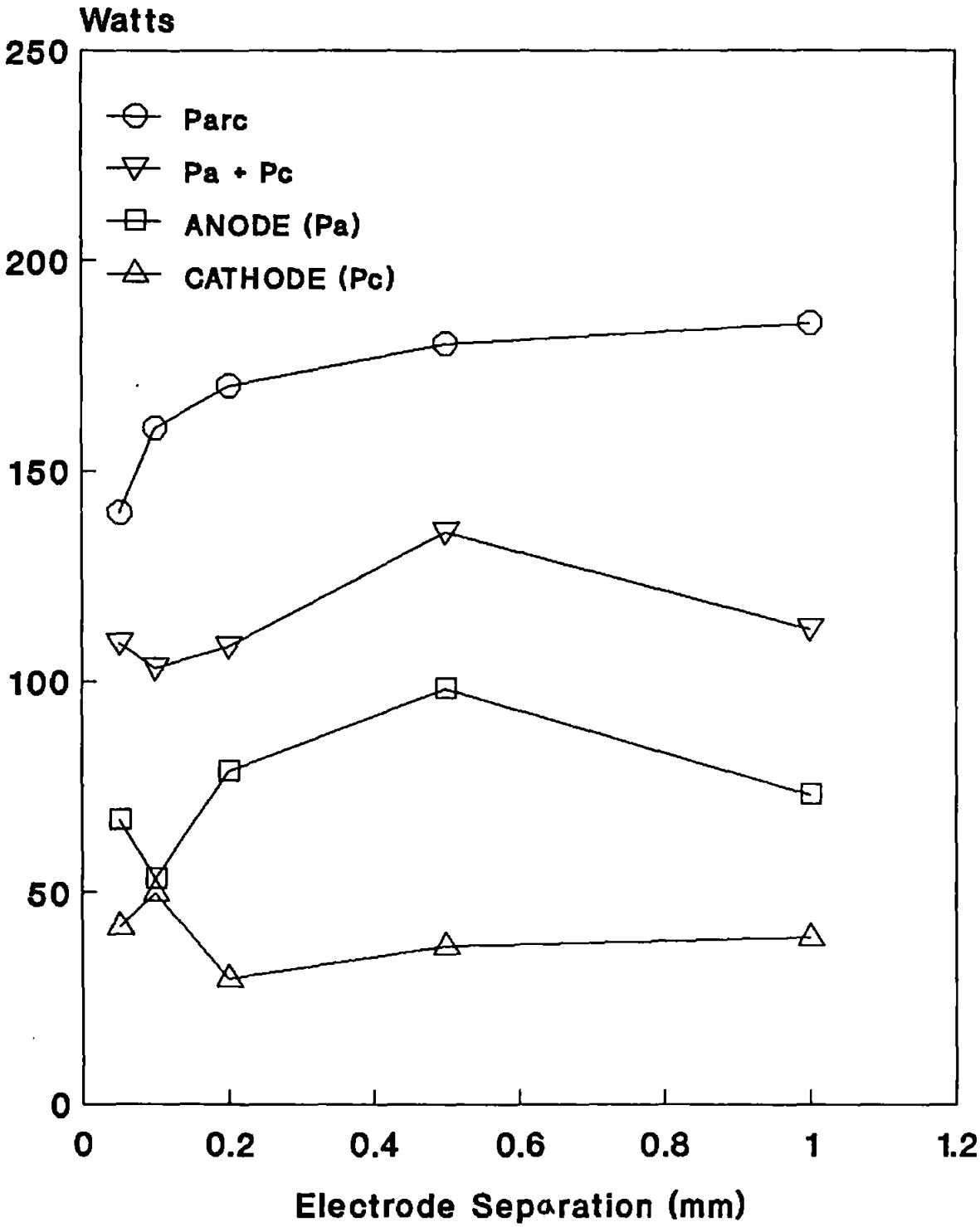
4.48b: Power transfer to the electrodes versus gap-length for a current of 6A and circuit voltage of 40 volts.



4.48c: Power transfer to the electrodes versus gap-length for a current of 8A and circuit voltage of 40 volts.



4.48d: Power transfer to the electrodes versus gap-length for a current of 10A and circuit voltage of 40 volts.



Sato⁽²³⁾, the material transfer occurs in the direction from cathode to anode at a testing current of 6.4 A, but in the opposite direction from anode to cathode around 10 A.

Here it was found by calculation, that for separation of 0.1 mm, the power dissipated at cathode and anode is the same at the currents 6.5 Ampere, and of around 11 A – in this case extending the power curves.

For gaps of 0.2 mm and 0.5 mm, one can observe from figure (4.47) that the cathode power decreases from 6 A upwards, but anode power is still increasing. The decrease of cathode power for gap of 0.5 mm starts from 8 A. For 1 mm gap the anode and cathode power both decrease from 8 A. This suggests that the significant loss of cathode power starts earlier than for the anode power.

Figure (4.48) suggests that for currents of 4 A, 8 A and 10 A the power curves of cathode and anode have similar patterns before and after 0.1 mm of gap. But for 6 A the difference is reversed below 0.1 mm gap, and as a result they cross each other at around 0.125 mm of gap.

As shown in figure (4.49), the cathode fall remains constant, so any increase in the power conducted into the cathode is as a result of increased power dissipation in the arc column.

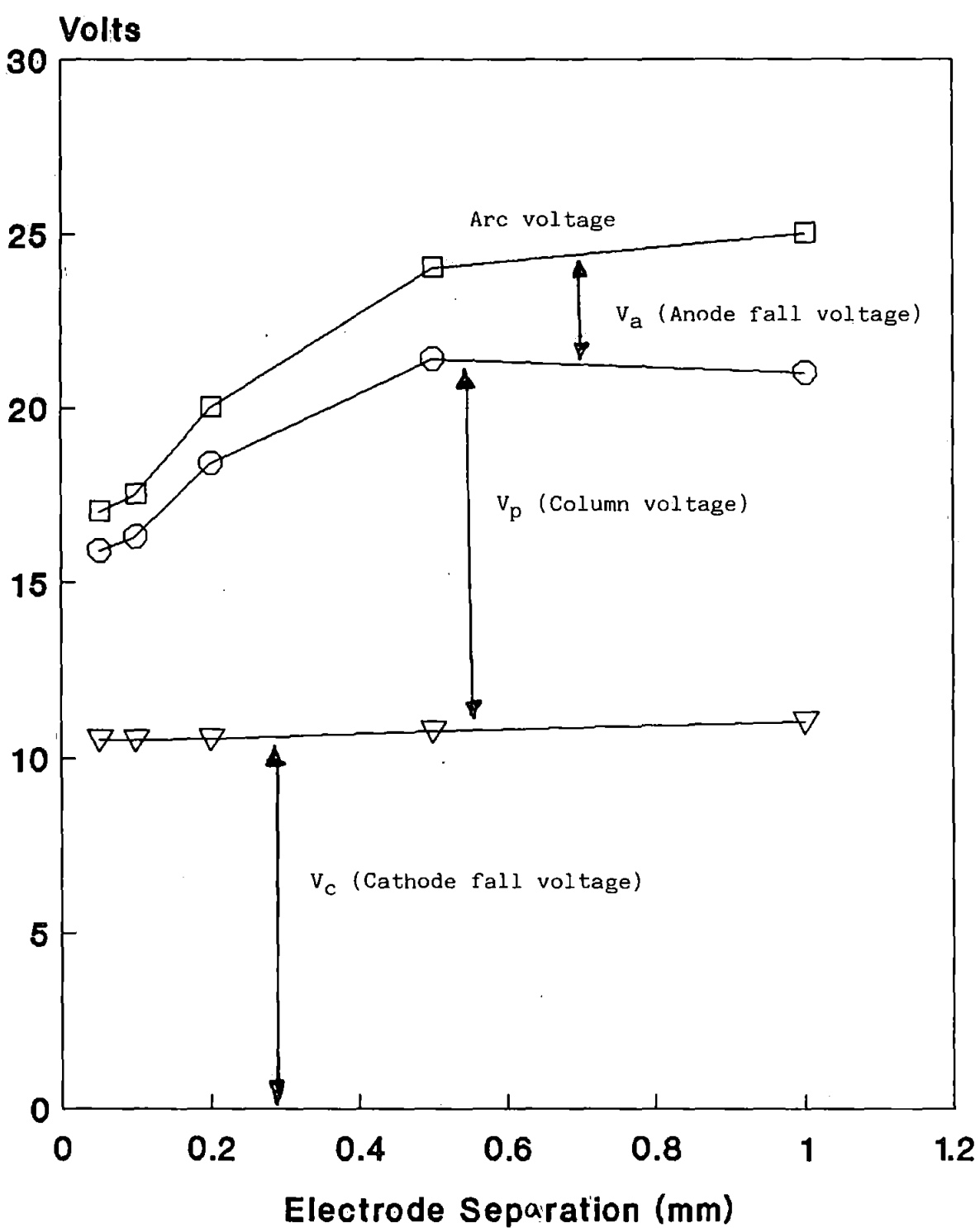
Figure (4.47) also shows that at some currents the sum of anode and cathode powers are not equal to the arc power. This can be related to the losses from the contacts which take place in the form of evaporation, or conduction to the air, etc.

Examinations of the contact surfaces, for all the different test conditions, by a Scanning Electron Microscope (S.E.M.), have revealed that most of the arc power has been used for melting and evaporation, and the resulting debris is scattered over the electrode surface.

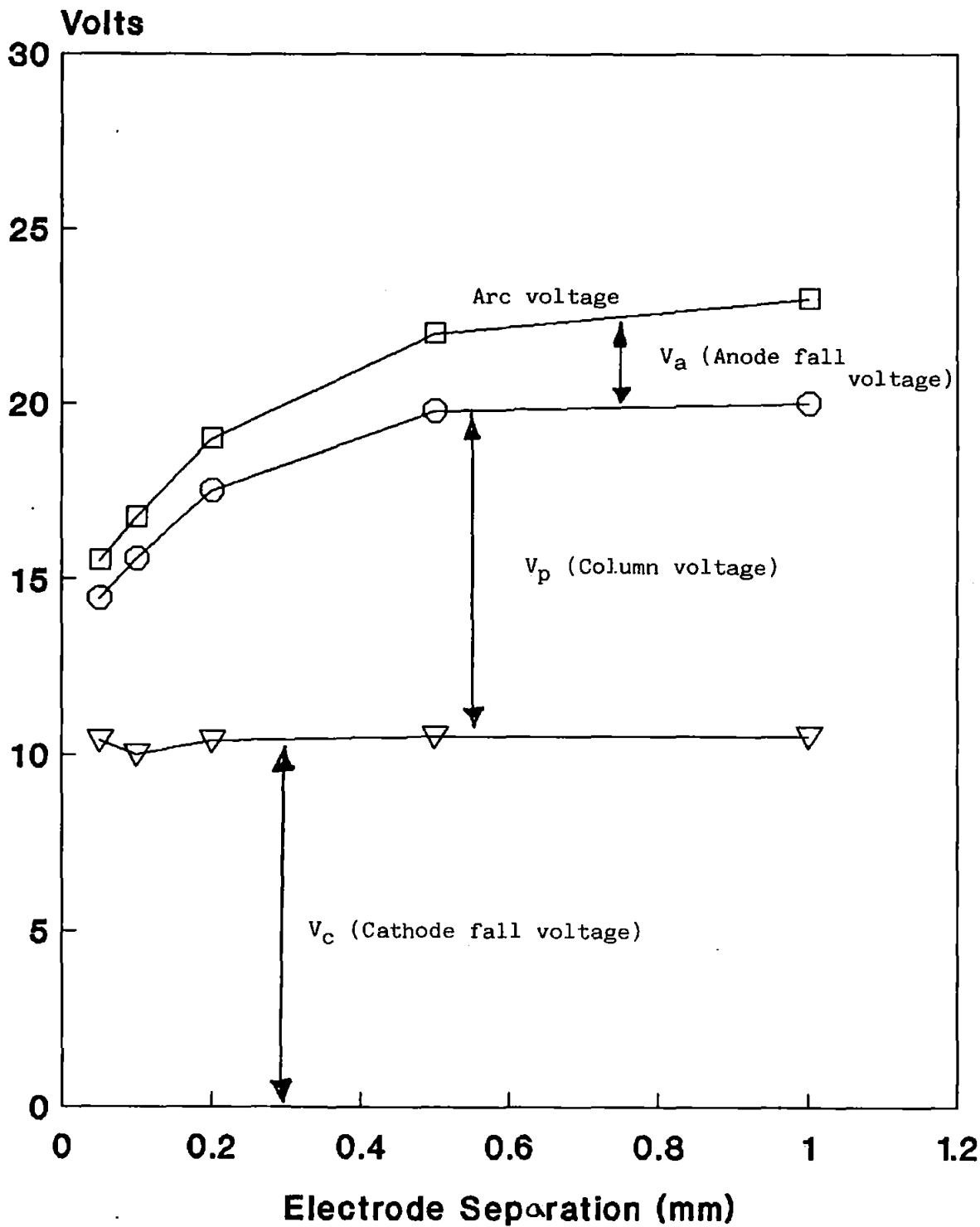
A typical S.E.M. photograph of a contact, for a current of 6 A, arc duration of 8 ms, operating voltage of 40 V and gap of 0.1 mm, after completing 10 operations, is shown in figure (4.50). In figure (4.50) photographs 1–3 are of the cathode and 4–6 of the anode.

Figure (4.49): Graphs of (a-d) show components of the arc voltage against electrode separation for a current of 4-10A and operating voltage of 40 volts.

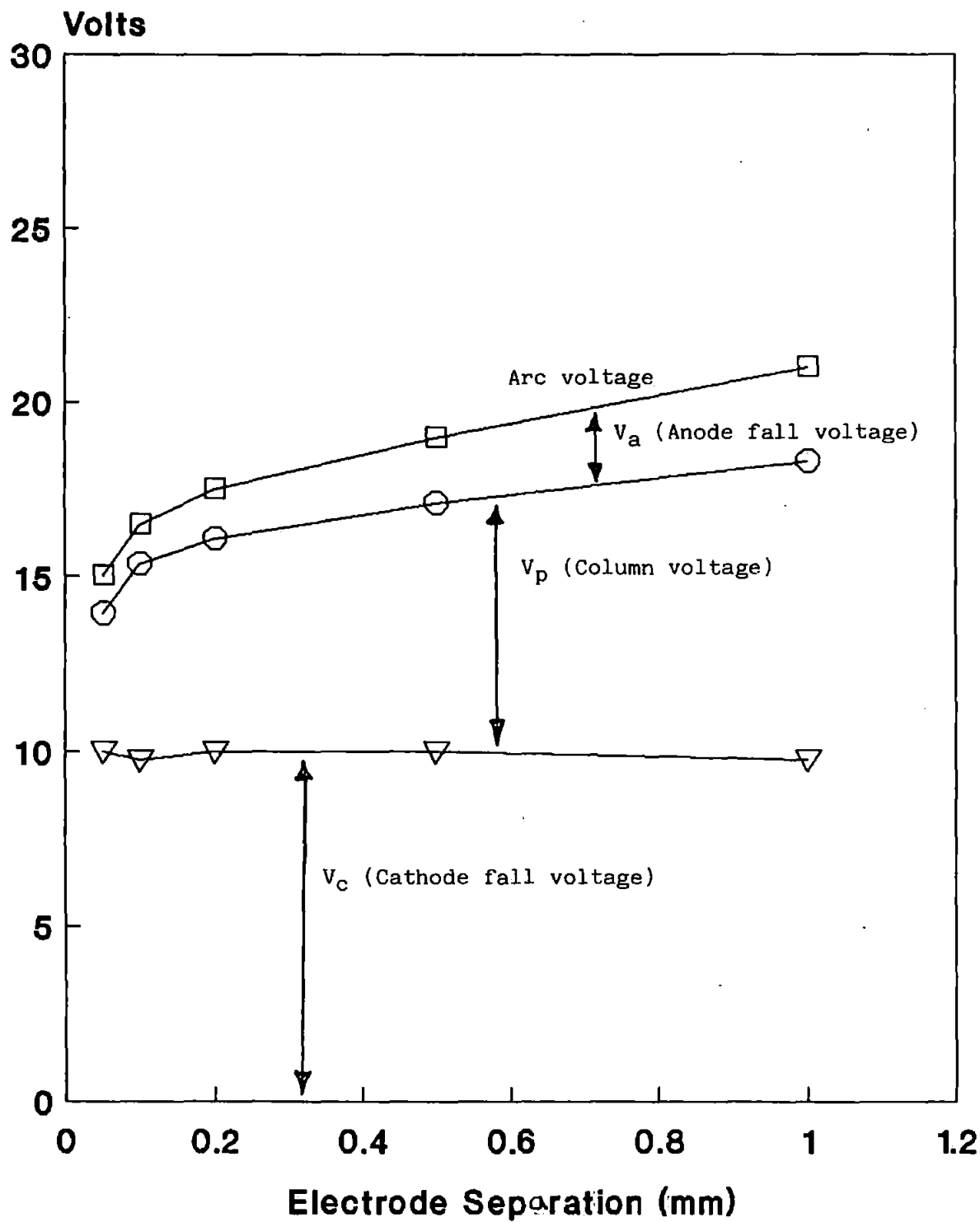
4.49a: Components of the arc voltage against electrode-seperation for a current of 4A and operating voltage of 40v.



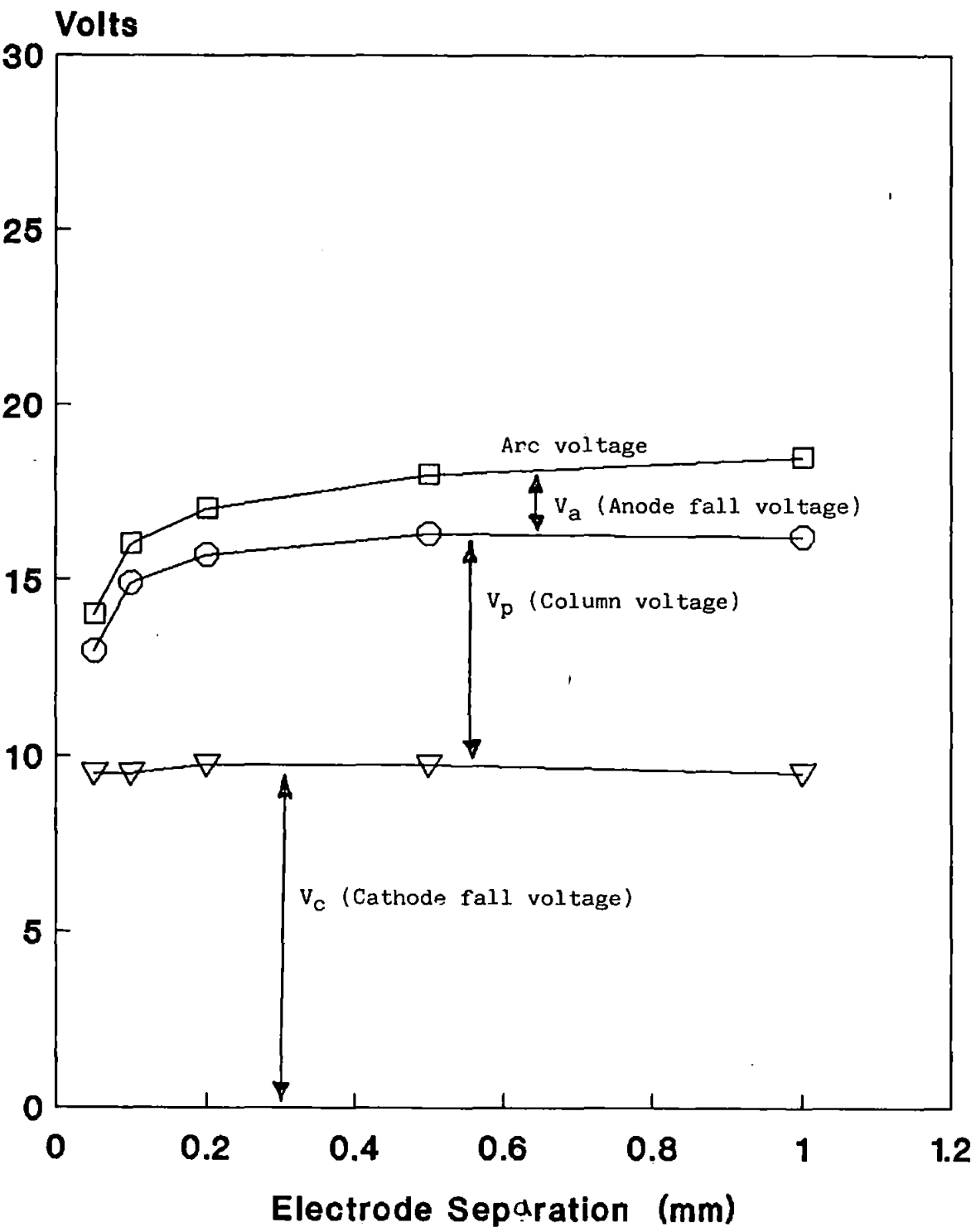
4.49b: Components of the arc voltage against electrode-separation for a current of 6A and operating voltage of 40v.



4.49c: Components of the arc voltage against electrode-seperation for a current of 8A and operating voltage of 40v.



4.49d: Components of the arc voltage against electrode-separation for a current of 10A and operating voltage of 40.



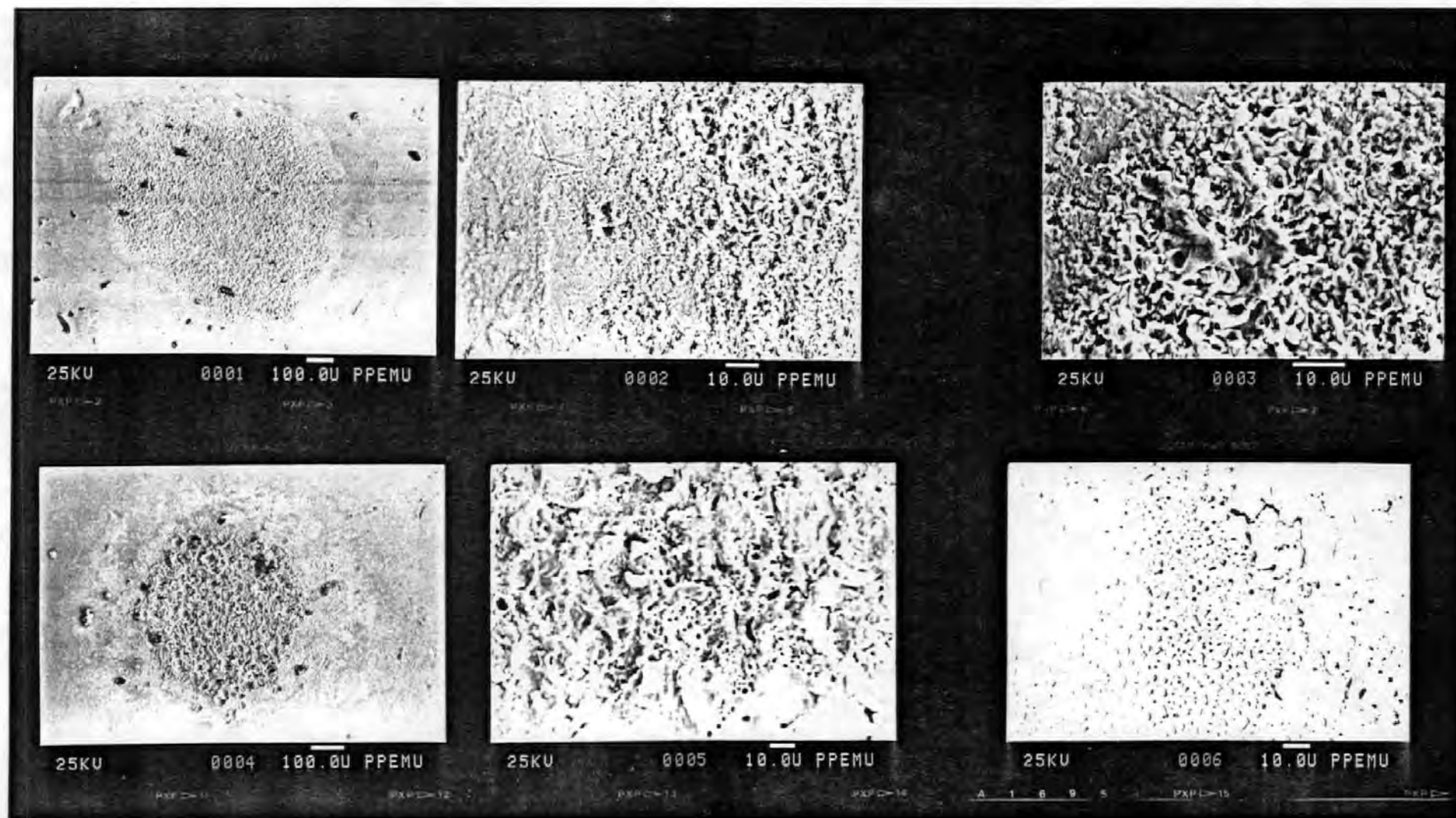


Figure (4.50): Shows S.E.M. photographs of the electrodes' surface after completing 10 operations at a current of 6A, arc duration of 8ms, operating voltage of 40 volts and gap-length of 0.1mm. Photographs 1-3 are of the cathode and 4-6 are of the anode.

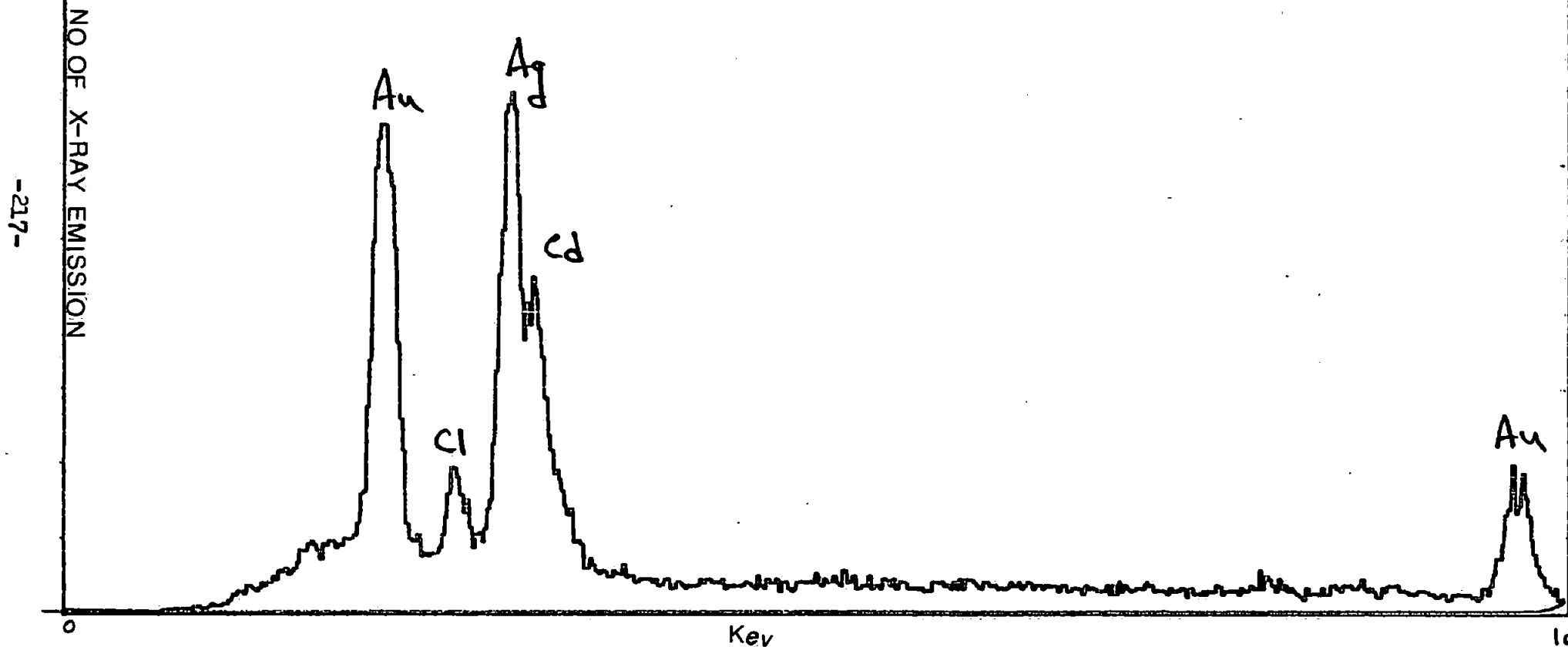


Figure (4.51a): Shows an X-ray analysis of the cathode surface after completing 10 tests at a current of 6A, arc duration of 8ms with operating voltage of 40 volts and gap-length of 0.1mm.

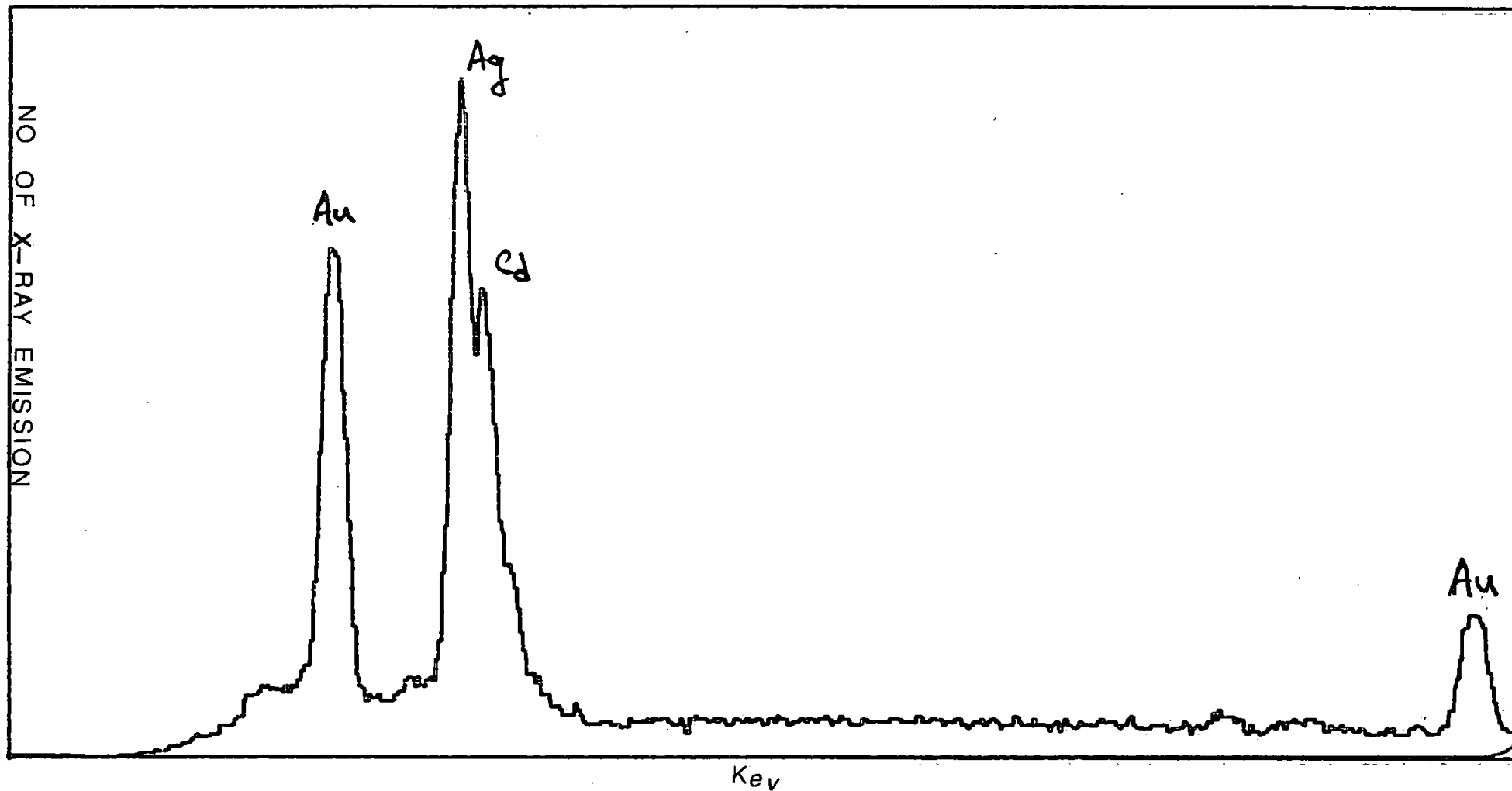


Figure (4.51b): Shows an X-ray analysis of the anode surface after completing 10 tests at a current of 6A, arc duration of 8ms, operating voltage of 40 volts and gap-length of 0.1mm.

From figure (4.50) one can observe that the cathode surface has low mounds and a fine surface roughness. The anode has a developed rim, surface cracks with holes, and is severely roughened. These cracks are probably formed by thermal stresses due to the mixed materials of the contact surface.

The above observation of the lack of cracks or a crater on the cathode surface suggests that the cathode spot must be mobile (because the heat does not concentrate on one area), and this has been suggested by Mapps et al⁽²¹⁾ and Slade et al⁽²²⁾.

However, both electrode surfaces exhibit the appearance of molten lava. The x-ray analysis of the electrode surfaces have revealed that the quantity of material making up this 'lava' at the anode is higher than at the cathode. This is shown in figure (4.51).

The losses from the electrodes can be calculated by knowing γ and V_e in equations (2) and (4). Here γ and V_e are calculated using power balance equations (1) and (3) and the relevant data from figures (4.47) and (4.49) for conditions where the sum of anode and cathode power is equal to the arc power, in which case no loss takes place.

It was found that in general where anode and cathode power are equal, or approximately equal, then γ is in the range of 0.51–0.54, and the thermal energy of the electron (V_e) is negligible, but where anode power is much greater than cathode power, γ is in the range of 0.47–0.5, and thermal energy of the electron is about 1.2 eV.

From the above results it can be concluded that for a relatively small gap (below 0.2 mm), where anode voltage is small and cathode voltage is almost equal to the arc voltage, then the value of thermal energy of electrons and the ratio of positive ion current to electron current ($\gamma = I_p/I$) play an important role in power balance relations.

The reasons why γ and V_e change in relation to gaps of below 0.5 mm has not been investigated.

In the thermal model, by using finite-element approach (as shown in appendix IV), it was assumed that all the heat *entering to* the contacts was received by the

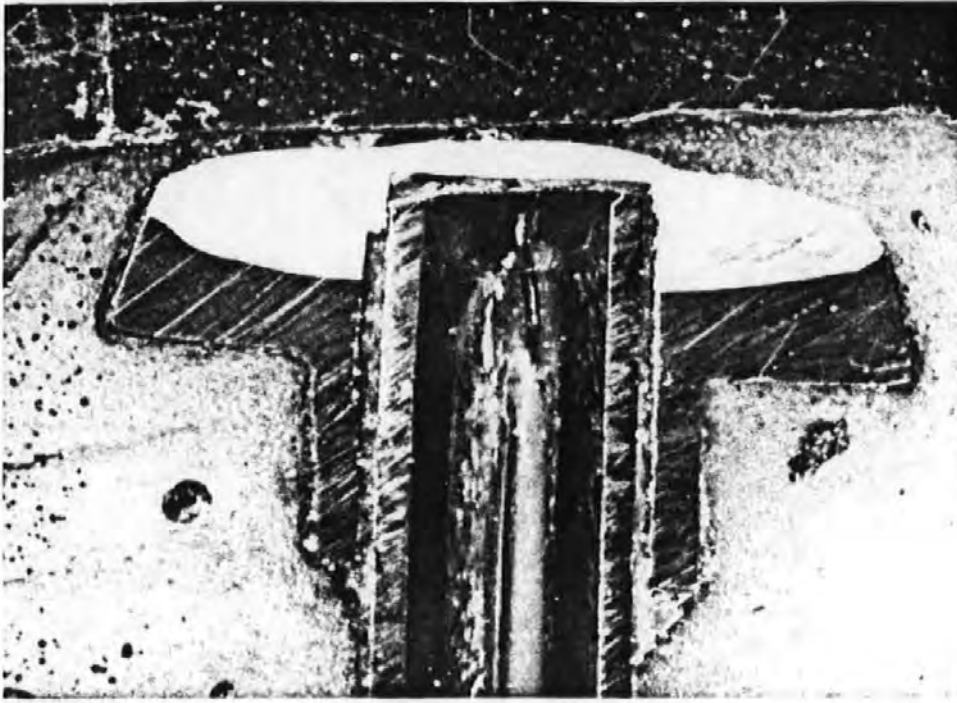


Figure (a): Shows a cut section of the probe.

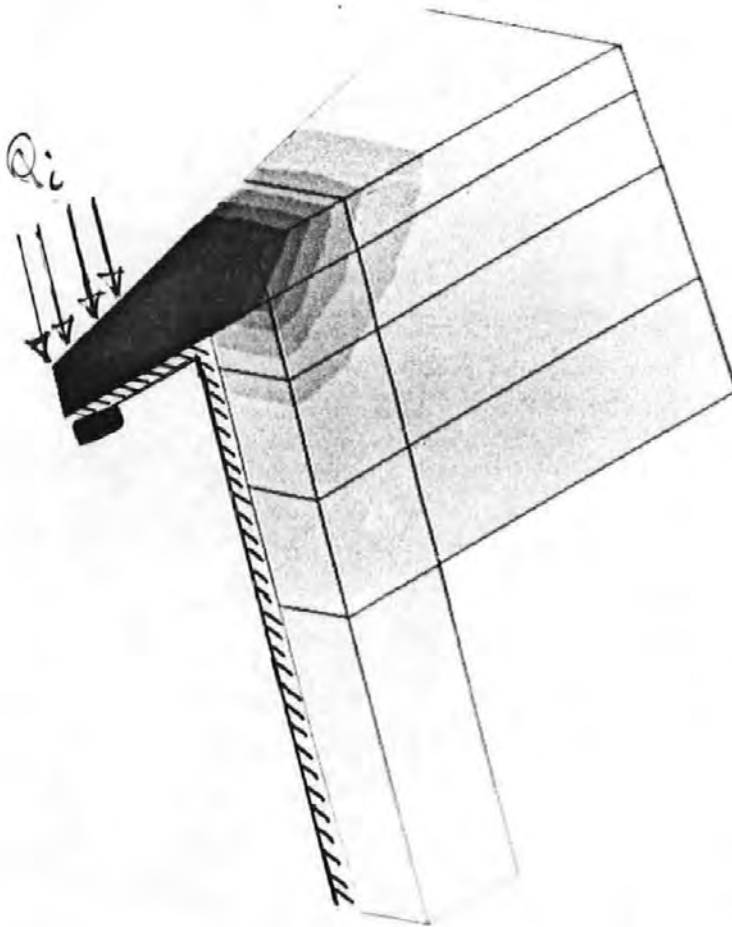


Figure (b): Shows generated 3-D volume of the model, tilted at 30 degrees.
Also the contour of heat distribution for 100 watts and 10ms.

APPENDIX IV

Modelling heat transfer in the contact body using FINITE ELEMENTS

Heat which flows in the contact due to arcing is very difficult to model directly using 3-D volume Finite Elements, as thermal capacity, thermal conductivity and density of the materials make the contacts change with input heat and internally generated heat.

The problem has been solved by assuming that no internal heat generation has taken place, no heat has been lost to the surrounding air under transient condition (no boundary condition) and *the heat expend Firevaporation and melting on the surface of the electrodes. does not contribute to the heat flow in the contact during arcing.*

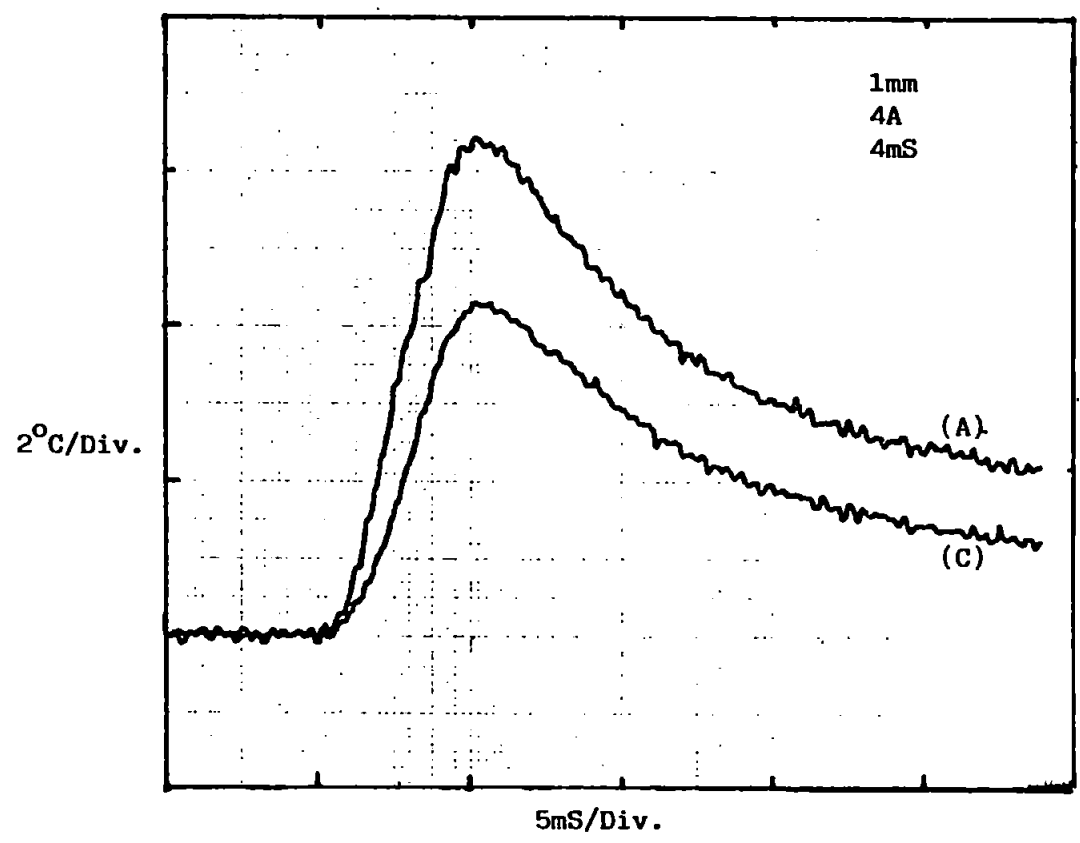
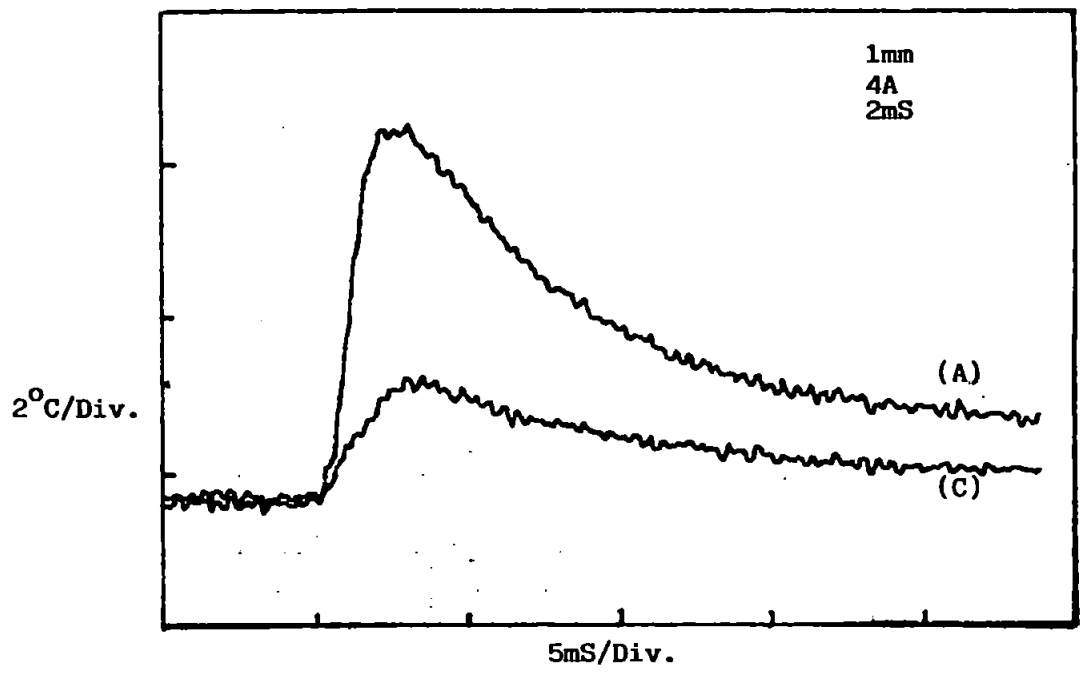
The dimensions of the required data, such as diameter and height of thermocouple weld junction, adhesive and etc..., are obtained from figure (a).

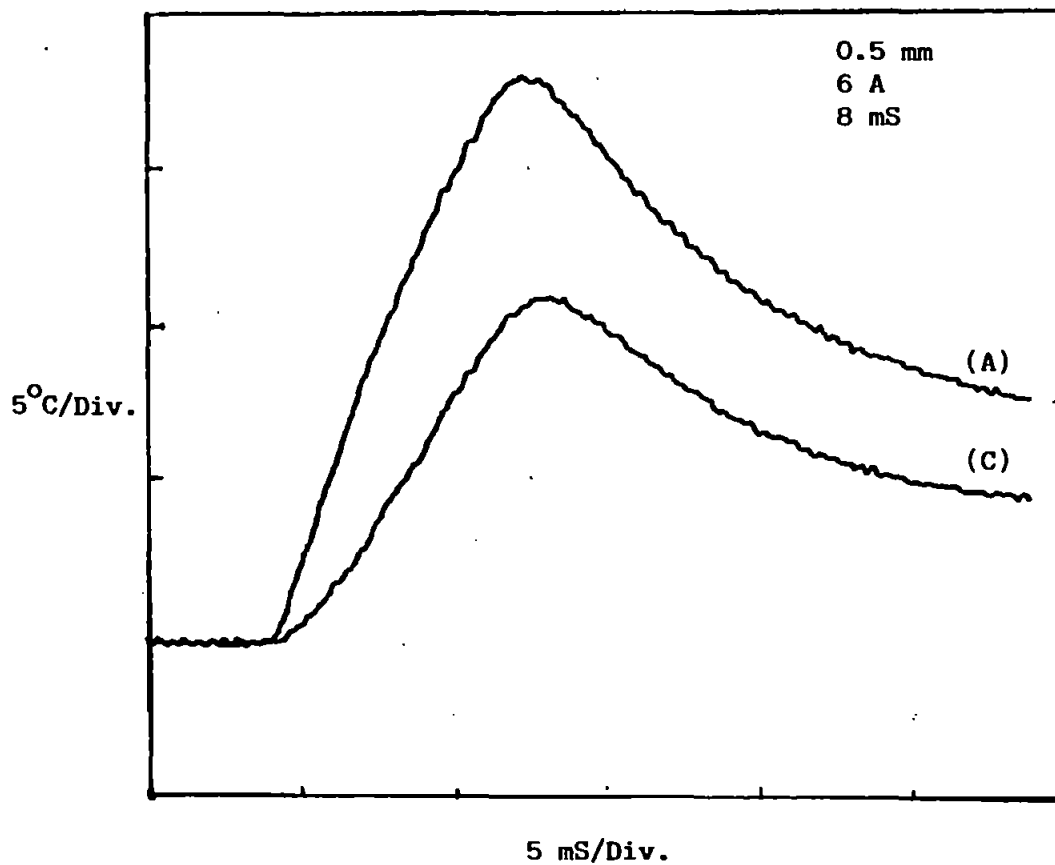
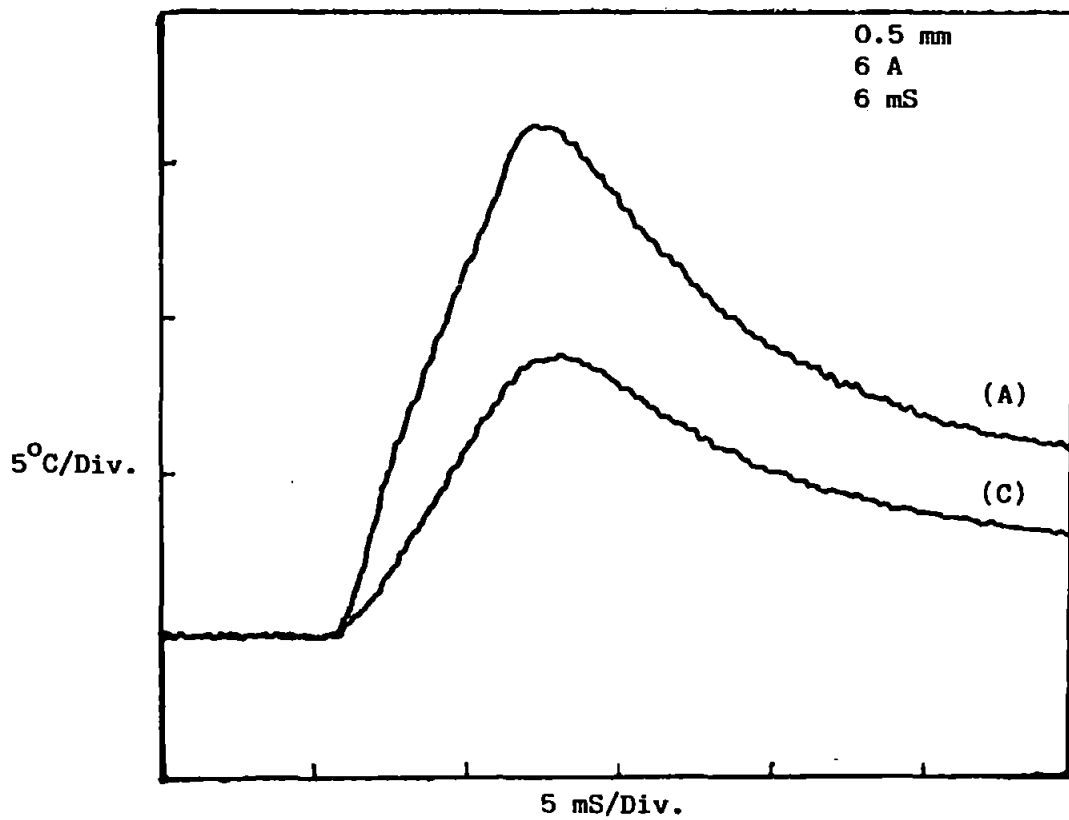
Figure (a) is a cut section (axially cut) of the probe (contact with thermocouple) which exposes more details of the construction.

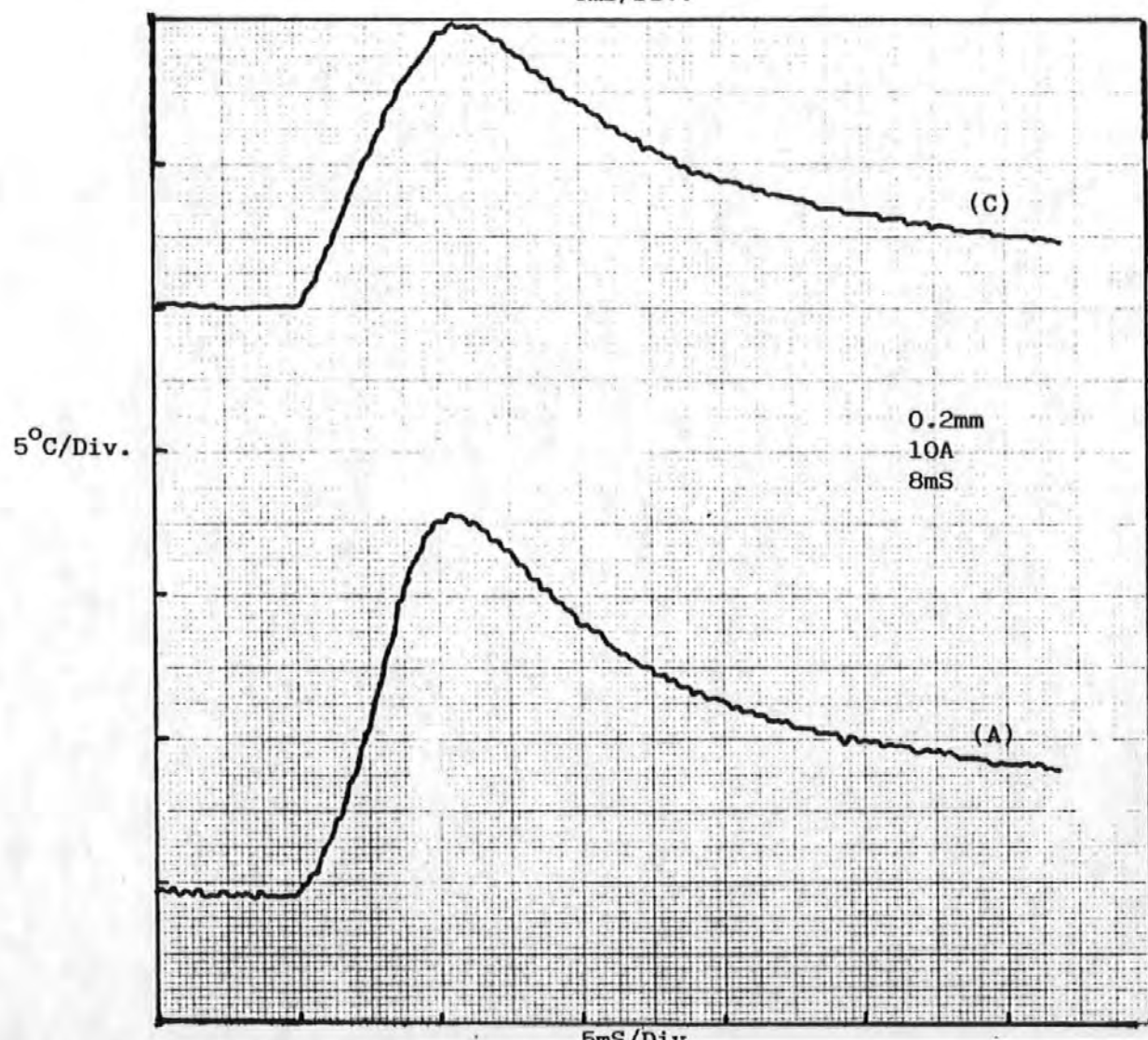
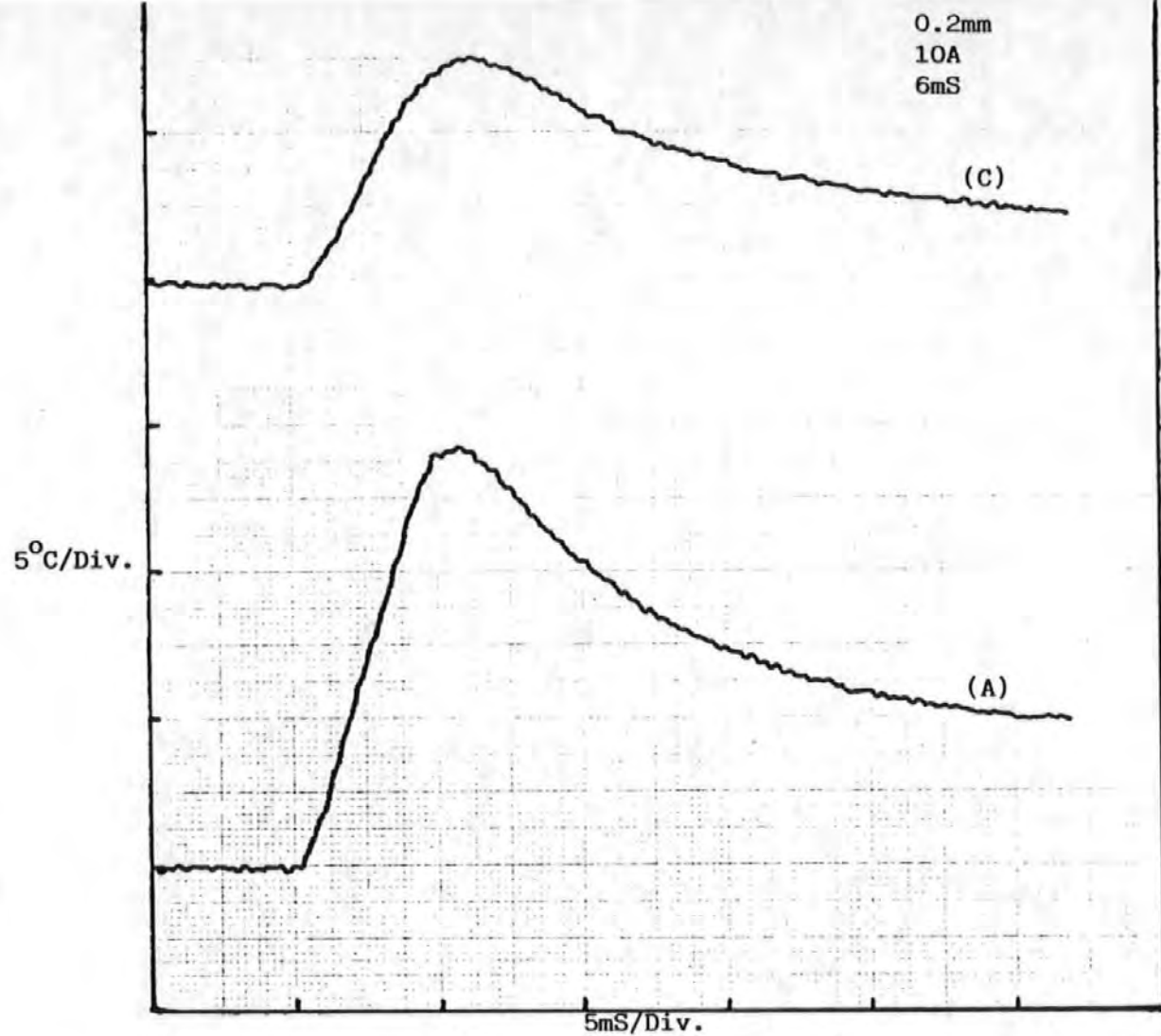
The package used was PAFEC-FE. With this package the contact is modelled by giving the co-ordinates (nodes) of the half section of the contact which is assumed to be asymmetrical about global x and y axis. This is then divided into four sections. The generated 3-D volume of this model which is tilted at 30 degrees is shown in figure (b).

Figure (b) also shows a typical contour of heat distribution within the contact for heat input of 100 watts which applied at the centre of the contact for duration of 10ms.

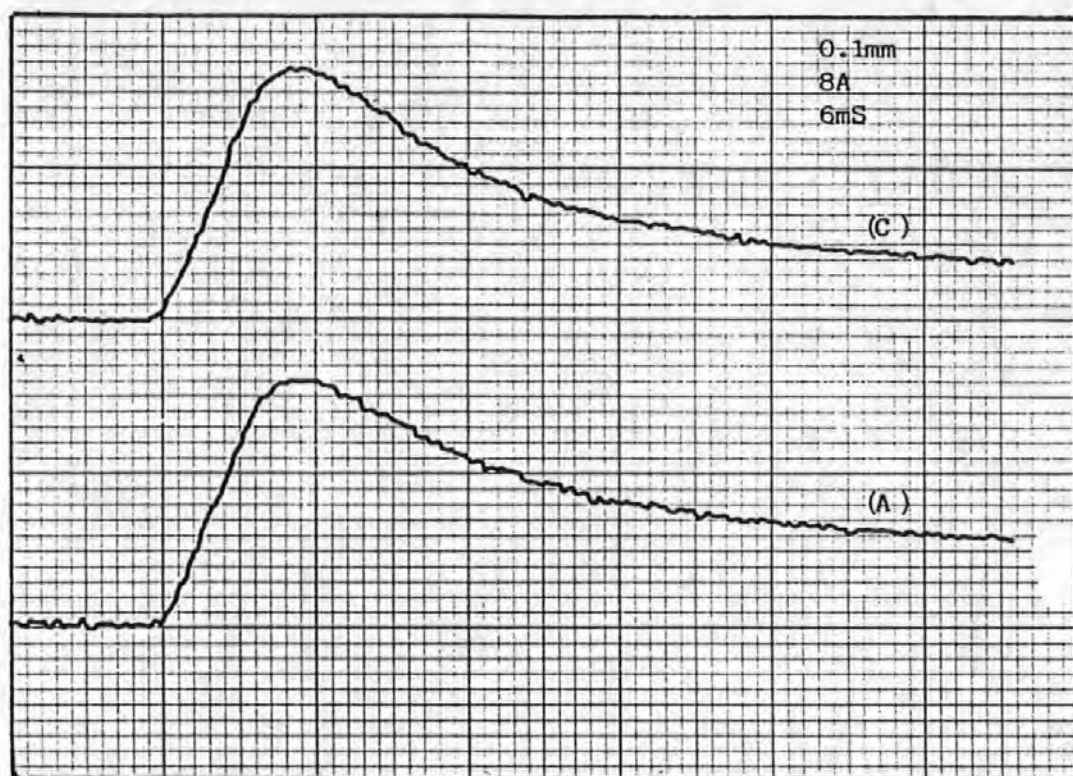
The observation of figure (b) suggests that most of the heat is concentrated within the line of contact (where the heat impulse is applied) and that at points remote from the impulse heat there is no rise in the temperature of the contact body from the room temperature.





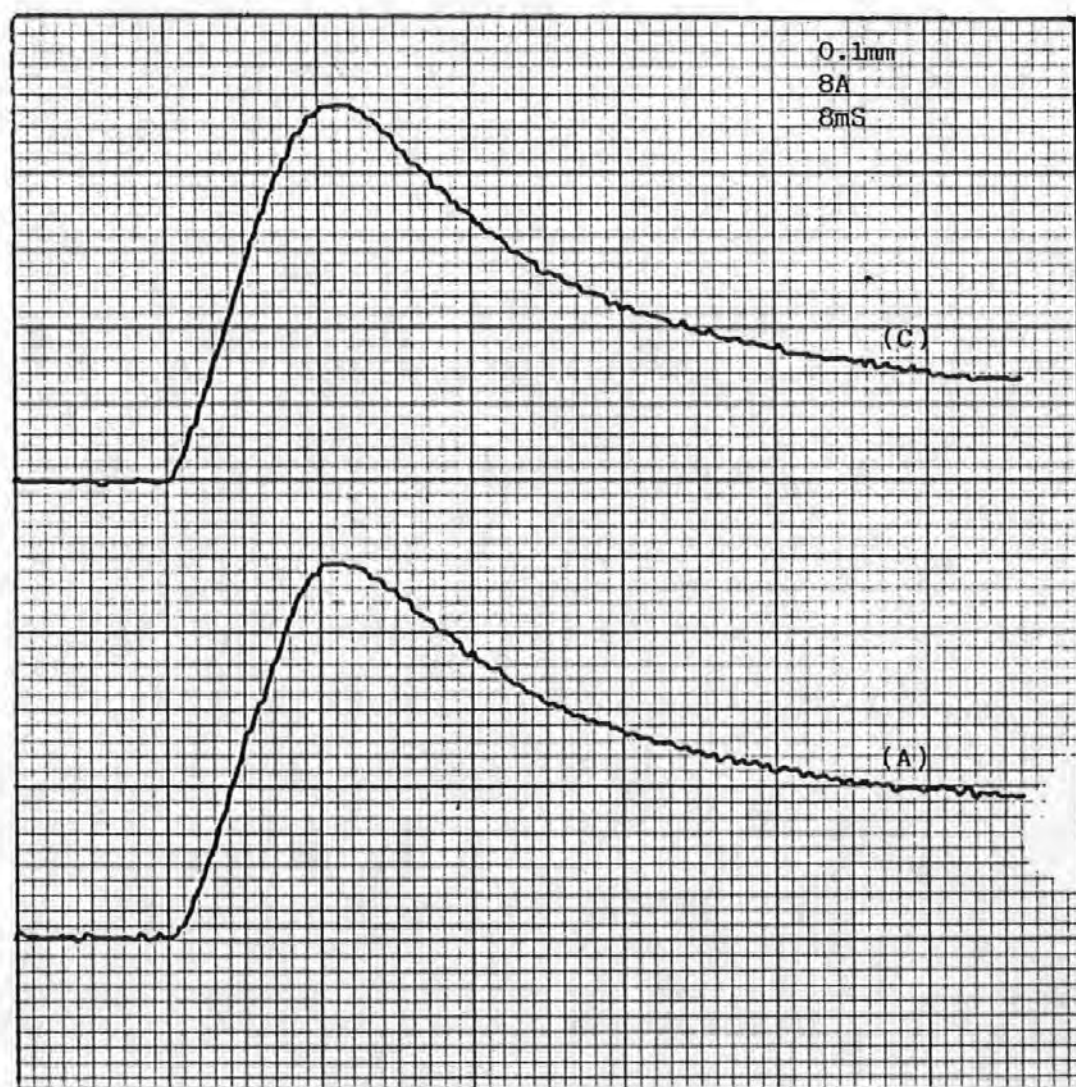


5°C/Div.

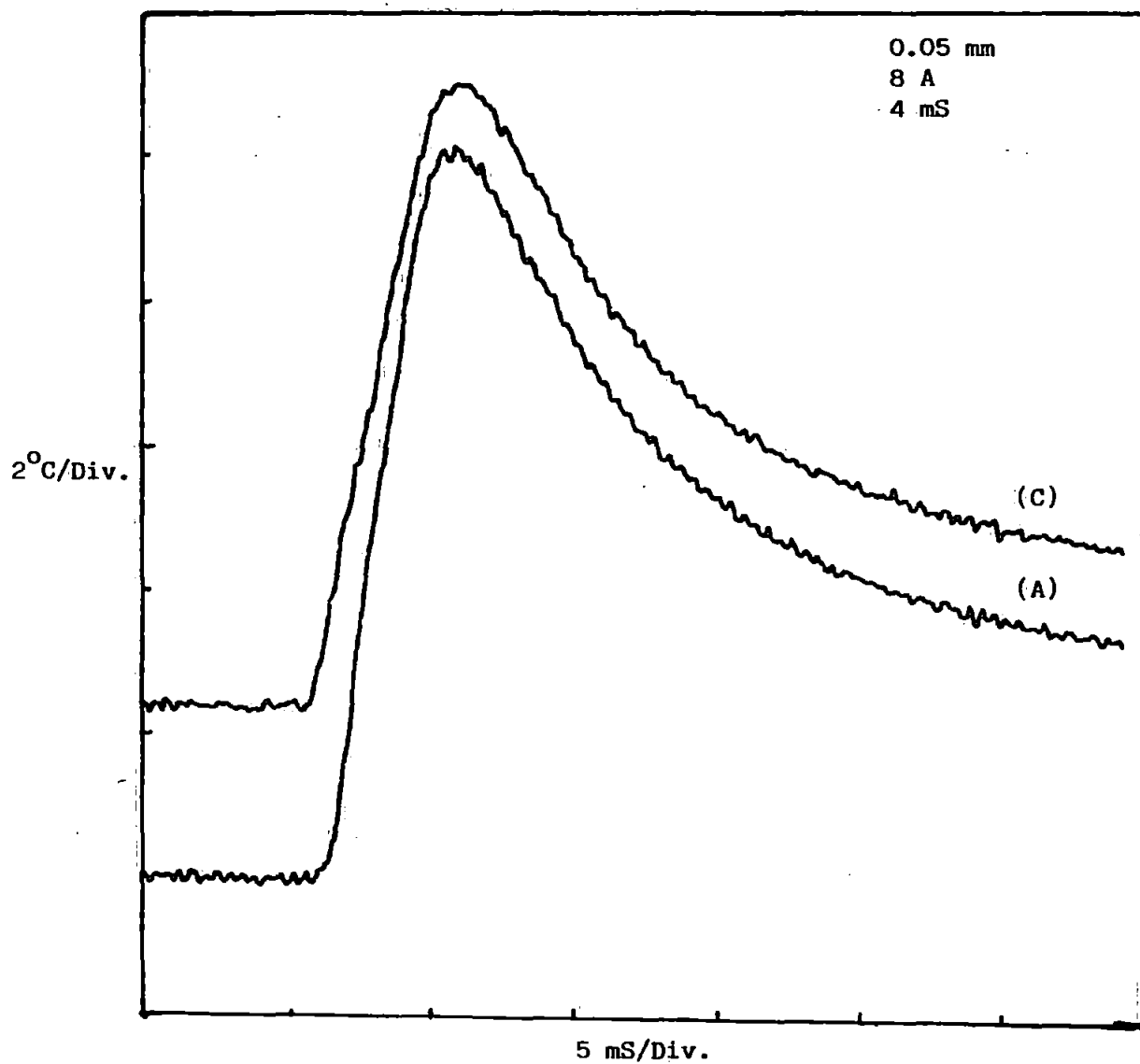
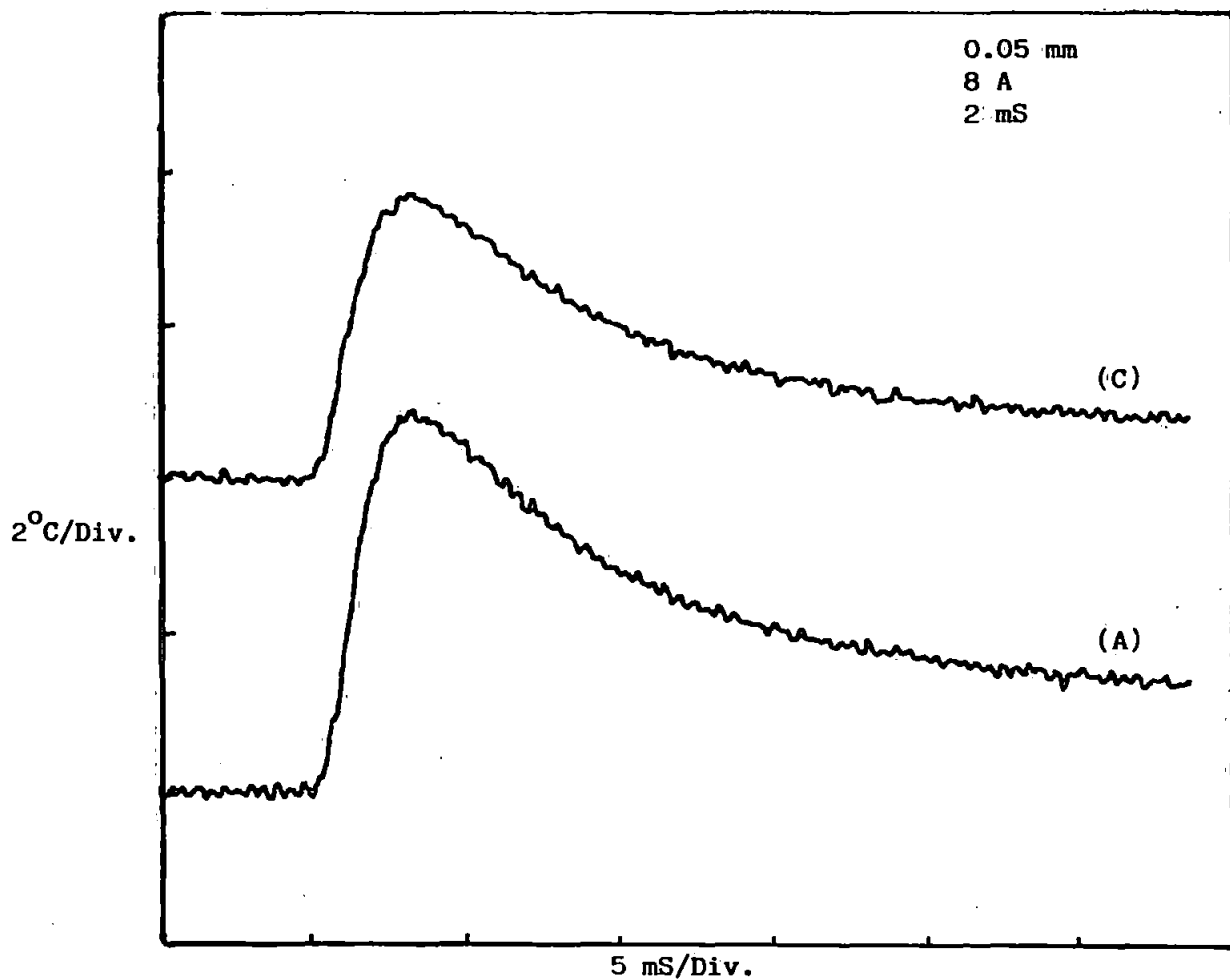


5mS/Div.

5°C/Div.



5mS/Div.



APPENDIX III

A sample of temperature-time curves of the anode and the cathode electrodes obtained by probes A and B respectively (these two probes are discussed in section 4.5.2) for a gap length of 0.05-1mm, and a current of 4-10 Amps at a supply voltage of 40 V.

(A) : Anode

(C) : Cathode


```

1340DRAW NZ,TR2,NZ;
1350NEXT NZ
1360ENDPROC
1370REM @@@@
1380DEFPROCheader
1390VDU 2
1400PRINT"Test results for filename ";filename$
1410PRINT"Step";TAB(10),"Time to";TAB(25);"Voltage"
1420PRINT" No.";TAB(12);"step";TAB(27);"step"
1430PRINT;TAB(12);"(uS)";TAB(28);"(V)"
1440PRINT:VDU 3
1450ENDPROC
1460REM @@@@
1470DEFPROCprint
1480VDU 2
1490FOR S%= 1 TO (step%-1)
1500PRINT;TAB(2);S%;TAB(12);time(S%);TAB(27);voltstep(S%),
1510NEXT S%
1520PRINT:VDU 3
1530ENDPROC
1540REM @@@@
1550DEFPROCfront
1560PTR#Y=1
1570FOR P1%=1 TO 11
1580F%(P1%)=BGET#Y:NEXT P1%
1590ENDPROC
1600REM @@@@
1610DEFPROCdump
1620PRINTTAB(5,30);"
1630*GDUMP
1640PRINT CHR$(12):REM page feed
1650ENDPROC
1660REM @@@@

```

```

720LOCAL A%,L%,P%,P1%
730REM GLOBEL P9%,SPACE%,X%
740IF MID$(F$,1,1)="R" THEN X%=1 ELSE X%=0
750P9%=LEN(F$); IF X%=1 THEN P9%=P9%-2
760P9%=P9%/2
770IF X%=1 THEN P%=3 ELSE P%=1
780L%=LEN(F$)-1
790FOR P1%=P% TO L% STEP 2
800A$=MID$(F$,P1%,2)
810AZ=EVAL("&"+A$)
820? ,SPACE$(P1%-P%)/2,=A%
830NEXT P1%
840ENDPROC
880DEFPROCinvest
890step%=1:start%=1
900P%=1
910REPEAT
920DZ=ABS(TR1(P%)-TR1(P%+3)),
930IF DZ>5 THEN PROCstep
940P%=P%+1
950UNTIL P%=122
960ENDPROC
1000DEFPROCstep
1010REPEAT
1020PZ=P%+1
1030DZ=ABS(TR1(P%)-TR1(PZ+1)),
1040UNTIL DZ>4
1050time(step%)=(P%-start%)*timescale
1060start%=P%
1070REPEAT
1080PZ=P%+1
1090DZ=ABS(TR1(P%)-TR1(PZ+1)),
1100UNTIL DZ<4
1110voltstep(step%)=INT((TR1(start%)-TR1(P%))*voltscale*1000/255)/1
00
1120start%=P%:step%=step%+1
1130ENDPROC
1140REM @@@@@@@@@@@@@@@@@@@@@@@@@@@@@@@@@@@@@@@@@
1150DEFPROClabel
1160PRINTTAB(10,20); "Step", "Time to", "Voltage"
1170PRINTTAB(10,21); "No.", "step", "step"
1175 PRINT; TAB(20); "(uS)", "(V)"
1180FOR SZ=1 TO (step%-1)
1190PRINT; TAB(10); SZ; TAB(22); time(SZ); TAB(31); voltstep(SZ)
1200NEXT SZ
1210INPUTTAB(5,28); "DUMP GRAPH TO PRINTER (Y or N)"; O$
1220IF O$="Y" THEN PROCdump
1230ENDPROC
1240REM @@@@@@@@@@@@@@@@@@@@@@@@@@@@@@@@@@@@@@@@@
1250DEFPROCgraph
1260GCOL 0,2
1270MOVE 1,TR1(1)
1280FOR NZ= 2 TO 125
1290DRAW NZ,TR1(NZ)
1300NEXT NZ
1310GCOL 0,1
1320MOVE 1,TR2(1)
1330FOR NZ= 2 TO 125

```

Appendix II

DATA Analysing Program Listing

```
80DIMR1$(2),F1$(1),R$(2),FS(1),TR1(125),TR2(125),time(50),voltstep(50),F%(11)
90CLS:PRINTTAB(10,10);"Enter data filename"
100INPUTTAB(16,14);filename$
110CLS:PRINTTAB(5,6);"Enter voltage scale, Volts/Div ";
120INPUTTAB(18,10);voltscale
130PRINTTAB(7,14);"Enter time scale, uS/sample";
140INPUTTAB(18,18);timescale
150MODE 1
160Y=OPENUP filename$:PTR#Y=0:samples=BGET#Y:CLOSE#Y
170PROCheader
180FOR T%= 1 TO samples
190CLS:GCOL 0,3
200PROC_READ
210PROCaxes
220PROCgraph
230PROCinvest
240PROClabel
250PROCprint
260NEXT T%
270MODE 7
280PRINT"ANALYSIS COMPLETE"
290END
310DEFPROCaxes
320*SCALE -20,-140,140,140
330 PRINTTAB(20,2);"Sample No: ";T%
340MOVE -20,0:DRAW 140,0
350MOVE 0,-140:DRAW 0,140
360MOVE 0,0
370FOR S=-128 TO 128 STEP 25.6
380MOVE -2,S:DRAW 2,S
390NEXT S
400FOR S%=-25 TO 140 STEP 25
410MOVE S%,-2:DRAW S%,2
420NEXT S%
430ENDPROC
440FOR S%=-140 TO 140 STEP 20
450MOVE -10,S%:PRINT S%
460NEXT S%
470FOR S% = -20 TO 140 STEP 20
480MOVE S%,-6:PRINT S%
490NEXT S%
500VDU 26
510ENDPROC
550DEFPROC_READ
560*DISC
570Y=OPENUP filename$:REM name of file
590PTR#Y=(T%-1)*250+12
600FOR P1%=1 TO 125:TR1(P1%)=BGET#Y
610IF TR1(P1%) > 127 THEN TR1(P1%)=TR1(P1%)-256
620NEXT P1%
630FOR P1%=1 TO 125:TR2(P1%)=BGET#Y
640IF TR2(P1%) > 127 THEN TR2(P1%)=TR2(P1%)-256
650NEXT P1%
660CLOSE#Y:REM closes file
670ENDPROC
710DEFPROC_CONINT(F$)
```

APPENDIX II

Shows program listing for the software used to retrieve the data previously stored on floppy disc, as illustrated in Appendix I, for analysis and printing.

```

3320DEFPROCfile
3330bytes=(no_test/ratio+5)*250+12
3340L$=STR$(bytes)
3350TS=&A80
3360$TS="*SAVE "+filename$+" 0000 "+L$
3370X%=TS MOD 256:Y%=TS DIV 256
3380CALL&FFF7
3390X=OPENUP filename$
3400PTR#X=0:BPUT#X,0:CLOSE#X
3410ENDPROC
3420DEFPROCfront
3430PROC CONINT(F$)
3440FOR P1%=0 TO P9%-1:BPUT#Y,?(SPACE%+P1%)
3450NEXT P1%
3460ENDPROC
3470REM @@@@@@@@@@@@@@@@@@@@@@@@@@@@@@@@@@@@@@

```

```

2810PRINTTAB(0,15),"
2820PRINTTAB(0,15)CHR$(131)"Supply"CHR$(129)" ON "CHR$(131),"
Contacts"CHR$(130)"OPEN"
2830?&FCC1=3:REM contactor CLOSED solenoid ENERGISED
2840ENDPROC
2850REM @@@@
2860REM @@@@ CONTACTORS CLOSED @@@@
2870REM @@@@ CONTACTS CLOSED @@@@
2880REM @@@@
2890DEFPROC_ConRoff
2900PRINTTAB(0,15),"
2910PRINTTAB(0,15,CHR$(131)"Supply"CHR$(129)" ON "CHR$(131),"
Contacts"CHR$(129)"CLOSED"
2920?&FCC1=2:REM contactor CLOSED solenoid DE-ENERGISED
2930ENDPROC
2940REM @@@@
2950REM @@@@ CONTACTORS OPEN @@@@
2960REM @@@@ CONTACTS CLOSED @@@@
2970REM @@@@
2980DEFPROC_CoffRoff
2990PRINTTAB(0,15),"
3000PRINTTAB(0,15,CHR$(131)"Supply"CHR$(130)" OFF "CHR$(131),"
Contacts"CHR$(129)"CLOSED"
3010?&FCC1=3:REM contactor CLOSE solenoid DE-ENERGISED
3020ENDPROC
3030DEFPROC_pause
3040TIME = 0
3050time=TIME+150
3060REPEAT
3070P=INKEY(0)
3080UNTIL P=80OR TIME>=time
3090IF P=80THEN GOTO 3100 ELSE IF P<>80 THEN ENDPROC
3100PRINTTAB(0,20)"
":PRINTTAB(0,20)CHR$(131)"Press"CHR$(135)"`C`"CHR$(131)"to
continue.":Y$=GET$
3110IF Y$="C" THEN PRINTTAB(0,20)"
":PRINTTAB(0,20)CHR$(131)"Press"CHR$(135)"`P`"CHR$(131)"to PAUSE
the program.":ENDPROC
3120ELSE IF Y$<>"C" THEN ENDPROC
3130ENDPROC
3140REM @@@@
3150REM @@@@ CONVERSION @@@@
3160REM @@@@
3170DEFPROC_CONINT(F$)
3180LOCAL A%,L%,P%,PI%
3190REM GLOBEL P%,SPACE%,X%
3200IF MID$(F$,1,1)="R"THEN X%=1 ELSE X%=0
3210P%=LEN(F$):IF X%=1 THEN P%=P%-2
3220P%=P%/2
3230IF X%=1 THEN P%=3 ELSE P%=1
3240L%=LEN(F$)-1
3250FOR PI%=P% TO L% STEP 2
3260A$=MID$(F$,PI%,2)
3270A%=EVAL("&"A$)
3280?(SPACE%+(PI%-P%)/2)=A%
3290NEXT PI%
3300ENDPROC
3310REM @@@@

```



```

1680NEXTI%
1690NEXTL%
1700FOR I%=1TOJ
1710INPUT#data%,sl$:REM sl$ IS LAST 3*2 BYTES OF DATA
1720NEXTI%
1730PRINT#cmd%,"UNTALK"
1740PRINT#cmd%,"GO TO LOCAL",cro%,"EXECUTE"
1750CLOSE#cro%
1760ENDPROC
1770REM @@@@@@@@@@@@@@@@@@@@@@@@@@@@@@@@@
1780REM @@@@ STORE 3 @@@@@@@@@@@@@
1790REM @@@@@@@@@@@@@@@@@@@@@@@@@@@@@@@@@
1800DEFPROC STO3
1810PROC _IEEEBUSINIT
1820N$=CHR$(27)+"ORN00":REM COMMAND TO O/P STO2
1830PRINT#cmd%,"UNLISTEN"
1840PRINT#cmd%,"LISTEN",cro%,"EXECUTE"
1850PRINT#data%,B$,N$
1860PRINT#cmd%,"UNLISTEN"
1870PRINT#cmd%,"TALK",cro%
1880FOR I%=1TO12
1890INPUT#data%,G$
1900F3$=F3$+G$:REM F3$ IS FRONT PANEL SETTING
1910NEXTI%
1920FOR I%=1TO3
1930INPUT#data%,s$:REM s$ FIRST 3*2 BYTES OF DATA
1940NEXTI%
1950FOR L%=1TO 2
1960FOR I%=1TO125
1970INPUT#data%,R3$
1980R3$(L%)=R3$(L%)+R3$:REM R3$(1) IS FIRST 125*2 BYTES OF TRACE
R3$(2) IS LAST 125*2 BYTES OF TRACE
1990NEXTI%
2000NEXTL%
2010FOR I%=1TO3
2020INPUT#data%,sl$:REM sl$ IS LAST 3*2 BYTES OF DATA
2030NEXTI%
2040PRINT#cmd%,"UNTALK"
2050PRINT#cmd%,"GO TO LOCAL",cro%,"EXECUTE"
2060CLOSE#cro%
2070ENDPROC
2080REM @@@@@@@@@@@@@@@@@@@@@@@@@@@@@@@@@
2090REM @@@@ WRITE TO FILE @@@@@@@
2100REM @@@@@@@@@@@@@@@@@@@@@@@@@@@@@@@@@
2110DEFPROC _WRITE
2120REM filename$ containsthe name of the file and MUST NOT exceed 7
characters
2130Y=OPENUP filename$:REM name of file
2140PTR#Y=0:pointer=BGET#Y
2150IF S%=1 THEN PROCfront
2160PTR#Y=(pointer*250+12)
2170PROC _CONINT(R$(1))
2180FOR P1%=0 TO P9%-1:BPUT#Y,?(SPACE%+P1%)
2190NEXT P1%
2200PROC _CONINT(R$(2))
2210FOR P1%=0 TO P9%-1:BPUT#Y,?(SPACE%+P1%)
2220NEXT P1%
2230pointer=pointer+1:PTR#Y=0:BPUT#Y,pointer

```



```

1120CLOSE#cro%
1130ENDPROC
1140REM @@@@@@@@@@@@@@@@@@@@@@@@@@@@@@@@@@@@@@
1150REM @@@@@@ STORE 1 @@@@@@@@@@
1160REM @@@@@@@@@@@@@@@@@@@@@@@@@@@@@@@@@@@@@@
1170DEFPROC_STO1
1180PROC_IEEEBUSINIT
1190L$=CHR$(27)+"ORLOO":REM COMMAND TO O/P STO1
1200PRINT#cmd%,"UNLISTEN"
1210PRINT#cmd%,"LISTEN",cro%,"EXECUTE"
1220PRINT#data%,B$,L$
1230PRINT#cmd%,"UNLISTEN"
1240PRINT#cmd%,"TALK",cro%
1250F1$="":R1$="":G$="":R1$(1)="":R1$(2)="
1260FOR I%=1TO12
1270INPUT#data%,G$
1280F1$=F1$+G$:REM F1$ IS FRONT PANEL SETTING
1290NEXTI%
1300FOR I%=1TO3
1310INPUT#data%,s$:REM s$ FIRST 3*2 BYTES OF DATA
1320NEXTI%
1330FOR L%=1TO 2
1340FOR I%=1TO125
1350INPUT#data%,R1$
1360R1$(L%)=R1$(L%)+R1$:REM R1$(1) IS FIRST 125*2 BYTES OF TRACE
R1$(2)IS LAST 125*2 BYTES OF TRACE
1370NEXTI%
1380NEXTL%
1390FOR I%=1TO3
1400INPUT#data%,s1$:REM s1$ IS LAST 3*2 BYTES OF DATA
1410NEXTI%
1420PRINT#cmd%,"UNTALK"
1430PRINT#cmd%,"GO TO LOCAL",cro%,"EXECUTE"
1440CLOSE#cro%
1450ENDPROC
1460REM @@@@@@@@@@@@@@@@@@@@@@@@@@@@@@@@@@@@@@
1470REM @@@@@@ STORE 2 @@@@@@@@@@
1480REM @@@@@@@@@@@@@@@@@@@@@@@@@@@@@@@@@@@@@@
1490DEFPROC_STO2
1500PROC_IEEEBUSINIT
1510M$=CHR$(27)+"ORMOO":REM COMMAND TO O/P STO2
1520PRINT#cmd%,"UNLISTEN"
1530PRINT#cmd%,"LISTEN",cro%,"EXECUTE"
1540PRINT#data%,B$,M$
1550PRINT#cmd%,"UNLISTEN"
1560PRINT#cmd%,"TALK",cro%
1570FOR I%=1TO12
1580INPUT#data%,G$
1590F2$=F2$+G$:REM F2$ IS FRONT PANEL SETTING
1600NEXTI%
1610FOR I%=1TO3
1620INPUT#data%,s$:REM s$ FIRST 3*2 BYTES OF DATA
1630NEXTI%
1640FOR L%=1TO 2
1650FOR I%=1TO125
1660INPUT#data%,R2$
1670R2$(L%)=R2$(L%)+R2$:REM R2$(1) IS FIRST 125*2 BYTES OF TRACE
R2$(2)IS LAST 125*2 BYTES OF TRACE

```

```

565PRINT#cmd%,"SERIAL POLL",cro%,1
566INPUT#cmd%,status$:PRINTTAB(0,7),status$:FORQ=1 TO 1000:NEXTQ
570PRINT#cmd%,"UNLISTEN"
580PRINT#cmd%,"LISTEN",cro%,"EXECUTE"
590PRINT#data%,B$:REM DELIMITER
600PRINT#data%,A$+"D00B64033810EE701EF00009"
610PRINT#cmd%,"UNLISTEN"
620CLOSE#cro%
630ENDPROC
640REM @@@@@@@@@@@@@@@@@@@@@@@@@@@@@@@@@@@@@@
650REM @@@@ READ FRONT @@@@@@@@@@@@@@@@
660REM @@@@@@@@@@@@@@@@@@@@@@@@@@@@@@@@@@@@@@
670DEFPROC READFRONT
680DIMfr$(13):REM TO SAVE FRONT PANEL ARRAY
690A$=CHR$(27)+"OMT00":REM COMMAND FOR O/P OF FRONT
700PRINT#cmd%,"UNLISTEN"
710PRINT#cmd%,"LISTEN",cro%,"EXECUTE"
720PRINT#data%,B$,A$
730PRINT#cmd%,"UNLISTEN"
740PRINT#cmd%,"TALK",cro%
750FORI%=1 TO13
760INPUT#data%,fr$
770FR$=FR$+fr$
780NEXTI%
790PRINT#cmd%,"UNTALK"
800CLOSE#cro%
810ENDPROC
820REM @@@@@@@@@@@@@@@@@@@@@@@@@@@@@@@@@@@@@@
830REM @@@@ ACCU @@@@@@@@@@@@@@@@
840REM @@@@@@@@@@@@@@@@@@@@@@@@@@@@@@@@@@@@@@
850DEFPROC REG
860PROC IEĒĒBUSINIT
870K$=CHR$(27)+"ORK00":REM COMMAND TO O/P ACCU
880PRINT#cmd%,"UNLISTEN"
890PRINT#cmd%,"LISTEN",cro%,"EXECUTE"
900PRINT#data%,B$,K$
910PRINT#cmd%,"UNLISTEN"
920PRINT#cmd%,"TALK",cro%
930F$="":R$="":G$="":R$(1)="":R$(2)="
940FOR I%=1TO12
950INPUT#data%,G$
960F$=F$+G$:REM F$ IS FRONT PANEL SETTING
970NEXTI%
980FOR I%=1TO3
990INPUT#data%,s$:REM s$ FIRST 3*2 BYTES OF DATA
1000NEXTI%
1010FOR L%=1TO 2
1020FOR I%=1TO125
1030INPUT#data%,R$
1040R$(L$)=R$(L$)+R$:REM R$(1) IS FIRST 125*2 BYTES OF TRACE R$(2)
IS LAST125*2 BYTES OF TRACE
1050NEXTI%
1060NEXTL%
1070FOR I%=1TO3
1080INPUT#data%,s$:REM s$ IS LAST 3*2 BYTES OF DATA
1090NEXTI%
1100PRINT#cmd%,"UNTALK"
1110PRINT#cmd%,"GO TO LOCAL",cro%,"EXECUTE"

```

Appendix I

DATA Collection Program Listing

```
10REM PROGRAM TO COLLECT DATA FROM
20REM THE PHILLIPS CRO
30REM @@@@@@@@@@@@@@@@@@@@@@@@@@@@@@@@@@@@@@
40REM @@@@@@@@@@@@@@@@@@@@@@@@@@@@@@@@@@@@@@
50REM @@@@ DIMENSION ALL @@@@@@@@@@@@
60REM @@@@ VARIABLE @@@@@@@@@@@@@@
70REM @@@@@@@@@@@@@@@@@@@@@@@@@@@@@@@@@@@@@@
80DIM R1$(2),F1$(1),R$(2),F$(1),SPACE% 125
90REM CLR
100CLS
110*DISC
120PRINTTAB(8,8);"Enter filename for data"
130INPUTTAB(16,10);filename$
140PRINTTAB(5,12);"Enter number of tests required"
150INPUTTAB(18,14);no_test
160INPUTTAB(9,18);"Sample/Test ratio= 1/";ratio
170CLS:no_samples=INT(no_test/ratio)
180PRINTTAB(12,18);"Test number: ",
190PROCfile
200number=0
210FOR S%=1 TO no_samples
220*IEEE
230FOR N%=1 TO ratio
240number=number+1
250PRINTTAB(26,18);number
260PROC_IEEEBUSINIT
270R$="":F$=""
280PROC_CONTACTOR
290PROC_REG
300NEXT N%
310*DISC
320PROC_WRITE
330NEXT S%
340PRINT"TEST FINISHED"
350END
360REM @@@@@@@@@@@@@@@@@@@@@@@@@@@@@@@@@@@@@@
370REM @@@@ IEEE BUS @@@@@@@@@@@@@@@@@@@@@@
380REM @@@@@@@@@@@@@@@@@@@@@@@@@@@@@@@@@@@@@@
390DEFPROC_IEEEBUSINIT
400*IEEE
410cmd%=OPENIN("COMMAND")
420data%=OPENIN("DATA")
430PRINT#cmd%,"BBC DEVICE NO",0
440PRINT#cmd%,"CLEAR"
450PRINT#cmd%,"REMOTE ENABLE"
460PRINT#cmd%,"END OF STRING",CHR$(13)
470cro%=OPENIN("5")
480PRINT#cmd%,"SERIAL POLL",cro%,1
490INPUT#cmd%,status$:PRINTTAB(0,5);status$:FORQ=1 TO 1000:NEXTQ
500A$=CHR$(27)+"OMT":REM PART OF FRONT SET STRING
510B$=CHR$(27)+"ODDO"+CHR$(13):REM DELIMITER COMAND
520ENDPROC
530REM @@@@@@@@@@@@@@@@@@@@@@@@@@@@@@@@@@@@@@
540REM @@@@ SET FRONT @@@@@@@@@@@@@@@@@@
550REM @@@@@@@@@@@@@@@@@@@@@@@@@@@@@@@@@@@@@@
560DEFPROC_SETFRONT
```

thermocouple, and then, with the aid of electric circuit analogy, a general relation between input power and measured temperature is obtained.

Since the degree of erosion depends upon the difference between the sum of the power absorbed by the electrodes and the arc power, the result obtained above (d.c. test) shows that the minimum contact erosion can be achieved if the maximum contact separation be in the region of 0.1mm.

However, minimum contact erosion between contacts used in a.c. switches (where the maximum separation between contacts is around 2mm) could only be achieved if the separation be maintained at or below 0.1mm for the first half-cycle.

1. White, P.J.
"Investigation of parameters affecting the operating characteristics of toggle switches with Ag-Cd 0 contacts",
CNA A PhD Thesis, Plymouth Polytechnic, 1979.
2. Dickson, D.J. and Von Engel, A.
"Resolving the electrode fall spaces of electric arcs",
Proc. R. Soc. A, Vol. 300, 1967, pp 316-325.
3. Maecker, H.
Z. Phys., Vol. 141, 1955, p 198.
4. Zhu, S.L. and Von Engel, A.
"Fall regions and electrode effects in atmospheric arcs of vanishing length",
J. Phys. D: Appl. Phys., Vol. 14, 1981, pp 2225-35.
5. Boddy, P.J. and Utsumi, T.
"Fluctuation of arc potential caused by metal vapour diffusion in arcs in air",
J. Appl. Phys., Vol. 42, No. 9, 1971, pp 3369-73.
6. Boylett, F.D.A. and Maclean, I.G.
"Cathode fall in potential and space in mercury arcs",
J. Phys. D: Appl. Phys., Vol. 4, 1971, pp 677-79.

7. Earhart, R.F.
Phil. Mag., Vol. 1, 1901, p 147 and Vol. 16, 1908, p 48.
8. Shaw, P.E.
Proc. Roy. Soc., Vol. 73, 1904, p 337.
9. Pearson, G.L.
Phys. Rev. Vol. 56, 1939, p 471.
10. Compton, K.T.
J. Am. Inst. Elec. Engrs., Vol. 46, 1927, p 868.
11. Mackeown, S.S.
Phys. Rev. Vol. 34, 1934, p 611.
12. Germer, L.H. and Haworth, F.E.
"Erosion of electrical contacts on make",
Journal of Applied Physics, Vol. 20, Nov. 1949, pp 1085-1109.
13. Germer, L.H.
"Arcing at electrical contacts on closure.
Part I - Dependence upon surface conditions and circuit
parameters",
Journal of Applied Physics, Vol. 22, No. 7, July 1951,
pp 955-964.
14. Germer, L.H.
"Heat dissipation at the electrodes of a short arc",
The Bell System Technical Journal, Oct. 1951, pp 933-44.

15. Germer, L.H.
"Arcing at electrical contacts on closure.
Part II - The initiation of an arc",
Journal of Applied Physics, Vol. 22, No. 9, Sept. 1951,
pp 1133-39.
16. Germer, L.H. and Smith, J.L.
"Arcing at electrical contacts on closure.
Part III - Development of an arc",
Journal of Applied Physics, Vol. 23, No. 5, May 1952,
pp 553-62.
17. Kisliuk, P.
"Electron emission at high fields due to positive ions",
Journal of Applied Physics, Vol. 30, No. 1, Jan. 1959,
pp 51-55.
18. Kisliuk, P.
"Arcing of electrical contacts on closure.
Part V - The cathode mechanism of extremely short arcs",
Journal of Applied Physics, Vol. 25, No. 7, July 1954,
pp 897-900.
19. Holm, R.
"Electric contacts",
Springer-Verlag, 1967.

20. Capp, B.
"The power balance in electrode-dominated arcs with a tungsten anode and cadmium or zinc cathode in nitrogen",
J. Phys. D: Appl. Phys., Vol. 5, 1972.
21. Mapps, D.J. and White, P.J.
"Investigation of available toggle switches for thermostatic control systems",
IEE Proc., Vol. 128, Pt. B., No. 5, Sept. 1981.
22. Slade, P.G. and Holmes, F.A.
"Pip and crater formation during interruption of a.c. circuit",
8th Int. Conf. on Electric Contact Phenomena, Japan 1976.
23. Sato, M.
"Studies on the silver base electrical contact materials",
Trans. of Nat. Research Inst. for Metals, Vol. 18, No. 2, 1976.

5.1 DISCUSSION

This thesis has presented a comprehensive investigation into the distribution of the arc power to the contacts at break using a power balance relation.

To achieve this objective the following were required: (a) to devise an accurate technique for construction of the probes (contact with thermocouple) for measurement of contact temperature due to arcing, (b) to measure anode and cathode fall voltages using the technique of Von Engel et al (reference 2, chapter 4) for Ag Cd-0 contacts and (c) To develop a power balance model, since the degree of the differences in the correlation between the two ~~power's~~ is related to the erosion rate.

The information obtained from (a) and (b) was subsequently applied to the relation obtained in (c) with a view to characterising the erosion rate and then attempting to reduce it. This data could be used for future design work and also give more insight into understanding the arcing effect between contacts of toggle switches used in thermostatically-controlled electrical appliances, e.g. refrigerators.

(i) Temperature-Time Characteristics of the Contacts:

The technique devised for the construction of the probe (contact with thermocouple, see section 3.5.2, figure 3.7) ensures that under transient conditions (defined as a condition in which, within arc duration of 2-10 ms, the contact body does not reach to a steady state) the temperature rise of the contact can be measured immediately before appreciable heat diffuses to its surroundings. The accuracy of the probe response was found to be subject to the degree of proximity of the arc contact-point to the probe.

The construction of the probe (contact with thermocouple) and the contact temperature measurements were found to be tedious and not straightforward.

Results obtained from temperature-time curves of anode and cathode sensors for

various test parameters such as current, gap-length and arc duration, at 40 Volts d.c. with speed of separation 300 mm/s, are detailed in section 4.5.3. These indicated that in most cases the anode is hotter than the cathode (see appendix III and figures 4.33 and 4.35). This is thought to be due to the cathode losing heat by way of latent heat of evaporation of lost metal.

The results also show that the temperatures of the electrodes at different current and gap-length have a linear relation to the arc duration, and that the temperatures increase from room temperature to approximately 30 °C, over a range of currents, gap-lengths and arc durations extending from 4-10 A, 0.05-1mm, and 2-10 ms respectively, as shown in figure (4.33).

The results of the measurements of the effects from contact newness show that initially there is inconsistency in the value of electrode temperatures and after about 50-100 operations, depending on circuit conditions, the electrodes' temperatures reach to steady values (figure 4.36).

This may be the reason why, where these contacts are to be used in switches for the temperature control of electrical appliances such as refrigerators, before their employment, a high level D.C. arc is drawn between them, probably in order to burn off the poorly-conducting surface deposits often found on metal components, which would otherwise adversely affect the switching function of the switches.

Results from tests on a pair of new contacts, under fixed test conditions, showed that the initial temperatures of both electrodes are high and that these temperatures decreased as the number of operations increased and eventually reached to a steady value (figure 4.36).

Where the change of polarity takes place after 500 operations, the contact which acts as anode (fixed contact) has a higher temperature than previously and the situation is reversed for the contact which now acts as cathode (moving contact), its temperature now being lower than previously and hence the difference between the temperature of the electrodes increases. This may be due to the moving contact causing a flow of air over its surface.

(ii) Electrodes Fall Voltages

A typical trace of the electrodes fall voltages, as observed on an oscilloscope, is shown in figure (4.4).

The results of fall measurements suggest that cathode and anode fall voltages decrease slightly with increase in the current, for the constant test conditions (figures 4.11, 4.14 and 4.15), and increase with increase of gap-length (figures 4.12, 4.13 and 4.17). The increase of the cathode fall is slight compared to the anode fall, to such an extent, in fact, that one can assume it is negligible. This may be because the difference in the number of positive and negative charges (which is basically a function of the cathode metal) in the cathode transition region does not vary significantly with the increase of the gap-length. (The transition regions are defined in section 2.5, and illustrated in figure 2.4.)

The results (figures 4.5b and 4.9) also show that the anode fall voltage can occur in a few steps (Voltage drop) within the arc. There are less steps at higher currents, or perhaps their magnitude is similar to fluctuation voltage, and they are not all distinguishable. Since for a particular gap-length or current the anode fall voltage is constant, if it occurs in steps, the sum of the steps value is equal to the fall voltage value (figure 4.9, samples 5, 25, 54).

The distance at which the second step (d2), third step (d3), etc. occur after the first drop (step) from the cathode surface is found to be dependent on the speed of closure (figure 4.8a). For example, at the faster speed (300 mm/s), the second step occurs within a few tens of microns, as opposed to a few hundreds of microns for the slower (75 mm/s) closing speed. The first step usually occurs within 5-15 μm from the cathode. Results (figures 4.4 and 4.9) also showed that speed has no influence on the magnitude of the electrodes fall voltages.

(iii) Arcing on Closure (Voltage Step Phenomena)

Arcing as a result of contact closure was observed from the oscilloscope trace (section 4.4).

A typical voltage characteristic is shown in figure (4.18), for test conditions for 50 volts, 5 A, and speed of closure 500 mm/s.

The steps within the arc voltage which resulted from contact closure are shown diagrammatically in figure (4.20).

In order to define these steps, e.g. V1 (1st Step Voltage), V2 (2nd Step Voltage) and VL (Last Step Voltage), and to identify the main causes of arcing, experimental work was concentrated on the influence of the parameters of operating voltages, currents, speeds of closure, and surface roughness.

The effect of various operating voltages (4.4.1.1) is that the amplitudes of V1, V2 and V3 (where existing) are increased with increase of operating voltage, but VL remains constant, typically at 10 volts (figure 4.19).

Observations of the effect of roughened surface (section 4.4.1.3) indicated that the steps can be seen at first operation for any fixed test condition (current, speed and voltage), whereas the surfaces of a new pair of contacts have to perform a great number of operations (i.e. they become disfigured) before steps can be seen.

This increased roughness also slightly decreases the cathode fall voltage (figure 4.24), which may be due to a reduced work-function required for the emission of the electrons because the surface state is changed.

The most interesting results obtained were that with the surface which had been roughened, an increase in the number of occurrences of steps was observed, but not in the number of steps (the maximum number of steps observed was three).

Having identified that the occurrence of steps increased at higher currents and faster speeds, and as it is known that these two parameters contribute to disfigurement of the contact surfaces (plastic deformation), and having also experimented with contacts having roughened surface, which showed that the steps occurred at every operation, so it was concluded that the initiation of the arc is strongly dependent on

the state of the electrodes' surfaces. It is postulated that the initiation of the arc is due to momentary points of contact, or it is as the result of field break-down due to the state of the electrodes' surfaces.

Whichever causes the initiation of the arc, in most cases after initiation, V_1 , V_2 , V_3 and V_L exist within the arc (these are defined in figure 4.20) until the two contacts come to rest on each other.

Since V_L has a steady value in the order of 10-11 Volts, which is characteristic of the metal electrode, it is considered to be cathode fall voltage. In most cases V_L follows after V_1 , V_2 and V_3 and the whole process becomes continuous. This indicates that there is inter-relation between them. The parameter required for the continuity of the arc is known to be the anode fall voltage (section 2.5.1.2).

When closure proceeds with steps (V_1 , V_2 , V_L), it is thought that field breakdown takes place. This is due to an intense field building up between the two electrode surfaces as they get closer (probably between spikes).

Closure which proceeds just by normal arc (V_L) as shown in figure (4.27a), is due to a first point of contact vaporising sufficient amount of metal from the electrode to provide ions. These ions charge the outer surface of the cathode and as a result create an intense field which is sufficient to drag out electrons from the cathode for the maintenance of the arc.

Such closures which proceed just by normal arc (figure 4.27a), can be interpreted as being due to field emission before a metallic contact takes place, as described above, or they may be perhaps due to surface impurities, as has been suggested by Germer et al (reference 16, chapter 4).

Those closures which are not preceded by an arc (figure 4.27d), can be explained as perhaps due to the first point of contact (e.g. spike) being covered by a good insulator, so that it did not vaporise. Germer, et al⁽¹⁶⁾ suggest it may be due to the absence of a foreign layer on the cathode surface.

The traverse of the arc voltage to zero [figure 4.26(b and d)] during closure is related to metal being thrown out, shorting the circuit, which then vaporises and

arcing continues.

The oscillation (figure 4.28) before the drop of supply voltage to V1 is related to the natural capacity and inductance of the oscilloscope probe, or wires in the circuit.

Since these values (V1, V2, VL) are in the range of values obtained from the measurements described in section 4.3, and also since the mechanism of the arc on closure has become clearer, one may be able to study the erosion of the contacts on closure in more detail, which is of great interest to the electrical contacts community.

(iv) Power Balance at the Electrodes

Contact erosion is assessed from a comparison of electrical and thermal power.

The electrical power, which is the input power, is the product of current and voltage drop between the contact's surfaces. The thermal power consists of power absorbed by the contact in raising the electrodes' temperatures and power used in the melting and evaporation of contact material.

Electrical power has been modelled using the equations derived by Capp (reference 20, chapter 4, section 4.6.1), and the thermal model is based on a simulation consisting of the response of an RC circuit to a d.c. pulse (section 4.6.2).

The equations derived from the electrical model were as follows:

$$\text{Voltage drop in front of cathode: } V_{CE} = \gamma V_c + \gamma V_i + 1/2 V_p - \phi_c$$

$$\text{Voltage drop in front of anode: } V_{AE} = V_a + V_e + 1/2 V_p + \phi_a$$

In the thermal model it was assumed that all the heat entering the contacts was received by the thermocouple, and then with the aid of electric circuit analogy a general relation between input power and measured temperatures was obtained which is as follows:

$$\text{Input power to contact (heating curve): } \dot{Q}_i = \frac{\theta_o}{\left[1 - e^{-\frac{T}{\alpha}} \right]}$$

$$\text{Input power to contact (cooling curve): } \dot{Q}_i = \frac{\theta_o}{\left[e^{-\frac{t}{\alpha}} \right] \left[e^{\frac{T}{\alpha}} - 1 \right]}$$

The equations of the above heating and cooling curves are truly exponential.

The log-linear (semi-log) plot of the heating curve (figure 4.45) revealed that it is not truly exponential, but the semi-log plot of the cooling curve as shown in figure (4.45), although in some cases at the mid-point of the cooling curve there was a kink (perhaps due to extra heat loss to the surrounding air at that time, etc.), it does satisfy the exponentiality required in order to use the equation of the cooling curve for the calculation of the input power.

The highest heat-flow rate was obtained using the points right at the start of the cooling curve. This has been followed in all the calculations of input power to the electrodes.

The results obtained from the thermal model showed (figure 4.47) that for gap of 0.05 mm and current less than 6 A, cathode power was less than anode power, for current of 6 A both cathode and anode power were the same, and for current greater than 6 A cathode power is less than anode power.

For gap of 0.1 mm and current less than 6.5 A cathode power was greater than anode power, for current 6.5 A they both had the same value, for currents greater than 6.5 A and less than 11 A, cathode power was less than anode power, at 11 A (by interpolation) they both had the same value, and for the currents greater than 11 A, the cathode power was always greater than the anode power.

At any other gaps (e.g. 0.2, 0.5 and 1 mm), for any current, the cathode power was always less than the anode power.

The results (figure 4.47) also showed that for gaps of 0.05 and 0.1 mm, up to a current of 8 A, the sum of cathode and anode power were equal to the arc power; in these cases it was thought no loss took place.

These findings agreed with the suggestion of White (reference 1, chapter 4) which is that, below 0.2 mm, the net power causing erosion is virtually the same as the net arc power (the study presented here was an extension of his investigations).

For conditions where the sum of anode and cathode power was equal to the arc power, γ and V_e were calculated using power balance equations (1) and (3) and with

the aid of data from figures (4.49) and (4.47). It was found that, in GENERAL, for the situation where anode and cathode power were equal, or approximately equal, then γ was in the range of 0.51– 0.54, and the thermal energy of the electron (V_e) was negligible, but where anode power was not equal to the cathode power, γ was in the range of 0.47–0.5, and the thermal energy of the electron was around 1.2 eV.

The results (figure 4.49) obtained for components of the arc voltage at 40 volts suggested that, since the cathode fall remained constant for any current and any gap-length, any increase in the power conducted into the cathode was as a result of increased power dissipation in the arc column.

The examination of Scanning Electron Micrographs of the contact surfaces has suggested that the arc has caused melting and evaporation. A typical example is shown in figure (4.50); the lack of cracks on the cathode surface shown in this figure was thought to be due to the cathode spot being mobile (i.e. the heat does not concentrate on one area). This agrees with the suggestion of Mapps et al (reference 21, chapter 4) and Slade et al (reference 22, chapter 4).

However, the x-ray analyses of the electrodes' surfaces have shown that the melted metal was composed mostly of silver. A typical example is shown in figure (4.51).

The degree of erosion depends upon the difference between the sum of the powers absorbed by the anode and cathode, and the arc power. Therefore the minimum contact erosion can be achieved if the maximum contact separation be in the order of up to 0.1 mm.

The adoption of this separation between contacts is not feasible for switches used in d.c. circuits due to electrical breakdown between the contacts of the switch.

In a.c. circuits the benefit of reduced contact erosion is made possible by reducing the initial rate of separation of the contacts, so that for the first half cycle (10 ms, which is the maximum possible duration of the arc in a.c. circuits) the contact separation only reaches to around 0.1 mm. After the occurrence of a zero-crossing during this 10 ms, the contacts can continue to separate to any required

gap.

It was thought that an opening velocity of 10 mm/s for the first 10 ms would achieve the above separation.

Finally, all the aspects of the proposed research have been studied in detail, but further research is desirable before an overall assessment of the above finding can be made.

5.2 FUTURE WORK

Here the results obtained with d.c. over a range of parameters (current, gap-length and arc-duration) relevant to the a.c. (mains) represents a foundation on which future work can be developed and progressed for optimising the design criteria and improving the performance of the switches. The proposed work is as follows:

(a) To investigate the effect of initial separation velocity of 10 mm/s for the first 10 ms on the erosion rate on switches which have separation of 2-2.5 mm, and also to find a suitable speed for them after the initial 10 ms.

(b) To develop a relation between contact erosion, arc duration and input power, using FINITE ELEMENT APPROACH. For designers, this will provide a rational method of predicting the erosion rate for specific working conditions.

(c) To investigate the effect of smaller size of contact on the performance of switches which have the above recommended characteristics. This may lead to the use of less silver on each contact, and hence a reduction in the material cost of each switch, which is of great interest to the manufacturers.

(d) The effect of the various shapes of contact (flat, round) on the distribution of the heat due to arcing is worth further study.

5.3 CONCLUSIONS

(i) Temperature-Time curves

- (1) In general the anode temperature is hotter than the cathode temperature except for gaps below 0.2 mm, they are the same. Appendix (III) and figure (4.29).
- (2) The effects from contact newness show that initially there is inconsistency in the value of electrode temperature before reaching to steady values, figure (4.36).
- (3) The effect of change of polarity reveals that the moving contact is always cooler compared to a situation where the same polarity acts on the fixed contact, figure (4.36).

(ii) Electrodes Fall Voltages

- (1) Cathode and anode fall voltage decrease slightly with increase in the current, and increase with increase of gap-length, figures (4.11-4.17).
- (2) The distance in which the anode fall occurs from the cathode surface is dependent on the speed of closure, also the anode fall can occur in a few steps. However, speed has no influence on the magnitude of the electrodes' fall voltage, figures (4.9 and 4.5b).

(iii) Arcing on closure (Voltage Step Phenomena)

- (1) The magnitude of 1st step (V1), 2nd step (V2) and 3rd step (V3) are directly proportional to the magnitude of operating voltages, but the magnitude of last step voltage (VL) remains constant, figure (4.21).
- (2) Current has no influence on the magnitude of 1st step (V1) see figure (4.19), but the magnitude of the first step (V1) is inversely proportional to the speed of closure, figure (4.22).
- (3) The surface roughness decreases the magnitude of the cathode fall voltage, figure (4.24), and on closure the initiation of the arc is strongly dependent on the state of the electrodes' surface.
- (4) In general arc on closure is due to momentary point of contact or it is as the result of a strong field which may exist between the electrodes.
- (5) The absence of the arc on closure is related to the absence of the foreign layers on the cathode surface, figure (4.27d).

(iv) Power Balance at the Electrodes

- (1) In general for the situation where anode and cathode power are equal or approximately equal, figures (4.47a and 4.47b), the ratio of positive ion current to total current (γ) is in the range of 0.51 - 0.54, and the thermal energy of the electron (V_e) is negligible, but where anode power is not equal to the cathode power, γ , is in the range of 0.47 - 0.5, and the thermal energy of the electron is around 1.2eV.
- (2) The minimum contact erosion can be achieved if the maximum contact separation be in the order of up to 0.1mm. It is thought that in a.c. circuit an opening velocity of 10mm/s for the first 10ms would achieve the above separation.

APPENDIX I

Shows the program listing of the data collection software, which is written in BASIC, for the communication of the BBC Microcomputer with the Philips Oscilloscope through the IEEE bus and controller of the test rig, through the PIO interface box (which energises the solenoid, contactor, etc...), and hence the test rig operates as a switch. This program also includes some software for transferring the digitised waveforms captured by the oscilloscope to the floppy disc.